JSCSEN 80(12)1461–1598(2015)

ISSN 1820-7421(Online)

Journal of the Serbian Chemical Society

Electronic version

Volume 80 : : 2015 : : 85 Years of the Journal

1930 Glasnik Hemijskog Društva Kraljevine Jugoslavije
Journal of the Chemical Society of the Kingdom of Yugoslavia

1947 Glasnik hemijskog društva Beograd
Journal of the Chemical Society of Belgrade

1985 Journal of the Serbian Chemical Society

VOLUME 80

No 12

BELGRADE 2015

Available on line at

www.shd.org.rs/JSCS/

The full search of JSCS
is available through

DOAJ DIRECTORY OF OPEN ACCESS JOURNALS
www.doaj.org

The **Journal of the Serbian Chemical Society** (formerly Glasnik Hemijskog društva Beograd), one volume (12 issues) per year, publishes articles from the fields of chemistry. The **Journal** is financially supported by the **Ministry of Education, Science and Technological Development of the Republic of Serbia.**
Articles published in the **Journal** are indexed in **Thompson Reuters products: Science Citation Index-Expanded™** – accessed *via* **Web of Science®**, part of **ISI Web of Knowledge℠** and **Journal of Citation Reports®**.
Impact Factor announced 2015: **0.871; 5-year Impact Factor**: **1.009**.
Articles appearing in the **Journal** are also abstracted by: **Scopus, Chemical Abstracts Plus (CAplus℠), Directory of Open Access Journals, Referativnii Zhurnal (VINITI), Analytical Abstracts** and **MINABS Online.**

Publisher: **Serbian Chemical Society**, Karnegijeva 4/III, P. O. Box 36, 1120 Belgrade 35, Serbia
tel./fax: ++381–11–3370–467, E-mails: **Society** – shd@shd.org.rs; **Journal** – jscs@shd.org.rs
Home Pages: **Society** – http://www.shd.org.rs/, **Journal** – http://www.shd.org.rs/JSCS/

Internet Service: Contents, Abstracts and full papers (from Vol 64, No. 1, 1999) are available in the electronic form at the Web Site of the **Journal** (http://www.shd.org.rs/JSCS/).

Former Editors: **Nikola A. Pušin** (1930–1947), **Aleksandar M. Leko** (1948–1954), **Panta S. Tutundžić** (1955–1961), **Miloš K. Mladenović** (1962–1964), **Đorde M. Dimitrijević** (1965–1969), **Aleksandar R. Despić** (1969–1975), **Slobodan V. Ribnikar** (1975–1985), **Dragutin M. Dražić** (1986–2006).

Editor-in-Chief: BRANISLAV Ž. **NIKOLIĆ**, Serbian Chemical Society (E-mail: jscs-ed@shd.org.rs)

Deputy Editor: DUŠAN **SLADIĆ**, Faculty of Chemistry, University of Belgrade

Sub editors:

Organic Chemistry DEJAN **OPSENICA**, Institute of Chemistry, Technology and Metallurgy, University of Belgrade
JÁNOS **CSANÁDI**, Faculty of Science, University of Novi Sad

Biochemistry and Biotechnology OLGICA **NEDIĆ**, INEP – Institute for the Application of Nuclear Energy, University of Belgrade

Inorganic Chemistry MILOŠ **ĐURAN**, Faculty of Science, University of Kragujevac

Theoretical Chemistry IVAN **JURANIĆ**, Serbian Chemical Society

Physical Chemistry LJILJANA **DAMJANOVIĆ**, Faculty of Physical Chemistry, University of Belgrade

Electrochemistry SNEŽANA **GOJKOVIĆ**, Faculty of Technology and Metallurgy, University of Belgrade

Analytical Chemistry SLAVICA **RAŽIĆ**, Faculty of Pharmacy, University of Belgrade

Polymers JASNA **ĐONLAGIĆ**, Faculty of Technology and Metallurgy, University of Belgrade

Thermodynamics MIRJANA **KIJEVČANIN**, Faculty of Technology and Metallurgy, University of Belgrade

Chemical Engineering MENKA **PETKOVSKA**, Faculty of Technology and Metallurgy, University of Belgrade

Materials RADA **PETROVIĆ**, Faculty of Technology and Metallurgy, University of Belgrade

Metallic Materials and Metallurgy NENAD **RADOVIĆ**, Faculty of Technology and Metallurgy, University of Belgrade

Environmental and Geochemistry BOJAN **RADAK**, Vinča Institute of Nuclear Science, University of Belgrade

History of and Education in Chemistry DRAGICA **TRIVIĆ**, Faculty of Chemistry, University of Belgrade

English Language Editor: LYNNE **KATSIKAS**, Faculty of Technology and Metallurgy, University of Belgrade

Technical Editors: VLADIMIR **PANIĆ**, ALEKSANDAR **DEKANSKI**, Institute of Chemistry, Technology and Metallurgy, University of Belgrade

Journal Manager & Web Master: ALEKSANDAR **DEKANSKI,** Institute of Chemistry, Technology and Metallurgy, University of Belgrade

Office: VERA **ĆUŠIĆ**, Serbian Chemical Society, Karnegijeva 4/III, P. O. Box 36, 1120 Belgrade 35, Serbia (E-mail: jscs-info@shd.org.rs)

Subscription: The annual subscription rate is **150.00 €** including postage (surface mail) and handling. For Society members from abroad rate is **50.00 €**. For the proforma invoice with the instruction for bank payment contact the Society Office (E-mail: shd@shd.org.rs) or see JSCS Web Site: http://www.shd.org.rs/JSCS/, option Subscription.

Godišnja pretplata: Za članove SHD: **2.500,00 RSD**, za penzionere i studente: **1000,00 RSD**, a za ostale: **3.500,00 RSD**:za organizacije i ustanove: **16.000,00 RSD**. Uplate se vrše na tekući račun Društva: **205-13815-62**, poziv na broj **320**, sa naznakom "pretplata za JSCS".

Nota: Radovi čiji su svi autori članovi SHD prioritetno se publikuju.

Odlukom Odbora za hemiju Republičkog fonda za nauku Srbije, br. 66788/1 od 22.11.1990. godine, koja je kasnije potvrđena odlukom Saveta Fonda, časopis je uvršten u kategoriju međunarodnih časopisa (**M-23**). Takođe, aktom Ministarstva za nauku i tehnologiju Republike Srbije, 413-00-247/2000-01 od 15.06.2000. godine, ovaj časopis je proglašen za publikaciju od posebnog interesa za nauku. **Impact Factor** časopisa objavljen 2015. godine iznosi **0,871**, a petogodišnji **Impact Factor 1,009**.

INSTRUCTIONS FOR AUTHORS (2013)

GENERAL

The ***Journal of the Serbian Chemical Society*** is an international journal publishing papers from all fields of chemistry and related disciplines. Twelve issues are published annually. The Editorial Board expects the editors, reviewers and authors to respect the well-known standard of professional ethics.

Types of Contributions

Original scientific papers	(about 10 typewritten pages) report original research which must not have been previously published.
Short communications	(about 5 pages) report unpublished preliminary results of sufficient importance to merit rapid publication.
Notes	(about 3 pages) report unpublished results of short, but complete, original research.
Authors' reviews	(about 30 pages) present an overview of the author's current research with comparison to data of other scientists working in the field.
Reviews	(about 30 pages) present a concise and critical survey of a specific research area.
Surveys	(about 15 pages) communicate a short reviews of a specific research area.
Book and Web site reviews	(1–2 pages)
Extended abstracts	(about 3 pages) of Lectures given at meetings of the Serbian Chemical Society Divisions.

Generally, Authors' reviews, Reviews and Surveys are prepared at the invitation of the Editor.

Submission of manuscripts

Manuscripts should be submitted using the **OnLine Submission Form**, available on the JSCS Web Site (www.shd.org.rs/JSCS/Form/). The manuscript must be uploaded as a Word.doc or .rtf file (tables and figures should follow the text, each on a separate page). Illustrations in TIF or EPS format (JPG format is acceptable for colour and greyscale photos, only), must be additionally uploaded as a separate archived (.zip, .rar or .arj) file. Figures and/or Schemes should be prepared according to the **Artwork Instructions**.

Manuscripts must be accompanied by a cover letter in which the type of the submitted manuscript and a warranty as given below are given. The Author warranties that the manuscript submitted to the *Journal* for review is original, has been written by the stated authors and has not been published elsewhere; is currently not being considered for publication by any other journal and will not be submitted for such a review while under review by the *Journal*; the manuscript contains no libellous or other unlawful statements and does not contain any materials that violate any personal or proprietary rights of any other person or entity. All manuscripts will be acknowledged on receipt (by e-mail) and given a reference number, which should be quoted in all subsequent correspondence. A password for "Article Tracking" (www.shd.org.rs/JSCS/) will also be supplied.

A MANUSCRIPT NOT PREPARED ACCORDING TO THESE INTRUCTIONS WILL BE RETURNED FOR RESUBMITION WITHOUT BEING ASSIGNED A REFERENCE NUMBER.

Conflict-of-Interest Statement*: Public trust in the peer review process and the credibility of published articles depend in part on how well conflict of interest is handled during writing, peer review, and editorial decision making. Conflict of interest exists when an author (or the author's institution), reviewer, or editor has financial or personal relationships that inappropriately influence (bias) his or her actions (such relationships are also known as dual commitments, competing interests, or competing loyalties). These relationships vary from those with negligible potential to those with great potential to influence judgment, and not all relationships represent true conflict of interest. The potential for conflict of interest can exist whether or not an individual believes that the relationship affects his or her scientific judgment. Financial relationships (such as employment, consultancies, stock ownership, honoraria, paid expert testimony) are the most easily identifiable conflicts of interest and the most likely to undermine the credibility of the journal, the authors, and of science itself. However, conflicts can occur for other reasons, such as personal relationships, academic competition, and intellectual passion.

Informed Consent Statement*: Patients have a right to privacy that should not be infringed without informed consent. Identifying information, including patients' names, initials, or hospital numbers, should not be published in written descriptions, photographs, and pedigrees unless the information is essential for scientific purposes and the patient (or parent or guardian) gives written informed consent for publication. Informed consent for this purpose requires that a patient who is identifiable be shown the manuscript to be published. Authors should identify Individuals who provide writing assistance and disclose the funding source for this assistance. Identifying details should be omitted if they are not essential. Complete anonymity is difficult to achieve, however, and informed consent should be obtained if there is any doubt. For example, masking the eye region in photographs of patients is inadequate protection of anonymity. If identifying characteristics are altered to protect anonymity, such as in genetic pedigrees, authors should provide assurance that alterations do not distort scientific meaning and editors should so note. The requirement for informed consent should be included in the journal's instructions for authors. When informed consent has been obtained it should be indicated in the published article.

Human and Animal Rights Statement*: When reporting experiments on human subjects, authors should indicate whether the procedures followed were in accordance with the ethical standards of the responsible committee on human experimentation (institutional and national) and with the Helsinki Declaration of 1975, as revised in 2000 (5). If doubt exists whether the research was conducted in accordance with the Helsinki Declaration, the authors must explain the rationale for their approach, and demonstrate that the institutional review body explicitly approved the doubtful aspects of the study. When reporting experiments on animals, authors should be asked to indicate whether the institutional and national guide for the care and use of laboratory animals was followed.

For detailed instructions please visit the JSCS website:
http://www.shd.org.rs/JSCS/JSCS-instruction.HTM

---

* **International Committee of Medical Journal Editors ("Uniform Requirements for Manuscripts Submitted to Biomedical Journals") -- February 2006**

PROCEDURE

All contributions will be peer reviewed and only those deemed worthy will be accepted for publication. The Editor has the final decision. To facilitate the reviewing process, authors are encouraged to suggest up to three persons competent to review their manuscript. Such suggestions will be taken into consideration but not always accepted.

Manuscripts requiring revision should be returned according to the requirement of the Editor, within 60 days or the manuscript will be considered as having been withdrawn. Later, the manuscript would have to be resubmitted.

The *Journal* maintains its policy and takes the liberty of correcting the English of manuscripts scientifically accepted for publication.

When a manuscript is ready for printing, the corresponding author will receive a PDF-formatted manuscript for proof reading, which should be returned to the *Journal* within 2 days. Failure to do so will be taken as the authors are in agreement with any alteration which may have occurred during the preparation of the manuscript.

Accepted manuscripts of active members of the Serbian Chemical Society (all authors) have publishing priority.

The corresponding author will receive by e-mail a PDF-formatted version of the paper as published in the journal.

MANUSCRIPT PRESENTATION

Manuscripts should be typed in English (either standard British or American English, but consistent throughout) with 1.5 spacing (12 points Times New Roman; Greek letters in the character font Symbol) in A4 format leaving 2.5 cm for margins. For Regional specific, non-standard save documents with Embed fonts Word option: *Save as -> (Tools) -> Save Options… -> Embed fonts in the text.*

The authors are requested to seek the assistance of competent English language expert, if necessary, to ensure their English is of a reasonable standard. The Serbian Chemical Society can provide this service in advance of submission of the manuscript. If this service is required, please contact the office of the Society by e-mail (jscs-info@shd.org.rs).

Tables and figures and/or schemes should not be embedded in the manuscript but their position in the text indicated. In electronic version (Word.doc document) tables and figures and/or schemes should follow the text, each on a separate page. Please number all pages of the manuscript including separate lists of references, tables and figures and their captions.

IUPAC recommendations for the naming of compounds should be followed. SI units, or other permissible units, should be employed. The designation of physical quantities must be in italic throughout the text (including figures, tables and equations), whereas the units are in upright letters. They should be in Times New Roman font. In graphs and tables, a slash should be used to separate the designation of a physical quantity from the unit (example: p / kPa, t /°C, T / K, τ / h…). Designations such as: p (kPa), t [min]…, are not acceptable. However, if the full name of a physical quantity is unavoidable, it should be given in upright letters and separated from the unit by a comma (example: Pressure, kPa, Temperature, K…). Please do not use the axes of graphs for additional explanations; these should be mentioned in the figure captions and/or the manuscript (example: "pressure at the inlet of the system, kPa" should be avoided). The axis name should follow the direction of the axis (the name of *y*–axis should be rotated by 90°). Top and right axes should be avoided in diagrams, unless they are absolutely necessary.

Latin words, as well as the names of species, should be in *italic*, as for example: *i.e.*, *e.g.*, *in vivo*, *ibid*, *Calendula officinalis* L., *etc*. The branching of organic compound should also be indicated in *italic*, for example, *n*-butanol, *tert*-butanol, *etc*.

Decimal numbers must have decimal points and not commas in the text (except in the Serbian abstract), tables and axis labels in graphical presentations of results.

Title page.

Title in bold letters, should be clear and concise, preferably 12 words or less. The use of non-standard abbreviations, symbols and formulae is discouraged.

AUTHORS' NAMES in capital letters with the full first name, initials of further names separated by a space and surname. Commas should separate the author's names except for the last two names when 'and' is to be used. In multi-affiliation manuscripts, the author's affiliation should be indicated by an Arabic number placed in superscript after the name and before the affiliation. Use * to denote the corresponding author(s).

Affiliations should be written in italic. The e-mail address of the corresponding author should be given after the affiliation(s).

Abstract: A one-paragraph abstract written of 150–200 words in an impersonal form indicating the aims of the work, the main results and conclusions should be given and clearly set off from the text. Domestic authors should also submit, on a separate page, an Abstract – Izvod, the author's name(s) and affiliation(s) in Serbian (Latin letters). For authors outside Serbia, the Editorial Board will provide a Serbian translation of their English abstract.

Keywords: Up to 6 keywords should be given. Do not use words appearing in the manuscript title

RUNNING TITLE: A one line (maximum five words) short title in capital letters should be provided.

Main text.

The main text should have the form: INTRODUCTION, EXPERIMENTAL (RESULTS AND DISCUSSION), RESULTS AND DISCUSSION (EXPERIMENTAL), CONCLUSIONS, NOMENCLATURE (optional), *Acknowledgements*: If any, REFERENCES (Citation of recent papers published in chemistry journals that highlight the significance of work to the general readership is encouraged.)

The sections should be arranged in a sequence generally accepted for publication in the respective fields. They subtitles should be in capital letters, centred and NOT numbered.

The INTRODUCTION should include the aim of the research and a concise description of background information and related studies directly connected to the paper.

The EXPERIMENTAL section should give the purity and source of all employed materials, as well as details of the instruments used. The employed methods should be described in sufficient detail to enable experienced persons to repeat them. Standard procedures should be referenced and only modifications described in detail. On no account should results be included in the experimental section.

The RESULTS AND DISCUSSION should include concisely presented results and there significance discussed and compared to relevant literature data. The results and discussion may be combined or kept separate.

The inclusion of a CONCLUSION section, which briefly summarizes the principal conclusions, is highly recommended. NOMENCLATURE is optional but, if the authors wish, a list of employed symbols may be included.

REFERENCES should be numbered sequentially as they appear in the text. When cited in the text, the reference number should be superscripted in Font 12, following any punctuation mark. In the reference list, they should be in normal position followed by a full stop. Reference entry must not be formatted using Carriage returns (enter key; ↵ key) or multiple space key. The formatting of references to published work should follow the *Journal*'s style as follows:

Journals*:	1. A. B. Surname1, C. D. Surname2, *J. Serb. Chem. Soc.* **Vol.** (Year) first page Number
Books:	2. A. B. Surname1, C. D. Surname2, *Name of Book*, Publisher, City, Year, p. 100
Compilations:	3. A. B. Surname1, C. D. Surname2, in: *Name of Compilation*, A. B. Editor1, C. D. Editor2, Ed(s)., Publisher, City, Year, p. 100
Proceedings:	4. A. B. Surname1, C. D. Surname2, , in: *Proceeding of Name of the Conference or Symposium*, *Title of the Proceeding*, (Year of publishing), Place of the Conference, Country, Year, p. 100
Patents:	5. A. B. Inventor1, C. D. Inventor2, (Holder), Country Code and patent number (registration year)
Chemical Abstracts:	6. A. B. Surname1, C. D. Surname2, Chem. Abstr. CA 234 567a For non-readily available literature, the Chemical Abstracts reference should be given in square brackets: [C.A. 139/2003 357348t] after the reference
Standards:	7. EN ISO 250: *Name of the Standard* (Year)
Websites:	8. Title of the website, URL in full (date accessed)

* International Library Journal abbreviation is required. Please consult *e.g.* http://www.library.ubc.ca/scieng/coden.html

Only the last entry in the reference list should end with a full stop.

The names of all authors should be given in the list of references; the abbreviation *et al.* may only be used in the text. The original journal title is to be retained in the case of publications published in any language other than English (please denote the language in parenthesis after the reference). Titles of publications in non-Latin alphabets should be transliterated. Russian references are to be transliterated using the following transcriptions:

ж→zh, х→kh, ц→ts, ч→ch, ш→sh, щ→shch, ы→y, ю→yu, я→ya, э→e, й→i, ь→'.

Table Captions. A separate list of table captions, which makes the tables comprehensible without reference to the text, should be provided in numerical order on a separate page.

Tables. Tables are part of the text but must be given on separate pages. The tables should be numbered consequently in Roman numbers. Quantities should be separated from units by a slash (/). Footnotes to tables, in size 10 font, are to be indicated consequently (line-by-line) in superscript letters. Tables should be prepared with the aid of the WORD table function, without vertical lines. The minimum size of the font in the tables should be 10 pt. Table columns must not be formatted using multiple spaces. Table rows must not be formatted using Carriage returns (enter key; ↵ key). Tables should not be incorporated as graphical objects. In setting up tables, Authors should keep in mind the area of the Journal's page (12.5 cm × 19 cm) and should make tables conform to the limitations of these dimensions.

Figure and/or Scheme Captions. A separate list of figure and/or scheme captions, which makes the figures and/or schemes comprehensible without reference to the text, should be provided in numerical order on a separate page.

Figures and/or Schemes. Figures and/or Schemes (of moderate resolution) should follow the captions, each on a separate page of the manuscript. High resolution illustrations in TIF or EPS format (JPG format is acceptable for colour and greyscale photos, only) must be uploaded as a separate archived (.zip, .rar or .arj) file.

Mathematical and chemical equations must be numbered, Arabic numbers, consecutively in parenthesis at the end of the line. All equations should be embedded in the text except when they contain graphical elements (tables, figures, schemes and formulae). Complex equations (fractions, inegrals, matrix…) should be prepared with the aid of the WORD Equation editor.

Reporting analytic and spectral data: Adequate evidence to enable the identity and purity of all newly synthesized compounds should be provided. The styles for the presentation of analytical and spectral data, which should be strictly adhered to (including the order), are as follows:

Compound (**3a**). Yield: 60 %; m.p. 120 °C. Anal. Calcd. for $C_{30}H_{23}N_3O_5$: C, 71.27; H 4.58; N, 8.31. Found: C, 71.30, H, 4.54, N, 8.70. IR (KBr, cm^{-1}): 1535, 1469 (C=C– stretching of aromatic ring), 1680s (–C=O stretching of -COOH group), 3128 (–NH stretching of secondary amine). ^{1}H-NMR (200 MHz, DMSO-d_6, δ / ppm): 1.38 (3H, *t*, *J* = 7.2 Hz, $–CH_2–CH_3$), 4.15 (2H, *q*, *J* = 7.2 Hz, $–CH_2–CH_3$), 10.92 (1H, *s*, –NH, D_2O exchangeable), 7.75 (2H, *t*, *J* = 7.8 Hz, aromatic), 2.26–2.75 (2H, *m*, $–CH_2$). ^{13}C-NMR (100 MHz, $CDCl_3$, δ / ppm): 157.76 (C_1), 146.89 (C_2), 177.69 (–COO), 33.44 (–CH), 38.55 ($–CH_2$). MS (*m*/*z*, (relative abundance, %)): 252 (M+, 32.5) 225, 213, 211 (BP, 100). UV–Vis (EtOH) (λ_{max} / nm, eV or cm^{-1} (ε / L mol^{-1} cm^{-1})): 205 (2300), 243 (1800). Optical rotation values, α (589 nm, 20 °C, 10 g dm^{-3} in H_2O, 10 cm): +66.470°. Specific rotation $[\alpha]^{20}_{589}$ / deg dm^{-1} g^{-1} cm^3. Magnetic moment, $\boldsymbol{\mu}_{eff}$ / μ_B: 3.1.

Deposition of crystallographic data

Prior to submission, the crystallographic data included in a manuscript presenting such data should be deposited at the appropriate database. Crystallographic data associated with organic and metal-organic structures should be deposited at the Cambridge Crystallographic Data Centre (CCDC) by e-mail to deposit@ccdc.cam.ac.uk

Crystallographic data associated with inorganic structures should be deposited with the Fachinformationszentrum Karlsruhe (FIZ) by e-mail to crysdata@fiz-karlsruhe.de. A deposition number will then be provided, which should be added to the reference section of the manuscript.

ARTWORK INSTRUCTIONS

JSCS accepts only **TIFF** or **EPS** formats, as well as **JPEG** format (only for colour and greyscale photographs) for electronic artwork and graphic files. **MS files** (Word, PowerPoint, Excel, Visio) **NOT acceptable**. Generally, scanned instrument data sheets should be avoided. Authors are responsible for the quality of their submitted artwork. Every single Figure or Scheme, as well as any part of the Figure (A, B, C…) should be prepared according to following instructions (every part of the figure, A, B, C…, must be submitted as an independent single graphic file).

TIFF - Virtually all common artwork and graphic creation software is capable of saving files in TIFF format. This "option" can normally be found under the "Save As..." or "Export..." commands in the "File" menu. TIFF (Tagged Image File Format) is the recommended file format for bitmap, greyscale and colour images. Colour images should be in the RGB mode. When supplying TIFF files, please ensure that the files are supplied at the correct resolution: Line artwork: minimum of 1000 dpi, RGB image: minimum of 300 dpi, Greyscale image: minimum of 300 dpi, Combination artwork (line/greyscale/RGB): minimum of 500 dpi, Images should be tightly cropped.

If applicable, please re-label artwork with a font supported by JSCS (Arial, Helvetica, Times, Symbol) and ensure it is of an appropriate font size. Save an image in TIFF format with LZW compression applied. It is recommended to remove Alpha channels before submitting TIFF files. It is recommended to flatten layers before submitting TIFF files.

EPS - Virtually all common artwork creation software, such as Canvas, ChemDraw, CorelDraw, SigmaPlot, Origin Lab…, are capable of saving files in EPS format. This "option" can normally be found under the "Save As..." or "Export..." commands in the "File" menu. For vector graphics, EPS (Encapsulated PostScript) files are the preferred format as long as they are provided in accordance with the following conditions: when they contain bitmap images, the bitmaps should be of good resolution (see instructions for TIFF files).

JPEG - (Joint Photographic Experts Group) is the acceptable file format only for colour and greyscale photographs. JPEG can be created with respect to photo quality (low, medium, high; from 1 to 10), ensuring file sizes are kept to a minimum to aid easy file transfer. Images should have a minimum resolution of 300 dpi. Image width: minimum 8.0 cm; maximum 12.0 cm.

When colour is involved, it should be encoded as RGB. An 8-bit preview/header at a resolution of 72 dpi should always be included. Embed fonts should be always included and only the following fonts should be used in artwork: Arial, Helvetica, Times, Symbol. The vertical space between the parts of an illustration should be limited to the bare necessity for visual clarity. No data should be present outside the actual illustration area. Line weights should range from 1 pt to 2 pt. When using layers, they should be reduced to one layer before saving the image (Flatten Artwork).

Sizing of artwork

JSCS aspires to have a uniform look for all artwork contained in a single article. Hence, it is important to be aware of the style of the journal. Figures should be submitted in black and white or, if required, colour (charged). If coloured figures or photographs are required, this must be stated in the cover letter and arrangements made for payment through the office of the Serbian Chemical Society. As a general rule, the lettering on an artwork should have a finished, printed size of 11 pt for normal text and no smaller than 7 pt for subscript and superscript characters. Smaller lettering will yield a text that is barely legible. This is a rule-of-thumb rather than a strict rule. There are instances where other factors in the artwork, (for example, tints and shadings) dictate a finished size of perhaps 10 pt. Lines should be of at least 1 pt thickness. When deciding on the size of a line art graphic, in addition to the lettering, there are several other factors to address. These all have a bearing on the reproducibility/readability of the final artwork. Tints and shadings have to be printable at the finished size. All relevant detail in the illustration, the graph symbols (squares, triangles, circles, *etc*.) and a key to the diagram (to explain the explanation of the graph symbols used) must be discernible. The sizing of halftones (photographs, micrographs,...) normally causes more problems than line art. It is sometimes difficult to know what an author is trying to emphasize on a photograph, so you can help us by identifying the important parts of the image, perhaps by highlighting the relevant areas on a photocopy. The best advice that can be given to graphics suppliers is not to over-reduce halftones. Attention should also be paid to magnification factors or scale bars on the artwork and they should be compared with the details inside. If a set of artwork contains more than one halftone, again please ensure that there is consistency in size between similar diagrams.

THE GRAPHS AND ARTWORK SHOULD BE **10 cm** WIDE AT LEAST.

Journal of the Serbian Chemical Society
JSCS-info@shd.org.rs • www.shd.org.rs/JSCS

J. Serb. Chem. Soc. Vol. 80, No. 12 (2015)

CONTENTS

Organic Chemistry

L. I. Socea, G. Saramet, C. Draghici, B. Socea, V. D. Constantin and *M. A. Radu-Popescu*: Synthesis of new derivatives of hydrazinecarbothioamides and 1,2,4-triazoles, and an evaluation of their antimicrobial activities 1461

V. Alagarsamy, V. Raja Solomon, G. Krishnamoorthy, M. T. Sulthana and *B. Narendar*: Syntheses and antimicrobial activities of 1-(3-benzyl-4-oxo-3,4-dihydroquinazolin--2-yl)-4-(substituted) thiosemicarbazide derivatives..... 1471

V. Dobričić, B. M. Francuski, V. Jaćević, M. V. Rodić, S. Vladimirov, O. Čudina and *Dj. Francuski*: Synthesis, crystal structure and local anti-inflammatory activity of the L-phenylalanine methyl ester derivative of dexamethasone-derived cortienic acid (Short communication) 1481

Inorganic Chemistry

W. Śmiszek-Lindert, A. Michta, A. Tyl, G. Małecki, E. Chełmecka and *S. Maślanka*: X-Ray, Hirshfeld surface analysis, spectroscopic and DFT studies of polycyclic aromatic hydrocarbons: fluoranthene and acenaphthene..... 1489

Physical Chemistry

M. Momčilović, J. Ciganović, D. Ranković, U. Jovanović, M. Stoiljković, J. Savović and *M. Trtica*: Analytical capability of the plasma induced by IR TEA CO_2 laser pulses on copper-based alloys..... 1505

Electrochemistry

S. M. Miulović, V. M. Nikolić, P. Z. Laušević, D. D. Aćimović, G. S. Tasić and *M. P. Marčeta Kaninski*: Electrochemistry of cobalt ethylenediamine complexes at high pH.... 1515

Materials

T. B. Novaković, Lj. S. Rožić, S. P. Petrović, Z. M. Vuković and *M. N. Mitrić*: Study of the effect of Mg(II) addition and the annealing conditions on the structure of mesoporous aluminum oxide using Plackett–Burman design 1529

I. Dimić, I. Cvijović-Alagić, N. Obradović, J. Petrović, S. Putić, M. Rakin and *B. Bugarski*: *In vitro* biocompatibility assessment of Co–Cr–Mo dental cast alloy 1541

Environmental

S. Li, S.-C. Yang, Y. Pan and *J.-H. Zhang*: Preparation of aluminum–ferric–magnesium polysilicate and its application on oily sludge..... 1553

History of and Education in Chemistry

J. N. Korolija, S. Rajić, M. Tošić and *Lj. M. Mandić*: "It happened, what's the problem?" and "A guide through the problem" – A model for consideration of ecological issues in chemistry education..... 1567

Contents of Volume 80 1581

Author index 1593

Subject index (electronic version only at www.shd.org.rs)..... (9 pages)

2015 List of Referees (electronic version only at www.shd.org.rs) ..... (8 pages)

Published by the Serbian Chemical Society
Karnegijeva 4/III, P.O. Box 36, 11120 Belgrade, Serbia
Printed by the Faculty of Technology and Metallurgy
Karnegijeva 4, P.O. Box 35-03, 11120 Belgrade, Serbia

Journal of the Serbian Chemical Society
JSCS-info@shd.org.rs • www.shd.org.rs/JSCS
J. Serb. Chem. Soc. 80 (12) 1461–1470 (2015)
JSCS–4811
UDC 547.298.4'264–304.3+547.78'367+542.913:615.28–188
Original scientific paper

Synthesis of new derivatives of hydrazinecarbothioamides and 1,2,4-triazoles, and an evaluation of their antimicrobial activities

LAURA I. SOCEA[1]*, GABRIEL SARAMET[2], CONSTANTIN DRAGHICI[3], BOGDAN SOCEA[4], VLAD D. CONSTANTIN[4] and MANUELA A. RADU-POPESCU[5]

[1]Organic Chemistry Department, Faculty of Pharmacy, "Carol Davila" University of Medicine and Pharmacy, 6 Traian Vuia Street, 020956, Bucharest, Romania, [2]Pharmaceutical Technology Department, Faculty of Pharmacy, "Carol Davila" University of Medicine and Pharmacy, 6 Traian Vuia, 020956 Bucharest, Romania, [3]"C. D. Nenitzescu" Institute of Organic Chemistry, Romanian Academy, 202B Splaiul Independentei, 060023 Bucharest, Romania, [4]Faculty of General Medicine, "Carol Davila" University of Medicine and Pharmacy, St. Pantelimon Emergency Hospital, 340–342, Soseaua Pantelimon Street, 021623, Bucharest, Romania and [5]General and Pharmaceutical Microbiology Department, Faculty of Pharmacy, "Carol Davila" University of Medicine and Pharmacy, 6 Traian Vuia Street, 020956, Bucharest, Romania

(Received 27 February, revised 15 May, accepted 18 May 2015)

Abstract: A new series of hydrazinecarbothioamides **6**–**9** bearing a 5*H*-dibenzo[*a*,*d*][7]annulene moiety were synthesized. Cyclization of **6**–**9** in NaOH solution produced the corresponding 4*H*-1,2,4-triazole-3-thiols **10**–**13**, which proved to be axial isomers. The thioethers **14**–**17** were prepared by alkylation of **10**–**13** with methyl iodide. All new compounds were characterized by elemental analysis, and IR, UV, ^{1}H-NMR and ^{13}C-NMR spectroscopy. An evaluation for antimicrobial activity against *Staphylococcus aureus*, *Pseudomonas aeruginosa*, *Escherichia coli*, *Bacillus subtilis*, *Salmonella enterica* subsp. *enterica* serovar Typhimurium, *Shigella flexneri* and *Candida albicans* was performed.

Keywords: acylhydrazinecarbothioamide; 1,2,4-triazole-3-thiol; dibenzo[*a*,*d*]-[7]annulene; antimicrobial activity.

INTRODUCTION

Bacterial infection remains a serious threat to human lives because of their capacity to develop resistance to existing antibiotics, which is an increasing public health problem. For this reason, obtaining new types of antibacterial agents is a very important task.

* Corresponding author. E-mail: laurasocea@gmail.com
doi: 10.2298/JSC150227039S

The tricyclic framework of 5*H*-dibenzo[*a*,*d*][7]annulene constitutes an integral part of the structure of molecules that are known to be effective for the treatment of depressive disorders.[1,2] Analogs of 5*H*-dibenzo[*a*,*d*][7]annulene, such as protriptyline and demexiptiline, are well known tricyclic antidepressants, which are used in the treatment of migraines, tension headaches, anxiety, psychosis, aggression and violent behavior. The anti-allergic drug cyproheptadine (Cyp) is known to have inhibitory activity for L-type calcium channels in addition to histamine and serotonin receptors.[3]

Recently, studies that were trying to detect other possible pharmacological actions of already known tricyclic antidepressants have received increasing interest.[4–13]

Dibenzo[*a*,*d*][7]annulene moieties are incorporated in biologically active compounds that exhibit muscarinic receptor antagonist properties and are useful in the treatment of Parkinson's disease, tardive dyskinesia and motion sickness.[4]

Dibenzo[*a*,*d*][7]annulene derivatives exhibit antidiabetic,[5] antiparasitic,[6] metalloprotease inhibitory[7] and antimicrobial activity.[8–13] Munoz-Bellido *et al.* realized an extensive study that demonstrated the intense antibacterial activities presented by some antidepressant from the group of serotonin recapture inhibitors, such as clomipramine and sertraline.[11] Similarly some psychiatric agents, such as protriptyline or cyclobenzaprine, are associated with some chemotherapy agents (sulfathiazole) that enhance the antibacterial activity of the latter and reduce the *MIC* up to 50 %.[11]

1,2,4-Triazole derivatives are known to show biological properties including antimicrobial,[14–19] anticancer,[20] anti-inflammatory,[21,22] anticonvulsant,[23] antiviral,[24,25] antitubercular,[25] hypolipidemic,[26] antioxidant activities[27,28] and others.

Several compounds containing 1,2,4-triazole rings are used in therapy. For example, fluconazole, terconazole and itraconazole are used as antimicrobial drugs, while vorozole, letrozole and anastrozole are non-steroidal drugs used for the treatment of cancer.[29] Other examples are ribavirin (antiviral agent), rizatriptan (antimigraine agent) and alprazolam (anxiolytic agent),[30] beside others.

Furthermore, a number of substituted hydrazinecarbothioamide were found to exhibit antifungal,[12,31–36] tuberculostatic,[36] cytostatic,[37] anticonvulsant,[38] antiviral[39] and antioxidant activities.[28,40]

Considering the above data, in continuation of ongoing research on biologically active compounds, the synthesis of new hydrazinecarbothioamides and 1,2,4--triazoles bearing the 5*H*-dibenzo[*a*,*d*][7]annulene moiety and their antimicrobial activities were considered.[41,42]

EXPERIMENTAL

Chemistry

All reactants and solvents of the highest purity were obtained commercially and used without further purification. Melting points were determined on a Boetius apparatus and are

uncorrected. The UV–Vis spectra were recorded on a SPECORD 40 Analytik Jena spectrometer, in methanol (2.5×10^{-5} M) in the wavelength range 200–600 nm. The IR spectra were recorded in KBr pellets using a Vertex 70 Bruker spectrometer. Elemental analyses were performed on an ECS-40-10-Costeh micro-dosimeter (and the values were within ±0.4 % of the theoretical ones). The NMR spectra were recorded on a Varian Gemini 300 BB instrument operating at 300 MHz for ^{1}H- and 75 MHz for ^{13}C-NMR, using DMSO-d_6 as solvent for the hydrazinecarbothioamides and $CDCl_3$ for the 1,2,4-triazole compounds. Chemical shifts (δ in ppm) were assigned according to the internal standard signal of tetramethylsilane in DMSO-d_6 (δ = 0 ppm). Coupling constants, J, are expressed in Hz.

Analytical and spectral data of the synthesized compounds are given in the Supplementary material to this paper.

General procedure for the preparation of N-*substituted 2-(5*H-*dibenzo[*a,d*][7]annulen-5-ylacetyl)-hydrazinecarbothioamides (**6**–**9**)*

A mixture of 2-(5*H*-dibenzo[*a*,*d*][7]annulen-5-yl)acetohydrazide (**1**, 4 mmol) and the required isothiocyanate **2**–**5** (4 mmol) in absolute ethanol (30–50 mL) was refluxed for 6–12 h. On cooling the reaction mixture to room temperature, a precipitate appeared. This was filtered off and recrystallized from ethanol to obtain the desired compound.

*General procedure for the preparation of 4-substituted 5-(5*H-*dibenzo[*a,d*][7]annulen-5-ylmethyl)-4*H-*1,2,4-triazole-3-thiols (**10**–**13**)*

A solution of the required hydrazinecarbothioamide (**6**–**9**, 1 mmol) in 8 mL of 8 % NaOH solution was refluxed for 3–9 h and then filtered. After cooling, the filtrate was neutralized with acetic acid. The obtained white precipitate was filtered and recrystallized from $CHCl_3$:petroleum ether (1:2, *V*:*V*, boiling range: 60–80 °C).

*General procedure for the preparation of 4-substituted 3-(5*H-*dibenzo[*a,d*][7]annulen-5-ylmethyl)-5-(methylsulfanyl)-4*H-*1,2,4-triazoles (**14**–**17**)*

To a solution of sodium ethoxide (1mmol of sodium in 10 mL of absolute ethanol) was added the required triazole **10**–**13** (1 mmol). The reaction mixture was stirred at room temperature until a solution was obtained. To this solution, methyl iodide (1 mmol) was added and stirring continued for 10 h. The reaction mixture was poured into ice water and the precipitate was filtered off, washed with water and recrystallized from ethanol.

Antimicrobial activity

The antibacterial and antifungal activities of the compounds were investigated by the broth microdilution method, in 96 flat-bottomed wells microplates (Nunc, Denmark). Dimethyl sulfoxide was used as the solvent for the preparation of stock solutions of the compounds, to obtain a concentration of 2048 μg mL^{-1}. The antimicrobial actions of the newly-synthesized compounds were tested against 6 reference bacterial strains, *i.e*., *Staphylococcus aureus* ATCC 25923, *Pseudomonas aeruginosa* ATCC 27853, *Escherichia coli* ATCC 25922, *Bacillus subtilis* ATCC 6633, *Salmonella enterica* subsp. *enterica* serovar Typhimurium ATCC 14028, *Shigella flexneri* ATCC 12022, and one reference yeast strain, *i.e*., *Candida albicans* ATCC 90028. Gentamicin was used as a positive control for *S. aureus*, *P. aeruginosa* and *E. coli*, and fluconazole for *C. albicans*. Bacterial susceptibility testing was performed according to the guidelines of the Clinical and Laboratory Standards Institute (CLSI) M100-S16 and European Committee on Antimicrobial Susceptibility Testing (EUCAST).[43,44]

All 96 wells of the microplate were filled in with 100 μL of Müller–Hinton broth (cation-adjusted) when testing compounds against bacteria and Sabouraud broth when testing against

the yeast. Series of two-fold dilutions of the newly-obtained compounds were performed in Műller–Hinton or Sabouraud broth. In the case of the reference bacterial strains, the inoculum was prepared by suspending 5 distinct colonies from a 24 h culture obtained on Columbia Blood Agar (BioMérieux, France), in a tube with Brain Heart Infusion broth (BHI broth). After vortex mixing and adjusting the density to the turbidity of the 0.5 McFarland standard, the bacterial suspension was diluted 1:100 in BHI broth, in order to obtain the working inoculum. Afterwards, each well of the microdilution plates containing 100 µL of Müller––Hinton broth with compound was inoculated within 15 min with 100 µL of the bacterial inoculum, including the growth control wells, but not the sterility control wells that were filled with 200 µL of compound-free Müller–Hinton broth.

In the case of the reference yeast strains, the inoculum was prepared by suspending 5 distinct colonies from a 24 h culture obtained on Sabouraud dextrose agar, in a tube with 5 mL of sterile distilled water. After vortex mixing and adjusting the density to the turbidity of the 0.5 McFarland standard, the fungal suspension was diluted in sterile distilled water in order to obtain a working inoculum. Each well of the microdilution plates containing 100 µL of Sabouraud broth with compound was inoculated with 100 µl yeast inoculum within 15 min, including the growth control wells, but not the sterility control wells, which were filled only with 200 µL compound-free Sabouraud broth. After performing the inoculum controls from the growth control wells, the microplates were incubated at 37 °C for 24 h.[48-50]

The lowest concentration of each compound able to inhibit visible microbial growth was considered the minimum inhibitory concentration (*MIC*) value.

RESULTS AND DISCUSSION

Chemistry

The reaction sequences employed for the syntheses of the title compounds are shown in Scheme 1. In the present work, *N*-aryl-2-(5*H*-dibenzo[*a*,*d*][7]-annulen-5-ylacetyl)hydrazinecarbothioamides **6**–**9** were synthesized by nucleophilic addition of 2-(5*H*-dibenzo[*a*,*d*][7]annulen-5-yl)acetohydrazide (**1**) to the aryl isothiocyanates **2**–**5**, in absolute ethanol under reflux. 2-(5*H*-Dibenzo[*a*,*d*]-[7]annulen-5-yl)acetohydrazide (**1**) was prepared starting from dibenzosuberenone, according to a literature method.[42,43,46]

Synthesis of the new 4-alkyl/aryl-5-(5*H*-dibenzo[*a*,*d*][7]annulen-5-yl-methyl)-4*H*-1,2,4-triazole-3-thiols **10**–**13** (that exist in equilibrium with their thione tautomer) consisted in intramolecular cyclization of acylhydrazine-carbothioamides **6**–**9** in 8 % sodium hydroxide solution under reflux.[41,46,47]

The treatment of 1,2,4-triazoles **10**–**13** with methyl iodide in basic media yielded the 4-substituted 3-(5*H*-dibenzo[*a*,*d*][7]annulen-5-ylmethyl)-5-(methylsulfanyl)-4*H*-1,2,4-triazoles **14**–**17** and not the *N*-methylated derivatives.

Analytical and spectral data of the newly synthesized compounds

All the synthesized compounds were analyzed by IR, UV–Vis, ^{1}H-NMR and ^{13}C-NMR spectroscopy. The analytical and spectral data of the new compounds are given in the Supplementary material to this paper.

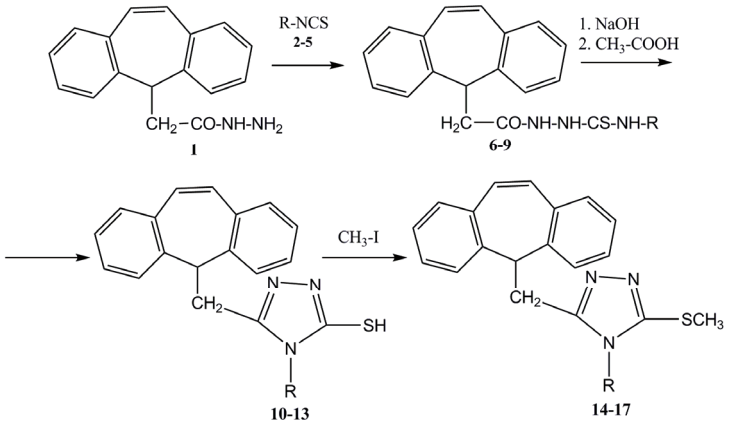

R= p-C_6H_4-Cl : 2, 6, 10, 14
R= p-C_6H_4-Br : 3, 7, 11, 15
R= p-C_6H_4-I : 4, 8, 12, 16
R= -CH_2-CH_2-C_6H_5 : 5, 9, 13, 17

Scheme 1. Synthetic route to the title compounds.

Infrared spectra of new hydrazinecarbothioamides **6**–**9** showed a new band at 1249–1258 cm^{-1} due to the stretching vibration of the C=S groups. This fact confirmed the addition of the 2-(5*H*-dibenzo[*a*,*d*][7]annulen-5-yl)acetohydrazides to different isothiocyanates. The C=O and N–H stretching bands were present at 1673–1699 and 3141–3359 cm^{-1}, respectively.

The hydrazinecarbothioamides **6**–**9** were present as two conformational isomers, 5′-axial and 5′-equatorial in about 3:1 ratio, interconvertible by inversion of the middle ring, which was confirmed by their ^{1}H-NMR spectra.[42] In **6**–**9**-axial isomers, the H-5′(eq) is deshielded, manifested as a triplet at 4.62–4.65 ppm (*J* in range 7.0–7.3 Hz), whereas the CH_2-12′ protons are shielded by the double bond, showing a doublet at 2.57–2.60 ppm (Scheme S-1 of the Supplementary material to this paper). Double bonds shield H-5′ axial, while aromatic rings deshield H-5′ equatorial, because of the current cycle. The H-5′(eq) appeared at δ = 4.62–4.65 ppm (triplet) and H-5′(ax) appeared at δ 3.74–3.76 ppm (triplet).[42]

The signals of NH protons appeared as singlets between 9.53–10.12 ppm and the double bond protons H-10′ and H-11′ appeared as a singlet at 7.02–7.03 ppm.

The ^{13}C-NMR spectrum of compounds **6**–**9** showed a narrow δ domain (123–140 ppm) with C-10′ and C-11′ easily recognizable at δ 130–131 ppm, corresponding to the dibenzo[*a*,*d*][7]annulene moiety. C=S carbon atom could be responsible for the appearance of a signal at $\delta \approx 181$ ppm.

Cyclization of **6**–**9** to **10**–**13** was proved by the IR spectra that showed the disappearance of the $\nu_{C=O}$ band. It appears that in KBr pellets, the 1,2,4-triazole-3-thiols **10**–**13** exist in their thionic tautomeric form.[41]

The presence of a single conformational isomer (the axial one) of the triazoles **10**–**13** was confirmed by their ^{1}H-NMR spectra. Cyclization of **6**–**9** to **10**––**13** and the subsequent reactions produced the loss of the minor equatorial isomer, probably due to an increased solubility in acidic water. H-5′(eq) appears at δ 4.35–4.45 ppm (triplet, J = 7.9 Hz) and the CH_2-12′ protons manifest as doublets at 2.67–2.93 ppm in **10**–**13**. The NH signals of **6**–**9** totally disappeared, and were replaced by singlets at δ 11.44–11.90 ppm, attributable to the SH proton. Thus, in solution, the above equilibrium was shifted towards the thiolic form.

Conversion of hydrazinecarbothioamides **6**–**9** to the triazoles **10**–**13** was also confirmed by the ^{13}C-NMR spectra. A new quaternary carbon signal (for C-3) appeared at δ 166.57–167.97 ppm (Scheme S-2 of the Supplementary material) simultaneously with the disappearance of the C=S signal of **6**–**9** (δ = 181 ppm). Furthermore, a new signal for C-5 of **10**–**13** appeared at $\delta \approx$ 155.5 ppm, instead of the C=O signal from **6**–**9** at δ 169–170 ppm.

A new band in 2929–2983 cm^{-1} region, due to presence of methyl group (ν_{CH_3}) in the IR spectra confirmed the structures of compounds **14**–**17**, obtained by alkylation of the triazoles **10**–**13** with methyl iodide. Proof of *S*-alkylation that led to the formation of compounds **14**–**17** was given by the disappearance of the C=S stretching band in the IR spectra.

The presence of new signals at 14.8 ppm corresponding to CH_3 group in the ^{13}C-NMR spectra of compounds **14**–**17** was the most significant proof of alkylation of triazoles **10**–**13** with methyl iodide. Heterocyclic carbons C-3 and C-5 from these methylated compounds resonated at 154.82–155.11 ppm (more shielded than the C-3 heterocyclic carbon from the 1,2,4-triazoles **10**–**13**) and δ 151.28––151.54 ppm, respectively.

^{1}H-NMR spectra of the 3-(methylsulfonyl)-1,2,4-triazoles indicated the presence of a single conformational isomer, the axial one, except for triazole **15**, which exists as two isomers, 5′-axial and 5′-equatorial in about 1:1 ratio.

Antimicrobial activity

The antimicrobial activities of all products were investigated *in vitro* against *S. aureus*, *P. aeruginosa*, *E. coli*, *B. subtilis*, *S. enterica* subsp. *enterica* serovar Typhimurium, *S. flexneri* and *C. albicans* by the dilution method. The *MIC* values were determined using the dilution method with dimethyl sulfoxide as solvent.

Dimethyl sulfoxide showed no antimicrobial activity against the tested strains. The *MIC* values (μg mL^{-1}) for the new compounds against the strains are presented in Table I.

The investigation of the antimicrobial activity of the compounds was performed in duplicate. As control, *S. aureus*, *E. coli* and *P. aeruginosa* were tested against gentamicin, and *C. albicans* against fluconazole by the broth micro-

dilution method.[44,45,49–51] The *MIC* value of gentamicin was 2 μg mL^{-1} for all tested strains and the *MIC* value of fluconazole was 2 μg mL^{-1} for the reference strain.

TABLE I. *In vitro* antimicrobial activity of compounds **6–17** as *MIC* values (μg mL^{-1})

Compd.	Bacterial strains						Yeast
	S. aureus	*P. aeruginosa*	*E. coli*	*B. subtilis*	*S. enterica* subsp. *enterica* serovar Typhimurium	*S. flexneri*	*C. albicans*
6	256	16	512	>1024	256	1024	>1024
7	512	256	>1024	>1024	256	256	>1024
8	>1024	1024	512	>1024	1024	512	>1024
9	512	256	512	>1024	512	512	>1024
10	512	>1024	64	128	64	512	>1024
11	256	128	512	128	>1024	1024	>1024
12	256	512	512	128	>1024	512	>1024
13	512	64	>1024	>1024	512	512	>1024
14	256	128	512	128	>1024	512	128
15	256	128	512	128	512	512	128
16	256	256	512	256	128	512	128
17	512	512	512	256	256	512	256
Gentamicin	2	2	2	–	–	–	–
Fluconazole	–	–	–	–	–	–	2

The antimicrobial screening data revealed that all the newly synthesized compounds exhibited weaker antimicrobial activities compared to those of the control drugs.

For the reference bacterial strains, the *MIC* values of the compounds ranged between: 16–1024 μg mL^{-1} for the hydrazinecarbothoamides **6**–**9**, 64–1024 μg mL^{-1} for the 1,2,4-triazole-3-thiols **10**–**13** and 128–512 μg mL^{-1} for the methylsulfamyl-1,2,4-triazoles **14**–**17**.

Hydrazinecarbothioamide **6** with a chlorine atom presented the strongest action against *P. aeruginosa* (*MIC* 16 μg mL^{-1}). 1,2,4-Triazole-3-thiol **13** with a 4-(2-phenylethyl) fragment presented the strongest action against *P. aeruginosa* (MIC 64 μg mL^{-1}).

Comparing the results of this study, it was observed: a) compounds containing 4-chlorophenyl group had moderate antibacterial activity, hydrazinecarbothioamides against *S. aureus*, *S. enterica* subsp. *enterica* serovar Typhimurium and *P. aeruginosa*, 1,2,4-triazole-3-thiol against *E. coli* and *S. enterica* subsp. *enterica* serovar Typhimurium, and methylsulfanyl-1,2,4-triazole against *P. aeruginosa*; b) hydrazinecarbothioamides containing 4-chlorophenyl or 4-bromophenyl had better action compared to derivatives containing 4-iodophenyl or 4-(2-phenylethyl); c) the presence of methylsulfanyl-1,2,4-triazole ring in the structures **14**–**17** were favorable for the activity against the bacterial strains; d)

hydrazinecarbothioamides **6**–**9** and 1,2,4-triazole-3-thiols **10**–**13** were almost inactive against *C. albicans* but methylsulfanyl-1,2,4- triazole showed moderate activity against fungus strain.

CONCLUSIONS

In this paper, the synthesis and characterization of four new acyl hydrazinecarbothioamides, four 4*H*-1,2,4-triazole-3-thiol derivatives and four methylsulfanyl-1,2,4-triazoles containing the 5*H*-dibenzo[*a*,*d*]annulene moiety were presented. The structures of new compounds were confirmed by spectral data (IR, UV, ^{1}H-NMR and ^{13}C-NMR) and elemental analysis. All the compounds were investigated for their antimicrobial activity against *S. aureus*, *P. aeruginosa*, *E. coli*, *B. subtilis*, *S. enterica* subsp. *enterica* serovar Typhimurium, *S. flexneri* and *C. albicans*.

The antibacterial screening data are given for all the tested compounds. The data indicated weak antibacterial activity, except for compound **6** (which presented good action against *P. aeruginosa*), **10** (which presented moderate action on *S. enterica* subsp. *enterica* serovar Typhimurium and *E. coli*) and **13** (which presented a moderate action on *P. aeruginosa*). Based on the *MIC* values presented by the tested compounds, it could be concluded that, in general, the derivatives containing a chlorine or bromine atom had better antibacterial activity against the tested strains.

SUPPLEMENTARY MATERIAL

Physical, analytical and spectral data for the synthesized compounds are available electronically from http://www.shd.org.rs/JSCS/, or from the corresponding author on request.

Acknowledgement. This work was supported by the University of Medicine and Pharmacy “Carol Davila” Bucharest, Project No. 28331/04.11.2013.

ИЗВОД

СИНТЕЗА НОВИХ ДЕРИВАТА ХИДРАЗИНКАРБОТИОАМИДА И 1,2,4-ТРИАЗОЛА И ЊИХОВА АНТИМИКРОБНА АКТИВНОСТ

LAURA I. SOCEA[1], GABRIEL SARAMET[2], CONSTANTIN DRAGHICI[3], BOGDAN SOCEA[4], VLAD D. CONSTANTIN[4] и MANUELA A. RADU-POPESCU[5]

[1]Organic Chemistry Department, Faculty of Pharmacy, „Carol Davila“ University of Medicine and Pharmacy, 6 Traian Vuia Street, 020956, Bucharest, Romania, [2]Pharmaceutical Technology Department, Faculty of Pharmacy, „Carol Davila“ University of Medicine and Pharmacy, 6 Traian Vuia, 020956 Bucharest, Romania, [3]“C.D. Nenitzescu” Institute of Organic Chemistry, Romanian Academy, 202B Splaiul Independentei, 060023 Bucharest, Romania, [4]Faculty of General Medicine, „Carol Davila“ University of Medicine and Pharmacy, St. Pantelimon Emergency Hospital, 340–342, Soseaua Pantelimon Street, 021623, Bucharest, Romania u [5]General and Pharmaceutical Microbiology Department, Faculty of Pharmacy, „Carol Davila“ University of Medicine and Pharmacy, 6 Traian Vuia Street, 020956, Bucharest, Romania

Синтетисана је серија деривата хидразинкарботиоамида **6**–**9** који садрже 5*H*-дибензо[*a*,*d*][7]ануленски део. Циклизација деривата **6**–**9** у раствору NaOH даје одговарајуће аксијалне изомере 4*H*-1,2,4-триазол-3-тиола **10**–**13**. Тиоетри **14**–**17** су добијени алкиловањем деривата **10**–**13** јодметаном. Сва нова једињења окарактерисана су елементалном

анализом, IR, UV, ^{1}H-NMR и ^{13}C-NMR спектроскопијом. Извршено је испитивање антимикробне активности према *Staphylococcus aureus* ATCC 25923, *Pseudomonas aeruginosa* ATCC 27853, *Escherichia coli* ATCC 25922, *Bacillus subtilis* ATCC 6633, *Salmonella enterica* subsp. *enterica* serovar Typhimurium ATCC 14028, *Shigella flexneri* ATCC 12022 и *Candida albicans* ATCC 90028.

(Примљено 27. фебруара, ревидирано 15. маја, прихваћено 18. маја 2015)

REFERENCES

1. P. E. Holtzheimer III, C. B. Nemeroff, *NeuroRx*. **3** (2006) 42
2. P. K. Gillman, *Br. J. Pharmacol*. **151** (2007) 737
3. K. G. Wu, T. H. Li, T. Y. Wang, C. L. Hsu, C. J. Chen, *Int. J. Immunopathol. Pharmacol*. **25** (2012) 231
4. M. Hibert, L. Van Hijfte, M. Richards, P. Mose (Merrell Pharmaceuticals, Inc.) US5508280 A, 1996
5. J. Inoue, Y. S. Cui, L. Rodriguez, Z. Chen, P. F. Kador, *Eur. J. Med. Chem*. **34** (1999) 399
6. A. T. Evans, S. L. Croft, *Biochem. Pharmacol*. **48** (1994) 61
7. M. Ilies, M. D. Banciu, A. Scozzafava, M. A. Ilies, M. T. Caproiu, C. T. Supuran, *Bioorg. Med. Chem.* **11** (2003) 2227
8. L. I. Socea, G. Şaramet, C. E. Dinu-Pârvu, C. Draghici, B. Socea, *Rev. Chim. (Bucharest, Rom.)* **65** (2014) 253
9. H. Cederlund, P. A. Mårdh, *J. Antimicrob. Chemother.* **32** (1993) 355
10. L. P Yunnikova, T. A Akenteva, G. A. Aleksandrova, *Pharm. Chem. J.* **46** (2013) 723
11. J. L. Munoz-Bellido, S. Munoz-Crido, J. A. Garcia Rodriguez, *Int. J. Antimicrob. Agents* **14** (2000) 177
12. R. G. Nelson, A. Rosowsky, *Antimicrob. Agents Chemother.* **45** (2001) 3293
13. A. Rosowsky, F. Hongning, G. F. Queener, *J. Heterocycl. Chem*. **37** (2000) 921
14. S. Sharad, M. Ganesh, G. Sunil, G. Charnsingh, *Bioorg. Med. Chem. Lett.* **20** (2010) 7200
15. M. Koparir, C. Orek, A. E. Parlak, A. Söylemez, P. Koparir, M. Karatepe, S. D. Dastan, *Eur. J. Med. Chem*. **63** (2013) 340
16. Y. Ruan, L. H. Jin, J. He, S. Yang, P. S. Bhadury, M. He, Z. C. Wang, B. A. Song, *Afr. J. Pharm. Pharmacol.* **5** (2011) 602
17. P. Zoumpoulakis, C. Camoutsis, G. Pairas, M. Soković, J. Glamočlija, C. Potamitis, A. Pitsas, *Bioorg. Med. Chem*. **20** (2012) 1569
18. S. Eswaran, A. V. Adhikari, N. S. Shetty, *Eur. J. Med. Chem.* **44** (2009), 4637
19. G. S. Hassan, S. M. El-Messery, F. A. M. Al-Omary, S. T. Al-Rashood, M. I. Shabayek, Y. S. Abulfadl, E. S. E. Habib, S. M. El-Hallouty, W. Fayad, K. M. Mohamed, B. S. El--Menshawi, H. I. El-Subbagh, *Eur. J. Med. Chem.* **66** (2013) 135
20. B. S. Holla, B. Veerendra, M. K. Shivanada, B. Poojary, *Eur. J. Med. Chem*. **38** (2003) 759
21. A. M. Abdel-Megeed, H. M. Abdel-Rahman, G. E. Alkaramany, M. A. El-Gendy, *Eur. J. Med. Chem*. **44** (2009) 117
22. S. G. Küçükgüzel, K. Küçükgüzel, E. Tatar, S. Rollas, F. Şahin, M. Güllüce, E. De Clercq, L. Kabasakal, *Eur. J. Med. Chem.* **42** (2007) 893
23. A. Almasirad, N. Vousooghi, S. A. Tabatabai, A. Kebriaeezadeh, A. Shafiee, *Acta Chim. Slov*. **54** (2007) 317
24. A. R. Farghaly, H. El-Kashef, *Arkivoc* (2006) 76

25. I. Küçükgüzel, E. Tatar, S. G. Küçükgüzel, S. Rollas, E. De Clercq, *Eur. J. Med. Chem*. **43** (2008) 381
26. G. A. Idrees, O. M. Aly, G. E. D. A. A. Abuo-Rahma, M. F. Radwan, *Eur. J. Med. Chem*. **44** (2009) 3973
27. W. A. Yehye, N. A. Rahman, A. A. Alhadi, H. Khaledi, S. W. Ng, A. Ariffin, *Molecules* **17** (2012) 7645
28. S. F. Barbuceanu, D. C. Ilies, G. Saramet, V. Uivarosi, C. Draghici, V. Radulescu, *Int. J. Mol. Sci.* **15** (2014) 10908
29. M. H. Morshed, M. F. Islam, M. A. Yousuf, G. M. G. Hossain, J. A. Khanam, M. A. Salam, *Dhaka Univ. J. Pharm. Sci.* **10** (2011), 43
30. S. Baytas, E. Kapc, T. Coban, H. Ozbilge, *Turk. J. Chem.* **36** (2012) 867
31. Ł. Popiołek, U. Kosikowska, M. Dobosz, A. Malm, *Phosphorus, Sulfur Silicon Relat. Elem.* **187** (2012) 468
32. M. Shukla, M. Dubey, H. Kulshrashtha, D. S. Seth, in *Chemistry of Phytopotentials: Health, Energy and Environmental Perspectives,* L. D. Khemani, M. M. Srivastava, S. Srivastava, Eds., Springer-Verlag, Berlin, 2012, p. 9
33. T. Plech, M. Wujec, A. Siwek, U. Kosikowska, A. Malm, *Eur. J. Med. Chem.* **46** (2011) 241
34. S. Shelke, G. Mhaske, S. Gadakh, C. Gill, *Bioorg. Med. Chem. Lett*. **20** (2010) 7200
35. J. Nevagi Reshma; S. Dhake Avinash, *Pharm. Chem.* **5** (2013) 45
36. D. Sriram, P. Yogeeswari, D. Y. Priya, *Biomed. Pharmacother*. **63** (2009) 36
37. K. Benci, L. Mandić, T. Suhina, M. Sedić, M. Klobučar, S. Kraljević Pavelić, K. Pavelić, K. Wittine, M. Mintas, *Molecules* **17** (2012) 11010
38. N. Siddiqui, S. Alam, W. Ahsan, *Acta Pharm.* **58** (2008) 445
39. J. B. McMahon, R. J. Gulakowski, O. S. Weislow, R. J. Schultz, V. L. Narayanan, D. J. Clanton, R. Pedemonte, F. W. Wassmundt, R. W. Buckheit Jr., W. D. Decker, *Antimicrob. Agents Chemother*. **37** (1993) 754
40. B. Šarkanj, M. Molnar, M. Čačić, L. Gille, *Food Chem.* **139** (2013) 488
41. L. I. Socea, T. V. Apostol, G. Şaramet, Ş. F. Bărbuceanu, C. Drăghici, M. Dinu, *J. Serb. Chem. Soc.* **77** (2012) 1541
42. I. Saramet, A. Banciu, L. Socea, C. Draghici, M. D. Banciu, *Heterocycl. Commun.* **9** (2003) 653
43. European Committee on Antimicrobial Susceptibility Testing. EUCAST Discussion Document E.Dis. 5.1, *Clin. Microbiol. Infect.* **9** (2003) 1
44. Clinical and Laboratory Standards Institute (CLSI), CLSI document M07-A9, approved standard, 9th ed., Wayne, PA, 2012
45. N. Nossek, *Bull. Stiintific Stud., I. P. B. Seria Chimie-Metalurgia* **I** (1977) 80
46. J. Burbiel, *Arkivoc* (2006) 16
47. L. I. Socea, I. Şaramet, B. Socea, B. Drăghici, *Rev. Chim. (Bucharest, Rom.)* **57** (2006) 1123
48. Clinical and Laboratory Standards Institute., CLSI document M27-A3, approved standard, 3rd ed., Clinical and Laboratory Standards Institute, Wayne, PA, 2008
49. Clinical and Laboratory Standards Institute. CLSI document M27-S4, approved standard, 4th Informational Supplement, Clinical and Laboratory Standards Institute, Wayne, PA, 2012
50. Subcommittee on Antifungal Susceptibility Testing (EUCAST-AFST) of the ESCMID European Committee for Antimicrobial Susceptibility Testing (EUCAST-AFST) 2008, EUCAST definitive document E Def 7.1, *Clin. Microbiol. Infect.* **14** (2008) 398.

Journal of the Serbian Chemical Society
JSCS@tmf.bg.ac.rs • www.shd.org.rs/JSCS
J. Serb. Chem. Soc. 80 (12) S370–S75 (2015) *Supplementary material*

SUPPLEMENTARY MATERIAL TO

Synthesis of new derivatives of hydrazinecarbothioamides and 1,2,4-triazoles and evaluation of their antimicrobial activity

LAURA I. SOCEA[1]*, GABRIEL SARAMET[2], CONSTANTIN DRAGHICI[3], BOGDAN SOCEA[4], VLAD D. CONSTANTIN[4] and MANUELA A. RADU-POPESCU[5]

[1]Organic Chemistry Department, Faculty of Pharmacy, "Carol Davila" University of Medicine and Pharmacy, 6 Traian Vuia Street, 020956, Bucharest, Romania, [2]Pharmaceutical Technology Department, Faculty of Pharmacy, "Carol Davila" University of Medicine and Pharmacy, 6 Traian Vuia, 020956 Bucharest, Romania, [3]"C. D. Nenitzescu" Institute of Organic Chemistry, Romanian Academy, 202B Splaiul Independentei, 060023 Bucharest, Romania, [4]Faculty of General Medicine, "Carol Davila" University of Medicine and Pharmacy, St. Pantelimon Emergency Hospital, 340–342, Soseaua Pantelimon Street, 021623, Bucharest, Romania and [5]General and Pharmaceutical Microbiology Department, Faculty of Pharmacy, "Carol Davila" University of Medicine and Pharmacy, 6 Traian Vuia Street, 020956, Bucharest, Romania

J. Serb. Chem. Soc. 80 (12) (2015) 1461–1470

PHYSICAL, ANALYTICAL AND SPECTRAL DATA FOR THE SYNTHESIZED COMPOUNDS

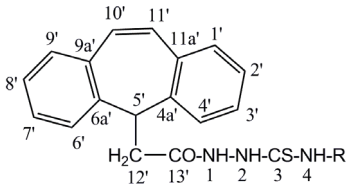

Scheme S-1. Atom numbering of the general structure for **6**–**9**.

N-*(4-Chlorophenyl)-2-(5*H-*dibenzo[*a,d*][7]annulen-5-ylacetyl)hydrazinecarbothioamide (**6**).* Yield: 78.6 %; m.p.: 172–173 °C; Anal. calcd. for $C_{24}H_{20}ClN_3OS$ (FW: 433.95): C, 66.43; H, 4.65; N, 9.68 %. Found: C, 66.40; H, 4.66; N, 9.70 %; IR (KBr, cm^{-1}): 3321, 3147 (N–H stretching), 3065, 3017 (C–H stretching of aromatic ring), 2976, 2851 (CH_2 stretching), 1682 (C=O stretching), 1605, 1595, 1522, 1492, 1253 (C=S stretching), 765 (C–Cl); ^{1}H-NMR (300 MHz, DMSO-d_6, δ / ppm): 9.80 (2H, *s*, NH), 9.68 (1H, *s*, NH), 7.50–7.20 (12H, *m*, Ar-H), 7.03 (2H, *s*, H10′, H11′), 4.66 (1H, *t*, J = 7.1 Hz, H5′) axial isomer, 3.76 (1H, *t*, J = 7.1 Hz, H5′) equatorial isomer, 2.62 (2H, *d*, J = 7.1 Hz, H12′)

* Corresponding author. E-mail: laurasocea@gmail.com

axial isomer; ^{13}C-NMR (75 MHz, DMSO-d_6, δ / ppm): 180.78 (C=S), 170.08 (C=O), 140.05 (2C_q), 139.55 (C_q), 138.87 (C_q), 137.99 (C_q), 133.76 (C_q), 131.27 (C10′, C11′) equatorial isomer, 130.98 (CH), 130.81 (C10′, C11′) axial isomer, 129.63 (CH), 129.52 (CH), 128.76 (CH), 128.51 (CH) equatorial isomer, 127.97 (CH), 127.58 (CH) equatorial isomer, 126.51 (CH), 125.51 (CH) equatorial isomer, 48.60 (C5′), 34.61 (C12′) axial isomer, 33.21 (C12′) equatorial isomer; UV–Vis (CH_3OH, 2.5×10^{-5} M, λ_{max} / nm (log (ε / L·mol^{-1}·cm^{-1}))): 206.2 (4.51), 224.7 (4.40), 279.3 (4.22).

N-*(4-Bromophenyl)-2-(5*H-*dibenzo[*a,d*][7]annulen-5-ylacetyl)hydrazinecarbothioamide (**7**)*. Yield: 83.1 %; m.p.: 197–198 °C; Anal. Calcd. for $C_{24}H_{20}BrN_3OS$ (FW: 478.40): C, 60.25; H, 4.21; N, 8.78 %. Found: C, 60.26; H, 4.22; 8.78 %; IR (KBr, cm^{-1}): 3342, 3340, 3141 (N–H stretching), 3052, 3019 (C–H stretching of aromatic ring), 2970, 2873 (CH_2 stretching), 1673 (C=O stretching), 1586, 1531, 1488, 1257 (C=S stretching), 621 (C–Br); ^{1}H-NMR (300 MHz, DMSO-d_6, δ / ppm): 9.72 (2H, *s*, NH), 9.53 (1H, *s*, NH), 7.50 (2H, *d*, *J* = = 8.6 Hz, H-bromophenyl), 7.45–7.20 (10H, *m*, Ar-H), 7.03 (2H, *s*, H10′, H11′), 4.65 (1H, *t*, *J* = 7.3 Hz, H5′) axial isomer, 3.80 (2H, *d*, *J* = 7.1 Hz, H12′) equatorial isomer, 3.75 (1H, *t*, *J* = 7.3 Hz, H5′) equatorial isomer, 2.61 (2H, *d*, *J*=7.1 Hz, H12′) axial isomer; ^{13}C-NMR (75 MHz, DMSO-d_6, δ / ppm): 180.73 (C=S), 170.03 (C=O), 140.05 (C_q), 139.55 (C_q), 138.43 (C_q), 133.74 (C_q), 131.27 (C10′, C11′) equatorial isomer, 130.89 (C10′, C11′) axial isomer, 130.87 (CH), 130.80 (CH), 129.62 (CH), 129.52 (CH), 128.51 (CH) equatorial isomer, 127.57 (CH), equatorial isomer, 126.50 (CH), 125.51 (CH) equatorial isomer, 122.55 (CH) equatorial isomer, 117.22 (C–Br), 48.57 (C5′), 34.59 (C12′) axial isomer, 33.19 (C12′) equatorial isomer; UV–Vis (CH_3OH, 2.5×10^{-5} M, λ_{max} / nm (log (ε / L·mol^{-1}·cm^{-1}))): 204.4 (4.35), 226.4 (4.20), 281.9 (4.20).

*2-(5*H-*Dibenzo[*a,d*][7]annulen-5-ylacetyl)*-N-*(4-iodophenyl)hydrazinecarbothioamide (**8**)*. Yield: 69.5 %; m.p.: 194–195 °C; Anal. Calcd. for $C_{24}H_{20}IN_3OS$ (FW: 525.40): C, 54.86; H, 3.84; N, 8.00 %. Found: C, 54.88; H, 3.84; N, 8.02 %; IR (KBr, cm^{-1}): 3339, 3304, 3141 (N–H stretching), 3051, 3015 (C–H stretching of aromatic ring), 2969, 2874 (CH_2 stretching), 1674 (C=O stretching), 1582, 1530, 1510, 1486, 1258 (C=S stretching); 516 (C–I); ^{1}H-NMR (300 MHz, DMSO-d_6, δ / ppm): 9.72 (2H, *s*, NH), 9.52 (H, *s*, NH), 7.66 (2H, *d*, *J* = 8.6 Hz, H-iodophenyl), 7.50–7.20 (10H, *m*, aromatic), 7.03 (2H, *s*, H10′, H11′), 4.65 (1H, *t*, *J* = 7.3 Hz, H5′) axial isomer, 3.75 (1H, *t*, *J* = 7.3 Hz, H5′) equatorial isomer, 2.60 (2H, *d*, *J* = 7.3 Hz, H12′); ^{13}C-NMR (75 MHz, DMSO-d_6, δ / ppm): 180.75 (C=S), 170.11 (C=O), 140.05 (C_q), 139.54 (C_q), 138.43 (C_q), 136.77 (C_q) 134.86 (C_q), 133.74 (C_q), 131.27 (C10′,C11′) equatorial isomer, 130.84 (C10′,C11′) axial isomer, 129.62 (CH), 129.52 (CH), 128.76 (CH), 128.54 (CH) equatorial isomer, 127.58 (CH) equatorial isomer, 126.50 (CH), 125.51 (CH) equatorial isomer, 122.95 (CH) equatorial isomer, 89.55

(C–I), 49.59 (C5′), 34.60 (C12′); UV–Vis (CH_3OH, 2.5×10^{-5} M, λ_{max} / nm (log (ε / L·mol^{-1}·cm^{-1}))): 207.0 (4.54), 223.8 (4.46), 283.7 (4.30).

*2-(5*H*-Dibenzo[*a,d*][7]annulen-5-ylacetyl)-*N*-(2-phenylethyl)hydrazinecarbothioamide* (***9***). Yield: 74.6 %; m.p.: 183–185 °C; Anal. Calcd. for $C_{26}H_{25}N_3OS$ (FW: 427.56): C, 73.04; H, 5.89; N, 9.83 %. Found: C, 73.04; H, 5.87; N, 9.81 %; IR (KBr, cm^{-1}): 3359, 3304, 3232 (N–H stretching), 3062, 3023 (C–H stretching of aromatic ring), 2969, 2862 (CH_2 stretching), 1699 (C=O stretching), 1562, 1542, 1493, 1249 (C=S stretching); ^{1}H-NMR (300 MHz, DMSO-d_6, δ / ppm): 10.12 (H, *s*, NH) equatorial isomer, 9.52 (H, *s*, NH) axial isomer, 9.36 (H, *s*, NH) equatorial isomer, 9.15 (H, *s*, NH) axial isomer, 7.40––7.10 (13H, *m*, Ar-H), 7.02 (2H, *s*, H10′, H11′), 4.62 (1H, *t*, *J* = 7.1 Hz, H5′) axial isomer, 3.74 (1H, *t*, *J* = 7.1 Hz, H5′) equatorial isomer, 3.53 (2H, *m*, NH–CH_2), 2.72 (2H, *t*, *J* = 8.2 Hz, C**H**$_2$–C_6H_5), 2.55 (2H, *d*, *J* = 7.1 Hz, H12′); ^{13}C-NMR (75 MHz, DMSO-d_6, δ / ppm): 181.16 (C=S), 170.03 (C=O), 140.25 (C_q) equatorial isomer, 139.85 (C_q), 139.47 (C_q), 139.10 (C_q), 133.75 (C_q), 131.25 (C10′, C11′) equatorial isomer, 130.77 (C10′, C11′) axial isomer, 129.57 (CH), 129.52 (CH), 128.76 (CH), 128.63 (CH), 127.58 (CH), 127.60 (CH), 127.42 (CH), 126.53 (CH), 126.15 (CH), 125.52 (CH) equatorial isomer, 48.73 (C5′), 45.10 (CH_2–NH), 34.84 (**C**H_2–C_6H_5), 34.43 (C12′); UV–Vis (CH_3OH, 2.5×10^{-5} M, λ_{max} / nm (log (ε / L·mol^{-1}·cm^{-1}))): 205.3 (4.50), 222.9 (4.46), 285.5 (4.04).

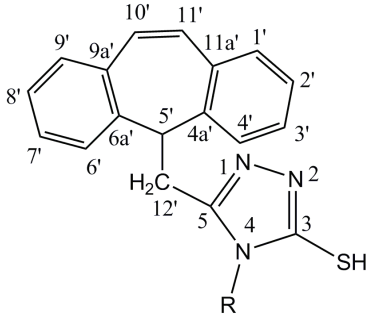

Scheme S-2. The general structure of **10–13** with atom numbering.

*4-(4-Chlorophenyl)-5-(5*H*-dibenzo[*a,d*][7]annulen-5-ylmethyl)-4*H*-1,2,4-triazole-3-thiol* (***10***). Yield: 78.6 %; m.p.: 177–179 °C; Anal. Calcd. for $C_{24}H_{18}ClN_3S$ (FW: 415.93): C, 69.30; H, 4.36; N, 10.10 %. Found: C, 69.28; H, 4.38; N, 10.10 %; IR (KBr, cm^{-1}): 3383 (N–H stretching), 3066, 3020 (C–H stretching of aromatic ring), 2929, 2845 (CH_2 stretching), 1566, 1495, 1458, 1231 (C=S stretching), 768 (C–Cl); ^{1}H-NMR (300 MHz, $CDCl_3$, δ / ppm): 11.90 (1H, *s*, SH), 7.43 (2H, *d*, *J* = 8.5 Hz, H-chlorophenyl), 7.35–7.10 (8H, *m*, Ar-H), 6.83 (2H, *s*, H10′, H11′), 6.77 (2H, *d*, *J* = 8.5 Hz, H-chlorophenyl), 4.41 (1H, *t*, *J* = 7.9 Hz, H5′), 2.98 (2H, *d*, *J* = 7.9 Hz, H12′); ^{13}C-NMR (75 MHz, $CDCl_3$,

δ / ppm): 167.97 (triazole-C3), 151.54 (triazole-C5), 138.48 ($2C_q$), 136.02 (C_q), 133.91 (C_q), 131.54 (C–Cl), 130.77 (C10′, C11′), 130.14 (CH), 129.92 (CH), 129.56 (CH), 129.28 (CH), 53.20 (C5′), 26.13 (C12′); UV–Vis (CH_3OH, 2.5×10^{-5} M, λ_{max} / nm (log (ε / L·mol^{-1}·cm^{-1}))): 207.0 (4.53), 222.9 (4.47), 277.5 (4.21).

*4-(4-Bromophenyl)-5-(5*H*-dibenzo[*a,d*][7]annulen-5-ylmethyl)-4*H*-1,2,4-triazole-3-thiol (**11**)*. Yield: 90.0% m.p.: 133–135°C; Anal. Calcd. for $C_{24}H_{18}BrN_3S$ (FW: 460.38 g/mol): C, 62.61; H, 3.94; N, 9.13; Found: C, 62.61; H, 3.92; N, 9.16; IR (KBr, cm^{-1}): 33392 (N–H stretching), 3066, 3020 (C–H stretching of aromatic ring), 2930, 2845 (CH_2 stretching), 1561, 1491, 1435, 1231 (C=S stretching), 570 (C–Br); ^{1}H-NMR (300 MHz, $CDCl_3$, δ / ppm): 11.82 (1H, *s*, SH), 7.59 (2H, *d*, *J* = 8.3 Hz, H-bromophenyl), 7.30–7.05 (8H, *m*, Ar-H), 6.71 (2H, *d*, *J* = 8.3 Hz, H-bromophenyl), 6.62 (2H, *s*, H10′, H11′) 4.41 (1H, *t*, *J* = 7.9 Hz, H5′), 2.98 (2H, *d*, *J* = 7.9 Hz, H12′); ^{13}C-NMR (75 MHz, $CDCl_3$, δ / ppm): 168.00 (triazole-C3), 151.51 (triazole-C5), 138.47 (C_q), 133.91 (C_q), 132.06 (Cq), 130.78 (C10′, C11′), 130.15 (CH), 129.81 (CH), 129.56 (CH), 129.28 (CH), 124.11 (C–Cl), 53.21 (C5′), 26.13 (C12′); UV–Vis (CH_3OH, 2.5×10^{-5} M, λ_{max} / nm (log (ε / L·mol^{-1}·cm^{-1}))): 202.6 (4.42), 222.3 (4.33), 283.7 (3.87).

*5-(5*H*-Dibenzo[*a,d*][7]annulen-5-ylmethyl)-4-(4-iodophenyl)-4*H*-1,2,4-triazole-3-thiol (**12**)*. Yield: 74.5 %; m.p.: 200–202 °C; Anal. Calcd. for $C_{24}H_{18}IN_3S$ (FW: 507.39): C, 56.81; H, 3.58; N, 8.26 %. Found: C, 56.81; H, 3.57; N, 8.28 %; IR (KBr, cm^{-1}): 3371 (N–H stretching), 3062, 3019 (C–H stretching of aromatic ring), 2928, 2840 (CH_2 stretching), 1578, 1563, 1491, 1459, 1228 (C=S stretching), 571 (C–I); ^{1}H-NMR (300 MHz, $CDCl_3$, δ / ppm): 11.58 (1H, *s*, SH), 7.75 (2H, *d*, *J* = 8.6 Hz, H-iodophenyl), 7.25–7.05 (8H, *m*, Ar-H), 6.59 (2H, *s*, H10′, H11′), 6.54 (2H, *d*, *J* = 8.6 Hz, H-iodophenyl), 4.35 (1H, *t*, *J* = 7.9 Hz, H5′), 2.93 (2H, *d*, *J* = 7.9 Hz, H12′); ^{13}C-NMR (75 MHz, $CDCl_3$, δ / ppm): 168.08 (triazole-C3), 151.50 (triazole-C5), 133.92 (C_q), 132.80 (C_q), 130.95 (CH), 130.80 (C10′, C11′), 130.47 (C_q), 130.18 (CH), 129.93 (CH), 129.62 (CH), 129.29 (CH), 95.77 (C–I), 53.20 (C5′), 26.16 (C12′); UV–Vis (CH_3OH, 2.5×10^{-5} M, λ_{max} / nm (log (ε / L·mol^{-1}·cm^{-1}))): 206.2 (4.53), 229.1 (4.44), 278.4 (4.21).

*5-(5*H*-Dibenzo[*a,d*][7]annulen-5-ylmethyl)-4-(2-phenylethyl)-4*H*-1,2,4-triazole-3-thiol (**13**)*. Yield: 77.0 %; m.p.: 107–109 °C; Anal. Calcd. for $C_{26}H_{23}N_3S$ (FW: 409.54): C, 76.25; H, 5.66; N, 10.26 %. Found: C, 76.26; H, 5.65; N, 10.26 %; IR (KBr, cm^{-1}): 3401 (N–H stretching), 3064, 3025 (C–H stretching of aromatic ring), 2945, 2861 (CH_2 stretching), 1566, 1493, 1454, 1277 (C=S stretching); ^{1}H-NMR (300 MHz, $CDCl_3$, δ / ppm): 11.44 (1H, *s*, SH), 7.35–7.10 (11H, *m*, Ar-H), 7.06 (2H, *d*, *J* = 6.8 Hz, arom. H-phenylethyl), 6.99 (2H, *s*, H10′, H11′), 4.45 (1H, *t*, *J* = 7.5 Hz, H5′), 3.73 (2H, *t*, *J* = 7.0 Hz, CH_2–N4––triazole), 2.80 (2H, *t*, *J* = 7.0 Hz, CH_2-phenyl), 2.67 (2H, *d*, *J* = 7.5 Hz, H12′); ^{13}C-NMR (75 MHz, $CDCl_3$, δ / ppm): 166.57 (triazole-C3), 151.70 (triazole-C5),

138.48 (C_q), 137.80 (C_q), 131.11 (C10′, C11′), 130.10 (CH), 129.98 (CH), 129.86 (CH), 129.41 (CH), 127.34 (CH), 127.15 (CH), 52.81 (C5′), 45.21 (CH_2––N4-triazole), 34.12 (CH_2--phenyl), 26.13 (C12′); UV–Vis (CH_3OH, 2.5×10^{-5} M, λ_{max} / nm (log (ε / L·mol^{-1}·cm^{-1}))): 207.0 (4.54), 225.6 (4.37), 256.4 (4.25), 287.2 (4.12).

*4-(4-Chlorophenyl)-3-(5*H*-dibenzo[*a,d*][7]annulen-5-ylmethyl)-5-(methylsulfanyl)- 4*H*-1,2,4-triazole (**14**)*. Yield: 69.1 %; m.p.: 81–83 °C; Anal. Calcd. for $C_{25}H_{20}ClN_3S$ (FW: 429.96): C, 69.84; H, 4.69; N, 9.77 %. Found: C, 69.82; H, 4.70; N, 9.77 %; IR (KBr, cm^{-1}): 3056, 3017 (aromatic C–H), 2983, 2928 (CH_2 + CH_3 stretching), 1493, 1448, 1432, 768 (C–Cl), 727 (C–S–C); ^{1}H-NMR (300 MHz, $CDCl_3$, δ / ppm): 7.36 (2H, *d*, *J* = 8.7 Hz, H-chlorophenyl), 7.30–7.05 (8H, *m*, Ar-H), 6.53 (2H, *s*, H10′, H11′), 6.51 (2H, *d*, *J* = 8.7 Hz, H-chlorophenyl), 4.62 (1H, *t*, *J* = 7.9 Hz, H5′), 3.09 (2H, *d*, *J* = 7.9 Hz, H12′), 2.57 (3H, *s*, CH_3–S); ^{13}C-NMR (75 MHz, $CDCl_3$, δ / ppm): 154.94 (triazole-C3), 151.43 (triazole-C5), 139.32 (C_q), 135.80 (C_q), 133.97 (C_q), 130.73 (C10′, C11′), 130.01 (CH), 129.95 (CH), 129.86 (CH), 129.15 (CH), 128.64 (CH), 126.94 (CH); 54.26 (C5′), 25.30 (C12′), 14.80 (CH_3–S); UV–Vis (CH_3OH, 2.5×10^{-5} M, λ_{max} / nm (log (ε / L mol^{-1}·cm^{-1}))): 207.9 (4.53), 220.0 (4.48), 287.2 (4.11).

*4-(4-Bromophenyl)-3-(5*H*-dibenzo[*a,d*][7]annulen-5-ylmethyl)-5-(methylsulfanyl)- 4*H*-1,2,4-triazole (**15**)*. Yield: 66.2 %; m.p.: 128–130 °C; Anal. Calcd. for $C_{25}H_{20}BrN_3S$ (FW: 474.41): C, 63.29; H, 4.25; N, 8.86 %. Found: C, 63.28; H, 4.27; N, 8.85 %; IR (KBr, cm^{-1}): 3041, 3015 (aromatic C–H), 2970, 2926, 2854 (CH_2 + CH_3 stretching), 1509, 1489, 1455, 768 (C–S–C), 563 (C–Br); ^{1}H--NMR (300 MHz, $CDCl_3$, δ / ppm): 7.69 (2H, *d*, *J* = 8.8 Hz, H-bromophenyl) equatorial isomer, 7.52 (2H, *d*, *J* = 8.8 Hz, H-bromophenyl) equatorial isomer, 7.50 (2H, *d*, *J* = 8.8 Hz, H-bromophenyl) axial isomer, 7.32–7.12 (H, *m*, Ar-H), 6.96 (2H, *m*, Ar-H), 6.73 (2H, *s*, H10′, H11′) axial isomer, 6.54 (2H, *s*, H10′, H11′) equatorial isomer, 6.46 (2H, *d*, *J* = 8.8 Hz, H-bromophenyl) axial isomer, 4.62 (1H, *t*, *J* = 7.7 Hz, H5′) axial isomer, 4.08 (1H, *t*, *J* = 7.7 Hz, H5′) equatorial isomer, 3.65 (2H, *d*, *J* = 7.7 Hz, H12′) equatorial isomer, 3.06 (2H, *d*, *J* = 7.7 Hz, H12′) axial isomer, 2.62 (3H, *s*, CH_3–S), 2.57 (3H, *s*, CH_3–S); ^{13}C-NMR (75 MHz, $CDCl_3$, δ / ppm): 155.11 (triazole-C3), 154.54 (triazole-C5), 139.22 (C_q), 136.73 (C_q), 133.89 (C_q), 133.74 (CH), 132.80 (CH), 130.94 (C10′, C11′), 130.71 (CH), 130.65 (CH), 129.62 (CH), 129.14 (CH), 129.06 (CH), 128.81 (CH), 128.55 (CH), 128.07 (CH), 127.89 (CH), 126.56 (C_q), 123.71 (C_q), 54.19 (C5′) axial isomer, 52.34 (C5′) equatorial isomer, 27.35 (C12′) equatorial isomer, 25.21 (C12′) axial isomer, 14.88 (CH_3–S) equatorial isomer, 14.74 (CH_3–S) axial isomer; UV–Vis (CH_3OH, 2.5×10^{-5} M, λ_{max} / nm (log (ε / L·mol^{-1}·cm^{-1}))): 207.9 (4.55), 222.9 (4.52), 287.2 (4.11).

*3-(5*H*-Dibenzo[*a,d*][7]annulen-5-ylmethyl)-4-(4-iodophenyl)-5-(methylsulfanyl)-4*H*-1,2,4-triazole (**16**)*. Yield: 69.3 %; m.p.: 99–101 °C; Anal. Calcd. for

$C_{25}H_{20}IN_3S$ (FW: 521.41): C, 57.59; H, 3.87; N, 8.06 %. Found: C, 57.57; H, 3.89; N, 8.05 %; IR (KBr, cm^{-1}): 3058, 3016 (aromatic C–H), 2927, 2852 (CH_2 + CH_3 stretching), 1489, 1447, 1431, 768 (C–S–C), 564 (C–I); ^{1}H-NMR (300 MHz, $CDCl_3$, δ / ppm): 7.71 (2H, *d*, *J* = 8.4 Hz, CH-iodophenyl), 7.35–7.10 (8H, *m*, Ar-H), 6.53 (2H, *s*, H10′, H11′), 6.31 (2H, *d*, 8.4, H-iodophenyl), 4.61 (1H, *t*, *J* = 7.7 Hz, H5′), 3.06 (2H, *d*, *J* = 7.7 Hz, H12′), 2.57 (3H, *s*, CH_3–S); ^{13}C-NMR (75 MHz, $CDCl_3$, δ / ppm): 154.82 (triazole-C3), 151.28 (triazole-C5), 139.21 (C_q), 138.85 (C_q), 133.90 (C_q), 132.50 (C_q), 130.69 (C10′, C11′), 129.24 (CH), 129.11 (CH), 128.96 (CH), 126.90 (CH); 95.24 (C–I), 54.21 (C5′), 25.18 (C12′), 14.79 (CH_3–S); UV–Vis (CH_3OH, 2.5×10^{-5} M, λ_{max} / nm (log (ε / $L\cdot mol^{-1}$ cm^{-1}))): 207.0 (4.56), 229.1 (4.24), 289.0 (4.11).

*3-(5*H*-Dibenzo[*a,d*][7]annulen-5-ylmethyl)-5-(methylsulfanyl)-4-(2-phenyl-ethyl)-4*H*-1,2,4-triazole (**17**)*. Yield: 67.6 %; m.p.: 100–102 °C; Anal. Calcd. for $C_{27}H_{25}N_3S$ (FW: 423.57): C, 76.56; H, 5.97; N, 9.92 %. Found: C, 76.56; H, 5.95; N, 9.93 %; IR (KBr, cm^{-1}): 3061, 3021 (aromatic C–H), 2929, 2854 (CH_2 & CH_3 stretching), 1515, 1495, 1466, 768 (C–S–C); ^{1}H-NMR (300 MHz, $CDCl_3$, δ / ppm): 7.25–7.10 (11H, *m*, Ar-H), 6.91 (2H, *s*, H10′, H11′), 6.81 (2H, *dd*, *J* = 1.6 and 7.7 Hz, arom. H-phenylethyl), 4.60 (1H, *t*, *J* = 7.7 Hz, H5′), 3.36 (2H, *t*, *J* = 7.4 Hz, CH_2–N4-triazole), 2.80 (2H, *d*, *J* = 7.7 Hz, C12′), 2.50 (2H, *t*, *J* = 7.4 Hz C**H**$_2$–C_6H_5), 2.48 (3H, *s*, S–CH_3); ^{13}C-NMR (75 MHz, $CDCl_3$, δ / ppm): 154.58 (triazole-C3), 150.34 (triazole-C5), 139.60 (C_q), 136.77 (C_q), 133.92 (C_q), 131.12 (C10′, C11′), 130.30 (CH), 129.91 (CH), 129.31 (CH), 128.87 (CH); 128.77 (CH), 127.22 (CH), 53.80 (C5′), 44.49 (CH_2–N4-triazole), 36.02 (CH_2–C_6H_5), 25.82 (C12′), 15.62 (CH_3–S); UV–Vis (CH_3OH, 2.5×10^{-5} M, λ_{max} / nm (log (ε / $L\cdot mol^{-1}\cdot cm^{-1}$))): 207.0 (4.34), 230.0 (4.15), 292.5 (3.79).

Journal of the Serbian Chemical Society
JSCS-info@shd.org.rs • www.shd.org.rs/JSCS
J. Serb. Chem. Soc. 80 (12) 1471–1479 (2015)
JSCS–4812
UDC 547.856+547.497.1:542.913:
615.28–188
Original scientific paper

Syntheses and antimicrobial activities of 1-(3-benzyl-4-oxo-3,4--dihydroquinazolin-2-yl)-4-(substituted) thiosemicarbazide derivatives

VEERACHAMY ALAGARSAMY[1]*, VISWAS RAJA SOLOMON[1], G. KRISHNAMOORTHY[2], M. T. SULTHANA[1] and B. NARENDAR[1]

[1]*Medicinal Chemistry Research Laboratory, MNR College of Pharmacy, Sangareddy, Gr. Hyderabad -502 294, India and* [2]*Department of Pharmaceutical Chemistry, Periyar College of Pharmaceutical Sciences for Girls, Trichy – 620 021, India*

(Received 3 January, revised 11 May, accepted 10 June 2015)

Abstract: A series of 1-(3-benzyl-4-oxo-3,4-dihydroquinazolin-2-yl)-4-(substituted) thiosemicarbazides (**AS1**–**AS10**) were obtained by the reaction of 3-benzyl-2-hydrazino-3*H*-quinazolin-4-one (**6**) with different dithiocarbamic acid methyl ester derivatives. The key intermediate, 3-benzyl-2-thioxo-2,3-dihydro-1*H*-quinazolin-4-one (**4**), was obtained by the reaction of benzyl amine (**1**) with carbon disulphide and sodium hydroxide in dimethyl sulphoxide to give sodium dithiocarbamate, which was methylated with dimethyl sulphate to yield the dithiocarbamic acid methyl ester **2** and condensation with methyl anthranilate (**3**) in ethanol yielded the desired compound (**4**) *via* the thiourea intermediate. The SH group of compound (**4**) was methylated in the favourable nucleophilic displacement reaction with hydrazine hydrate, which afforded 3-benzyl-2-hydrazino-3*H*-quinazolin-4-one (**6**). The IR, and ^{1}H- and ^{13}C-NMR spectra of these compounds showed the presence of peaks due to thiosemicarbazides, carbonyl (C=O), NH and aryl groups. The molecular ion peaks of the quinazolin-4-one moiety (*m*/*z* 144) were observed in all the mass spectra of the compounds **AS1**–**AS10**. Elemental (C, H, N) analysis satisfactorily confirmed purity and elemental composition of the synthesized compounds. All the synthesized compounds were screened for their antimicrobial activity against selective gram positive and gram negative bacteria by agar dilution method. In the present study, compounds **AS8** and **AS9** emerged as the most active compounds of the series.

Keywords: quinazolinone; substituted thiosemicarbazide; anti-bacterial; anti-tubercular activity.

* Corresponding author. E-mail: drvalagarsamy@gmail.com
doi: 10.2298/JSC150103053A

INTRODUCTION

Worldwide, tuberculosis (TB) is one of the leading causes of death. TB is an infection, primarily in the lungs (a pneumonia), caused by the bacteria *Mycobacterium tuberculosis*. Emergence of multi drug resistant tuberculosis (MDR-TB) makes the conditions most alarming.[1,2] Some of the MDR isolates are resistant to as many as seven of the commonly employed antimycobacterial drugs.[3] Quinazolines and condensed quinazolines have received the attention of medicinal chemists due to their potential biological activities. Among the biological activities exhibited by quinazolines, the antimicrobial activities of 2,3-disubstituted quinazolines are promising.[4] A literature survey indicated that the quinazolines nucleus substituted at the 2,3-positions (Fig. 1, **I** and **II**) showed significant antitubercular activity.[5,6] Pharmacophore such as thiosemicarbazides and thiosemicarbazones groups (Fig 1, **III** and **IV**) in different heterocyclic moieties were also found to exhibit antitubercular activity.[7–15] The present work is an extension of ongoing efforts towards developing effective antitubercular and antimicrobial agents by a hybrid approach using the quinazoline scaffold (Fig. 1). In this approach, two or more pharmacophores are merged into a single molecule. Therefore, with a single molecule containing more than one pharmacophore, each pharmacophore may address the active site of targets and offer the possibility of selectivity; further it can also reduce unwanted side effects.[16] In the present study, a substituted thiosemicarbazide moiety was placed at the C-2 position and a benzyl ring at the N-3 position of the quinazoline ring[17,18] and the antitubercular and antibacterial activities of the resulting compounds were studied against selected gram positive and negative bacteria.

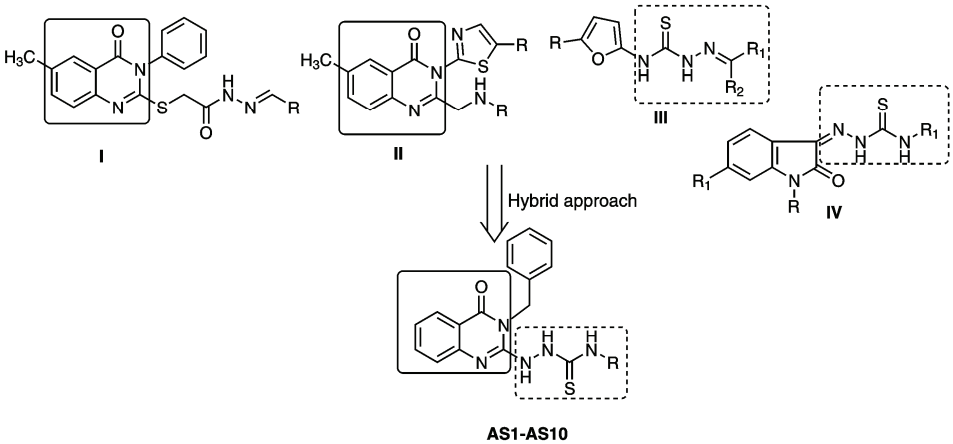

Fig. 1. Hybrid approach design of 1-[3-benzyl-4-oxo-3,4-dihydroquinazolin-2-yl]-4--[substituted] thiosemicarbazide analogues.

EXPERIMENTAL

Chemistry

Melting points (m.p.) were taken in open capillaries on a Thomas Hoover melting point apparatus (Thomas Hoover, USA) and are uncorrected. The IR spectra were recorded as films or in potassium bromide disks on a Perkin–Elmer 398 spectrometer (Perkin–Elmer). The ^{1}H-spectra were recorded on a DPX-300 MHz Bruker FT-NMR spectrometer (Bruker, USA). The chemical shifts are reported as parts per million (δ / ppm) with tetramethylsilane (TMS) as an internal standard. The mass spectra were obtained on a JEOL-SX-102 instrument (JEOL, Japan) using fast atom bombardment (FAB positive). The elemental analyses were realised on a Perkin–Elmer 2400 CHN analyzer (Perkin–Elmer) and the values were within acceptable limits of the calculated values (±0.4 %). The progress of the reactions were monitored on ready-made silica gel plates (Merck, Norway) using chloroform–methanol (9:1) as the solvent system. Iodine was used as the developing agent. All chemicals and reagents used in the synthesis were obtained from Aldrich (USA), Lancaster (USA) or Spectrochem (India) and were used without further purification.

The physical, analytical and spectral data for the compounds are given in the Supplementary material to this paper.

*3-Benzyl-2-thioxo-2,3-dihydro-1*H*-quinazolin-4-one (**4**)*

A solution of benzylamine **1** (0.02 mol) in dimethyl sulphoxide (10 ml) was stirred vigorously. To this mixture was added carbon disulphide (1.6 mL) and aqueous sodium hydroxide (1.2 mL, 20 M) dropwise during 30 min under stirring. Dimethyl sulphate (0.02 mol) was added gradually keeping the reaction mixture stirring in a freezing mixture for 2 h. The reaction mixture was then poured into ice water. The obtained solid **2** was filtered, washed with water, dried and recrystallised from ethanol. Methyl anthranilate (**3**, 0.01 mol) and the above prepared methyl *N*-(benzyl)carbamodithioate (**2**, 0.01 mol), were dissolved in ethanol (20 mL). To this, anhydrous potassium carbonate (100 mg) was added and the mixture refluxed for 22 h. The reaction mixture was cooled in ice and the solid that separated was filtered and purified by dissolving in 10 % alcoholic sodium hydroxide solution and re-precipitated by treating with dilute hydrochloric acid. The thus obtained solid was filtered, washed with water, dried and recrystallised from ethanol.

*3-Benzyl-2-(methylsulphanyl)-3*H*-quinazolin-4-one (**5**)*

3-Benzyl-2-thioxo-2,3-dihydro-1*H*-quinazolin-4-one (**4**, 0.01 mol) was dissolved in 40 mL of 2 % alcoholic sodium hydroxide solution. To this, dimethyl sulphate (0.01 mol) was added dropwise with stirring. After further stirring for 1 h, the reaction mixture was poured into ice water. The obtained solid was filtered, washed with water, dried and recrystallised from ethanol–chloroform (75:25) mixture.

*3-Benzyl-2-hydrazino-3*H*-quinazolin-4-one (**6**)*

3-Benzyl-2-(methylsulphanyl)-3*H*-quinazolin-4-one (**5**, 0.01 mol) was dissolved in ethanol (25 mL). To this, hydrazine hydrate (99 %, 0.1 mol) and anhydrous potassium carbonate (100 mg) were added and refluxed for 33 h. The reaction mixture was cooled and poured into ice–water. The so obtained solid was filtered, washed with water, dried and recrystallised from chloroform–benzene (25:75) mixture.

*General procedure for synthesis of 1-(3-benzyl-4-oxo-3,4-dihydroquinazolin-2-yl)-4--(substituted) thiosemicarbazides (**AS1**–**AS10**)*

A solution of primary alkyl/aryl amine (0.02 mol) in dimethyl sulphoxide (10 mL) was stirred vigorously. To this, simultaneously, carbon disulphide (1.6 mL) and aqueous sodium hydroxide 1.2 mL (20 M) were added dropwise during 30 min with stirring. Dimethyl sulphate (0.02 mol) was added gradually to the stirred reaction mixture in a freezing mixture and the stirring was continued for further 2 h. The reaction mixture was then poured into ice water and the obtained solid was filtered, washed with water, dried and recrystallised from ethanol to afford methyl *N*-(substituted) dithiocarbamates (**7**).

3-Benzyl-2-hydrazino-3*H*-quinazolin-4-one (**6**, 2.32 g, 0.01 mol) and methyl *N*-(substituted) dithiocarbamate (**7**, 0.01 mol) were dissolved in ethanol and refluxed for 22–30 h (until the evolution of methanethiol ceased). After completion of the reaction, the reaction mixture was cooled to room temperature. The obtained solid was filtered, dried and recrystallised from ethanol. By adapting the above procedure, the compounds **AS1–AS10** were prepared. It should be noted that the synthesis of compounds **AS1**–**AS3**, **AS5** and **AS6** were previously reported.[19-21] However, none of these compounds has been examined for their antitubercular activities.

Pharmacology

Antibacterial activity. Evaluation of antibacterial activity was realized using the agar dilution method.[10,11] The standard strains were procured from the American Type Culture Collection (ATCC), Rockville, MD, USA, and the pathological strains were procured from the Department of Microbiology, MNR Medical College, Sangareddy, India. The antibacterial activity of the synthesized compounds was screened against the following bacterial strains: *Proteus vulgaris* ATCC 9484, *Salmonella enterica* subsp. *enterica* sarovar Typhimurium ATCC 33068, *Klebsiella pneumoniae* ATCC 13883, *Edwardsiella tarda*, *Pseudomonas aeruginosa* ATCC 27853, *Bacillus subtilis* ATCC 6051 and *Salmonella enterica* subsp. *enterica* sarovar Paratyphi. All bacteria were grown on Muller–Hinton Agar (Hi-media) plates (37 °C, 24 h) and the minimum inhibitory concentration (*MIC*) was considered to be the lowest concentration that completely inhibited the growth on agar plates, disregarding a single colony or faint haze caused by the inoculums.[22,23] The *MIC* values of the test compounds were compared with those the reference drug ciprofloxacin. The data given in Table I were calculated from at least three different experiments in duplicate.

Antitubercular activity. Ten-fold serial dilutions of each test compound/drug were incurporated into Middlebrook 7H11 agar slants with OADC growth supplement. Inoculums of *Mycobacterium tuberculosis* $H37R_V$ were prepared from fresh Middlebrook 7H11 agar slants with OADC Growth Supplement adjusted to 1 mg mL^{-1} in Tween 80 (0.05 %, *w*/*V*) saline diluted to 10^{-2} to give a concentrate of approximately 107 CFU mL^{-1}. A 5 μL amount of bacterial suspension was spotted into 7H11 agar tubes containing 10-fold serial dilutions of the drugs per mL. The tubes were incubated at 37 °C, and final readings were recorded after 28 days. Tubes having the compounds were compared with control tubes in which medium alone were incubated with $H37R_V$. The concentration at which complete inhibition of colonies occurred was taken as the active concentration of test compound. The *MIC* is defined as the minimum concentration of compound required to give complete inhibition of bacterial growth.[24-26] The *MIC* values of the test compounds were compared with that of the reference drug gatifloxacin.

Cytotoxicity profile of the tested compounds. For cytotoxic assay with HeLa, approximately 10,000 cells were seeded with 0.1 mL RPMI 1640 culture medium per well of 96-well

micro-plates. HeLa cells were pre-incubated for 48 h without the test substances. The solutions of the compounds of the corresponding concentrations were applied carefully on the monolayers of HeLa cells after the pre-incubation time. The monolayers of the adherent HeLa cells were fixed by glutaraldehyde and stained with a 0.05 % solution of methylene blue for 15 min. After gently washing, the stain was eluted by 0.2 mL of 0.33 M HCl in the wells. The optical densities were measured at 630 nm in a micro plate reader. In general, the compounds showed no significant cytotoxic effect at the tested concentration.[27]

RESULTS AND DISCUSSION

Chemistry

Synthetic route depicted in Scheme 1 outlines the chemistry part of the present work. The key intermediate 3-benzyl-2-thioxo-2,3-dihydro-1*H*-quinazolin-4--one (**4**) was obtained by reacting aniline (**1**) with carbon disulphide and sodium hydroxide in dimethyl sulphoxide to give sodium dithiocarbamate, which was methylated with dimethyl sulphate to afford the dithiocarbamic acid methyl ester **2**. Compound **2** on reflux with methyl anthranilate (**3**) in ethanol yielded the desired 3-benzyl-2-thioxo-2,3-dihydro-1*H*-quinazolin-4-one (**4**) *via* the thiourea intermediate in good yield (80 %). The obtained product was cyclic and not an open chain thiourea **3a**. The 3-benzyl-2-(methylsulphanyl)-3*H*-quinazolin-4-one (**5**) was obtained by dissolving **4** in 2 % alcoholic sodium hydroxide solution and methylating with dimethyl sulphate under stirring at room temperature. Nucleophilic displacement of the methylthio group of **5** with hydrazine hydrate was performed using ethanol as solvent to afford 3-benzyl-2-hydrazino-3*H*-quinazolin-4--one (**6**). The required long duration of the reaction (33 h) might be due to the presence of the bulky aromatic ring at position 3, which might have reduced the reactivity of quinazoline ring system at the C-2 position. The title compounds 1-(3-benzyl-4-oxo-3,4-dihydroquinazolin-2-yl)-4-(substituted) thiosemicarbazides (**AS1**–**AS10**) were obtained by the condensation of the amino group of 3-benzyl--2-hydrazino-3*H*-quinazolin-4-one (**6**) with a variety of methyl ester of dithiocarbamic esters. The formation of title products was indicated by the disappearance of peak due to NH, NH_2 of the starting material in IR and ^{1}H-NMR spectra of all the compounds **AS1**–**AS10**. The IR and ^{1}H-NMR spectra of these compounds showed the presence of peaks due to thiosemicarbazides, carbonyl (C=O), NH and aryl groups. The mass spectra of the title compounds showed molecular ion peaks corresponding to their molecular formulae. In the mass spectrum of compounds **AS1–AS10**, a common peak at *m*/*z* 144 corresponding to the quinazolin-4-one moiety appeared. Elemental (C, H, N) analysis satisfactorily confirmed the elemental composition and purity of the synthesized compounds.

Antitubercular activity

The synthesized compounds were screened for their *in vitro* antimycobacterial activity against *M. tuberculosis* strain $H37R_V$. The results are expressed in

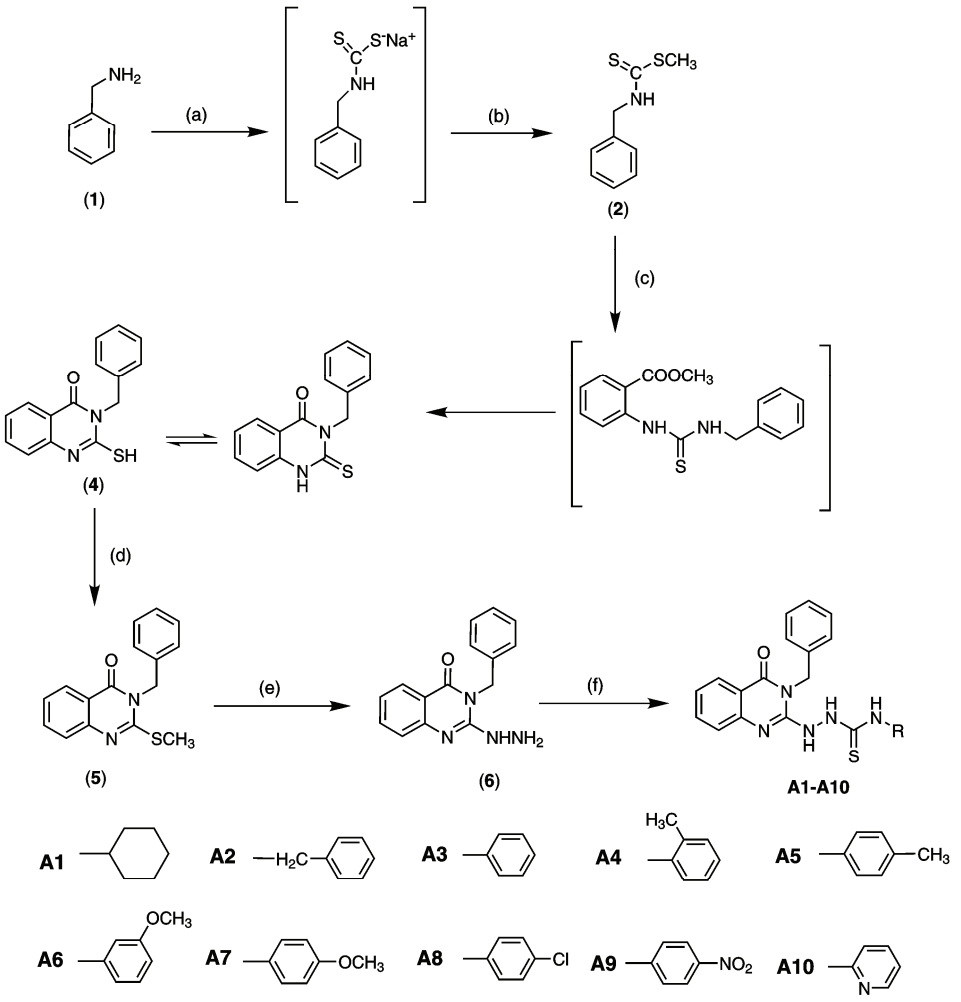

Scheme 1. Synthesis of 1-(4-oxo-3-phenyl-3,4-dihydroquinazolin-2-yl)-4-(substituted) thiosemicarbazides. Reagents and conditions: a) CS_2, NaOH, DMSO, 30 min; b) dimethyl sulphate, 2 h; c) methyl anthranilate, anhydrous K_2CO_3, EtOH reflux, 22 h; the product is **3a**; d) 2 % alcoholic NaOH, dimethyl suphate, 1 h; e) hydrazine hydrate, anhydrous K_2CO_3, EtOH reflux, 33 h; f) methyl N-(substituted) carbamodithioate, EtOH reflux, 22–30 h; notation "**A**" in the Scheme replaces notation "**AS**" from the text.

terms of minimum inhibitory concentration (*MIC*). The results of antimycobacterial activity depicted in Table I, indicate that the test compounds inhibited the growth of *Mycobacterium* to varying degree. Compounds with aliphatic substituents showed lower antitubercular activity over the aryl and heteroaryl substituents. The compounds with electron withdrawing substituent on the aryl ring showed better activity over the unsubstituted or electron donating substituent on

the aryl ring. Among the test compounds, 2-(3-benzyl-4-oxo-3,4-dihydroquinazolin-2-yl)-*N*-(4-chlorophenyl)hydrazinecarbothioamide (**AS8**) and 1-(3-benzyl--4-oxo-3,5-dihydroquinazolin-2-yl)-4-(4-nitrophenyl)hydrazinecarbothioamide (**AS9**) exhibited antitubercular activity at the minimum microgram concentration (3 μg mL^{-1}).

TABLE I. Antitubercular and antibacterial activity of the synthesized compounds **AS1**–**AS10**; (*MIC* in μg mL^{-1}); na – no activity

Microorganism	Test Compound										Standard[a]
	AS1	**AS2**	**AS3**	**AS4**	**AS5**	**AS6**	**AS7**	**AS8**	**AS9**	**AS10**	
M. tuberculosis	125	63	63	6	13	13	6	3	3	6	1
S. enterica serovar Typhimurium	66	63	63	63	63	125	63	8	8	16	4
P. vulgaris	63	63	125	125	63	63	63	8	16	32	1
K. pneumoniae	63	125	125	32	63	125	63	16	16	63	1
B. subtilis	63	125	63	125	63	32	32	8	8	16	1
P. aeruginosa	125	125	16	63	32	32	63	16	8	32	1
E. tarda	na	na	na	na	na	na	na	na	na	na	na

[a]Gatifloxacin was used as a reference standard against *M. tuberculosis*, whereas ciprofloxacin was used as a reference standard for the other bacteria

Antibacterial activity

Among the different substituents, aryl and heteroaryl substituents exhibited better activity over the aliphatic cyclic substituents. Compounds with electron withdrawing substituents, such as –Cl and $–NO_2$ showed better activity over the unsubstituted and electron donating substituents. Compounds **AS8** and **AS9** emerged as the most active compounds of the series. Compound **AS8** showed the most potent activity against *E. coli*, *P. vulgaris*, *B. subtilis* and *S. enterica* subsp. *enterica* serovar Typhimurium, while compound **AS9** showed the most potent activity against *E. coli*, *B. subtilis*, *P. aeruginosa* and *S. enterica* subsp. *enterica* serovar Typhimurium.

CONCLUSIONS

In summary, the syntheses of a new series of 1-(4-oxo-3-phenyl-3,4-dihydroquinazolin-2-yl)-4-(substituted) thiosemicarbazides was described. These derivatives exhibited significant antibacterial activity against various Gram-positive and Gram-negative bacteria, including *M. tuberculosis.* Among the series, compound **AS8** showed the most potent activity against *E. coli*, *P. vulgaris*, *B. subtilis* and *S. enterica* subsp. *enterica* serovar Typhimurium, while compound **AS9** showed the most potent activity against *E. coli*, *B. subtilis*, *P. aeruginosa* and *S. enterica* subsp. *enterica* serovar Typhimurium. The test compounds **AS8** and **AS9** exhibited antitubercular activity at the minimum microgram concentration

(3 μg mL^{-1}) and show potential for further optimization and development to new antitubercular agents.

SUPPLEMENTARY MATERIAL

The physical, analytical and spectral data for the compounds are available electronically from http://www.shd.org.rs/JSCS/, or from the corresponding author on request.

Acknowledgements. The authors gratefully acknowledge the Central Instrumentation Facility, IIT Chennai, India for the spectral analysis of the compounds synthesised in this study and Dr. D. Sriram, Birla Institute of Technology & Sciences, Hyderabad Campus for performing the antitubercular screening of the test compounds.

ИЗВОД

СИНТЕЗА И АНТИМИКРОБНА АКТИВНОСТ 1-(3-БЕНЗИЛ-4-ОКСО-3,4-ДИХИДРОКИНАЗОЛИН-2-ИЛ)-4-СУПСТИТУИСАНИХ ДЕРИВАТА ТИОСЕМИКАРБАЗИДА

VEERACHAMY ALAGARSAMY[1], VISWAS RAJA SOLOMON[1], G. KRISHNAMOORTHY[2], M. T. SULTHANA[1] и B. NARENDAR[1]

[1]*Medicinal Chemistry Research Laboratory, MNR College of Pharmacy, Sangareddy, Gr. Hyderabad -502 294, India u* [2]*Department of Pharmaceutical Chemistry, Periyar College of Pharmaceutical sciences for Girls, Trichy – 620 021, India*

Синтетисана је серија 1-(3-бензил-4-оксо-3,4-дихидрокиназолин-2-ил)-4-супституисаних деривата тиосемикарбазида (**AS1**–**AS10**), реакцијом 3-бензил-2-хидразино-3*H*-хиназолин-4-она (**6**) и различитих деривата метил-естара дитиокарбаминске киселине. Главни интермедијер 3-бензил-2-тиоксо-2,3-дихидро-1*H*-хиназолин-4-он (**4**) добијен је после секвенције у којој је реакцијом бензиламина (**1**) са угљен-дисулфидом и натријум-хидроксидом у диметил-сулфоксиду добијен дитиокарбамат, који је метилован диметил-сулфатом при чему је добијен метил-естар дитиокарбаминске киселине **2** и који је кондензацијом са метил-антранилатом (**3**) у етанолу дао жељени производ **4** преко тиоуреидног интермедијера. Тиол-група у једињењу **4** метилована је да би била извршена нуклеофилна замена помоћу хидразин хидрата, чиме је добијен 3-бензил-2-хидразинохиназолин-4-он (**6**). IR, ^{1}H- и ^{13}C-NMR спектри једињења показују присуство сигнала тиосемикарбазидних, карбонилних (C=O), NH и арил-група. У свим масеним спектрима деривата **AS1–AS10** присутан је сигнал хиназолин-4-он јона (m/z 144). Елементална анализа (C, H, N) је показала добру чистоћу једињења. Испитана је антимикробна активност свих синтетисаних једињења према одабраним грам-позитивним и грам-негативним бактеријама. Деривати **AS8** и **AS9** показују најбоље активности у овој серији испитаних једињења.

(Примљено 3. јануара, ревидирано 11. маја, прихваћено 10. јуна 2015)

REFERENCES

1. E. N. Houben, L. Nguyen, J. Pieters, *Curr. Opin. Microbiol*. **9** (2001) 76
2. M. C. Venuti, in *Burger's Medicinal Chemistry and Drug Discovery: Principles and Practice*, 5th ed., M. E. Wolff, Ed., Wiley, New York, 1995, p. 661
3. World Health Organization, Fact sheet No. 104, Reviewed March, 2014, http://www.who.int/mediacentre/factsheets/fs104/en

4. M. Zia-ur-Rehman, J. A. Choudary, S. Ahmad, H. L. Siddiqui, *Chem. Pharm. Bull.* **54** (2006) 1175
5. A. Gürsoy, B. Ünal, N. Karalı, G. Ötük, *Turk. J. Chem.* **29** (2005) 233
6. S. R. Pattan, V. V. K. Reddy, F. V. Manvi, B. G. Desai, A. R. Bhat, *Indian J. Chem., B* **45** (2006) 1778
7. F. R. Pavan, P. I. da S Maia, S. R. Leite, V. M. Deflon, A. A. Batista, D. N. Sato, S. G. Franzblau, C. Q. Leite, *Eur. J. Med. Chem.* **45** (2010) 1898
8. O. Güzel, N. Karali, A. Salman, *Bioorg. Med. Chem.* **16** (2008) 8976
9. N. Karali, A. Gürsoy, F. Kandemirli, N. Shvets, F. B. Kaynak, S. Ozbey, V. Kovalishyn, A. Dimoglo, *Bioorg. Med. Chem.* **15** (2007) 5888
10. D. Sriram, P. Yogeeswari, R. Thirumurugan, R. K. Pavana, *J. Med. Chem.* **49** (2006) 3448
11. D. Sriram, P. Yogeeswari, P. Dhakla, P. Senthilkumar, D. Banerjee, T. H. Manjashetty, *Bioorg. Med. Chem. Lett.* **19** (2009) 1152
12. E. Saripinar, Y. Güzel, S. Patat, I. Yildirim, Y. Akçamur, A. S. Dimoglo, *Arzneim. Forsch.* **46** (1996) 824
13. B. Milczarska, H. Foks, J. Sokołowska, M. Janowiec, Z. Zwolska, Z. Andrzejczyk, *Acta Pol. Pharm.* **56** (1999) 121
14. G. Turan-Zitouni, A. Ozdemir, Z. A. Kaplancikli, K. Benkli, P. Chevallet, G. Akalin, *Eur. J. Med. Chem.* **43** (2008) 981
15. S. N. Pandeya, S. Smitha, M. Jyoti, S. K. Sridhar, *Acta Pharm. (Zagreb, Croatia)* **55** (2005) 27
16. B. Meunier. *Acc. Chem. Res.* **41** (2008) 69
17. V. Alagarsamy, V. R. Solomon, R. V. Sheorey, R. Jayakumar, *Chem. Biol. Drug Des.* **73** (2009) 471
18. V. Alagarsamy, D. Shankar. V. R. Solomon, R. V. Sheorey, P. Parthiban, *Acta Pharm. (Zagreb, Croatia)***59** (2009) 75
19. S. K. Pandey, A. Singh, A. Singh, A. Nizamuddin, *Eur. J. Med. Chem.* **44** (2009) 1188
20. A. M. M. E. Omar, S. A. S. El-Dine, A. A. Ghobashy, M. A. Khalil, *Eur. J. Med. Chem.* **16** (1981) 77
21. G. Krishnamoorthy, *Indian J. Heterocycl. Chem.* **20** (2010) 33
22. A Barry, *Antibiotics in Laboratory Medicine*, 5th ed., William and Wilkins, Baltimore, MD, 1991, p. 1
23. S. N. Pandeya, D. Sriram, G. Nath, E De Clercq, *Farmaco* **54** (1999) 624
24. D. Sriram, P. Yogeeswari, J. S. Basha, D. R. Radha, V. Nagaraja, *Bioorg. Med. Chem.* **13** (2005) 5774
25. P. Shanmugavelan, S. Nagarajan, M. Sathishkumar, A. Ponnuswamy, P. Yogeeswari, D. Sriram, *Bioorg. Med. Chem. Lett.* **21** (2011) 7273
26. J. Kunes, J. Bazant, M. Pour, K. Waisser, M. Slosárek, J. Janota, *Farmaco* **55** (2000) 725
27. V. Alagarsamy, V. R. Solomon, R. Meena, K. V. Ramaseshu, K. Thirumurugan, S. Murugesan, *Med. Chem.* **3** (2007) 67.

Journal of the Serbian Chemical Society
JSCS@tmf.bg.ac.rs • www.shd.org.rs/JSCS
J. Serb. Chem. Soc. 80 (12) S376–S380 (2015) *Supplementary material*

SUPPLEMENTARY MATERIAL TO

Syntheses and antimicrobial activities of 1-(3-benzyl-4-oxo-3,4--dihydroquinazolin-2-yl)-4-(substituted) thiosemicarbazide derivatives

VEERACHAMY ALAGARSAMY[1]*, VISWAS RAJA SOLOMON[1], G. KRISHNAMOORTHY[2], M. T. SULTHANA[1] and B. NARENDAR[1]

[1]Medicinal Chemistry Research Laboratory, MNR College of Pharmacy, Sangareddy, Gr. Hyderabad -502 294, India and [2]Department of Pharmaceutical Chemistry, Periyar College of Pharmaceutical sciences for Girls, Trichy – 620 021, India

J. Serb. Chem. Soc. 80 (12) (2015) 1471–1479

*3-Benzyl-2-thioxo-2,3-dihydro-1*H*-quinazolin-4-one (**4**)*. Yield: 85 %; m.p.: 230–231 °C; Anal. Calcd for $C_{15}H_{12}N_2OS$: C, 67.14; H, 4.51; N, 10.44 %. Found: C, 67.19; H, 4.49; N, 10.46 %; IR (KBr, cm^{-1}): 3200 (NH), 1680 (C=O), 1208 (C=S); ^{1}H-NMR (300 MHz, $CDCl_3$, δ / ppm): 4.65 (2H, *s*, CH_2), 7.01–7.03 (3H, *m*, Ar-H), 7.13 (2H, *d*, J = 7.5 Hz, Ar-H), 7.85–7.91 (4H, *m*, Ar-H), 8.15 (1H, *brs*, NH); ^{13}C-NMR (75 MHz, $CDCl_3$, δ / ppm): 39.75, 120.11, 121.79, 125.69, 126.25, 126.88, 127.23, 127.95, 132.89, 140.75, 145.89, 160.25, 162.89; MS (*m*/*z*): 268 (M^+).

*3-Benzyl-2-(methylsulphanyl)-3*H*-quinazolin-4-one (**5**)*. Yield: 78 %; m.p.: 150–152 °C; Anal. Calcd for $C_{16}H_{14}N_2OS$: C, 68.06; H, 5.00; N, 9.92 %. Found: C, 68.03; H, 5.01; N, 9.96 %; IR (KBr, cm^{-1}): 1681 (C=O), 1616 (C=C); ^{1}H-NMR (300 MHz, $CDCl_3$, δ / ppm): 2.02 (3H, *s*, SCH_3), 4.35 (2H, *s*, CH_2), 7.00–7.02 (3H, *m*, Ar-H), 7.14 (2H, *d*, J = 7.5 Hz, Ar-H), 7.95–7.99 (4H, *m*, Ar-H); ^{13}C-NMR (75 MHz, $CDCl_3$, δ / ppm): 9.85, 39.89, 120.22, 121.65, 125.73, 126.55, 126.87, 127.42, 127.85, 132.65, 140.75, 145.89, 160.35, 162.75; MS (*m*/*z*): 282 (M^+).

*3-Benzyl-2-hydrazino-3*H*-quinazolin-4-one (**6**)*. Yield: 81 %; m.p.: 242–245 °C; Anal. Calcd. for $C_{15}H_{14}N_4O$: C, 67.65; H, 5.30; N, 21.04 %. Found: C, 67.69; H, 5.32; N, 21.09 %; IR (KBr, cm^{-1}): 3383, 3295 ($NHNH_2$), 1677 (C=O); ^{1}H-NMR (300 MHz. $CDCl_3$, δ / ppm): 4.45 (2H, *s*, CH_2), 4.65 (2H, *s*, NH_2), 7.01–7.03 (3H, *m*, Ar-H), 7.14 (2H, *d*, J = 7.5 Hz, Ar-H), 8.01–8.03 (4H, *m*, Ar-H), 9.89 (1H, *s*, NH); ^{13}C-NMR (75 MHz, $CDCl_3$, δ / ppm): 39.89, 120.35,

* Corresponding author. E-mail: drvalagarsamy@gmail.com

121.77, 125.65, 126.55, 126.88, 127.23, 127.95, 132.89, 140.85, 145.91, 160.25, 162.93; MS (*m*/*z*): 266 (M^+).

*1-[3-Benzyl-4-oxo-3,4-dihydroquinazolin-2-yl]-4-[cyclohexyl]hydrazinecarbothioamide (**AS1**)*.[1] Yield: 76 %; m.p.: 215–218 °C; Anal. Calcd. for $C_{22}H_{25}N_5OS$: C, 64.84; H, 6.18; N, 17.18. Found: C, 64.81; H, 6.20; N, 17.22 %; IR (KBr, cm^{-1}): 3247 (NH), 3265 (NH), 3212 (NH), 1616 (C=O), 1600 (C=N), 1220 (C=S); ^{1}H-NMR (300 Hz, $CDCl_3$, δ / ppm): 1.42–1.69 (6H, *m*, CH_2), 1.78 (2H, *s*, CH_2), 1.82 (2H, *s*, CH_2), 2.99 (1H, *s*, CH), 4.72 (2H, *s*, CH_2), 7.11–7.62 (2H, *m*, Ar-H), 7.83–7.98 (1H, *m*, Ar-H), 8.04 (2H, *d*, J = 7.5 Hz, Ar-H), 8.10–8.14 (1H, *m*, Ar-H), 8.17 (2H, *d*, J = 8.0 Hz, Ar-H), 8.19–8.21 (1H, *m*, Ar-H), 8.85 (1H, *s*, NH), 8.96 (1H, *s*, NH), 11.15 (1H, *s*, NH); ^{13}C-NMR (75 MHz, $CDCl_3$, δ / ppm): 22.14, 25.89, 32.33, 39.89, 52.75, 120.56, 123.35, 123.68, 125.28, 127.78, 127.85, 128.61, 130.81, 131.86, 138.75, 158.69, 162.45, 183.74; MS (*m*/*z*): 407 (M^+).

N-*Benzyl-2-(3-benzyl-4-oxo-3,4-dihydroquinazolin-2-yl)hydrazinecarbothioamide (**AS2**)*.[2] Yield: 72 %; m.p.: 231–233 °C; Anal. Calcd. for $C_{23}H_{21}N_5OS$: C, 66.41; H, 5.07; N, 16.83 %. Found: C, 66.38; H, 4.99; N, 16.85 %; IR (KBr, cm^{-1}): 3281 (NH), 3261 (NH), 3233 (NH), 1690 (C=O), 1620 (C=N), 1215 (C=S); ^{1}H-NMR (300 MHz, $CDCl_3$, δ / ppm): 1.31 (2H, *s*, CH_2), 4.31 (2H, *s*, CH_2), 6.32–6.43 (2H, *m*, Ar-H), 6.83–6.91 (2H, *m*, Ar-H), 7.07 (2H, *d*, J = 8.0 Hz, Ar-H), 7.17 (2H, *d*, J = 7.5 Hz, Ar-H), 7.94 (2H, *d*, J = 8.0 Hz, Ar-H), 7.98–8.03 (1H, *m*, Ar-H), 8.10 (2H, *d*, J = 8.0 Hz, Ar-H), 8.31–8.38 (1H, *m*, Ar-H), 8.36 (1H, *s*, NH), 8.91 (1H, *s*, NH), 9.51 (1H, *s*, NH); ^{13}C-NMR (75 MHz, $CDCl_3$, δ / ppm): 39.87, 49.68, 120.71, 123.48, 123.68, 125.28, 125.68, 126.74, 127.22, 127.78, 127.85, 128.61, 130.81, 131.86, 138.75, 140.35, 158.69, 162.35, 183.58; MS (*m*/*z*): 415 (M^+).

2-(3-Benzyl-4-oxo-3,4-dihydroquinazolin-2-yl)-N-*phenylhydrazinecarbothioamide (**AS3**)*.[1] Yield: 72 %; m.p.: 150–153 °C; Anal. Calcd. for $C_{22}H_{19}N_5OS$: C, 65.81; H, 4.77; N, 17.44 %. Found: C, 65.78; H, 4.69; N, 17.39 %; IR (KBr, cm^{-1}): 3389 (NH), 3360 (NH), 3280 (NH), 1675 (C=O), 1600 (C=N), 1168 (C=S); ^{1}H-NMR (300 MHz, $CDCl_3$, δ / ppm): 4.19 (2H, *s*, CH_2), 7.14–7.31 (2H, *m*, Ar-H), 7.51–7.74 (2H, *m*, Ar-H), 7.88 (2H, *d*, J = 8.0 Hz, Ar-H), 8.02 (2H, *d*, J = 7.5 Hz, Ar-H), 8.10 (2H, *d*, J = 8.0 Hz, Ar-H), 8.20–8.32 (1H, *m*, Ar-H), 8.38 (2H, *d*, J = 8.0 Hz, Ar-H), 8.45–8.49 (1H, *m*, Ar-H), 8.95 (1H, *s*, NH), 9.03 (1H, *s*, NH), 10.18 (1H, *s*, NH); ^{13}C-NMR (75 MHz, $CDCl_3$, δ / ppm): 39.77, 120.68, 123.55, 123.74 125.18, 125.36, 126.74, 127.22, 127.78, 127.85, 128.61, 130.81, 131.86, 138.75, 140.35, 158.69, 162.75, 183.75; MS (*m*/*z*): 401 (M^+).

2-(3-Benzyl-4-oxo-3,4-dihydroquinazolin-2-yl)-N-*(2-methylphenyl)hydrazinecarbothioate (**AS4**)*. Yield: 78 %; m.p.: 190–193 °C; Anal. Calcd. for $C_{23}H_{21}N_5OS$: C, 66.48; H, 5.09; N, 16.85 %. Found: C, 67.01; H, 5.20; N, 16.83

%; IR (KBr, cm^{-1}): 3323 (NH), 3305 (NH), 3274 (NH), 1604 (C=O), 1610 (C=N), 1243 (C=S); ^{1}H-NMR (300 MHz, $CDCl_3$, δ / ppm): 2.42 (3H, *s*, CH_3), 4.71 (2H, *s*, CH_2), 6.80 (1H, *brs*, NH), 6.71–6.78 (2H, *m*, Ar-H), 7.01–7.08 (1H, *m*, Ar-H), 7.25 (2H, *d*, *J* = 7.5 Hz, Ar-H), 7.48 (2H, *d*, *J* = 7.5 Hz, Ar-H), 7.66 (2H, *d*, *J* = 7.5 Hz, Ar-H), 7.83–7.92 (1H, *m*, ArH), 7.99 (2H, *d*, *J* = 7.5 Hz, Ar-H), 8.32–8.41 (1H, *m*, Ar-H), 8.86 (1H, *brs*, NH), 10.50 (1H, *brs*, NH); ^{13}C--NMR (75 MHz, $CDCl_3$, δ / ppm): 12.58, 39.85, 120.68, 123.55, 123.74 125.18, 125.36, 126.74, 127.22, 127.78, 127.85, 128.61, 130.81, 131.86, 138.75, 138.85, 140.35, 158.69, 162.75, 181.75; MS (*m*/*z*): 415 (M^+).

2-(3-Benzyl-4-oxo-3,4-dihydroquinazolin-2-yl)-N-*(4-methylphenyl)hydrazinecarbothioate (**AS5**)*.[3] Yield: 74 %; m.p.: 260–263 °C; Anal. Calcd. for $C_{23}H_{21}N_5OS$: C, 66.48; H, 5.09; N, 16.85 %. Found: C, 66.50; H, 5.12; N, 16.87 %; IR (KBr, cm^{-1}): 3340 (NH), 3288 (NH), 3259 (NH), 1612 (C=O), 1174 (C=N), 1255 (C=S); ^{1}H-NMR ($CDCl_3$, δ / ppm): 2.56 (3H, *s*, CH_3), 4.78 (2H, *s*, CH_2), 6.85 (1H, *brs*, NH), 7.09–7.13 (2H, *m*, Ar-H), 7.25–7.36 (1H, *m*, Ar-H), 7.55 (2H, *d*, *J* = 7.5 Hz, Ar-H), 7.81 (2H, *d*, *J* = 8.0 Hz, Ar-H), 7.87 (2H, *d*, *J* = = 7.5 Hz, Ar-H), 7.92–7.96 (1H, *m*, Ar-H), 8.00 (2H, *d*, *J* = 8.0 Hz, Ar-H), 8.06––8.09 (1H, *m*, Ar-H), 8.94 (1H, *brs*, NH), 10.62 (1H, *brs*, NH); ^{13}C-NMR (75 MHz, $CDCl_3$, δ / ppm): 12.98, 39.85, 120.52, 123.71, 123.84, 125.42, 125.87, 126.74, 127.22, 127.78, 127.85, 128.61, 130.81, 131.86, 138.75, 140.45, 158.69, 162.59, 183.61; MS (*m*/*z*): 415 (M^+).

2-(3-Benzyl-4-oxo-3,4-dihydroquinazolin-2-yl)-N-*3-methoxyphenylhydrazinecarbothioate (**AS6**)*.[1] Yield: 70 %; m.p.: 205–208 °C; Anal. Calcd. for $C_{23}H_{21}N_5O_2S$: C, 64.02; H, 4.91; N, 16.23 %. Found: C, 64.01; H, 4.88; N, 16.32 %; IR (KBr, cm^{-1}): 3353 (NH), 3321 (NH), 3274 (NH), 1640 (C=O), 1621 (C=N), 1286 (OCH_3), 1243 (C=S); ^{1}H-NMR (300 MHz, $CDCl_3$, δ / ppm): 2.31 (3H, *s*, OCH_3), 5.23 (2H, *s*, CH_2), 6.83 (1H, *brs*, NH), 7.13–7.17 (1H, *m*, Ar-H), 7.21–7.25 (2H, *m*, Ar-H), 7.34 (2H, *d*, *J* = 7.5 Hz, Ar-H), 7.45 (2H, *d*, *J* = 8.0 Hz, Ar-H), 7.54 (2H, *d*, *J* = 7.5 Hz, Ar-H), 7.59–7.62 (1H, *m*, Ar-H), 7.68 (2H, *d*, *J* = 7.5 Hz, Ar-H), 8.06–8.09 (1H, *m*, Ar-H), 8.53 (1H, *brs*, NH), 10.31 (1H, *brs*, NH); ^{13}C-NMR (75 MHz, $CDCl_3$, δ / ppm): 39.89, 53.85, 108.75, 109.87, 117.85, 120.48, 123.51, 123.25, 125.42, 127.53, 127.85, 128.61, 129.57, 129.99, 130.81, 131.86, 137.57, 138.75, 158.69, 162.42, 179.53; MS (*m*/*z*): 431 (M^+).

2-(3-Benzyl-4-oxo-3,4-dihydroquinazolin-2-yl)-N-*4-methoxyphenylhydrazinecarbothioate (**AS7**)*. Yield: 79 %; m.p.: 210–212 °C; Anal. Calcd. for $C_{23}H_{21}N_5O_2S$: C, 64.02; H, 4.91; N, 16.23 %. Found: C, 64.05; H, 4.92; N, 16.26 %; IR (KBr, cm^{-1}): 3310 (NH), 3300 (NH), 3260 (NH), 1682 (C=O), 1608 (C=N), 1290 (OCH_3), 1212 (C=S); ^{1}H-NMR (300 MHz, $CDCl_3$, δ / ppm): 3.92 (3H, *s*, OCH_3), 4.15 (2H, *s*, CH_2), 6.52 (1H, *brs*, NH), 6.52–6.56 (1H, *m*, Ar-H), 6.91–6.94 (2H, *m*, Ar-H), 7.24 (2H, *d*, *J* = 7.5 Hz, Ar-H), 7.33 (2H, *d*, *J* = 8.0 Hz, Ar-H), 7.42 (2H, *d*, *J* = 7.5 Hz, Ar-H), 7.82–7.88 (1H, *m*, Ar-H), 8.13 (2H, *d*, *J* =

= 7.5 Hz, Ar-H), 8.21–8.26 (1H, *m*, ArH), 8.81 (1H, *brs*, NH), 10.63 (1H, *brs*, NH); ^{13}C-NMR (75 MHz, $CDCl_3$, δ / ppm): 39.75, 53.75, 120.61, 123.85, 123.98, 125.42, 125.87, 126.74, 127.22, 127.78, 127.85, 128.35, 128.61, 130.81, 131.86, 138.75, 140.45, 156.79, 162.59, 181.61; MS (*m*/*z*): 431 (M^+).

2-(3-Benzyl-4-oxo-3,4-dihydroquinazolin-2-yl)-N-*(4-chlorophenyl)hydrazinecarbothioate (**AS8**)*. Yield: 83 %; m.p.: 188–190 °C; Anal. Calcd. for $C_{22}H_{18}ClN_5OS$: C, 60.47; H, 4.12; N, 16.01 %. Found: C, 60.45; H, 4.13; N, 16.06 %; IR (KBr, cm^{-1}): 3321 (NH), 3310 (NH), 3221 (NH), 1690 (C=O), 1620 (C=N), 1210 (C=S); ^{1}H-NMR (300 MHz, $CDCl_3$, δ / ppm): 4.36 (2H, *s*, CH_2), 6.52–6.57 (2H, *m*, Ar-H), 6.92–6.95 (1H, *m*, Ar-H), 7.07 (2H, *d*, *J* = 7.5 Hz, Ar-H), 7.14 (2H, *d*, *J* = 7.5 Hz, Ar-H), 7.65 (2H, *d*, *J* = 7.5 Hz, Ar-H), 7.81–7.84 (1H, *m*, Ar-H), 7.91 (2H, *d*, *J* = 8.0 Hz, Ar-H), 7.93–7.97 (1H, *m*, Ar-H), 9.21 (1H, *brs*, NH), 10.51 (1H, *brs*, NH); ^{13}C-NMR (75 MHz, $CDCl_3$, δ / ppm): 39.75, 120.45, 123.77, 123.89, 125.23, 125.87, 126.81, 127.09, 127.58, 128.34, 127.99, 128.61, 130.81, 131.86, 138.75, 140.45, 156.79, 162.59, 181.61; MS (*m*/*z*): 435 (M^+).

2-(3-Benzyl-4-oxo-3,4-dihydroquinazolin-2-yl)-N-*(4-nitrophenyl)hydrazinecarbothioate (**AS9**)*. Yield: 72 %; m.p.: 251–253 °C; Anal. calcd. for $C_{22}H_{18}N_6O_3S$: C, 59.02; H, 4.02; N, 18.83 %. Found: C, 59.06; H, 4.00; N, 18.85 %; IR (KBr, cm^{-1}): 3342 (NH), 3313 (NH), 3262 (NH), 1691 (C=O), 1615 (C=N), 1222 (C=S); ^{1}H-NMR (300 MHz. $CDCl_3$, δ / ppm): 4.22 (2H, *s*, CH_2), 6.61–6.65 (2H, *m*, Ar-H), 6.72–6.78 (1H, *m*, ArH), 7.07 (2H, *d*, *J* = 8.0 Hz, Ar-H), 7.15 (2H, *d*, *J* = 8.0 Hz, Ar-H), 7.44 (2H, *d*, *J* = 7.5 Hz, Ar-H), 7.78–7.80 (1H, *m*, Ar-H), 7.91 (2H, *d*, *J* = 7.5 Hz, Ar-H), 7.93–7.95 (1H, *m*, A-rH), 8.62 (1H, *brs*, NH), 8.81 (1H, *brs*, NH), 10.51 (1H, *brs*, NH); ^{13}C-NMR (75 MHz, $CDCl_3$ δ ppm): 39.83, 120.39, 123.47, 123.84, 125.42, 125.87, 126.74, 127.22, 127.78, 127.85, 128.35, 128.61, 130.81, 131.66, 138.75, 139.45, 158.69, 161.79, 181.61; MS (*m*/*z*): 446 (M^+).

2-(3-Benzyl-4-oxo-3,4-dihydroquinazolin-2-yl)-N-*(pyridin-2-yl)hydrazinecarbothioate (**AS10**)*. Yield: 79 %; m.p.: 171–172 °C; Anal. Calcd. for $C_{21}H_{18}N_6OS$: C, 62.53; H, 4.45; N, 21.03 %. Found: C, 62.56; H, 4.46; N, 21.05 %; IR (KBr, cm^{-1}): 3350 (NH), 3323 (NH), 3242 (NH), 1691 (C=O), 1615 (C=N), 1210 (C=S); ^{1}H-NMR ($CDCl_3$, δ / ppm): 4.12 (2H, *s*, CH_2), 6.50–6.53 (1H, *m*, Ar-H), 6.51–6.53 (2H, *m*, ArH), 7.25 (2H, *d*, *J* = 8.0 Hz, Ar-H), 7.17 (2H, *d*, *J* = 8.0 Hz, Ar-H), 7.13 (2H, *d*, *J* = 7.5 Hz, Ar-H), 7.35–7.39 (1H, *m*, Ar-H), 7.44 (2H, *d*, *J* = 7.5 Hz, Ar-H), 7.64–7.66 (1H, *m*, Ar-H), 8.35 (1H, *s*, NH), 8.82 (1H, *s*, NH), 9.50 (1H, *s*, NH); ^{13}C-NMR (75 MHz, $CDCl_3$ δ / ppm): 39.83, 108.75, 112.89, 120.48, 123.51, 123.25, 125.42, 127.53, 127.85, 128.35, 128.61, 130.81, 131.86, 137.89, 138.75, 147.75, 157.85, 158.69, 161.78, 181.25; MS (*m*/*z*): 402 (M^+).

REFERENCES

1. S. K. Pandey, A. Singh, A. Singh, A. Nizamuddin, *Eur. J. Med. Chem*. **44** (2009) 1188
2. A. M. M. E. Omar, S. A. S. El-Dine, A. A. Ghobashy, M. A. Khalil, *Eur. J. Med. Chem*. **16** (1981) 77
3. G. Krishnamoorthy, *Indian J. Heterocycl. Chem*. **20** (2010) 33.

Journal of the Serbian Chemical Society
JSCS-info@shd.org.rs • www.shd.org.rs/JSCS
J. Serb. Chem. Soc. 80 (12) 1481–1488 (2015)
JSCS–4813
UDC 547.586.2:547.447.4:548.7:542.913:535.4:57–188
Short communication

SHORT COMMUNICATION

Synthesis, crystal structure and local anti-inflammatory activity of the L-phenylalanine methyl ester derivative of dexamethasone-derived cortienic acid

VLADIMIR DOBRIČIĆ[1]*, BOJANA M. FRANCUSKI[2], VESNA JAĆEVIĆ[3], MARKO V. RODIĆ[4#], SOTE VLADIMIROV[1#], OLIVERA ČUDINA[1] and DJORDJE FRANCUSKI[5]

[1]*University of Belgrade – Faculty of Pharmacy, Vojvode Stepe 450, 11000 Belgrade, Serbia,* [2]*Vinča Institute of Nuclear Sciences, Laboratory of Theoretical Physics and Condensed Matter Physics, University of Belgrade, P. O. Box 522, 11001 Belgrade, Serbia,* [3]*National Poison Control Centre, Medical Faculty, Military Medical Academy, University of Defense, Crnotravska 17, 11000 Belgrade, Serbia,* [4]*Faculty of Sciences, University of Novi Sad, Trg D. Obradovića 3, 21000 Novi Sad, Serbia and* [5]*Institute of Molecular Genetics and Genetic Engineering, University of Belgrade, Vojvode Stepe 444a, P. O. Box 23, 11010 Belgrade, Serbia*

(Received 5 May, revised 6 July, accepted 4 August 2015)

Abstract: The L-phenylalanine methyl ester derivative of dexamethasone-derived cortienic acid (DF) was synthesized and its crystal structure characterized by the X-ray diffraction method. The crystal system is orthorhombic with space group $P2_12_12_1$ and cell constants a = 8.2969(3) Å, b = 18.9358(8) Å, c = 20.0904(6) Å, V = 3156.4(2) Å^3 and Z = 4. Ring A of the steroid nucleus and phenyl ring in the 17β-side chain are almost planar. Rings B and C have a slightly distorted chair conformation, whereas ring D has an envelope conformation. The packing of DF is characterized by a network of intermolecular hydrogen bonds involving the O4 atom from one side of the steroid nucleus and O1 and F1 atoms from the other side as hydrogen bond acceptors. Apart from the intermolecular hydrogen bonds in the crystal packing, there are also numerous intramolecular hydrogen bonds of the N–H···O, C–H···O and C–H···F type. The local anti-inflammatory activity of DF was evaluated using the croton oil-induced ear oedema test. This derivative achieved maximal inhibition of ear oedema at significantly lower concentration in comparison with dexamethasone.

Keywords: 17β-carboxamide steroids; X-ray diffraction; biological activity; ear oedema test.

* Corresponding author. E-mail: vladimir@pharmacy.bg.ac.rs
# Serbian Chemical Society member.
doi: 10.2298/JSC150505067D

INTRODUCTION

Soft glucocorticoids are compounds synthesized using the retrometabolic approach and usually administered locally near the site of action. After local administration, these derivatives are easily biotransformed to non-toxic and inactive metabolites, resulting in fewer side effects than traditional glucocorticoids. The first (loteprednol etabonate) and second (etiprednol dicloacetate) generations of soft glucocorticoids are derived from cortienic acid (an inactive glucocorticoid metabolite).[1–3] Generally, other derivatives of glucocorticoids that are easily metabolized after local administration to non-toxic and inactive metabolites could also be denoted as soft (antedrug) glucocorticoids.[4] Several groups of 7β-carboxamide steroids were synthesized and tested for glucocorticoid activity. Some of these compounds showed significant glucocorticoid activity (inhibition of phytohaemagglutinin-induced blastogenesis of lymphocytes).[5–7] However, their metabolic properties and toxicity have not been tested so far.

A novel class of 17β-carboxamide derivatives of glucocorticoids was recently presented. These derivatives are amides of cortienic acids obtained from hydrocortisone, prednisolone, methylprednisolone, dexamethasone and betamethasone with amino acids. Molecular docking calculations indicate that introduction of an amino acid moiety in the 17β side chain enables favourable orientation in the glucocorticoid receptor (GR) and key binding interactions with the amino acids from the GR.[8] Their permeability and retention in human skin were predicted by use of *in vitro* tests – parallel artificial membrane permeability assay (PAMPA) and biopartitioning micellar chromatography.[9,10] According to these results, L-phenylalanine methyl ester derivatives should have significant local anti-inflammatory activity and a better skin retention/permeability ratio in comparison with corresponding parent glucocorticoids.

The aim of this study was to synthesize the L-phenylalanine methyl ester derivative of dexamethasone-derived cortienic acid (DF), perform crystallographic analysis of its structure and test the local anti-inflammatory activity of this derivative.

EXPERIMENTAL

Materials and methods

Dexamethasone was purchased from Tokyo Chemical Industry (Tokyo, Japan), whereas *N*-hydroxybenzotriazole (HOBt), *N*,*N*′-dicyclohexylcarbodiimide (DCC), croton oil, acetonitrile, *N*,*N*-dimethylformamide (DMF) and silica gel for preparative thin-layer chromatography were purchased from Sigma–Aldrich (Steinheim, Germany). Triethylamine (TEA) and L-phenylalanine methyl ester hydrochloride were purchased from Acros Organics (Geel, Belgium), chloroform and methanol from JT Baker (Loughborough, UK) and acetone from Zorka (Šabac, Serbia). Silica gel for column chromatography was purchased from Merck (Darmstadt, Germany).

Apparatus

The melting point was determined using a Boetius PHMK 05 apparatus (Radebeul, Germany). The UV spectrum was recorded on an Evolution 300 spectrophotometer (Thermo Scientific, UK), whereas the IR spectrum was recorded using a Nicolet iS10 ATR-FTIR spectrophotometer (Thermo Scientific, Madison, WI, USA). The ^{1}H- and ^{13}C-NMR spectra were acquired on a Bruker Avance III 400 NMR spectrometer (Bruker Biospin GmbH, Rheinstetten, Germany), operating at 400 MHz for protons and 100 MHz for carbons. The accurate mass was determined using an Agilent 6210 time-of-flight mass spectrometer (Agilent Technologies, Palo Alto, CA, USA). The crystallographic data were collected on an Oxford Diffraction Gemini S diffractometer.

Synthesis

The precursor (dexamethasone-derived cortienic acid, CD) was synthesized by periodic acid oxidation of dexamethasone, following a reported method.[9]

DF was synthesized from CD and L-phenylalanine methyl ester hydrochloride by use of DCC, HOBt and TEA according to a reported procedure,[8] which was a modification of a previously published method.[11] CD (53 mg, 0.14 mmol, 1 eq) was dissolved in DMF (2 mL) and the solution was cooled to 0 °C. Subsequently, DCC (58 mg, 0.28 mmol, 2 eq) and HOBt (28 mg, 0.21 mmol, 1.5 eq) were added. The mixture was stirred at 0 °C for 1 h and thereafter maintained at a temperature not exceeding 8 °C for 15 h. L-Phenylalanine methyl ester hydrochloride (30 mg, 0.14 mmol, 1 eq) was dissolved in DMF (1 mL), TEA was added (39 μL, 2 eq) and the mixture was cooled to 0 °C. Finally, the mixture of CD, DCC and HOBt was filtered and added dropwise. This reaction mixture was stirred at 0 °C for 1 h and maintained at a temperature not exceeding 8 °C for 15 h. The reaction mixture was filtered and evaporated to dryness under reduced pressure. Column chromatography was employed for the initial purification of the reaction mixture, whereas the final purification was realised by preparative thin-layer chromatography. Mobile phase used for column chromatography purification was chloroform/methanol 99:1 (*V*/*V*), whereas the mobile phase used for the purification by preparative thin-layer chromatography was chloroform/methanol 95:5 (*V*/*V*). The purified compound was recrystallized from water/acetonitrile 50:50 (*V*/*V*). Yield: 83.5 %.

X-Ray crystallography

Details of crystal data, data collection and structure refinement are summarized in Table S-I of the Supplementary material to this paper.

The structure was solved by the direct method using the program SHELXS-97[12] and refined by SHELXL-97.[13] The H atoms bonded to the N and O atoms were located from difference Fourier maps and the H atoms bonded to C atoms were placed at the geometrically calculated positions and refined using a riding model. C–H distances were fixed at 0.93 Å for aromatic C atoms, 0.97 Å for secondary C–H2 groups, 0.98 Å for tertiary C–H groups and 0.96 Å for methyl C–H3 groups. Their U_{iso}(H) values are equal to 1.2U_{eq} of the corresponding C atom, except for the methyl groups where the U_{iso}(H) values were set to 1.5U_{eq}(C). In the absence of significant anomalous scattering, the absolute configuration could not be reliably determined and any reference to the Flack parameter[14] was removed. In the phenyl ring, atoms C27, C28 and C29 show slightly elongated atomic displacement ellipsoids. Attempts to model disorder for the rings, even by employing extensive restraints, proved fruitless. Examination of the refined structure using PLATON[15] revealed a total void volume of 280 Å^3 distributed over two sites (–0.060, 0.250, 0.500) and (0.031, 0.750, 0.000).

Local anti-inflammatory activity assay

The local anti-inflammatory activities of DF and dexamethasone were evaluated using the croton oil-induced ear oedema test,[16-19] following the procedure described elsewhere.[8] The experimental procedure was in accordance with the institutional guidelines for care and use of animals in research No 03/10-2013 (Ethics Committee in research of the Military Medical Academy, Belgrade, Serbia). Croton oil solution (35 μg mL^{-1}), five solutions of DF (1.15, 2.29, 4.58, 9.17 and 13.75 μM) and five solutions of dexamethasone (9.17, 13.75, 27.50, 36.70 and 45.80 μM) were prepared in acetone. Eleven groups of experimental animals were formed – a control group and ten test groups (five groups for DF and five groups for dexamethasone, each containing five rats).

RESULTS AND DISCUSSION

Synthesis and physicochemical characterization

DF was previously synthesized using a single-step procedure, which utilizes 1-ethyl-3-(3-(dimethylamino)propyl)carbodiimide (EDC), HOBt and TEA.[9] In this paper, an alternative two-step synthesis of DF is presented (Scheme 1). By use of the two-step procedure, DF was synthesized in good yield (83.5 %), which is significantly higher in comparison with that obtained using the single-step synthesis (52.1 %).

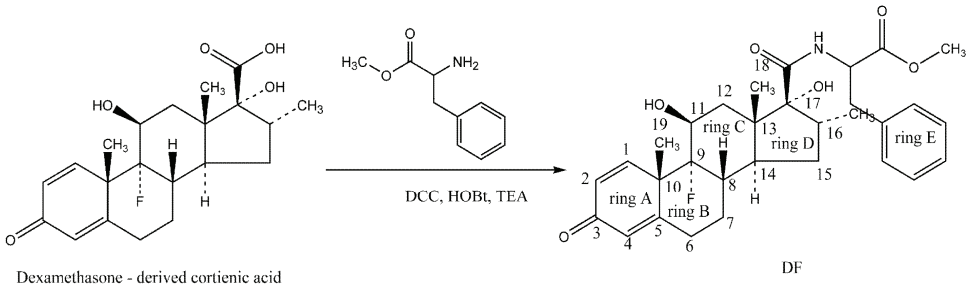

Scheme 1. Synthesis of DF.

DF was characterized by determining the melting point as well as by use of spectroscopy techniques (UV, IR, NMR, MS/MS and MS-TOF spectroscopy). The physical, analytical and spectral data for the title compound are given in the Supplementary material to this paper.

Crystal structure

DF crystallizes in the space group $P2_12_12_1$. Its molecular structure with the atom-labelling scheme is shown in Fig. 1. Selected bond lengths and bond angles are listed in Table S-II of the Supplementary material to this paper.

There are four fused rings, one five-membered (D) and three six-membered (A, B and C) rings. The five-membered ring D has an envelope conformation, with atom C13 at the flap position displaced by 0.757(2) Å from the best plane of the other four C atoms of the D ring ($Q(2)$ = 0.5038(17) Å, $\varphi(2)$ = 177.6(2)°).

The cyclohexane rings B and C have a slightly distorted chair conformation. The key puckering parameter[20] for a chair conformation should be $\theta = 0°$ for an ideal chair. The values of θ are 10.16(18) and 9.26(18)° for rings B and C, respectively. Other puckering parameters for ring B are Q = 0.5607(18) Å and φ = = 283.6(10)°, whereas for ring C, they are Q = 0.5311(17) Å and φ = 271.9(11)°. Rings A (C1–C2–C3–C4–C5–C10) and E (C24–C25–C26–C27–C28–C29) are almost planar with an average atom displacement of 0.015 Å for C24–C25–C26––C27–C28–C29 and 0.010 Å for C1–C2–C3–C4–C5–C10 from the plane defined by all atoms of the cyclohexane ring.

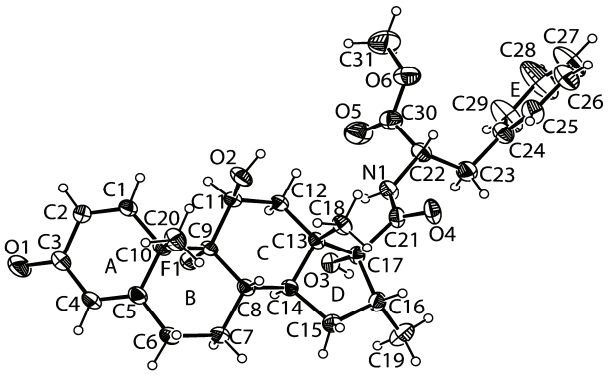

Fig. 1. Molecular structure of DF showing the atom-labelling scheme. Displacement ellipsoids are drawn at the 30 % probability level. The H atoms are shown as small circles of arbitrary radii.

The bonds C10–C20 and C9–F1 adopt the axial position at 2.95(10) and 8.89(9)°, respectively, with respect to ring B of the steroid nucleus, whereas bond C16–C19 occupies a bisectional position at 56.1(1)° with respect to ring D. Bonds C13–C18 and C11–O2 adopt axial positions at 5.43(9) and 15.50(10)°, respectively, with respect to the ring C of the steroid nucleus.

The length of the steroid nucleus C3···C16 is 8.586 Å and the dihedral angle between the mean planes of the steroid nucleus and the phenyl moiety (ring E) is 78.73(12)°.

The packing of DF is characterized by a network of hydrogen bonds involving the O4 atom from one side of the steroid nucleus and the O1 and F1 atoms from the other side as hydrogen bond acceptors. In the crystallographic *b* direction, chain growth is ensured by means of the O3–H···O1 and C29–H···F1 interactions, forming a zigzag pattern (Fig. 2a and Table S-III of the Supplementary material). Similar zigzag pattern is formed down the crystallographic *a*-axis by O2–H···O4 hydrogen bonds (Fig. 2b and Table S-III). Besides the intermolecular hydrogen bonds in the crystal packing, there are numerous intramolecular hydrogen bonds of the N–H···O, C–H···O and C–H···F type (Table S-III).

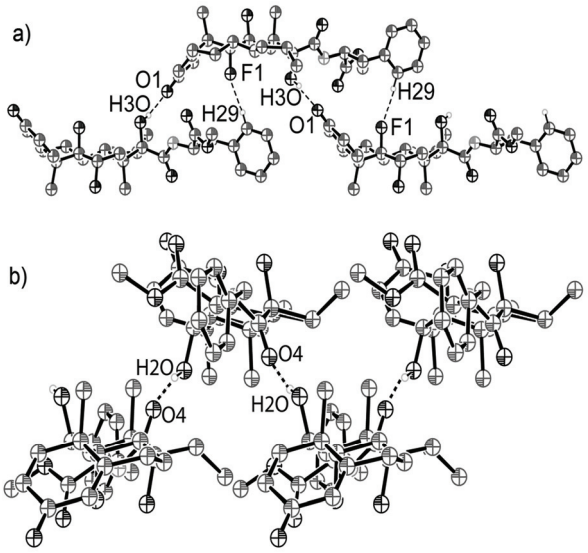

Fig. 2. The crystal packing of DF viewed down: a) [100] showing the O3–H3O…O1 and C29––H29…F1 hydrogen bonds, and b) [010] showing the O2––H2O…O4 hydrogen bond. The hydrogen bonds are shown as dotted lines. For clarity H atoms not participating in the interactions are omitted.

Local anti-inflammatory activity

Maximal inhibition of ear oedema caused by DF (29.54 %) was lower than the maximal inhibition caused by dexamethasone (55.54 %). However, DF could be applied at a lower concentration, because this derivative caused maximal inhibition of ear oedema at a significantly lower concentration (4.58 μM) in comparison with dexamethasone (45.8 μM). Additionally, DF should have significantly better skin retention/permeability ratio.[9] The local anti-inflammatory profile of DF is presented in Fig. 3.

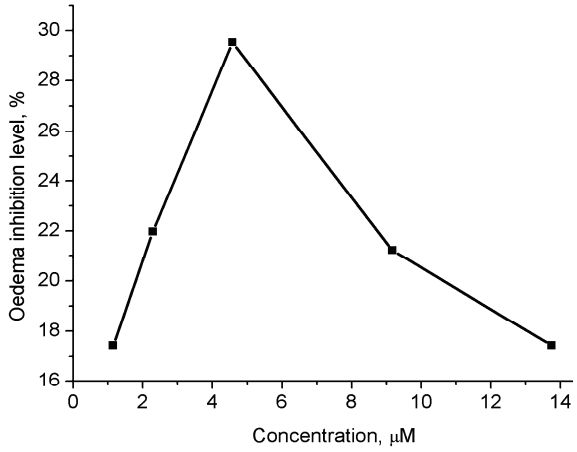

Fig. 3. Local anti-inflammatory profile of DF.

CONCLUSIONS

The L-phenylalanine methyl ester derivative of dexamethasone-derived cortienic acid (DF) was synthesized and structurally characterized. This derivative is a potential soft drug with fewer side effects and a better skin retention/permeability ratio than dexamethasone. Its crystal structure was characterized by the X-ray diffraction method. Ring A of the steroid nucleus and the phenyl ring (17β-side chain) are almost planar, rings B and C have a slightly distorted chair conformation and ring D has an envelope conformation. Hydrogen bonds that influence crystal packing of this derivative were identified, *i.e.*, O2–H···O4 (crystallographic *a* direction), and O3–H···O1 and C29–H···F1 interactions (crystallographic *b* direction). The local anti-inflammatory activity of DF was evaluated by the croton oil-induced ear oedema test. This derivative possesses local anti-inflammatory activity with the maximal inhibition of ear oedema achieved at significantly lower concentration in comparison with dexamethasone.

SUPPLEMENTARY MATERIAL

The physical, spectral and crystal data for DF, selected bond lengths and angles, as well as hydrogen bond geometry of DF are available electronically from http://www.shd.org.rs/JSCS/, or from the corresponding author on request.

Crystallographic data for the structure reported in this paper have been deposited with the Cambridge Crystallographic Data Centre with deposition number CCDC-1034681. Copies of these can be obtained free of charge on written application to CCDC, 12 Union Road, Cambridge, CB2 1EZ, UK (fax: +44 1223 336033); on request by e-mail to deposit@ccdc.cam.ac.uk or by access to http://www.ccdc.cam.ac.uk.

Acknowledgements. The first two authors contributed equally to this work, which was financially supported by the Ministry of Education, Science and Technological Development of the Republic of Serbia, as parts of Projects No. 172041, 172014 and 172035.

ИЗВОД

СИНТЕЗА, КРИСТАЛНА СТРУКТУРА И ЛОКАЛНА АНТИИНФЛАМАТОРНА АКТИВНОСТ ДЕРИВАТА КОРТИЕНСКЕ КИСЕЛИНЕ ИЗ ДЕКСАМЕТАЗОНА И МЕТИЛ-ЕСТРА L-ФЕНИЛАЛАНИНА

ВЛАДИМИР ДОБРИЧИЋ[1], БОЈАНА М. ФРАНЦУСКИ[2], ВЕСНА ЈАЋЕВИЋ[3], МАРКО В. РОДИЋ[4], СОТЕ ВЛАДИМИРОВ[1], ОЛИВЕРА ЧУДИНА[1] и ЂОРЂЕ ФРАНЦУСКИ[5]

[1]Универзитет у Београду – Фармацеутски факултет, Војводе Степе 450, 11000 Београд, [2]Институт за нуклеарне науке "Винча", Лабораторија за теоријску физику и физику кондензоване материје, Универзитет у Београду, п. пр. 522, 11001 Београд, [3]Национални центар за контролу тровања, Медицински факултет Војномедицинске академије, Универзитет одбране, Црнотравска 17, 11000 Београд, [4]Природно–математички факултет, Универзитет у Новом Саду, Трг Д. Обрадовића 3, 21000 Нови Сад, и [5]Институт за молекуларну генетику и генетичко инжењерство, Универзитет у Београду, Војводе Степе 444а, п. пр. 23, 11010 Београд

Синтетисан је дериват кортиенске киселине из дексаметазона и метил-естра L-фенилаланина (DF), а кристална структура овог једињења окарактерисана је методом дифракције X-зрака. Кристални систем је орторомбичан, са просторном групом $P2_12_12_1$ и константама a = 8,2969(3) Å^3, b = 18,9358(8) Å^3, c = 20,0904(6) Å^3, V = 3156,4 Å^3 и

Z = 4. Прстен A стероидне структуре и бензенов прстен у 17β-бочном низу су скоро планарни. Прстенови B и C су у благо искривљеној конформацији столице, док је прстен D у конформацији коверте. Кристална структура DF се карактерише мрежом интермолекулских водоничних веза преко којих се атом O4 са једне стране стероидне структуре повезује са атомима O1 и F1 (акцептори водоничне везе) са друге стране стероидне структуре. Поред интермолекулских, присутне су и бројне интрамолекулске водоничне везе N–H···O, C–H···O и C–H···F типа. Локална антиинфламаторна активност DF је испитана применом теста инхибиције едема уха изазваног кротонским уљем. Овај дериват постиже максималну инхибицију едема уха при значајно нижој концентрацији у односу на дексаметазон.

(Примљено 5. маја, ревидирано 6. јула, прихваћено 4. августа 2015)

REFERENCES

1. N. Bodor, P. Buchwald, *Curr. Pharm. Des.* **12** (2006) 3241
2. N. Chandegara, M. Chorawala, *Int. J. Pharm. Sci. Res.* **3** (2012) 311
3. N. Bodor, P. Buchwald, *Med. Res. Rev.* **20** (2000) 58
4. M. O. F. Khan, H. J. Lee, *Chem. Rev.* **108** (2008) 5131
5. P. A. Formstecher, P. Lefebvre, T. Burollaud, *J. Pharm. Belg.* **46** (1991) 37
6. B. Manz, M. Rehder, A. Heubner, R. Kreienberg, H. J. Grill, K. Pollow, *J. Clin. Chem. Clin. Biochem.* **22** (1984) 209
7. B. Manz, J. Grill, R. Kreienberg, M. Rehder, K. Pollow, *J. Clin. Chem. Clin. Biochem.* **21** (1983) 69
8. V. Dobričić, B. Marković, N. Milenković, V. Savić, V. Jaćević, N. Rančić, S. Vladimirov, O. Čudina, *Arch. Pharm. (Weinheim, Germany)* **347** (2014) 786
9. V. Dobričić, B. Marković, K. Nikolic, S. Vladimirov, O. Čudina, *Eur. J. Pharm. Sci.* **52** (2014) 95
10. V. Dobričić, K. Nikolic, S. Vladimirov, O. Čudina, *Eur. J. Pharm. Sci.* **56** (2014) 105
11. P. Formstecher, P. Lustenberger, M. Dautrevaux, *Steroids* **35** (1980) 265
12. G. M. Sheldrick, *SHELXS97: Program for Crystal Structure solution*, University of Göttingen, Göttingen, 1997
13. G. M. Sheldrick, *SHELXL97: Program for crystal structure refinement*, University of Göttingen, Göttingen, 1997
14. H. D. Flack, *Acta Crystallogr., A* **39** (1983) 876
15. A. L. Spek, *Acta Crystallogr., A* **46** (1990) C34
16. G. Tonelli, L. Thibault, I. Ringler, *Endocrinology* **77** (1965) 625
17. L. Baumgartner, S. Sosa, A. Atanasov, A. Bodensieck, N. Fakhrudin, J. Bauer, G. Del Favero, C. Ponti, E. Heiss, S. Schwaiger, A. Ladurner, U. Widowitz, R. Della Loggia, J. Rolinger, O. Werz, R. Bauer, V. Dirsch, A. Tubaro, H. Stuppner, *J. Nat. Prod.* **74** (2011) 1779
18. A. Tubaro, P. Dri, G. Delbello, C. Zilli, R. Della Loggia, *Agents Actions* **17** (1985) 347
19. A. Vassallo, N. De Tommasi, I. Merfort, R. Sanogo, L. Severino, M. Pelin, R. Della Logia, A. Tubaro, S. Sosa, *Phytochemistry* **96** (2013) 288
20. D. Cremer, J. A. Pople, *J. Am. Chem. Soc.* **97** (1975) 1354.

Journal of the Serbian Chemical Society
JSCS@tmf.bg.ac.rs • www.shd.org.rs/JSCS
J. Serb. Chem. Soc. 80 (12) S381–S384 (2015) *Supplementary material*

SUPPLEMENTARY MATERIAL TO

Synthesis, crystal structure and local anti-inflammatory activity of the L-phenylalanine methyl ester derivative of dexamethasone-derived cortienic acid

VLADIMIR DOBRIČIĆ[1]*, BOJANA M. FRANCUSKI[2], VESNA JAĆEVIĆ[3], MARKO V. RODIĆ[4], SOTE VLADIMIROV[1], OLIVERA ČUDINA[1] and DJORDJE FRANCUSKI[5]

[1]University of Belgrade – Faculty of Pharmacy, Vojvode Stepe 450, 11000 Belgrade, Serbia, [2]Vinča Institute of Nuclear Sciences, Laboratory of Theoretical Physics and Condensed Matter Physics, University of Belgrade, P. O. Box 522, 11001 Belgrade, Serbia, [3]National Poison Control Centre, Medical Faculty, Military Medical Academy, University of Defense, Crnotravska 17, 11000 Belgrade, Serbia, [4]Faculty of Sciences, University of Novi Sad, Trg D. Obradovića 3, 21000 Novi Sad, Serbia and [5]Institute of Molecular Genetics and Genetic Engineering, University of Belgrade, Vojvode Stepe 444a, P. O. Box 23, 11010 Belgrade, Serbia

J. Serb. Chem. Soc. 80 (12) (2015) 1481–1488

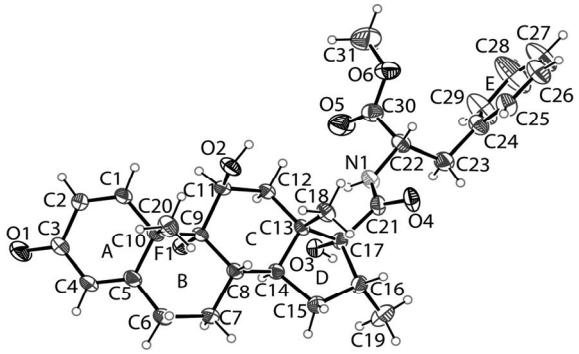

Fig. S-1. Structure of DF with atomic labelling.

PHYSICAL AND SPECTRAL DATA FOR DF

Yield: 83.5 %; m.p.: 119.3–122.0 °C; IR (ATR, cm^{-1}): 1269.02 (ester C–O stretching), 1658.36 (amide C=O stretching), 1670.71 (C_3=O stretching), 1718.18 (ester C=O stretching), 3407.79 (N–H stretching); ^{1}H-NMR (400 MHz, DMSO-d_6, δ / ppm): 0.75 (3H, *d*, J = 7.2 Hz, CH_3 at C16), 0.91 (3H, *s*, H18), 1.05–1.41 (3H, *m*, H6, H12, H15), 1.48 (3H, *s*, H19), 1.61 (1H, *m*, H6), 1.74 (1H,

* Corresponding author. E-mail: vladimir@pharmacy.bg.ac.rs

m, H15), 1.90–2.10 (2H, *m*, H14, H12), 2.22–2.40 (2H, *m*, H7, H8), 2.61 (1H, *m*, H7), 2.92 (1H, *m*, H16), 3.05 (2H, *d*, *J* = 6.4 Hz, C**H**$_2$C$_6$H$_5$), 3.61 (3H, *s*, OCH$_3$), 4.08 (1H, *m*, H11), 4.54 (1H, *q*, *J* = 7.6 Hz, NH–C**H**), 6.01 (1H, *s*, H4), 6.22 (1H, *dd*, *J* = 1.6 Hz, *J* = 10.2 Hz, H2), 7.18–7.31 (5H, *m*, Ar-H), 7.44 (1H, *d*, *J* = 7.6 Hz, H1); ^{13}C-NMR (100 MHz, DMSO-d_6, δ / ppm): 15.26 (CH$_3$ at C16), 17.11 (C18), 23.40 (*d*, *J* = 5 Hz, C19), 27.76 (C15), 32.27 (C7), 33.79 (C6), 34.28 (*d*, *J* = 19 Hz, C8), 35.21 (C16), 35.71 (C12), 37.20 (**C**H$_2$C$_6$H$_5$), 43.58 (C14), 48.39 (C13), 48.53 (*d, J* = 22 Hz, C10), 52.25 (OCH$_3$), 53.65 (NH–CH), 71.12 (*d, J* = 37 Hz C11), 86.88 (C17), 102.07 (*d, J* = 175 Hz C9), 124.51 (C4), 127.06 (C4′), 128.75 (C3′), 129.41 (C2), 129.56 (C2′), 137.45 (C1′), 157.17 (C1), 167.82 (C=O, ester), 172.25 (C20), 172.82 (C5), 185.86 (C3); MS $[M+H]^+$: calcd. for C$_{31}$H$_{38}$FNO$_6$: 540.27560. Observed: 540.27426; UV-Vis (CH$_3$OH) (λ_{max} / nm): 239.

TABLE S-I. Experimental details; crystal data

Chemical formula	C$_{31}$H$_{38}$FNO$_6$
Mr	539.62
Crystal system, space group	Orthorhombic, $P2_12_12_1$
Temperature, K	293
a, *b*, *c* / Å	8.2969 (3), 18.9358 (8), 20.0904 (6)
V / Å^3	3156.4 (2)
Z	4
Radiation type	MoK_α
μ / mm^{-1}	0.08
Crystal size, mm^3	0.18×0.02×0.02
Data collection	
No. of measured, independent and observed ($I > 2\sigma(I)$) reflections	18785, 7284, 5651
R_{int}	0.024
(sin $\theta/\lambda)_{max}$ / Å^{-1}	0.683
Refinement	
$R[F^2 > 2\sigma(F^2)]$, $wR(F^2)$, *S*	0.044, 0.104, 0.984
No. of reflections	7284
No. of parameters	368
H-atom treatment	H atoms treated by a mixture of independent and constrained refinement
$\Delta\rho_{max}$, $\Delta\rho_{min}$ / e Å^{-3}	0.16, –0.16

TABLE S-II. Selected bond lengths and angles (standard uncertainties (s.u.) are given in parentheses)

Bond	Bond length, Å	Bond	Bond length, Å
F1–C9	1.4237(17)	C9–C10	1.567(2)
N1–C21	1.339(2)	C10–C20	1.557(2)
N1–C22	1.447(2)	C11–C12	1.534(2)
O1–C3	1.222(2)	C12–C13	1.518(2)
O2–C11	1.413(2)	C13–C14	1.535(2)
O3–C17	1.4250(18)	C13–C18	1.543(2)
O4–C21	1.2239(19)	C13–C17	1.558(2)
O5–C30	1.188(2)	C14–C15	1.534(2)
O6–C30	1.318(2)	C15–C16	1.553(2)
O6–C31	1.451(3)	C16–C19	1.507(3)
C1–C2	1.320(2)	C16–C17	1.552(2)
C1–C10	1.494(3)	C17–C21	1.533(2)
C2–C3	1.460(3)	C22–C30	1.509(3)
C3–C4	1.442(3)	C22–C23	1.535(3)
C4–C5	1.325(3)	C23–C24	1.510(3)
C5–C6	1.489(3)	C24–C25	1.365(3)
C5–C10	1.520(2)	C24–C29	1.373(3)
C6–C7	1.532(3)	C25–C26	1.369(3)
C7–C8	1.530(2)	C26–C27	1.352(3)
C8–C14	1.518(2)	C27–C28	1.346(4)
C8–C9	1.533(2)	C28–C29	1.387(4)
C9–C11	1.549(2)		
Bond	Bond angle, °	Bond	Bond angle, °
C21–N1–C22	124.21(15)	C12–C13–C17	115.57(12)
C30–O6–C31	116.7(2)	C14–C13–C17	98.60(12)
C2–C1–C10	124.69(16)	C18–C13–C17	110.42(13)
C1–C2–C3	120.84(18)	C8–C14–C15	119.64(13)
O1–C3–C4	122.51(18)	C15–C16–C17	104.70(13)
O1–C3–C2	120.41(19)	O3–C17–C21	109.16(13)
C4–C3–C2	117.07(16)	O3–C17–C16	111.96(13)
C5–C4–C3	123.20(16)	C21–C17–C16	113.84(13)
C4–C5–C6	122.84(16)	O3–C17–C13	106.41(12)
C4–C5–C10	121.88(17)	C21–C17–C13	113.13(13)
C6–C5–C10	115.24(15)	C16–C17–C13	101.98(12)
C5–C6–C7	111.33(15)	O4–C21–N1	122.89(16)
C8–C7–C6	114.64(15)	O4–C21–C17	123.17(15)
C14–C8–C7	110.49(14)	N1–C21–C17	113.89(14)
C14–C8–C9	109.16(13)	N1–C22–C30	107.47(15)
C7–C8–C9	110.34(13)	N1–C22–C23	111.22(15)
F1–C9–C8	106.19(12)	C30–C22–C23	109.67(15)
F1–C9–C11	101.99(12)	C24–C23–C22	113.24(16)
C8–C9–C11	115.62(13)	C25–C24–C29	117.02(19)
F1–C9–C10	104.00(12)	C25–C24–C23	120.87(18)
C8–C9–C10	112.26(13)	C29–C24–C23	122.01(18)

TABLE S-II. Continued

Bond	Bond angle, °	Bond	Bond angle, °
C11–C9–C10	115.04(13)	C24–C25–C26	122.02(19)
C1–C10–C5	112.26(14)	C27–C26–C25	119.7(2)
C1–C10–C20	107.72(15)	C28–C27–C26	120.3(2)
C5–C10–C20	108.39(15)	C27–C28–C29	119.7(3)
C1–C10–C9	109.69(14)	C24–C29–C28	121.1(2)
C5–C10–C9	105.52(13)	O5–C30–O6	124.7(2)
C20–C10–C9	113.34(14)	O5–C30–C22	123.84(19)
O2–C11–C12	114.16(13)	O6–C30–C22	111.41(18)
O2–C11–C9	108.02(13)	C8–C14–C13	114.35(13)
C12–C11–C9	112.51(13)	C15–C14–C13	103.68(12)
C13–C12–C11	113.65(13)	C14–C15–C16	105.00(13)
C12–C13–C14	108.88(12)	C19–C16–C15	114.11(17)
C12–C13–C18	110.47(14)	C19–C16–C17	115.34(15)
C14–C13–C18	112.43(13)		

TABLE S-III. Hydrogen bond geometry of DF

D–H···A	Symmetry code	D–H	H···A	D···A	D–H···A
O2–H2O···O4	$-1/2+x$, $1/2-y$, $-z$	0.84(2)	1.97(2)	2.791(2)	165(2)
O3–H3O···O1	$1-x$, $-1/2+y$, $1/2-z$	0.76(2)	2.00(2)	2.750(2)	167(2)
C29–H29···F1	$1-x$, $-1/2+y$, $1/2-z$	0.93	2.52	3.376(3)	154
N1–H1N···O3		0.86(2)	2.114(18)	2.587(2)	114(2)
N1–H1N···O5		0.86(2)	2.415(18)	2.716(2)	101(1)
C14–H14···F1		0.980(1)	2.46	2.851(2)	103
C14–H14···O3		0.98	2.31	2.736(2)	105
C12–H12A···O3		0.97	2.40	2.832(2)	107
C18–H18C···O2		0.96	2.44	3.043(2)	120
C16–H16···O4		0.98	2.56	2.953(2)	104
C20–H20A···O2		0.96	2.32	2.921(2)	120

Journal of the Serbian Chemical Society
JSCS-info@shd.org.rs • www.shd.org.rs/JSCS
J. Serb. Chem. Soc. 80 (12) 1489–1504 (2015)
JSCS–4814
UDC 547.686+547.678.2:548.7:
543.424.2+543.42–74:519.677
Original scientific paper

X-Ray, Hirshfeld surface analysis, spectroscopic and DFT studies of polycyclic aromatic hydrocarbons: fluoranthene and acenaphthene

WIOLETA ŚMISZEK-LINDERT[1]*, ANNA MICHTA[2], ALEKSANDRA TYL[2], GRZEGORZ MAŁECKI[2], ELŻBIETA CHEŁMECKA[3] and SŁAWOMIR MAŚLANKA[2]

[1]Institute of Mechanized Construction and Rock Mining, W. Korfantego 193A Street, 40-157 Katowice, Poland, [2]Institute of Chemistry, University of Silesia, 9 Szkolna Street, 40-006 Katowice, Poland and [3]School of Pharmacy with Division of Laboratory Medicine in Sosnowiec, Medical University of Silesia, Katowice, Poland, Department of Statistics, 30 Ostrogórska Street, 41-200 Sosnowiec, Poland

(Received 4 March, revised 27 June, accepted 6 July 2015)

Abstract: The X-ray structure, theoretical calculation, Hirshfeld surfaces analysis, IR and Raman spectra of fluoranthene and acenaphthene were reported. Acenaphthene crystallizes in the orthorhombic crystal system and space group $P2_1ma$, with crystal parameters a = 7.2053(9) Å, b = 13.9800(15) Å, c = = 8.2638 (8) Å, Z = 4 and V = 832.41(16) Å^3. In turn, the grown crystals of fluoranthene are in the monoclinic system with space group $P2_1/n$. The unit cell parameters are a = 18.3490(2) Å, b = 6.2273(5) Å, c = 19.8610(2) Å, β = = 109.787(13)°, Z = 8 and the unit cell volume is 2135.50(4) Å^3. Theoretical calculations of isolated molecules of the title compounds were performed using DFT at the B3LYP level. The intermolecular interactions in the crystal structure, for both the title polycyclic aromatic hydrocarbons were analyzed using the Hirshfeld surfaces computational method.

Keywords: crystal structure; IR spectroscopy; Raman; density functional theory (DFT) calculation; Hirshfeld surfaces.

INTRODUCTION

Polycyclic aromatic hydrocarbons (PAHs) are important persistent organic pollutants (POPs) of the environment, which generally occur in all its parts: atmosphere, water, soils, sediments and vegetation.[1,2] The presence of PAHs in all these environmental elements may establish a risk for humans as well as all living organisms. Migration and distribution of PAHs in the environment depends on their physicochemical properties, *i.e.*, water solubility, octanol–water

* Corresponding author. E-mail: w.lindert@imbigs.pl
doi: 10.2298/JSC150304060S

distribution constant, or Henry's constants (volatility).[3–5] Besides, in the gas-phase of the atmosphere, PAHs can react with nitrogen oxides, ozone, OH radicals and NO_3 radicals, yielding, *e.g.*, nitrated, oxygenated, and hydroxylated derivatives of PAHs.[6–9] The nitrated PAH compounds are potentially more mutagenic and carcinogenic than the polycyclic aromatic hydrocarbon precursors.[10]

PAHs are released into the environment from domestic, industrial and natural sources. Anthropogenic PAHs are usually generated from incomplete combustion of fossil fuels (*e.g.*, oil, coal, crude oil, gasoline),[11,12] waste treatment,[11] combustion of synthetic chemicals,[11] and other human activities, such as cooking, tobacco smoking, or vehicle traffic.[13] The natural sources of emissions of PAHs pertain to forest fires,[11] volcanic eruptions[7] and carbonization processes, such as products of humus conversion by microorganisms,[14] diagenesis of organic matter,[15] *etc*.

Fluoranthene and acenaphthene are examples of PAHs, which are classified as priority control organic pollutants by the US Environmental Protection Agency (US EPA).[16] Acenaphthene is also on the Hazardous Substance List. Fluoranthene and acenaphthene are considered non-carcinogens for humans, but should be handled with caution.[17] Additionally, acenaphthene could be applied as an intermediary in pharmaceutical, agricultural and chemical industries.[17]

Molecular crystals of fluoranthene and acenaphthene, as well as their derivatives, were the subject of studies for the generation of the mechanism of their interactions by hydrogen bonds with other molecules in asphalt (a product from the distillation of petroleum). PAHs and their derivatives could be emitted from asphalt, and could migrate in the environment, for example, from contaminated soils into the ground water.[18] Therefore, they could be potential health hazards for humans.[19] The next aim of research is to obtain knowledge of the manner of interactions of PAHs and their derivatives with proteins by performing computer simulations using CLC Drug Discovery Workbench.[20] The experiments will be performed under conditions simulating the physiological pH.

EXPERIMENTAL

Materials

Fluoranthene (**I**) and acenaphthene (**II**) were provided by Sigma–Aldrich (Poland) at 98 and 99 % purity, respectively. The substances were investigated without further purification. Colourless crystals of **I,** suitable for X-ray analysis, were obtained by slow evaporation of ethanol–acetone mixture (1:1, *V*/*V*) at room temperature. On the other hand the crystals of acenaphthene were obtained upon recrystallization from petroleum ether, giving plate-shaped single crystals.

X-Ray crystal structure determination

The crystals of **I** and **II** were mounted in turn on a Gemini A Ultra Oxford Diffraction automatic diffractometer equipped with a CCD detector, and used for data collection. X-Ray intensity data were collected with graphite monochromated MoK_α radiation (λ = 0.71073 Å)

at room temperature, in the ω scan mode. Ewald sphere reflections were collected up to 2θ = = 50.10°. Lorentz, polarization and empirical absorption corrections using spherical harmonics implemented in SCALE3 ABSPACK scaling algorithm were applied.[21] The structures were solved by the direct method and subsequently completed by difference Fourier recycling. All non-hydrogen atoms were refined anisotropically using full-matrix, least-squares techniques. All hydrogen atoms were positioned in geometrically idealized positions and were allowed to ride on their parent atoms with U_{iso}(H) = 1.2 U_{eq}. The OLEX2[22] and SHELXS, SHELXL[23] programs were used for all calculations. Atomic scattering factors were those incorporated in the computer programs. All graphics were prepared using ORTEP-3[24] for Windows, Platon[25] and Mercury.[26]

Physical measurements

The infrared spectra of polycrystalline samples (dispersed in KBr pellets) and monocrystalline samples of fluoranthene and acenaphthene were recorded on a FT-IR Nicolet Magna 560 spectrometer in the transmission mode with 2 cm^{-1} resolution. The IR spectra of polycrystalline samples were measured at temperature 298 K, while the monocrystalline samples were measured at two temperatures, 298 and 77 K. The IR spectra were recorded in the spectral range of 4000–400 cm^{-1}. Crystals of **I** and **II** suitable for spectral studies were obtained by crystallization from melted samples occurring between two closely spaced CaF_2 windows. In this way, sufficiently thin crystals could be obtained, characterized by a maximum absorbance at the ν_{C-H} band frequency range close to 0.5. Monocrystalline fragments were selected from the crystalline mosaic and spatially oriented using a polarization microscope. In the next step, these selected crystals were exposed to the experiment with the use of a metal plate diaphragm with a 1.5 mm diameter hole. The Raman experiment was performed using a WITec confocal CRM alpha 300 Raman microscope (Jagiellonian Centre for Experimental Therapeutics – JCET, Kraków, Poland). The spectrometer was equipped with an air cooled solid state laser operating at 532 nm and CCD detector which was cooled to –58 °C. The laser was coupled to the microscope *via* a single mode optical fibre with a diameter of 50 μm. The scattered radiation was focused onto a multi-mode fibre (50 μm diameter) and a monochromator. A dry Olympus MPLAN (50×/0.76NA) objective was used. The integration time for a single spectrum was 2 s. The spectra were collected in the range between 4000–120 cm^{-1} with a spectral resolution of 3 cm^{-1}.

Theoretical calculations

The theoretical calculations were performed by means of the Gaussian 09[27] software package, using density functional theory (DFT) at the B3LYP level and with 6-31G(d,p) and 6-31G*(d,p) basis sets for acenaphthene, as well as 6-31+G(d,p) and 6-311++G(3df,2pd) basis sets for fluoranthene.[28,29]

The Hirshfeld surface analyses were realized using the CrystalExplorer program.[30] The distance from the Hirshfeld surface to the nearest nucleus inside and outside the surface were marked by d_i and d_e, respectively, whereas d_{norm} is a normalized contact distance, which is defined in turns of d_i, d_e and the van der Waals (vdW) radii of the atoms:[31]

$$d_{norm} = \frac{d_i - r_i^{vdW}}{r_i^{vdW}} + \frac{d_e - r_e^{vdW}}{r_e^{vdW}} \quad (1)$$

d_{norm} was visualized using a red–white–blue colour scheme. If the atoms make intermolecular contacts closer than the sum of their vdW radii, these contacts were represented as red spots

on the surface. Longer contacts were blue, while white was used for contacts around the sum of the van der Waals radii.[31]

RESULTS AND DISCUSSION

The crystal structures of fluoranthene (**I**) and acenaphthene (**II**) have already been described in the literature, *i.e.*, by Chakrabarti[32] and Hazell *et al.*,[33] and later by Munakata *et al.*[34], Ehrlich[35] and then by Hazell *et al.*,[36] respectively. The crystallographic data were re-collected in the present study because other conditions of crystals growth than in the literature were used, and these data were needed to perform the computer simulations of the binding processes of fluoranthene and acenaphthene with the selected human proteins.

The crystal data and final refinement details of compound **I** and **II** are given in Table I. The molecular structure of fluoranthene and acenaphthene are illustrated in Fig. 1a and b, respectively.

TABLE I. Crystal data and structure refinement details of fluoranthene (**I**) and acenaphthene (**II**)

Parameter	Fluoranthene (**I**)	Acenaphthene (**II**)
Empirical formula	$C_{16}H_{10}$	$C_{12}H_{10}$
Compound weight	202.24	154.20
Temperature, K	295.0(2)	295.0(2)
Crystal system	Monoclinic	Orthorhombic
Space group	$P2_1/n$	$P2_1ma$
Crystal dimension, mm	0.39 x 0.32 × 0.09	0.41 × 0.22 × 0.12
Crystal form, colour	Plate, colourless	Plate, colourless
	Unit cell dimensions	
a / Å	18.3490(2)	7.2053(9)
b / Å	6.2273(5)	13.9800(15)
c / Å	19.8610(2)	8.2638(8)
β / °	109.787(13)	90.00
V / Å^3	2135.50(4)	832.41(16)
Z	8	4
D_c / g cm^{-3}	1.258	1.230
F(000)	848	328
Θ range for data collection, °	4.0–29.2	4.8–27.5
Data collection method	ω scan	ω scan
Absorption coefficient, mm^{-1}	0.071	0.069
Final R indices ($I > 2\sigma(I)$)	R_1 =0.0696 , wR_2 = 0.1711	R_1 = 0.0442, wR_2 = 0.0964
R indices (all data)	R_1 = 0.1043, wR_2 = 0.1936	R_1 = 0.0550, wR_2 = 0.1022
Reflections collected/unique	2527 [R_{int} = 0.089]	1075 [R_{int} = 0.020]
Limiting indices	$-21 \le h \le 20$, $-7 \le k \le 7$, $-23 \le l \le 23$	$-8 \le h \le 6$, $-16 \le k \le 16$, $-7 \le l \le 9$
Refinement method	Full-matrix least-squares on F^2	Full-matrix least-squares on F^2
S	1.10	1.05
Parameters refined	289	105
$\Delta\rho_{max}$, $\Delta\rho_{min}$ / e Å^{-3}	0.22–0.21	0.25–0.28

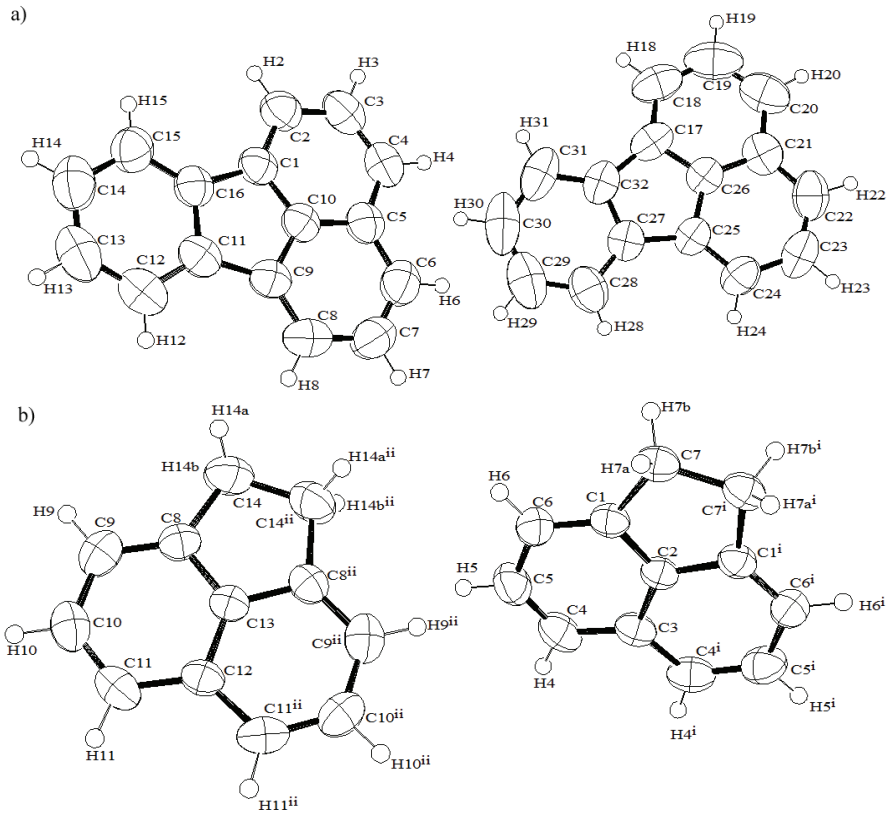

Fig. 1. The conformation of a) fluoranthene and b) acenaphthene molecules with the atom numbering scheme. Atomic displacement ellipsoids represent the 50 % probability level. H atoms are shown as small spheres of arbitrary radius. Symmetry code: *i*) *x*, *y*, *z*; *ii*) *x*, –*y*, *z*.

Compound **I** crystallizes with eight molecules in an asymmetric unit. The molecules in the unit cell are connected by weak C–H···π interactions between nearest neighbours. The intermolecular C–H···C interactions existing between carbon atoms of the condensed rings of the naphthalene structure nearest neighbouring molecules are shown in Fig. 2a (marked with blue dashed lines). Fluoranthene also contains π···π (C···C) interactions, but they are less dominant in this crystal structure. The C···C distances between neighbouring molecules are approximately 3.33 Å (Fig. 2a; red dashed line). Generally, the C···C van der Waals distance of 3.40 Å has been adopted as the reference distance for chemical stability.[37] Additionally, it is worth noting that the C···C distances are longer than the 2.6 Å distance observed in crystalline benzene.[38] The intermolecular C···C distance is also comparable to the C···C distance of dibenz[*a*,*h*]anthracene (3.37 Å).[39]

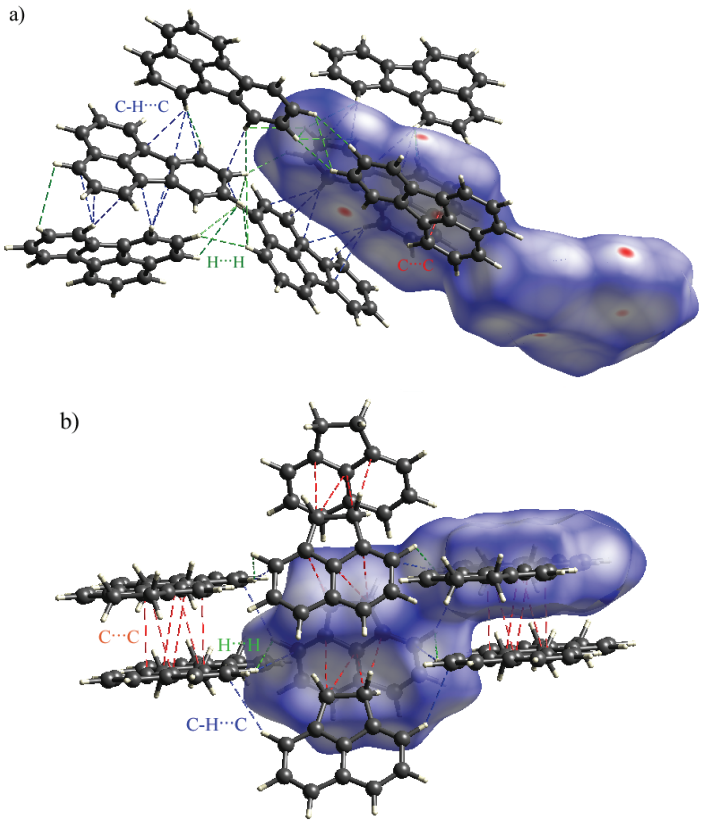

Fig. 2. Hirshfeld surfaces mapped with d_{norm} and part of the crystal structure of: a) fluoranthene and b) acenaphthene showing the intermolecular interactions.

The H···H contacts are marked green with a dashed line in Fig. 2a. The shortest close contacts between hydrogen atoms have a distance of approximately 2.37 Å (van der Waals radius for hydrogen atom is 1.2 Å). The shortest C–H···π close contacts have a distance of approximately 2.80 Å.

The intermolecular close contacts were likewise substantiated by examination of Hirshfeld surfaces. However, the fingerprint plots (2D representation of a Hirshfeld surface) provide a quantitative measure of the intermolecular interactions on the surface.[31,40] The C···H and H···C intermolecular interactions are depicted as two characteristic and distinct "spikes" in the two-dimensional fingerprint plot, Fig. 3a. The C···H (π···H) interactions (30.8 %) are represented by a spike (d_i = 1.74 Å, d_e = 1.75 Å) in the bottom right area of the fingerprint plot (these contacts are marked with a green ellipse; see Fig. 3a). Then the H···C (H···π) interactions (25.1 %) are represented by a spike (d_i = 1.74 Å, d_e = 1.75 Å) in the upper left area of the fingerprint plot (contacts are marked with a red

ellipse). Two small areas, visible on the fingerprint plot (Fig. 3b), are characteristic of π···π interactions (2.0 %). Besides, the presented results showed that the structure of **I** is also dominated by the H···H contacts (42.1 %), Fig. 3c.

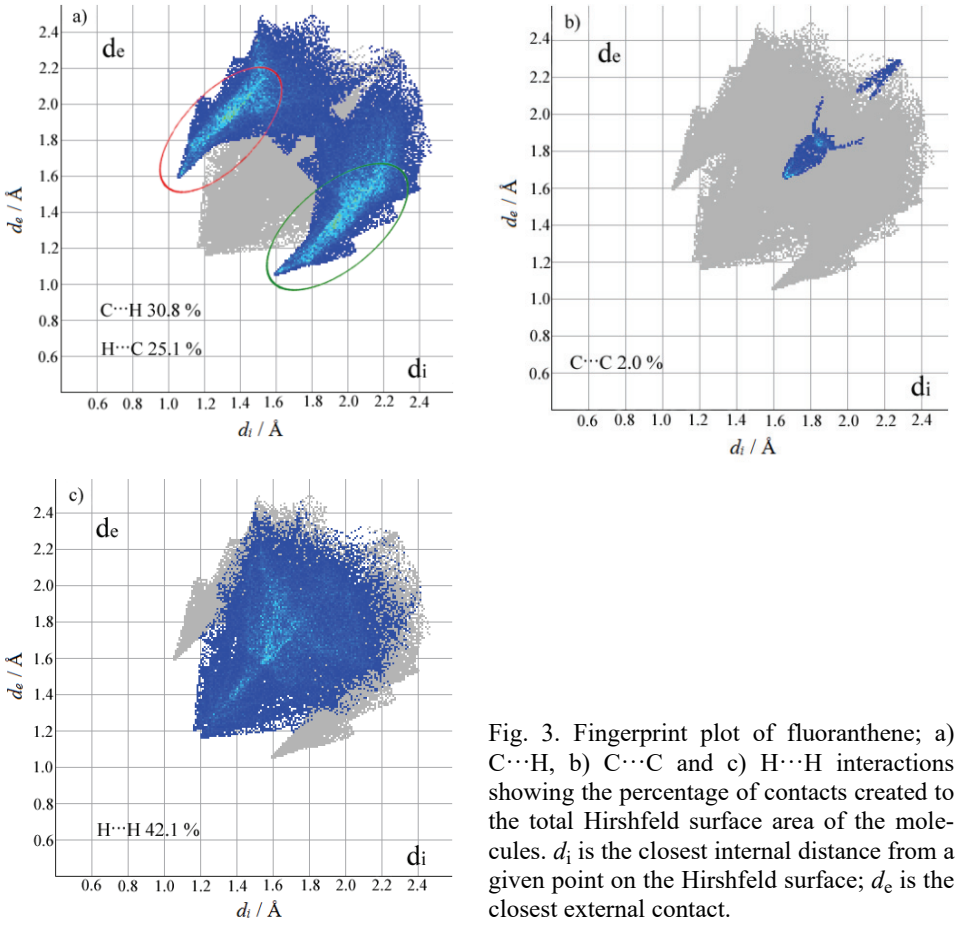

Fig. 3. Fingerprint plot of fluoranthene; a) C···H, b) C···C and c) H···H interactions showing the percentage of contacts created to the total Hirshfeld surface area of the molecules. d_i is the closest internal distance from a given point on the Hirshfeld surface; d_e is the closest external contact.

According to the classification of Desiraju and Gavezzotti,[41] the crystal packing of **I** follows a herringbone (HB) motif. The ratio of C···H to C···C interactions is 27.95 > 4.5.[42]

Hirshfeld surface analysis was also used for visual analysis of intermolecular interactions in the crystal structure of acenaphthene. The asymmetric unit of **II** contains four acenaphthene molecules that are linked by C–H···π interactions. The intermolecular C–H···C interactions, existing between carbon atoms of the condensed rings of the naphthalene structure nearest neighbouring molecules, are shown in Fig. 2b (blue dashed line). The shortest C–H···π close contacts have a distance of approximately 2.90 Å. The π···H (C–H) interactions provide 39.30

%, which is appreciably lower when compared to **I**. The C···H interactions (23.2 %) are represented by the characteristic wing (d_i = d_e = 1.66 Å) in the bottom right area of the fingerprint plot, Fig. 4a (contacts are denoted by a green ellipse). Then the H···C contacts (16.0 %) are illustrated by a wing (d_i = d_e = 1.66 Å) in the upper left area of the fingerprint plot, (the contacts are denoted by a red ellipse, see Fig. 4a).

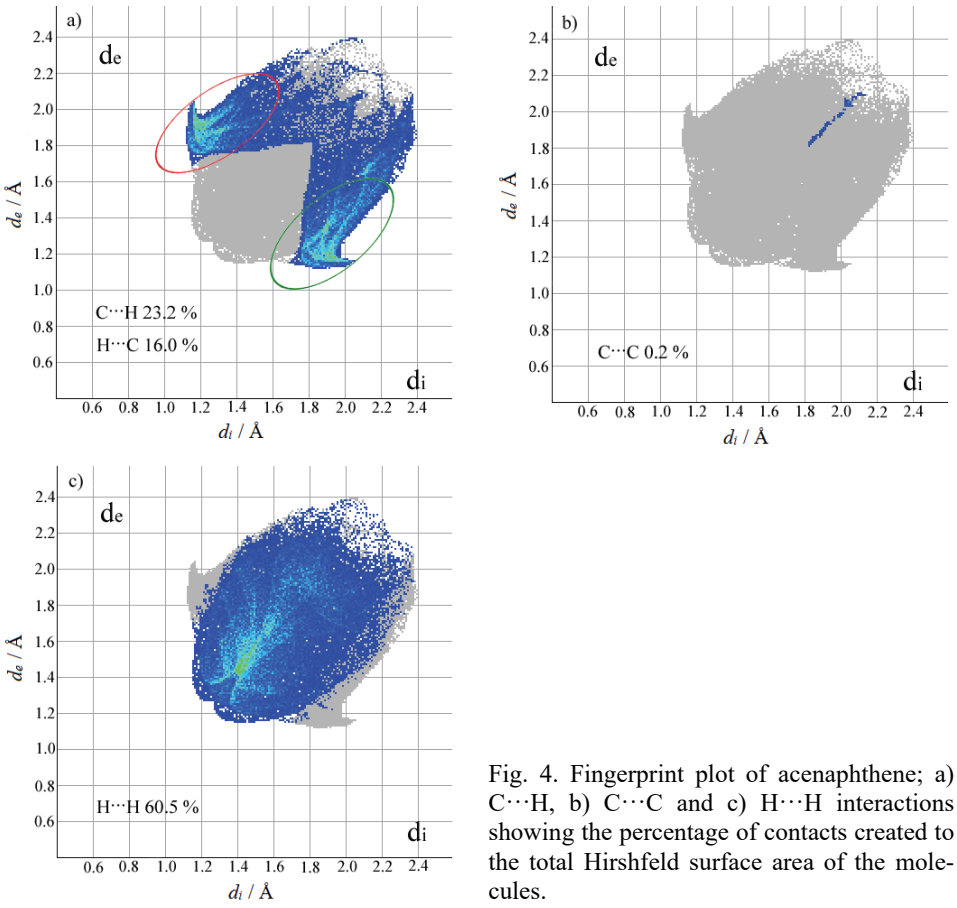

Fig. 4. Fingerprint plot of acenaphthene; a) C···H, b) C···C and c) H···H interactions showing the percentage of contacts created to the total Hirshfeld surface area of the molecules.

A significant difference between the molecular interactions in **I** and **II** in terms of H···H interactions is also noticeable in the fingerprint plots (Figs. 3c and 4c). In this case, H···H contacts comprise 60.5 % of the surface area. The shortest close contacts between hydrogen atoms have a distance of approximately 2.53 Å, Fig. 2b (green dashed line).

The π···π contacts are almost zero, and there are no significant interactions in the crystal structure of acenaphthene (C···C contacts make 0.2 % of the sur-

face area). The shortest close contacts between carbon atoms have a distance approximately 3.70 Å, Fig. 2b (red dashed line). The visual analysis of the fingerprint plots (C···H contact) of other PAHs, *e.g.*, naphthalene and anthracene, show that acenaphthene is more similar to them, than to fluoranthene.[43]

According to the method of Lootos and Barbour, the molecules of acenaphthene are arranged in a herringbone motif. The ratio of C···H to C···C is considerably greater than 4.5, and is 196.50.[42]

It should also be noted that in the unit cell, the molecules of fluoranthene and acenaphthene are not connected by hydrogen bonds. This fact was also proven by spectroscopic studies.

The Hirshfeld surface and 2D fingerprint plots were used for visualizing, exploring and quantifying intermolecular interactions in the crystal lattice of both PAHs. Besides, quantitative measures of Hirshfeld surfaces for fluoranthene and acenaphthene were obtained, such as molecular volume (V_H) 542,96 and 408,61 Å^3, surface area (S_H) 464,90 and 374,07 Å^2, globularity (G) 0.677 and 0.712, as well as asphericity (Ω) 0,456 and 0,333, respectively.

*IR spectra of compounds **I** and **II***

The IR spectra of polycrystalline samples of fluoranthene and acenaphthene, measured at 298 K using the KBr pellet technique, are shown in Fig. 5a and b, respectively. Additionally, the Raman spectra of **I** and **II** are also presented in Fig. 5a and b, respectively. The Raman spectra were measured at room temperature for polycrystalline samples. The Raman spectra allow for additional identification of the $\nu_{C–H}$ band positions, which are attributed to the C–H bond stretching vibrations in the molecules.[44]

Polarized IR spectra of **I** and **II** single crystals measured at 77 K, in the frequency ranges of the $\nu_{C–H}$ bands, are shown in Fig. 6a and b, respectively. The temperature dependence of the polarized crystalline spectra of fluoranthene and acenaphthene in the frequency ranges of the $\nu_{C–H}$ bands is presented in Fig. 7a and b, respectively.

The vibrations of crystalline acenaphthene can be divided into types: aromatic ring C–H stretching (3071–3036 cm^{-1}), CH_2 asymmetric stretching (2937––2914 cm^{-1}), CH_2 symmetric stretching (2840 cm^{-1}) (see Fig. 5b), in plane CH_2 group deformation (≈1423 cm^{-1}), aromatic ring stretching (≈1616–1593 cm^{-1}) and skeletal vibrations representing C=C stretching (≈1370 cm^{-1}). In Fig. 5b, C–H bending bands appear in the region 841–749 cm^{-1} (out-of-plane bending), and are very strong. In the case of crystalline fluoranthene, the characteristic IR bands in the five regions of the spectrum are illustrated in Figs. 5a and 6a. The main types of vibration are C–H stretching vibration, C=C stretching vibration, C–H out-of-plane vibration, C–H bending vibration and lattice vibration.[45]

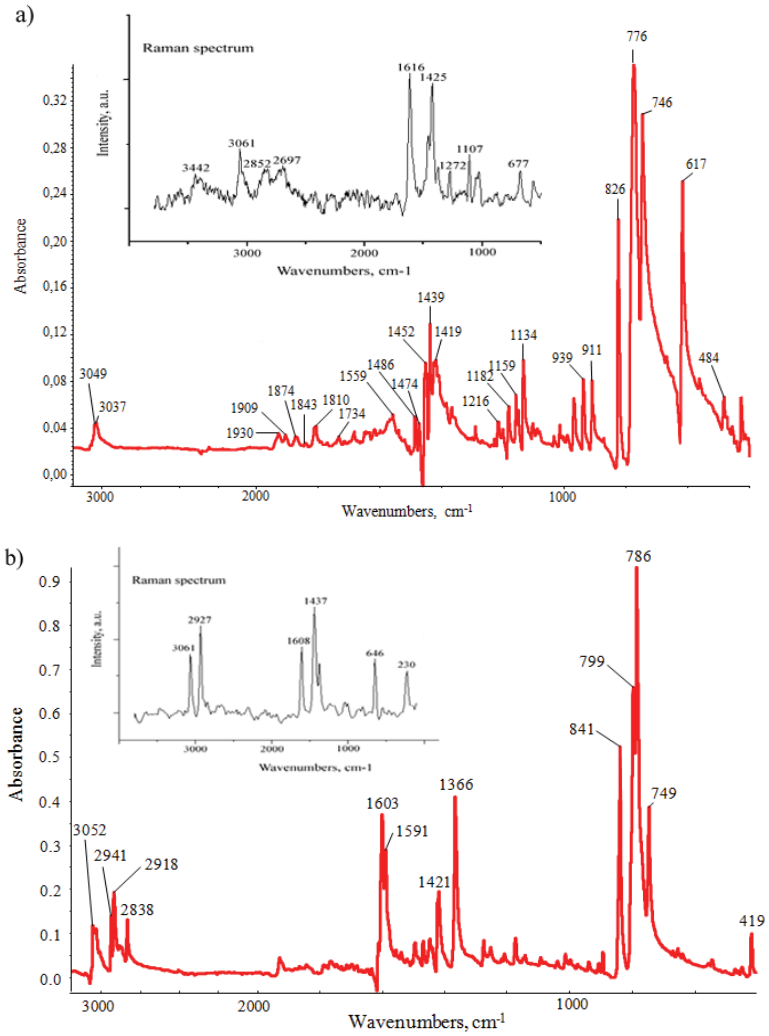

Fig. 5. IR spectra of polycrystalline samples of a) fluoranthene and b) acenaphthene measured at 298 K using the KBr pellet technique. Raman spectra for the identification of the vibration lines of the C–H bonds.

Analyzing the IR spectra of monocrystalline samples of acenaphthene, measured at the different orientations of the electric field vector *E*, the incident light on the crystal, large variability of the intensity of some bands could be observed, Fig. 6b. The ν_{C-H} bands (in the frequency range from 3060 to 2836 cm^{-1}) in the spectra of **II** crystals were characterized by the two-branch structure with their unique and relatively simple intensity distribution patterns. The polarized light

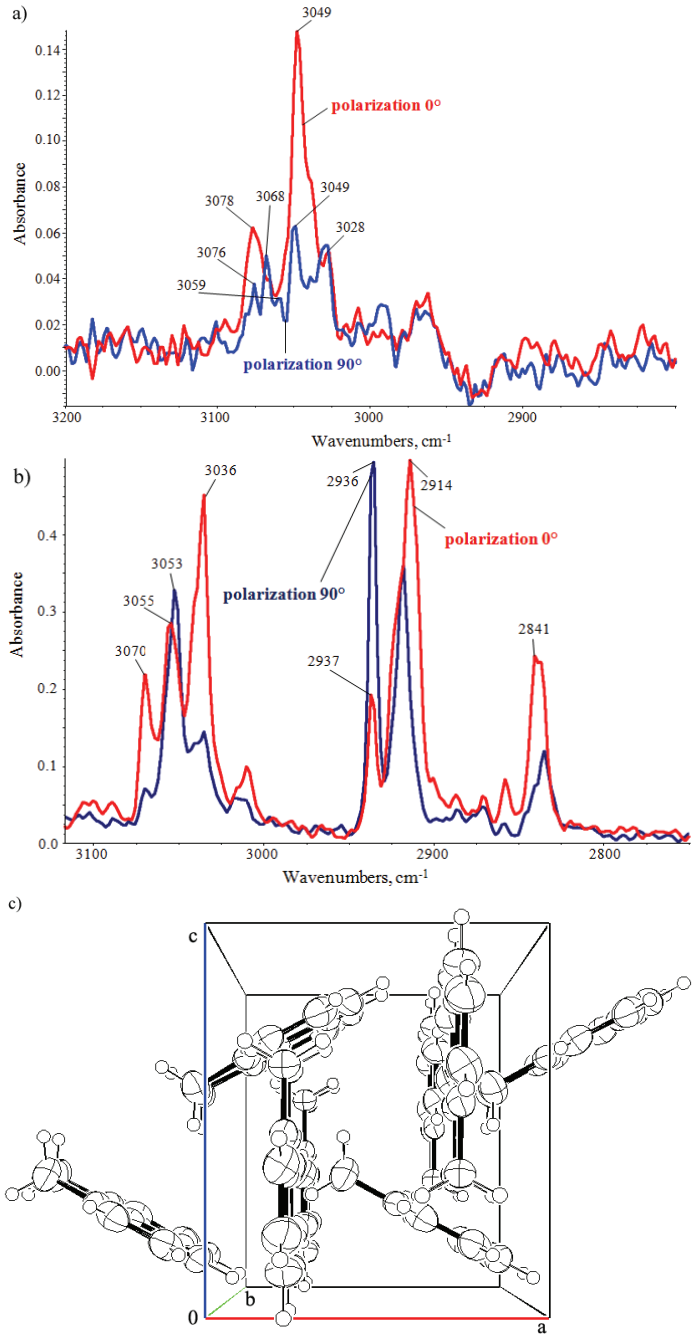

Fig. 6. Polarized spectra of a single crystal of: a) fluoranthene and b) acenaphthene measured at 77 K; c) packing diagram of acenaphthene viewed along the *b* axis.

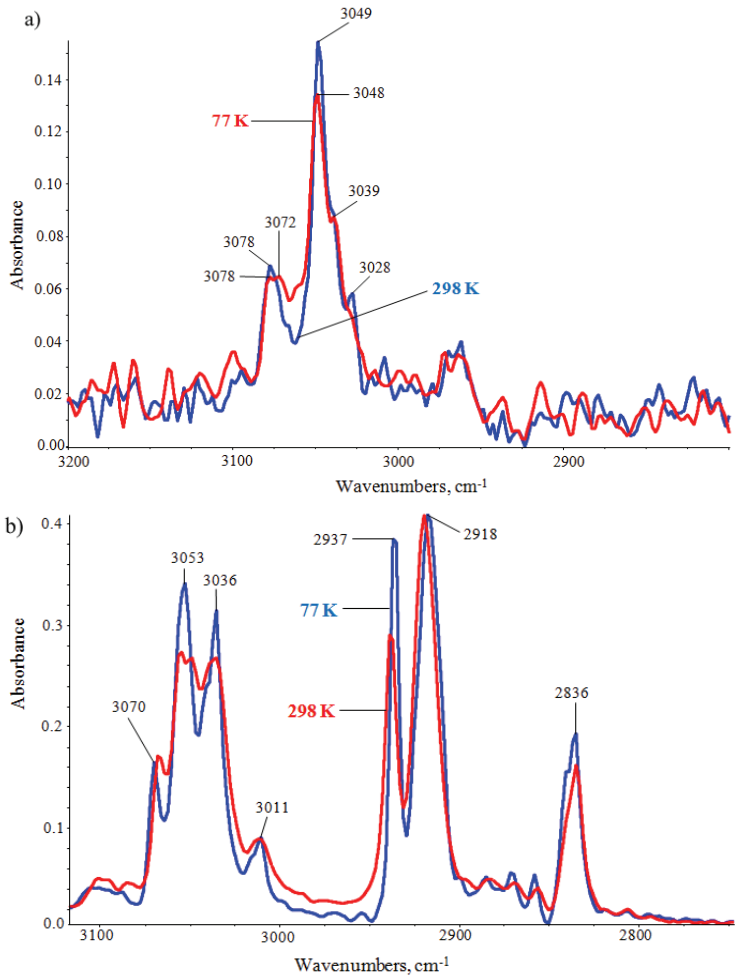

Fig. 7. Polarized spectra of a single crystal of: a) fluoranthene and b) acenaphthene are illustrative of the temperature effect.

especially strongly influenced the intensity of the bands of the stretching of C–H bonds vibrations in the molecules. Based on the results in Fig. 6b, it could be seen that the longer-wave branch (3060–3040 cm^{-1}) of the band was of relatively high intensity when compared with the branch properties of the shorter-wave band (3061–3075 cm^{-1}). These effects are related to the arrangement of the molecules in the unit cell. Two molecules lie in the crystalline plane *bc*, while the other two are arranged obliquely to them, Fig. 6c. Such an arrangement of the molecules means that, regardless of the type, C–H vibrations of different fragments of the molecules will be excited by the polarized light. Therefore, different intensity of the lines in the ν_{C-H} bands was observed in the spectra of the

acenaphthene crystals. For example, in the case of polarization 0°, the line 2937 cm^{-1} of the asymmetric CH_2 vibrations had significantly lower intensity compared with the 2914 cm^{-1} line (Fig. 6b). The opposite phenomenon was observed for polarization 90°. It may be noted that the polarization effects are also visible in some bands lying at lower frequencies.

The IR spectra of acenaphthene crystals showed that a temperature decrease to 77 K was responsible for a slight growth in the intensity of the longer-wave branch, whereas the intensity of the shorter-wave branch remained unchanged, Fig 7b.

Very similar phenomena were observed in the spectra of fluoranthene crystals (Figs. 6a and 7a). In this case, the largest differences in the intensities of the bands were also visible in the frequency range of the C–H bond stretching vibration in the molecules. On the other hand, the differences between the spectra measured at room temperature and the temperature of liquid nitrogen were a result of stiffening of the molecules. Therefore, there was a discernible sharpening of the $\nu_{C–H}$ bands contour, as well as a slight growth in their intensities.

The analysis of the IR and Raman spectra indicated that the skeletal vibrations of the C–C bands in the aromatic nucleus were much weaker in the IR spectra than in the Raman spectra. These data were also based on experimental data available in the literature.[44]

*DFT calculation results for compounds **I** and **II***

The studies showed satisfactory correlation between the calculated and XRD experimental structural parameters (Tables S-I and S-II of the Supplementary material to this paper). Significant differences in the DFT and XRD geometries were observed in case of fluoranthene in the C8–C9–C10–C1, C24–C25–C26––C17, C2–C1–C10–C9, C18–C17–C26–C25, C27–C25–C26–C21 and C32––C17–C26–C21 torsion angles, which had the values –178.5, –179.3, –179.5, –178.1, –178.7 and 179.1°, respectively.

Figure S-1 of the Supplementary material demonstrates a comparison of the calculated IR (non-scaled) spectra of fluoranthene and acenaphthene. It should be noted that the theoretical model satisfactorily reproduced the experimental infrared spectra for both PAHs. The results also showed slight discrepancies between the modelling and experimental data, which is not unusual since the calculations corresponded to the gas phase of a single isolated molecule, whereas the experiment was performed on crystal structures.

CONCLUSIONS

In the present paper, the crystal structure, the DFT calculations, analysis of Hirshfeld surfaces and fingerprint plots, as well as spectroscopic properties of the title PAHs are reported.

These results showed that Hirshfeld surface and fingerprint plot analysis provides rapid quantitative insight into intermolecular interactions in molecular solids. The close contacts, in the case of both analyzed compounds, are dominated by H···C (C–H···π) and H···H contacts and these relatively weak interactions have evident signatures in the fingerprint plots. In addition, it should be emphasized that the analysis of a Hirshfeld surface is well correlated to the spectroscopic studies. Moreover, the comparison of the DFT model with XRD in the present study may be considered good.

SUPPLEMENTARY MATERIAL

Calculated and XRD experimental structural parameters and calculated IR spectra of fluoranthene and acenaphthene are available electronically from http://www.shd.org.rs/JSCS/, or from the corresponding author on request.

CCDC-1011192 and CCDC-1011193 contain the supplementary crystallographic data for this paper. These data can be obtained free of charge at www.ccdc.cam.ac.uk/conts/retrieving.html or from the Cambridge Crystallographic Data Centre (CCDC), 12 Union Road, Cambridge CB2 1EZ, UK; fax: +44(0)1223-336033; e-mail: deposit@ccdc.cam.ac.uk

Acknowledgements. This work was founded by a grant of the Medical University of Silesia (No. KNW-1-026/N/5/0). All of the calculations were performed with the aid of hardware and software at the Wrocław Centre for Networking and Supercomputing WCSS, Wrocław, Poland.

ИЗВОД

РЕНДГЕНОСТРУКТУРНА АНАЛИЗА, МЕТОДА АНАЛИЗЕ ХИРШФЕЛДОВИХ ПОВРШИНА, СПЕКТРОСКОПСКА И DFT ИСПИТИВАЊА ФЛУОРАНТЕНА И АЦЕНАФТЕНА

WIOLETA ŚMISZEK-LINDERT[1], ANNA MICHTA[2], ALEKSANDRA TYL[2], GRZEGORZ MAŁECKI[2], ELŻBIETA CHEŁMECKA[3] и SŁAWOMIR MAŚLANKA[2]

[1]*Institute of Mechanized Construction & Rock Mining, W. Korfantego 193A Street, 40-157 Katowice, Poland,* [2]*Institute of Chemistry, University of Silesia, 9 Szkolna Street, 40-006 Katowice, Poland and* [3]*School of Pharmacy with Division of Laboratory Medicine in Sosnowiec, Medical University of Silesia, Katowice, Poland, Department of Statistics, 30 Ostrogórska Street, 41-200 Sosnowiec, Poland*

Дат је приказ рендгенске структуре, теоријских израчунавања, Хиршфелдове анализе површина, IR и Раманових спектара за флуорантен и аценафтен. Аценафтен кристалише као орторомбични кристални систем са $P2_1ma$ просторном групом и параметрима јединичне ћелије: a = 7,2053(9) Å, b = 13,9800(15) Å, c = 8,2638(8) Å, Z = 4 и V = = 832,41(16) Å^3. Супротно томе, флуорантен кристалише као моноклинични кристални систем са $P2_1/n$ просторном групом и следећим параметрима јединичне ћелије: a = = 18,3490(2) Å, b = 6,2273(5) Å, c = 19,8610(2) Å, β = 109,787(13)°, Z = 8 и V = 2135,50(4) Å^3. Теоријска израчунавања за изоловане молекуле наведених једињења су извршена помоћу DFT израчунавања и B3LYP методе. Применом Хиршфелдове компјутерске методе засноване на анализи површина одређене су интермолекулске интеракције у кристалним структурама оба PAHs једињења.

(Примљено 4. марта, ревидирано 27. јуна, прихваћено 6. јула 2015)

REFERENCES

1. A. Mrozik, Z. Piotrowska-Seget, S. Łabużek, *Pol. J. Environ. Stud.* **12** (2003) 15
2. B. Maliszewska-Kordybach, *Pol. J. Environ. Stud.* **8** (1999) 131
3. A. Baklanov, O. Hänninen, L. H. Slørdal, J. Kukkonen, N. Bjergene, B. Fay, S. Finardi, S. C. Hoe, M. Jantunen, A. Karppinen, A. Rasmussen, A. Skouloudis, R. S. Sokhi, J. H. Sørensen, V. Ødegaard, *Atmos. Chem. Phys.* **7** (2007) 855
4. K. H. Kim, S. A. Jahan, E. Kabir, R. J. C. Brown, *Environ. Int*. **60** (2013) 71
5. M. J. Ahrens, C. V. Depree, *Chemosphere* **81** (2010) 1526
6. A. J. Cohen, *Environ. Health Persp*. **108** (2000) 743
7. M. P. Holloway, M. C. Biaglow, E. C. McCoy, M. Anders, H. S. Rosenkranz, P. C. Howard, *Mutat. Res*. **187** (1987) 199
8. D. Helmig, J. Arey, R. Atkinson, W. P. Harger, P. A. McElroy, *Atmos. Environ., A* **26** (1992) 1735
9. J. Arey, B. Zielinska, R. Atkinson, A. M. Winer, T. Ramdahl, I. N. Pitts, *Atmos. Environ.* **20** (1986) 2339
10. Y. Zhang, S. Tao, *Atmos. Environ.* **43** (2009) 812
11. J. Lewtas, *Mutat. Res.* **636** (2007) 95
12. K. Ravindra, R. Sokhi, R. Van Grieken, *Atmos. Environ.* **42** (2008) 2895
13. M. A. Bari, G. Baumbach, B. Kuch, G. Scheffknecht, *Air Qual. Atmos. Health* **3** (2010) 103
14. K. Skupińska, I. Misiewicz, T. Kasprzycka-Guttman, *Acta Pol. Pharm*. **61** (2004) 233
15. K. Banger, G. S. Toor, T. Chirenje, L. Ma, *Soil Sediment Contam*. **19** (2010) 231
16. EPA United States Environmental Protection Agency, *Priority Pollutants*, http:// //water.epa.gov/scitech/methods/cwa/pollutants.cfm (accessed 21 February 2015)
17. Agency for Toxic Substances and Disease Registry (ATSDR), *Toxicological profile for aromatic hydrocarbons*, U.S. Department of Health and Human Services, U.S. Public Health Services, Washington D.C., 1990, pp. 7, 226
18. I. R. DeLeon, C. J. Byrne, E. L. Peuler, S. R. Antoine, J. Schaefer, R. C. Murphy, *Chemosphere* **15** (1986) 795
19. S. Binet, P. Bonnet, H. Brandt, M. Castegnaro, P. Delsaut, J. F. Fabries, C. K. Huynh, M. Lafontaine, G. Morel, H. Nunge, B. Rihn, T. Vu Duc, R. Wrobel, *Ann. Occup. Hyg*. **46** (2002) 617
20. CLC Drug Discovery Workbench 2.4, 2015 CLC bio, QIAGEN Company
21. Oxford Diffraction, CrysAlis CCD & CrysAlis RED, Version 1.171.29.2, Oxford Diffraction Ltd., Wrocław, Poland, 2006
22. O. V. Dolomanov, L. J. Bourhis, R. J. Gildea, J. A. K. Howard, H. Puschmann, *J. Appl. Crystallogr*. **42** (2009) 339
23. G. M. Sheldrick, *Acta Crystallogr., A* **64** (2008) 112
24. L. J. Farrugia, *J. Appl. Cryst*. **45** (2012) 849
25. A. L. Spek, *Acta Crystallogr., D* **65** (2009) 148
26. C. F. Macrae, P. R. Edgington, P. McCabe, E. Pidcock, G. P. Shields, R. Taylor, M. Towler, J. van de Streek, *J. Appl. Crystallogr.* **39** (2006) 453
27. Gaussian 09, Revision A.02, Gaussian, Inc., Wallingford, CT, 2009
28. A. D. Becke, *J. Chem. Phys*. **98** (1993) 5648
29. C. Lee, W. Yang, R. G. Parr, *Phys. Rev., B* **37** (1998) 785
30. S. K. Wolff, D. J. Grimwood, J. J. McKinnon, D. Jayatilaka, M. A. Spackamn, *Crystal Explorer 3.0*, University of Western Australia, Perth, 2007
31. M. A. Spackman, D. Jayatilaka, *CrysEngComm* **11** (2009) 19

32. S. C. Chakrabarti, *Proc. Natl. Inst. Sci. India* **21** (1955) 263
33. A. C. Hazell, D. W. Jones, J. M. Sowden, *Acta Cryst*. **33** (1977) 1516
34. M. Munakata, L. P. Wu, G. L. Ning, T. Kuroda-Sowa, M. Maekawa, Y. Suenaga, N. Maeno, *J. Am. Chem. Soc*. **121** (1999) 4968
35. H. W. W. Ehrlich, *Acta Crystallogr*. **10** (1957) 699
36. A. C. Hazell, R. G. Hazell, L. Nørskov-Lauritsen, *Acta Crystallogr*. **42** (1986) 690
37. B. Schatschneider, J. J. Liang, *J. Chem. Phys*. **135** (2011) 164508
38. L. Ciabini, M. Santoro, F. A. Gorelli, R. Bini, V. Schettino, S. Raugei, *Nature Mater*. **6** (2007) 39
39. J. M. Robertson, J. G. White, *J. Chem. Soc*. (1956) 925
40. P. A. Wood, J. J. McKinnon, S. Parsons, E. Pidcock, M. A. Spackman, *CrystEngComm* **10** (2008) 368
41. G. R. Desiraju, A. Gavezzotti, *Acta Crystallogr., B* **45** (1989) 473
42. L. Loots, L. J. Barbour, *CrystEngComm* **14** (2012) 300
43. A. Parkin, G. Barr, W. Dong, C. J. Gilmore, D. Jayatilaka, J. J. McKinnon, M. A. Spackman, C. C. Wilson, *CrystEngComm* **9** (2007) 648
44. H. T. Flakus, W. Śmiszek-Lindert, K. Stadnicka, *Chem. Phys*. **335** (2007) 221
45. M. Hesse, H. Meier, B. Zeeh, *Spectroscopic Methods in Organic Chemistry*, Thieme, Stuttgart, 2007, p. 72.

Journal of the Serbian Chemical Society
JSCS@tmf.bg.ac.rs • www.shd.org.rs/JSCS
J. Serb. Chem. Soc. 80 (12) S385–S388 (2015) *Supplementary material*

SUPPLEMENTARY MATERIAL TO

X-Ray, Hirshfeld surface analysis, spectroscopic and DFT studies of polycyclic aromatic hydrocarbons: fluoranthene and acenaphthene

WIOLETA ŚMISZEK-LINDERT[1]*, ANNA MICHTA[2], ALEKSANDRA TYL[2], GRZEGORZ MAŁECKI[2], ELŻBIETA CHEŁMECKA[3] and SŁAWOMIR MAŚLANKA[2]

[1]Institute of Mechanized Construction & Rock Mining, W. Korfantego 193A Street, 40-157 Katowice, Poland, [2]Institute of Chemistry, University of Silesia, 9 Szkolna Street, 40-006 Katowice, Poland and [3]School of Pharmacy with Division of Laboratory Medicine in Sosnowiec, Medical University of Silesia, Katowice, Poland, Department of Statistics, 30 Ostrogórska Street, 41-200 Sosnowiec, Poland

J. Serb. Chem. Soc. 80 (12) (2015) 1489–1504

TABLE S-I. Comparison of selected calculated geometric parameters of fluoranthene with experiment values

Experimental (XRD)				Theoretical	
				6-31+G (d, p)	6-311++G(3df,2pd)
Bond length, Å					
C1–C2	1.396	C17–C18	1.365	1.381	1.374
C2–C3	1.406	C18–C19	1.401	1.425	1.419
C3–C4	1.358	C19–C20	1.361	1.386	1.379
C4–C5	1.410	C20–C21	1.410	1.426	1.420
C5–C6	1.416	C21–C22	1.410	1.419	1.416
C6–C7	1.356	C22–C23	1.357	1.386	1.379
C7–C8	1.399	C23–C24	1.401	1.425	1.418
C8–C9	1.368	C24–C25	1.356	1.381	1.374
C9–C10	1.403	C25–C26	1.405	1.404	1.398
C10–C5	1.396	C26–C21	1.396	1.419	1.413
C10–C1	1.407	C26–C17	1.405	1.393	1.386
C9–C11	1.477	C25–C27	1.472	1.477	1.473
C11–C12	1.381	C27–C28	1.376	1.402	1.395
C12–C13	1.394	C28–C29	1.362	1.400	1.392
C13–C14	1.370	C29–C30	1.372	1.380	1.379
C14–C15	1.383	C30–C31	1.393	1.402	1.395
C15–C16	1.380	C31–C32	1.383	1.393	1.386
C16–C11	1.410	C32–C27	1.416	1.428	1.422
C16–C1	1.473	C32–C17	1.475	1.477	1.472

* Corresponding author. E-mail: w.lindert@imbigs.pl

TABLE S-I. Continued

Experimental (XRD)				Theoretical	
				6-31+G (d, p)	6-311++G(3df,2pd)
Angle, °					
C10–C1–C2	118.00	C26–C17–C18	117.16	118.34	118.31
C1–C2–C3	119.00	C17–C18–C19	119.00	118.71	118.74
C2–C3–C4	122.60	C18–C19–C20	122.50	122.48	122.48
C3–C4–C5	120.50	C19–C20–C21	120.40	120.07	120.08
C4–C5–C10	115.60	C20–C21–C26	115.70	116.13	116.12
C5–C10–C1	124.20	C21–C26–C17	124.40	124.27	124.26
C10–C5–C6	115.50	C26–C21–C22	115.40	116.13	116.12
C5–C6–C7	120.70	C21–C22–C23	120.50	120.07	120.08
C6–C7–C8	122.40	C22–C23–C24	122.90	122.48	122.48
C7–C8–C9	119.30	C23–C24–C25	118.70	118.71	118.75
C8–C9–C10	118.00	C24–C25–C26	118.50	118.34	118.31
C9–C10–C5	124.10	C25–C26–C21	124.00	124.27	124.26
C9–C10–C1	111.60	C25–C26–C17	111.60	111.45	111.48
C10–C9–C11	106.20	C26–C25–C27	106.30	106.20	106.18
C9–C11–C16	107.90	C25–C27–C32	107.90	108.08	108.07
C11–C16–C1	108.30	C27–C32–C17	108.00	108.08	108.08
C16–C1–C10	106.00	C32–C17–C26	106.20	106.20	106.19
C9–C11–C12	131.90	C25–C27–C28	131.80	131.66	131.71
C11–C12–C13	118.10	C27–C28–C29	119.50	119.02	119.04
C12–C13–C14	121.30	C28–C29–C30	120.90	120.72	120.73
C13–C14–C15	121.20	C29–C30–C31	121.50	120.72	120.73
C14–C15–C16	118.30	C30–C31–C32	118.10	119.02	119.03
C15–C16–C11	120.80	C31–C32–C27	119.80	120.26	120.26
Dihedral angle, °					
C15–C16–C1–C2	–0.006	C31–C32–C–17–C18	–4.1(6)	0.002	0.023
C15–C16–C1–C10	179.4(3)	C31–C32–C17–C26	179.0(3)	179.99	–179.99
C12–C11–C9–C8	–2.4(6)	C28–C27–C25–C24	–0.3(6)	0.01	–0.01
C12–C11–C9–C10	179.3(3)	C28–C27–C25–C26	179.5(3)	179.98	179.98
C8–C9–C1–C1	–178.5(3)	C24–C25–C26–C17	–179.3(3)	179.99	179.99
C2–C1–C10–C9	–179.5(2)	C18–C17–C26–C25	–178.1(3)	179.99	179.99
C16–C1–C10–C5	–177.6(2)	C32–C17–C26–C21	179.1(3)	–179.99	179.98
C11–C9–C10–C5	178.7(2)	C27–C25–C26–C21	–178.7(3)	180.00	–180.00

TABLE S-II. Comparison of selected calculated geometric parameters of acenaphthene with experiment values

Experimental (XRD)				Theoretical	
				6-31G (d, p)	6-31G* (d, p)
Bond length, Å					
$C1^{i}$–$C6^{i}$	1.358	$C8^{ii}$–$C9^{ii}$	1.358	1.370	1.377
C6–C5	1.403	$C9^{ii}$–$C10^{ii}$	1.397	1.426	1.423
C5–C4	1.359	$C10^{ii}$–$C11^{ii}$	1.354	1.384	1.383
$C4^{i}$–C3	1.410	$C11^{ii}$–C12	1.414	1.425	1.422
C3–C4	1.410	C12–C11	1.414	1.425	1.422
C4–C5	1.359	C11–C10	1.354	1.384	1.383
C5–C6	1.403	C10–C9	1.397	1.426	1.423
C6–C1	1.358	C9–C8	1.358	1.378	1.377
C1–C2	1.400	C8–C13	1.400	1.414	1.412
C2–C3	1.398	C13–C12	1.393	1.414	1.414
$C2–C1^{i}$	1.400	$C13–C8^{ii}$	1.400	1.414	1.412
C1–C7	1.506	C8–C14	1.503	1.523	1.520
$C7–C7^{i}$	1.547	$C14–C14^{ii}$	1.534	1.575	1.570
$C7^{i}$–$C1^{i}$	1.506	$C14^{ii}$–$C8^{ii}$	1.503	1.523	1.520
Angle, °					
$C7^{i}$–$C1^{i}$–$C6^{i}$	132.93	$C14^{ii}$–$C8^{ii}$–$C9^{ii}$	133.14	132.40	132.40
$C7^{i}$–$C1^{i}$–C2	108.41	$C14^{ii}$–$C8^{ii}$–C13	108.21	108.70	108.70
$C1^{i}$–$C6^{i}$–$C5^{i}$	119.14	$C8^{ii}$–$C9^{ii}$–$C10^{ii}$	118.90	118.80	118.80
$C6^{i}$–$C5^{i}$–$C4^{i}$	122.20	$C9^{ii}$–$C10^{ii}$–$C11^{ii}$	122.80	122.30	122.30
$C5^{i}$–$C4^{i}$–C3	120.60	$C10^{ii}$–$C11^{ii}$–12	120.20	120.30	120.20
$C4^{i}$–C3–C2	115.87	$C11^{ii}$–C12–C13	115.86	116.30	116.30
$C4^{i}$–C3–C4	128.30	$C11^{ii}$–C12–C11	128.30	127.40	127.40
C3–C4–C5	120.60	C12–C11–C10	120.20	120.20	120.20
C4–C5–C6	122.20	C11–C10–C9	122.80	122.30	122.30
C5–C6–C1	119.14	C10–C9–C8	118.30	118.90	118.80
C6–C1–C2	118.66	C9–C8–C13	118.60	118.90	118.90
C6–C1–C7	132.93	C9–C8–C14	133.14	132.40	132.40
$C1–C7–C7^{i}$	105.13	$C8–C14–C14^{ii}$	105.40	104.80	104.80
$C7–C7^{i}–C1^{i}$	105.13	$C14–C14^{ii}–C8^{ii}$	105.40	104.80	104.80
$C1–C2–C1^{i}$	112.90	C8–C13–$C8^{ii}$	112.80	112.80	112.80
Dihedral angle, °					
$C7^{i}$–$C1^{i}$–$C6^{i}$–$C5^{i}$	179.3(2)	$C14^{ii}$–$C8^{ii}$–$C9^{ii}$–$C10^{ii}$	179.4(2)	180.00	180.00
C7–C1–C6–C5	–179.3(2)	C14–C8–C9–C10	–179.4(2)	–180.00	–180.00
$C1–C2–C1^{i}–C6^{i}$	179.2(2)	$C8–C13–C8^{ii}–C9^{ii}$	179.9(2)	180.00	180.00
$C4^{i}$–C3–C4–C5	–179.6(3)	$C11^{ii}$–C12–C11–C10	–179.6(3)	–180.00	–180.00

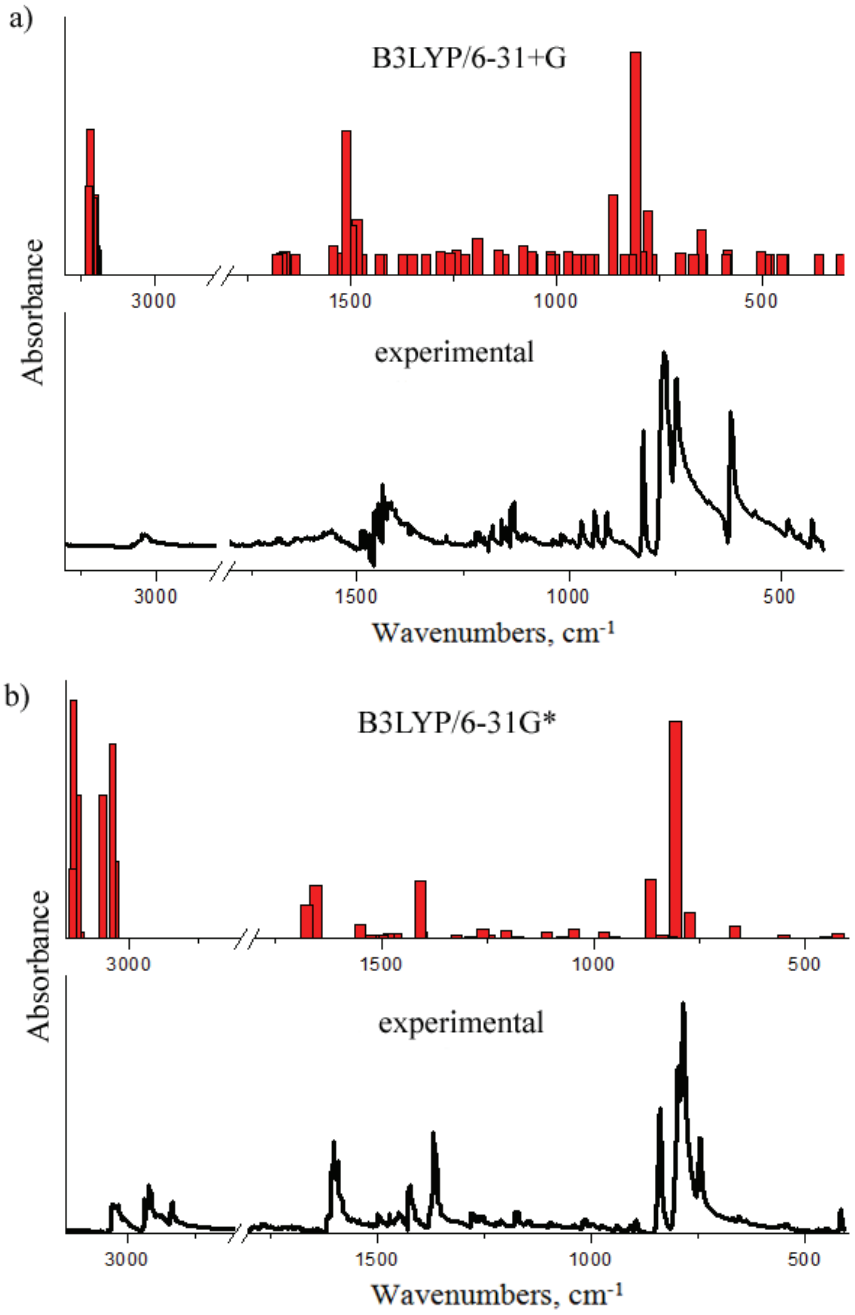

Fig. S-1. Comparison of B3LYP calculated IR spectra of: a) fluoranthene and b) acenaphthene with the corresponding experimental spectra.

Journal of the Serbian Chemical Society
JSCS-info@shd.org.rs • www.shd.org.rs/JSCS
J. Serb. Chem. Soc. 80 (12) 1505–1513 (2015)
JSCS–4815
UDC 533.9+546.264–31:544.537/.538:669.35'6'24
Original Scientific paper

Analytical capability of the plasma induced by IR TEA CO_2 laser pulses on copper-based alloys

MILOŠ MOMČILOVIĆ[1], JOVAN CIGANOVIĆ[1], DRAGAN RANKOVIĆ[2], UROŠ JOVANOVIĆ[1], MILOVAN STOILJKOVIĆ[1], JELENA SAVOVIĆ[1] and MILAN TRTICA[1]*

[1]*Vinča Institute of Nuclear Sciences, University of Belgrade, P. O. Box 522, 11001 Belgrade, Serbia and* [2]*Faculty of Physical Chemistry, University of Belgrade, P. O. Box 276, 11001 Belgrade, Serbia*

(Received 16 April, revised 11 June, accepted 3 July 2015)

Abstract: The applicability of a nanosecond infrared (IR) transversely excited atmospheric (TEA) CO_2 laser, operating at 10.6 μm and 100 ns pulse length (initial spike), induced plasma under reduced air pressure for spectrochemical analysis of bronze and brass samples was investigated. The plasma consisted of two clearly distinguished and spatially separated regions and expanded to a distance of about 10 mm from the surface. The elemental composition of the samples was determined using a time-integrated space-resolved laser-induced plasma spectroscopic (TISR–LIPS) technique. Sharp and well-resolved spectral lines mostly atomic, and negligibly low background emission, were obtained from a plasma region 7 mm from the target surface. Good signal to background and signal to noise ratios were obtained. The estimated detection limits for the trace elements Mg, Fe, Al and Ca were in the order of 10 ppm in bronze and around 50 ppm in brass. Damage on the investigated samples induced by TEA CO_2 laser radiation was negligible.

Keywords: TEA CO_2 laser; LIBS; copper-based alloys.

INTRODUCTION

Laser-induced breakdown spectroscopy (LIBS) is a powerful analytical technique for rapid analysis of a large variety of materials. A number of works report LIBS application for the analysis of bronze and brass samples,[1–5] and many of the samples were cultural heritage materials. This is not surprising because copper-based alloys were often used in ancient times and LIBS appears to be the most suitable technique for dating and rapid classification of metal objects.[6] Nowadays, a variety of techniques, including X-ray photoelectron spectroscopy, X-ray fluorescence and diffraction spectroscopy, Raman spectroscopy, Fourier

* Corresponding author. E-mail: etrtica@vinca.rs
doi: 10.2298/JSC150416061M

transform infrared spectroscopy, scanning electron microscopy, inductively--coupled-plasma atomic-emission spectrometry and (laser ablation) inductively--coupled mass spectrometry have been successfully used for the characterization of archaeological objects.[7,8] Although some of the aforementioned techniques may have better analytical figures of merit (such as accuracy, precision and limits of detection), the specific features of LIBS makes this technique particularly suitable for elemental analysis of cultural heritage objects. LIBS combines the capability of providing fast multi-elemental analysis with no sample pretreatment, potential for *in situ* and remote analysis, micro-destructiveness and the ability to provide isotopic ratio information additionally to elemental composition. Besides, virtually unique to LIBS is the possibility of surface cleaning, analyzing multilayered samples and performing depth profiling. One of the main difficulties for a precise and accurate quantitative analysis by LIBS is due to matrix effects, to which laser induced plasmas can be very sensitive.

Although various laser systems were used for plasma generation,[5,9,10] LIBS analysis of copper-based alloys was most often accomplished by means of Nd:YAG lasers. To the best of our knowledge, the possible use of transversely excited atmospheric (TEA) CO_2 laser has not hitherto been examined. There are two main reasons for this. First, the photon energy of CO_2 laser radiation is relatively low (≈0.12 eV whereas, for comparison, Nd:YAG laser photon energy is ≈1.17 eV). Second, copper strongly reflects the incident light in the infrared spectral range (for CO_2 laser emission wavelength of 10.6 μm, the reflectivity is ≈98 %). Considering the analysis of metal samples, the most critical stage for plasma generation using a TEA CO_2 laser is heating and evaporation of the target. However, once the initial plasma is produced, the long wavelength and long pulse duration of CO_2 laser becomes advantageous. The initial plasma absorbs the remaining laser pulse energy through inverse "Bremsstrahlung" and this absorption is much stronger in the case of a TEA CO_2 laser than for an Nd:YAG laser.[11] This is because the plasma absorption coefficient is proportional to the square of the laser wavelength. Thus, when a CO_2 laser is used, appreciable laser heating of the plasma occurs at low density far from the target surface. Consequently, spatial discrimination between line and continuum emission is improved and line broadening reduced. It was shown that under reduced air pressure, plasma could readily be induced by irradiation of a copper target with TEA CO_2 laser peak intensity of 30 MW cm^{-2}.[12–14]

The aim of the present study was to test the applicability of TEA CO_2 laser induced plasma under reduced air pressure for spectrochemical analysis of copper-based alloys: bronze (Cu–Sn) and brass (Cu–Zn). The obtained results should provide a basis for potential applications of TEA CO_2 laser based LIBS for the analysis of cultural heritage objects made of copper alloys.

EXPERIMENTAL

Schematic diagram of experimental setup used for LIBS analysis of bronze and brass samples is shown in Fig. 1. Plasma was initiated by irradiation of a metal target with a nanosecond infrared (IR) transversely excited atmospheric (TEA) CO_2 laser, operating at 10.6 μm. A typical output pulse energy was 150 mJ, and the repetition rate during the experiments was 1.5 Hz. The laser/optical pulse had a gain switched spike followed by a slowly decaying tail. The full width at half maximum, FWHM, of the spike was about 100 ns while the tail duration was ≈2 μs. The energy sustained in the initial spike was about 35 % of the total irradiated laser energy.

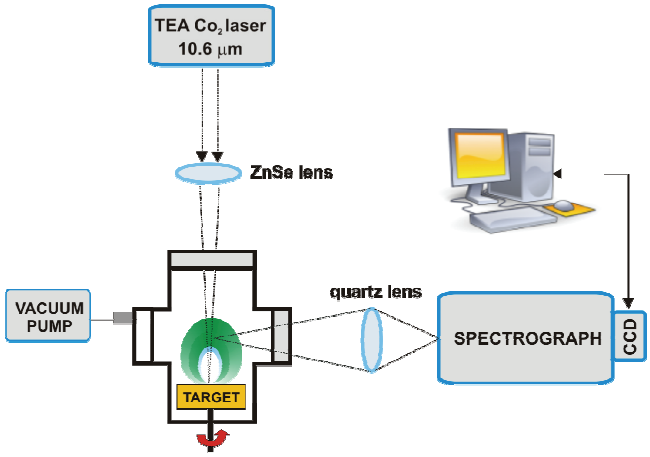

Fig. 1. Schematic diagram of experimental setup used for LIBS analysis of bronze and brass samples.

The samples were placed in a glass vacuum chamber closed with NaCl and CaF_2 windows. The air pressure during the experiments was ≈0.1 mbar. The production of stable and reproducible plasma required a "fresh" area at the target surface between two successive laser pulses, which was achieved by rotation of the sample at 0.5 rpm using a step motor.

The optical emission from the plasma was viewed in the direction parallel to the target surface. By changing the position of the plasma along the direction of the laser beam, while keeping a constant distance between the focusing lens and the target, different parts of the plasma were observed, *i.e.*, a spatial plasma resolution was achieved. The horizontal part of the plume was projected by a lens on the entrance slit of a monochromator (Carl-Zeiss PGS2 dispersion 0.7 nm/mm). For the time-integrated spatially resolved measurements, an Apogee Alta F1007 CCD camera was used. Each emission spectrum was obtained by integration of 30 laser shots impinging on fresh spots of the target.

The high electron density of the plasma immediately after laser ablation gives rise to a strong continuum emission and to broadening of the lines because of the Stark effect. Usually temporal gating of the emission is used in order to discriminate the atomic emission from the continuum background. In this work, time-integrated space-resolved laser induced plasma spectroscopy (TISR–LIPS) was used.[14,15] This method relies on the fact that the intense plasma background spectral continuum emission is mostly emitted from a region close to the sample surface, while in the further-out regions of the plasma, the continuum emission is

largely reduced. The fact that the plasma reaches a given distance above the analyzed surface with a certain time delay enables replacing temporal with spatial resolution. Thus, instead of time-gated detection, the position-selective spectra were recorded.

RESULTS AND DISCUSSION

The plasma was initiated by irradiation of a copper alloy target with a fluence of ≈8.6 J cm^{-2} in an air atmosphere at a pressure of 0.1 mbar. The plasma consisted of two clearly distinguished and spatially separated regions, Fig. 2. The first region, close to the target surface (length about 5 mm), was characterized by a whitish color and is known as primary plasma. The second region, also known as the secondary plasma, was larger in volume, had a hemispherical shape and intense green color, due to emission of the spectral lines of the target. The plasma expanded to a distance of about 10 mm from the surface.

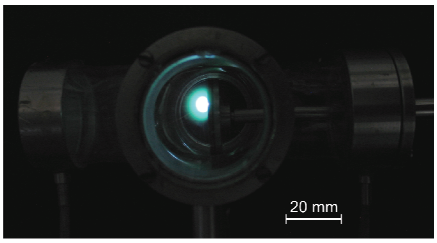

Fig. 2. Image of the plasma induced over a brass sample.

The composition of bronze and brass samples used in this study were determined by inductively coupled plasma atomic emission spectroscopy (ICP--AES), Table I.

TABLE I. Elemental composition of bronze and brass samples; nd: not detected

Sample	Metal											
	Cu	Sn	Zn	Pb	Ni	Ca	Fe	Al	Co	Mg	Mn	Cr
	wt. %						μg g^{-1}					
Bronze	56	41	1.7	1.1	0.07	0.04	60	40	32	26	8	6
Brass	69	nd	30	nd	nd	0.23	260	125	nd	300	<5	nd

The time-integrated emission spectra of the major and trace elements present in the bronze and brass samples are shown in Figs. 3 and 4; the optical emission was analyzed in the wavelength region ranging from about 250 to 650 nm, but the LIBS experimental spectra in the most significant wavelength windows are shown. The spectrum consisted of well-resolved sharp emission lines, and low background emission intensity. Good signal to noise and signal to background ratios were obtained. The signal to background, and signal to noise ratios together with the estimated limits of detection (*LOD*) are presented in Table II. The limits of detection were calculated using the formula:

$$LOD = 3BEC \times RSD_B$$

where *BEC* is the background equivalent concentration and RSD_B is the relative standard deviation of the background.

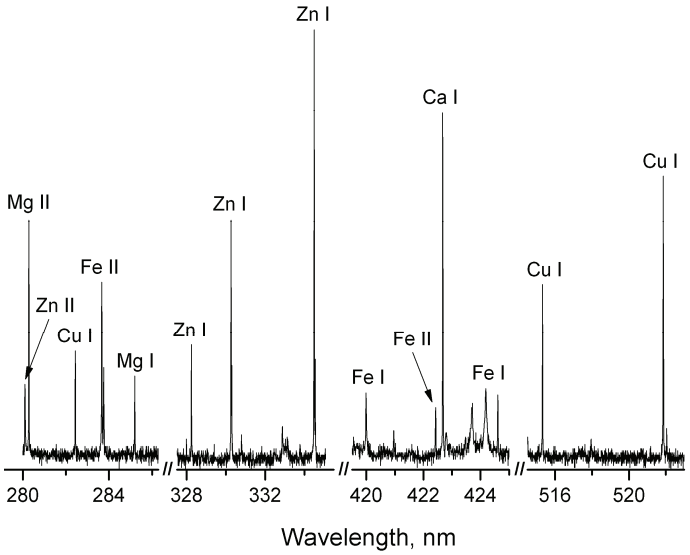

Fig. 3. LIBS spectra of the brass sample. The composition of the sample is given in Table I. The main emission lines are labeled in the spectrum. Air pressure 0.1 mbar, laser fluence 8.6 J cm^{-2} (intensity 30 MW cm^{-2}).

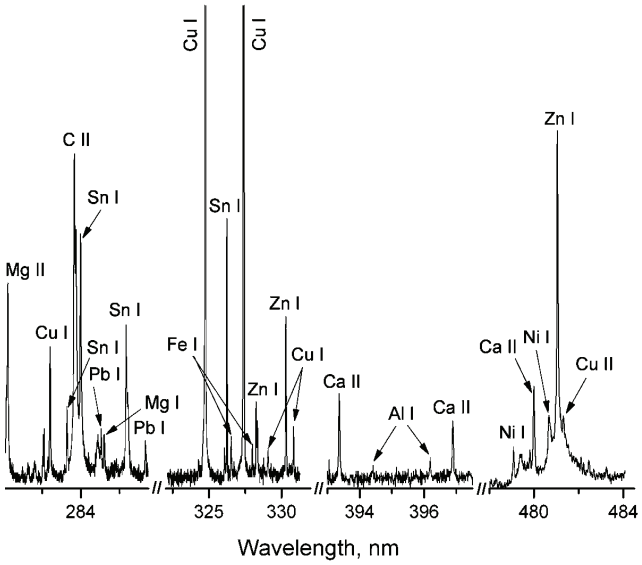

Fig. 4. LIBS spectra of bronze sample. The composition of the sample is given in Table I. The main emission lines are labeled in the spectrum. Air pressure: 0.1 mbar, laser fluence 8.6 J cm^{-2} (intensity 30 MW cm^{-2}).

TABLE II. Signal to noise (*S*/*N*) and signal to background (*S*/*B*) ratio, and the estimated limits of detection (*LOD*) for bronze and brass

Element	Wavelength, nm	*S*/*N*	*S*/*B*	*LOD* / mg kg^{-1}
Bronze				
Mg	280.27	40	4	2
Fe	328.02	14	2	13
Al	396.15	9	1	13
Ca	422.67	56	2	21
Brass				
Mg	285.21	26	5	35
Fe	288.13	20	3	40
Al	396.15	30	36	13
Ca	422.67	126	16	55

Higher *LOD* obtained for brass compared to bronze may be a consequence of a matrix effect that leads to variations in the plasma parameters. In the case of metallic samples, stronger matrix effects were found for alloys with high Zn contents, such as brass.[2,5] Thermal vaporization may significantly influence the ablation processes, especially when the ablation is accomplished by a low power density, long-pulse duration laser, as in the present study.

There are a large number of research papers devoted to the application of LIBS for the analyses of copper-based alloys. However, they are mainly limited to the determination of major elements, while there are still very few works that report *LOD* values for minor or trace elements. Furthermore, different elements were analyzed, thus comparison of the present results with literature data is rather limited. One exception is iron, for which *LOD* values of 22.3[16] and 150 ppm[17] were evaluated for Fe I 372.26 nm and Fe II 234.83 nm lines, respectively. For other minor elements, such as Ag, As, Ni and Pb, the limits of detection were in the range from 1.4 to 250 ppm;[16,17] in both papers, an Nd:YAG laser and time gated detection (iCCD camera) was used. Limits of detection are element dependent, nevertheless the *LOD* values obtained using TEA CO_2 laser and non-gated detection are of the same order of magnitude (ppm) as the ones obtained with standard LIBS.

Each analytical technique available for the characterization of archaeological objects is characterized by its own strengths and weaknesses. The selection of the most appropriate depends on the analytical problem, on possible limitations imposed by the object or sample examined, and on the capabilities of the technique. Although the *LOD* of a spectral line is an important characteristic, it is just one of many parameters that are considered in the method selection process. For example, the *LOD* values of inductively coupled mass spectrometry are among the lowest (μg–ng per kg), however this method is destructive (the sample to be analyzed must be digested prior to analysis) and could not be used if there is a need for *in situ* analysis. Special features of LIBS, such as rapidity, low invasive-

ness, high spatial discrimination and possibility to perform *in situ* measurements, make this technique quite competitive compared with other techniques commonly used in archaeological science for obtaining information about elemental composition.

An important characteristic of the proposed LIBS system is position-selective emission spectroscopy, which eliminates the need for time-gated detection. This is not a new concept, it was already successfully applied for studying various laser induced plasmas.[18,19] For instance, Bulatov *et al*.[18] applied non-gated detection for the analysis of brass samples using a Nd:YAG laser (400 mJ, 7 ns, 2.25×10^9 W cm^{-2}). Compared to the Nd:YAG laser, the TEA CO_2 laser has a longer wavelength and longer pulse duration. Both these characteristics are favorable for non-gated detection of spectral lines. In general, the dimensions and lifetime of a plasma increase with pulse duration. The plasma takes longer to decay and hence, the emission lasts longer. The leading part of the TEA CO_2 laser pulse (FWHM ≈100 ns) produces the plasma, while the tail part (≈2 μs) interacts with it by means of laser absorption. Absorption of the laser radiation in the plasma occurs mainly by inverse "Bremsstrahlung", which increases as the laser wavelength increases.[11] Absorption by the plume causes an additional plasma excitation and expansion, which increase the LIBS signal through enhancement of emission lines. Simultaneously, because of the longer wavelength of CO_2 laser radiation, heating of the plasma by optical absorption occurs at lower plasma densities.[11] Strong line emission is therefore observed at greater distances from the target surface, where the background is negligibly low. In general, a shorter pulse gives a higher ablation rate, if the pulse energy or the fluence is constant.[19,20] This means that the higher emission intensities obtained by the elongated pulses do not indicate a higher ablation rate, but rather a higher efficiency of the emission.[18]

The goal of this investigation was to test the applicability of a TEA CO_2 laser based LIBS for the analysis of copper alloys, with the intention to (eventually) use this system for the analysis of cultural heritage objects made of bronze and brass. In this regard, it is important to mention that the TEA CO_2 laser radiation induced negligible damage on the investigated samples. Previous results showed that irradiation of a pure copper target with a TEA CO_2 laser intensity of approx. 100 MW cm^{-2} under 0.1 mbar air pressure induced only superficial damage, practically invisible in the OM image (magnification 50×).[14]

Taking all into consideration (compact, low-cost detection system; well-resolved spectral lines; *LOD* values in the ppm range, typical for LIBS; minimal destructivity), it could be concluded that for the elemental analysis of copper alloys, the proposed LIBS system based on a TEA CO_2 laser may be a suitable alternative to conventional LIBS using an Nd:YAG laser.

CONCLUSIONS

The plasma was induced by irradiation of a copper alloy target with 30 MW cm^{-2} of TEA CO_2 laser peak intensity, in air at 0.1 mbar. Time-integrated emission spectra of elements present in the bronze and brass samples were used for an evaluation of the signal to background and signal to noise ratios, and an estimation of the limits of detection. Detection limits for trace elements were in the order of 10 ppm in brass and around 50 ppm in bronze. The single-shot TEA CO_2 LIBS has significant potential for cultural heritage applications.

Acknowledgement. This work was supported by the Ministry of Education, Science and Technological Development of the Republic Serbia, Project No. 172019.

И З В О Д

ПЛАЗМА ИНДУКОВАНА ИНФРАЦРВЕНИМ TEA CO_2 ЛАСЕРОМ НА ЛЕГУРАМА БАКРА – МОГУЋНОСТИ АНАЛИТИЧКЕ ПРИМЕНЕ

МИЛОШ МОМЧИЛОВИЋ[1], ЈОВАН ЦИГАНОВИЋ[1], ДРАГАН РАНКОВИЋ[2], УРОШ ЈОВАНОВИЋ[1], МИЛОВАН СТОИЉКОВИЋ[1], ЈЕЛЕНА САВОВИЋ[1] и МИЛАН ТРТИЦА[1]

[1]Институт за нуклеарне науке Винча, Универзитет у Београду, 11001 Београд и [2]Факултет за физичку хемију, Универзитет у Београду, Студентски трг 12–16, 11001 Београд

Испитана је могућност спектрохемијске примене плазме индуковане дејством зрачења импулсног TEA CO_2 ласера (10,6 μm, 100 nm) на мете од бронзе и месинга. Димензија плазме индуковане на сниженом притиску ваздуха износила је 10 mm са јасно израженим и просторно раздвојеним областима. Елементни састав узорака одређен је временски интегрираном просторно разложеном емисионом спектроскопијом ласерски индуковане плазме (TISR–LIPS). Оштре и добро разложене спектралне линије (углавном атомске), уз занемарљиво ниску емисију позадине, добијене су посматрањем плазме на растојању 7 mm од површине мете. Такође, добијен је добар однос линије према позадини и линије према шуму. Добијене границе детекције за елементе у траговима, Mg, Fe, Al и Ca, биле су реда величине око 10 ppm у бронзи и око 50 ppm у месингу. Оштећења настала дејством ласерског TEA CO_2 зрачења на испитиваним узорцима била су незнатна.

(Примљено 16. априла, ревидирано 11. јуна, прихваћено 3. јула 2015

REFERENCES

1. F. Colao, R. Fantoni, V. Lazic, V. Spizzichino, *Spectrochim. Acta, B* **57** (2002) 1219
2. L. Fornarini, R. Fantoni, F. Colao, A. Santagata, R. Teghil, A. Elhassan, M. A. Harith, *J. Phys. Chem., A* **113** (2009) 14364
3. F. J. Fortes, M. Cortes, M. D. Simon, L. M. Cabalın, J. J. Laserna, *Anal. Chim. Acta* **554** (2005) 136
4. A. A. Shaltout, M. S. Abdel-Aal, N. Y. Mostafa, *J. Appl. Spectrosc.* **78** (2011) 594
5. V. Margetic, A. Pakulev, A. Stockhaus, M. Bolshov, K. Niemax, R. Hergenroder, *Spectrochim. Acta, B* **55** (2000) 1771
6. R. Gaudiuso, M. Dell'Aglio, O. De Pascale, G. S. Senesi, A. De Giacomo, *Sensors* **10** (2010) 7434
7. E. Ciliberto, G. Spoto, Eds., *Modern Analytical Methods in Art and Archaeology*, Wiley/Interscience, New York, 2000

8. A. Giakoumaki, K. Melessanaki, D. Anglos, *Anal. Bioanal. Chem.* **387** (2007) 749
9. A. Elhassan, A. Giakoumaki, D. Anglos, G. M. Ingo, L. Robbiola, M. A. Harith, *Spectrochim. Acta, B* **63** (2008) 504
10. A. De Giacomo, M. Dell'Aglio, O. De Pascale, R. Gaudiuso, R. Teghil, A. Santagata, G. P. Parisi, *Appl. Surf. Sci*. **253** (2007) 7677
11. A. Khumaeni, Z. S. Lie, H. Niki, K. H. Kurniawan, E. Tjoeng, Y. I. Lee, K. Kurihara, Y. Deguchi, K. Kagawa, *Anal. Bioanal. Chem.* **400** (2011) 3279
12. M. Momcilovic, M. Trtica, J. Ciganovic, J. Savovic, J. Stasic, M. Kuzmanovic, *Appl. Surf. Sci.* **270** (2013) 486
13. M. Kuzmanovic, M. Momcilovic, J. Ciganovic, D. Rankovic, J. Savovic, D. Milovanovic, M. Stoiljkovic, M. S. Pavlovic, M. Trtica, *Phys. Scr. T.* **162** (2014) 014011
14. M. Momcilovic, M. Kuzmanovic, D. Rankovic, J. Ciganovic, M. Stoiljkovic, J. Savovic, M. Trtica, *Appl. Spectrosc*. **69** (2015) 419
15. M. A. Khater, P. van Kampen, J. T Costello, J. P. Mosnier, E. T. Kennedy, *J. Phys., D: Appl. Phys.* **33** (2000) 2252
16. M. Sabsabi, P. Cielo, *J. Anal. At. Spectrom.* **10** (1995) 643
17. F. J. Fortes, M. Cortes, M. D. Simon, L. M. Cabalın, J. J. Laserna, *Anal. Chim. Acta* **554** (2005) 136
18. V. Bulatov, R. Krasniker, I. Schechter, *Anal. Chem.* **72** (2000) 2987
19. A. Matsumoto, A. Tamura, K. Fukami, Y. H. Ogata, T. Sakka, *Anal. Chem.* **85** (2013) 3807
20. T. Sakka, H. Oguchi, S. Masai, K. Hirata, Y. H. Ogata, M. Saeki, H. Ohba, *Appl. Phys. Lett.* **88** (2006) 061120.

Journal of the Serbian Chemical Society
JSCS-info@shd.org.rs • www.shd.org.rs/JSCS
J. Serb. Chem. Soc. 80 (12) 1515–1527 (2015)
JSCS–4816
UDC 546.73+547.313.2'415.1:544.653.3
Original Scientific paper

Electrochemistry of cobalt ethylenediamine complexes at high pH

SNEŽANA M. MIULOVIĆ*, VLADIMIR M. NIKOLIĆ, PETAR Z. LAUŠEVIĆ, DANKA D. AĆIMOVIĆ, GVOZDEN S. TASIĆ and MILICA P. MARČETA KANINSKI

Institute of Nuclear Sciences – Vinča, Laboratory of Physical Chemistry, University of Belgrade, 11000 Belgrade, Mike Alasa 12–14, Serbia

(Received 27 March, revised 23 June, accepted 30 June 2015)

Abstract: The electrochemical behavior of cobalt ethylenediamine complexes (Co(en)), at pH 12 was investigated by cyclic voltammetry (CV), the potentiostatic pulse technique and polarization curve measurements at stationary and rotating glassy carbon (GC) electrodes. It was shown that sixteen different species could be formed in a solution containing $Co(en)_3$, with the most stable one at all pH values being $[Co(en)_3]^{3+}$. The reduction of $[Co(en)_3]^{3+}$ into $[Co(en)_3]^{2+}$ was shown to be a totally irreversible, one-electron exchange reaction. Further reduction of $[Co(en)_3]^{2+}$ was found to be a complex process leading to cobalt deposition at potentials more negative than –1.45 V *vs*. SCE. The process of $[Co(en)_3]^{2+}$ oxidation was also complex and most probably coupled with chemical reactions.

Keywords: distribution of $Co(en)_3$-based complexes; irreversible reduction of $[Co(en)_3]^{3+}/[Co(en)_3]^{2+}$; reduction of $[Co(en)_3]^{2+}$ to Co.

INTRODUCTION

The $Co(en)_3Cl_3$ was first described and isolated as yellow–gold needle-like crystals by Werner.[1] This was important in the history of coordination chemistry due to its stability and stereochemistry. The cation $[Co(en)_3]^{3+}$ has an octahedral structure with Co–N distance in the range 0.1947–0.1981 nm, with N–Co–N angles of 85° within the chelate rings and 90° between the N atoms on adjacent rings.[2] The acid–base, *cis–trans*, and complex equilibria in the cobalt(III)(en) system was investigated by Bjerrum and Rasmunssen.[3] It was shown that in an inert cobalt(III)(en) system, the first hydrolysis constant of the tris(en) ion could be estimated by analytical methods. In the system of diaquobis(en) cobalt(III) ions, *cis–trans* equilibria are established spontaneously. All acidic dissociation and *cis–trans* equilibrium constants were determined. In addition, it was shown

* Corresponding author. E-mail: snezana.miulovic@vinca.rs
doi: 10.2298/JSC150327079M

that the partial formation constants could be estimated by glass electrode and spectrophotometric measurements.[3]

It was shown that $[Co(en)_3]^{3+}$ became reversibly reduced to the divalent state at a dropping mercury electrode in an excess of (en), while irreversible behavior was detected in the absence of the complexing agent.[4,5] Using the cyclic voltammetry (CV) technique, the formal potential for the reduction of $[Co(en)_3]^{3+}$ into $[Co(en)_3]^{2+}$ in an aqueous solution of 0.1 mol dm^{-3} $LiClO_4$ was found to be about –0.46 V *vs*. SCE.[6] It was stated by the same authors that, although $[Co(en)_3]^{2+}$ is labile, a small excess (0.002–0.01 mol dm^{-3}) of (en) was required in order to prevent dissociation of $[Co(en)_3]^{2+}$.[7] At the same time. the authors claimed that equal cathodic and anodic peak currents were obtained at the CV, with the separation of the peak potentials varying between 60 and 90 mV in the investigated solution.[7] In many electrochemical investigations, the redox reaction $[Co(en)_3]^{3+}/[Co(en)_3]^{2+}$ was examined in order to determine the influence of the outer-sphere effects on the reduction process.[8,9]

One of the important applications of $Co(en)_3Cl_3$ is its use as an ionic activator for the *in situ* activation of the hydrogen evolution reaction (HER) in combination with molybdate ions.[10–12] The addition of small concentrations (0.001––0.01 mol dm^{-3}) of ionic activators reduced the overvoltage for HER and the energy needs per mass unit of hydrogen produced.[13] A possible mechanism for the *in situ* activation of the HER has not yet been offered. It is supposed that both metals deposit on the cathode surface producing large surface area of active centers.[14–17] At the same time the catalytic activity of (en), which is present in the electrolyte after decomposition of cobalt complex, has been discussed in the light of Rowland's effect.[18,19] It is assumed that (en) cleans the cathode surface by removing the oxide film and preparing it for deposition of Co and Mo. Since it is found that both metals are present in a very rough deposit formed during the process of *in situ* activation,[14,15] the question arises what is the current efficiency for the deposition of such coatings and how often these chemicals should be added to the electrolyte in order to maintain the same catalytic activity for the HER.

In this work, an attempt was made to better understand the process of $[Co(en)_3]^{3+}$ reduction to metallic cobalt in the presence of an excess of (en) at high pH.

EXPERIMENTAL

All experiments were performed with extra pure UV water (Smart2PureUV, TKA) and p.a. chemicals in a standard electrochemical cell (EuroCell, Gamry Instruments). The working electrode was a glassy carbon (GC) rotating disc electrode (RDE, Gamry Instruments). A saturated calomel electrode (SCE), connected to the working electrode by means of a Luggin capillary, was used as the reference electrode, while a Pt wire was the counter electrode. Rotating experiments were performed with an RDE710 rotating system (Gamry Instruments). Before the experiments, the GC electrode was polished on polishing cloths impregnated with

polishing alumina (0.05 μm), kept in an ultrasonic bath for 10 min and rinsed with UV--purified water. CV, pulse experiments and polarization measurements were performed with a Reference 600 potentiostat using PHE 200 software (Gamry Instruments).

The distribution of the Co^{3+} and Co^{2+} complexes in the investigated solutions was obtained with the commercial software HySS2009 (Protonic Software).

RESULTS AND DISCUSSION

Distribution of different cobalt complexes

In the solution containing excess of ethylenediamine (en) of 0.2 mol dm^{-3} and 0.01 mol dm^{-3} Co^{2+} (as $CoCl_2$), the following species could be formed:[20] (en), (en)H, (en)H_2, Co^{2+}, $[Co(OH)]^+$, $[Co(OH)_2]$, $[Co(OH)_3]^-$, $[Co_4(OH)_4]^{4+}$, $[Co(en)]^{2+}$, $[Co(en)_2]^{2+}$ and $[Co(en)_3]^{2+}$. In the same solution of ethylenediamine and 0.01 mol dm^{-3} Co^{3+} (as $Co(en)_3Cl_3$), among (en), (en)H and (en)H_2, additional species, Co^{3+}, $[Co(OH)]^{2+}$, $[Co(en)]^{3+}$, $[Co(en)_2]^{3+}$ and $[Co(en)_3]^{3+}$ could be formed. Hence, if both Co^{2+} and Co^{3+} are present in 0.2 mol dm^{-3} (en), sixteen different species could be formed. Taking into account the stability constants for all the above-mentioned species, it is possible to obtain distributions of all species as a function of *pH* (using HySS 2009 software).[20] The results of such an analysis are presented in Fig. 1: a) only Co^{2+} is present in the solution, b) only Co^{3+} is present in the solution or c) both Co^{2+} and Co^{3+} are present in the solution. As could be seen in Fig. 1a, at pH values higher than 10, only the $[Co(en)_3]^{2+}$ complex is present in the solution. Figure 1b shows that the $[Co(en)_3]^{3+}$ complex is dominant at all pH values with its concentration being 0.01 mol dm^{-3} (concentration of (en) is also independent of pH), while Fig. 1c confirms that at pH > 10 $[Co(en)_3]^{2+}$ and $[Co(en)_3]^{3+}$ complexes dominate in 0.2 mol dm^{-3} (en). Hence, in an excess of (en) and at pH 12 (Fig. 1c), it should be possible to investigate the oxidation of $[Co(en)_3]^{2+}$ to $[Co(en)_3]^{3+}$, as well as the reduction of $[Co(en)_3]^{3+}$ to $[Co(en)_3]^{2+}$.

Electrochemical behavior of Co^{3+} in 0.2 mol dm^{-3} ethylenediamine

The CVs recorded on a GC electrode at a sweep rate of 100 mV s^{-1} in (a) a solution containing 0.01 mol dm^{-3} $Co(en)_3Cl_3$ + 0.2 mol dm^{-3} (en) and (b) 0.001 mol dm^{-3} $Co(en)_3Cl_3$ + 0.2 mol dm^{-3} (en) are shown in Fig. 2. The CV's were recorded at a stationary (0 r.p.m.) and rotating electrodes (1000 r.p.m. and 2000 r.p.m.). Identical behavior was observed in both solutions, except that the current densities were one order of magnitude lower in the solution containing the lower concentration of cobalt ions (Fig. 2b). The starting potential was set at –0.4 V and electrode was cycled first towards anodic potentials (up to 0.5 V). As expected, no oxidation peak was recorded during the first sweep, since only the $[Co(en)_3]^{3+}$ complex was present in the solution. During the reverse sweep down to –1.0 V, well defined reduction peaks at about –0.7 V (a) and –0.6 V (b) were obtained at the stationary electrode. In both cases, reduction of $[Co(en)_3]^{3+}$ to

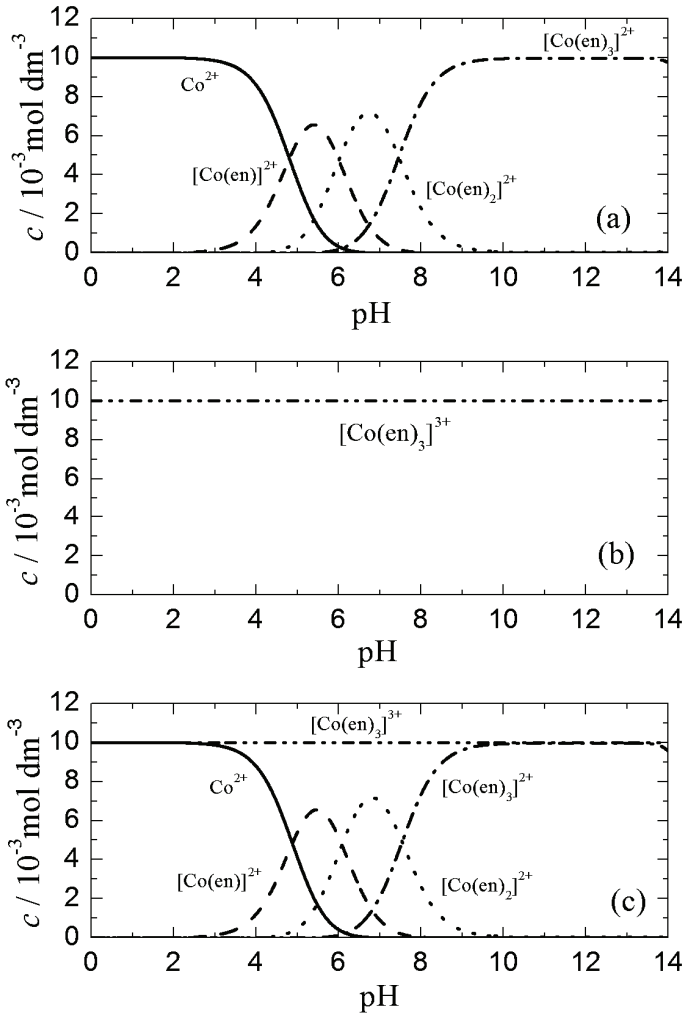

Fig. 1. Distribution of different cobalt complexes in the solution 0.2 mol dm^{-3} ethylenediamine, pH 12: (a) 0.01 mol dm^{-3} Co^{2+}; (b) 0.01 mol dm^{-3} Co^{3+}; (c) 0.01 mol dm^{-3} Co^{2+} + 0.01 mol dm^{-3} Co^{3+}.

$[Co(en)_3]^{2+}$ commenced at about –0.45 V, being defined by cathodic peaks at the stationary electrode (0 rpm) and current density plateaus at the rotating electrode (1000 and 2000 rpm). The oxidation of $[Co(en)_3]^{2+}$ to $[Co(en)_3]^{3+}$ was evidenced only at the stationary electrode after the formation of the $[Co(en)_3]^{2+}$ complex during the first sweep that remained in the vicinity of the electrode surface, being characterized by a broad anodic peak for all subsequent sweeps (2^{nd}–n^{th}). At the rotating electrode, this reaction did not occur, since all the $[Co(en)_3]^{2+}$ complexes formed during the reduction of $[Co(en)_3]^{3+}$ were transfer-

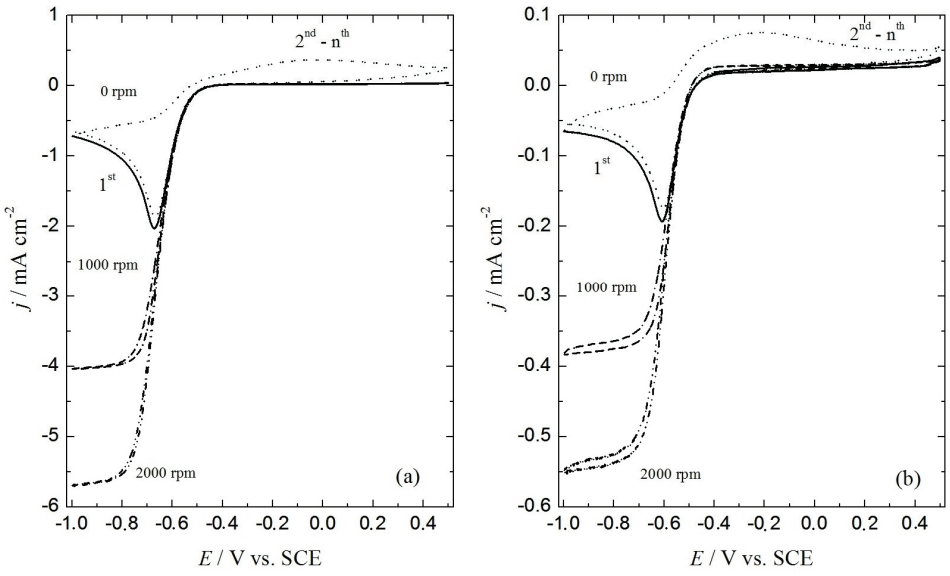

Fig. 2. CVs recorded at v = 100 mV s^{-1} at different rotation speeds (marked in the figure) in (a) solutions containing 0.01 mol dm^{-3} $Co(en)_3Cl_3$ + 0.2 mol dm^{-3} (en) and (b) 0.001 mol dm^{-3} $Co(en)_3Cl_3$ + 0.2 mol dm^{-3} (en).

red from the electrode surface to the bulk electrolyte during electrode rotation. Hence, it could be concluded that only a certain amount of $[Co(en)_3]^{2+}$, *i.e.*, that which remained in the vicinity of the surface of the stationary electrode after reduction of $[Co(en)_3]^{3+}$ to $[Co(en)_3]^{2+}$, could be oxidized to $[Co(en)_3]^{3+}$ during the anodic sweep. Taking into account that the whole amount of cobalt in both solutions is in the form of $[Co(en)_3]^{3+}$ complex (Fig. 1b), such behavior could be expected. This finding is in accordance with certain literature data,[5] while some authors claimed that the reduction/oxidation process is reversible with differences in the peak potentials varying from 60 to 90 mV.[7]

Polarization curves for reduction of $[Co(en)_3]^{3+}$ to $[Co(en)_3]^{2+}$, recorded at a sweep rate of 5 mV s^{-1} at different rotation speeds are presented in Fig. 3a. As can be seen, well-defined diffusion limiting current density plateaus were obtained at potentials more negative than –0.7 V with the shape of the j–E curves being typical for a totally irreversible reaction. The j^{-1} *vs.* $\omega^{-1/2}$ dependences, obtained by analysis of the polarization curves presented in Fig. 2a, are plotted in Fig. 3b for different potentials and the j^{-1} *vs.* $\omega^{-1/2}$ dependence recorded for E = –0.80 V was the linear one passing through zero. The diffusion coefficient calculated from the slope of this dependence (using the Koutecky–Levich Equation for a one-electron exchange)[21] amounted to 1.60×10^{-5} cm^2 s^{-1}. As expected, in the region of mixed activation–diffusion control of the reduction process (potential range from –0.45 to –0.65 V), the values of intercepts on the j^{-1} axes

increased with decreasing cathodic potential, producing higher values of the kinetic current density (j_k) and accordingly higher values of the rate constants ($k_f(E)$) at a given potential, since:[21]

$$j_k = Fk_f(E)c_0 \quad (1)$$

where c_0 is the bulk concentration of the $[Co(en)_3]^{3+}$ complex. Corresponding values of the rate constants were E = –0.60 V, $k_f(E)$ = 0.0497 cm s^{-1}; E = –0.55 V, $k_f(E)$ = 0.0122 cm s^{-1} and E = –0.50 V, $k_f(E)$ = 0.0022 cm s^{-1}.

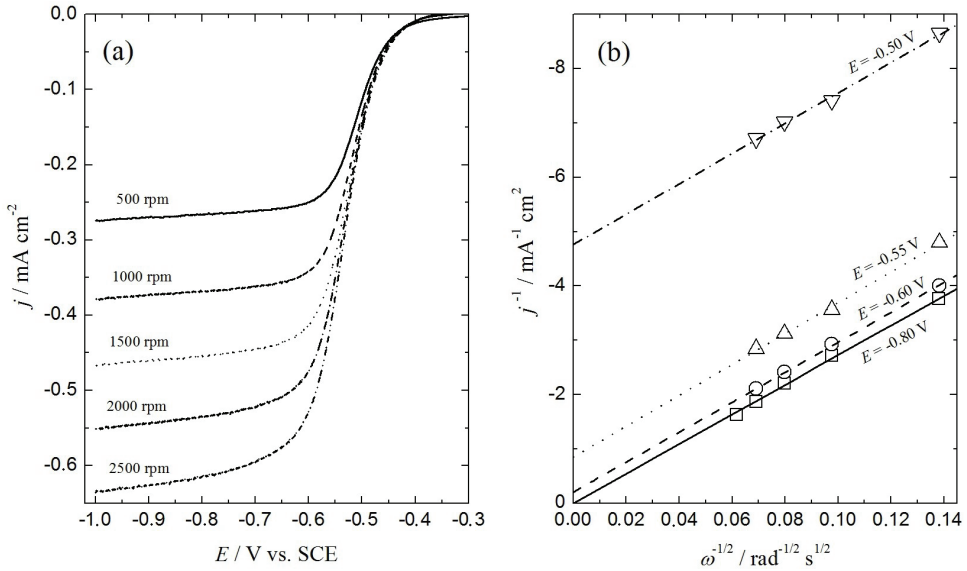

Fig. 3. a) Polarization curves for the reduction of $[Co(en)_3]^{3+}$ to $[Co(en)_3]^{2+}$, recorded at v = 5 mV s^{-1} at different rotation speeds (marked in the figure) in the solution: 0.001 mol dm^{-3} $Co(en)_3Cl_3$ + 0.2 mol dm^{-3} (en). b) The j^{-1} *vs.* $\omega^{1/2}$ dependences obtained by analysis of the polarization curves presented in (a) for different potentials (marked in the figure).

Similar results were obtained for 0.01 mol dm^{-3} $Co(en)_3Cl_3$ + 0.2 mol dm^{-3} (en) solution at pH 12. In order to determine the next step in the process of $[Co(en)_3]^{3+}$ reduction, the cathodic potential limit was adjusted to –1.5 V and the CV with v = 20 mV s^{-1} was recorded (Fig. 4a). As can be seen, a stable cathodic current density was detected at potentials more negative than –1.0 V, while it suddenly increases at about –1.47 V. This current density increase reflects simultaneous hydrogen evolution and deposition of cobalt. During the reverse sweep, three anodic peaks appeared on the CV at about –0.85 V (I_a), –0.70 V (II_a) and –0.45 V (III_a), respectively. The first two peaks (I_a and II_a) correspond most likely to the dissolution of deposited Co and formation of the $[Co(en)_3]^{2+}$ complex, while the third one (III_a) could be ascribed to further oxidation of $[Co(en)_3]^{2+}$ to $[Co(en)_3]^{3+}$. Hence, before the deposition of cobalt from this solution occurs,

the reduction of $[Co(en)_3]^{3+}$ into $[Co(en)_3]^{2+}$ takes place (I_c) at potentials about 1.00 V more positive, indicating that the current efficiency for the deposition process (which occurs with simultaneous hydrogen evolution) is very low. At the higher concentration of $Co(en)_3Cl_3$ of 0.1 mol dm^{-3}, two more peaks could be detected on the CV recorded at a sweep rate of 2 mV s^{-1} (Fig. 4b). The peak (wave) II_c indicates the commencement of cobalt deposition at about –1.25 V, while peak IV_a corresponds to the oxidation of deposited cobalt that could not be quantitatively dissolved from the GC surface and its presence could be detected on the GC surface after the experiment.[22]

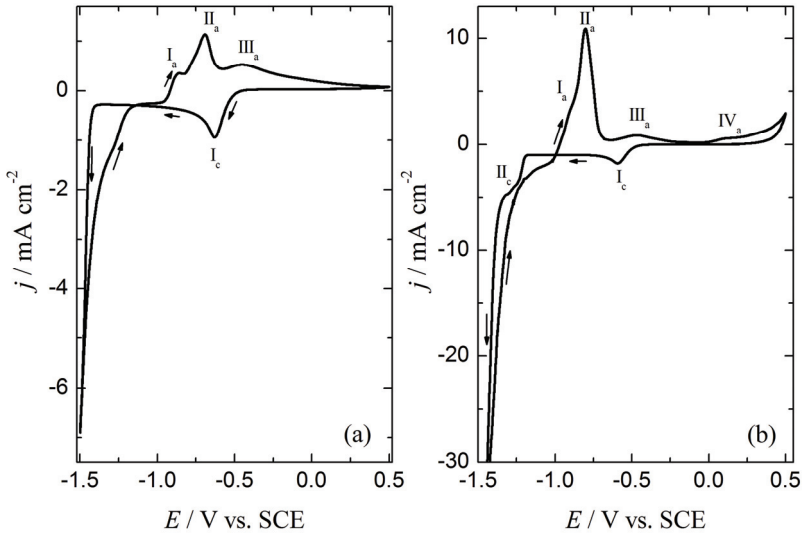

Fig. 4. a) CV with v = 20 mV s^{-1} recorded in the solution 0.01 mol dm^{-3} $Co(en)_3Cl_3$ + 0.2 mol dm^{-3} (en). b) CV with v = 2 mV s^{-1} recorded in the solution 0.1 mol dm^{-3} $Co(en)_3Cl_3$ + 0.2 mol dm^{-3} (en), both obtained at a stationary electrode at pH 12.

Electrochemical behavior of Co^{2+} in 0.2 mol dm^{-3} ethylenediamine

The CVs recorded on the GC electrode at a sweep rate of 100 mV s^{-1} onto stationary and rotating electrodes (1000 and 2000 rpm) in a solution containing 0.001 mol dm^{-3} $CoCl_2$ + 0.2 mol dm^{-3} (en) are shown in Fig. 5a. The potential was swept in the anodic direction from the starting potential marked with the arrow. Considering the CV obtained at a stationary electrode, it appears that the oxidation of $[Co(en)_3]^{2+}$ (dominant complex at pH 12, Fig. 1a) to $[Co(en)_3]^{3+}$ did not occur during the first cycle (solid line) and that its reduction takes place at potentials more negative than –0.70 V through a current density wave characterized with the plateau. During the reverse sweep, the oxidation of $[Co(en)_3]^{2+}$ to $[Co(en)_3]^{3+}$ did occur through a broad anodic peak, while the reduction of $[Co(en)_3]^{3+}$ (which is formed during the oxidation process) into $[Co(en)_3]^{2+}$

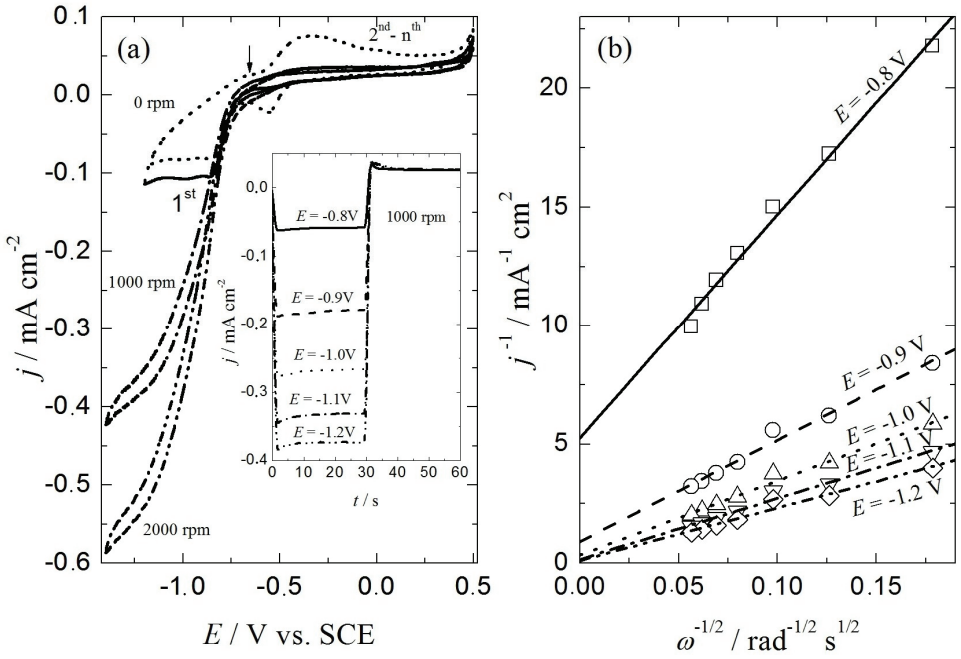

Fig. 5. a) CVs recorded with v = 100 mV s^{-1} at different rotation speeds (marked in the figure) in solutions containing 0.001 mol dm^{-3} $CoCl_2$ + 0.2 mol dm^{-3} (en). Inset: potentiostatic j *vs*. t transients recorded at different cathodic potentials (marked in the figure) and constant anodic potential E = –0.2 V at 1000 rpm. b) The j^{-1} *vs*. $\omega^{1/2}$ dependences obtained from the potentiostatic j *vs*. t transients recorded at different potentials (marked in the figure).

takes place through a sharper cathodic peak positioned between about –0.45 and –0.65 V during the 2nd and subsequent cycles. Under the conditions of convective diffusion, oxidation of $[Co(en)_3]^{2+}$ to $[Co(en)_3]^{3+}$ cannot be detected on the CVs in this solution. The process of reduction of $[Co(en)_3]^{2+}$ commenced at about –0.75 V, being expressed by a sudden increase in the cathodic current density without indication of a diffusion limiting current density plateau. The j *vs*. t transients recorded at 1000 rpm, presented in the inset of Fig. 5a, are characterized with a constant current density response at all applied potentials. As can be seen, the values of the cathodic current density increased with increasing cathodic potential, while the values of the anodic current density recorded during the anodic pulse at E = –0.2 V (as well as the amount of anodic charge for the oxidation reaction) was independent of the cathodic potential, *i.e*., of the amount of reduced $[Co(en)_3]^{2+}$. Taking into account that all reduced species during the cathodic process are removed to the bulk of the solution by electrode rotation, it is reasonable to expect that only a limited amount could be oxidized during the anodic pulse. It should be stated here that even in the case of a stationary electrode only a small amount (about 10 %) of reduced species could be oxidized,

although certain amount of them remain near the electrode surface after the cathodic current density pulse. Hence, it could be concluded that, as in the solution containing only the $[Co(en)_3]^{3+}$ complex, the oxidation process of $[Co(en)_3]^{2+}$ to $[Co(en)_3]^{3+}$ is complex. Considering the results presented in Fig. 5b, it is obvious that the reduction process is complex, since the slopes of the j^{-1} *vs.* $\omega^{-1/2}$ dependences change with the potential, indicating that most likely different species undergo the reduction process in the investigated potential range.[21] It is also possible that some chemical reactions occur, but it is not possible to predict what is really occurring in the system from the presented results.[21]

When the concentration of $CoCl_2$ was increased to 0.01 mol dm^{-3}, slightly different results were obtained. As can be seen in Fig. 6a, at the stationary electrode, the first and subsequent sweeps were identical, indicating oxidation of $[Co(en)_3]^{2+}$ to $[Co(en)_3]^{3+}$ immediately at the beginning of cycling (the starting potential is marked with an arrow). It appears that in order to be able to detect this process by CV at 100 mV s^{-1}, it is necessary to increase the concentration of $CoCl_2$. During the reverse (cathodic) sweep, a sharp peak of the reduction of $[Co(en)_3]^{3+}$ (formed during the oxidation reaction) to $[Co(en)_3]^{2+}$ appeared at about –0.6 V, while further reduction of $[Co(en)_3]^{2+}$ species was characterized by the presence of an additional, smaller peak at about –0.8 V. As in previous cases, the increase in the anodic current density at the oxidation peak on all the CVs recorded at 100 mV s^{-1} was positioned at more negative potentials than expected for a totally irreversible oxidation/reduction mechanism. This could be the consequence of the occurrence of some other reaction, most probably a coupled chemical reaction, during the oxidation process, since the shape of the CVs was similar to those theoretically predicted for such reactions.[21] In the case of electrode rotation, the anodic peak became more pronounced, but practically independent of the rotation speed. During the reverse sweep (from 0.5 to –1.2 V), a first current density plateau appeared between 0.0 and –0.3 V, indicating the occurrence of a diffusion controlled oxidation reaction at a current density of about 0.4 mA cm^{-2}. An additional, much shorter current density plateau, between –0.50 and –0.75 V, at zero current density indicates that no reduction of $[Co(en)_3]^{3+}$ to $[Co(en)_3]^{2+}$ occurred under conditions of convective diffusion. The increase in the cathodic current density at potentials more negative than –0.75 V corresponded to further reduction of the $[Co(en)_3]^{2+}$ complex. In order to understand better these processes, the potentiostatic pulse experiments were performed and the results are presented in Fig. 6b and c. Figure 6b shows that the species formed during the anodic potential step (E = 0.1 V) started to be reduced at –0.70 V. The amount of species being reduced during the cathodic potential steps increased with increasing cathodic potential reaching a maximum of about 12 % at E = –1.1 V. The results presented in Fig. 6c show that about 28 % of the species formed at E = –0.2 V on the stationary electrode become reduced at

E = –0.6 V (peak potential, Fig. 6a), while no reduction could be detected under convective diffusion conditions. Simultaneously, it could be seen that the oxidation process was practically insensitive to the rotation speed. It should be noted here that similar j^{-1} *vs.* $\omega^{-1/2}$ dependences (changing slopes and intercepts as a function of the cathodic potential) compared to those recorded for 0.001 mol dm^{-3} $CoCl_2$ were obtained.

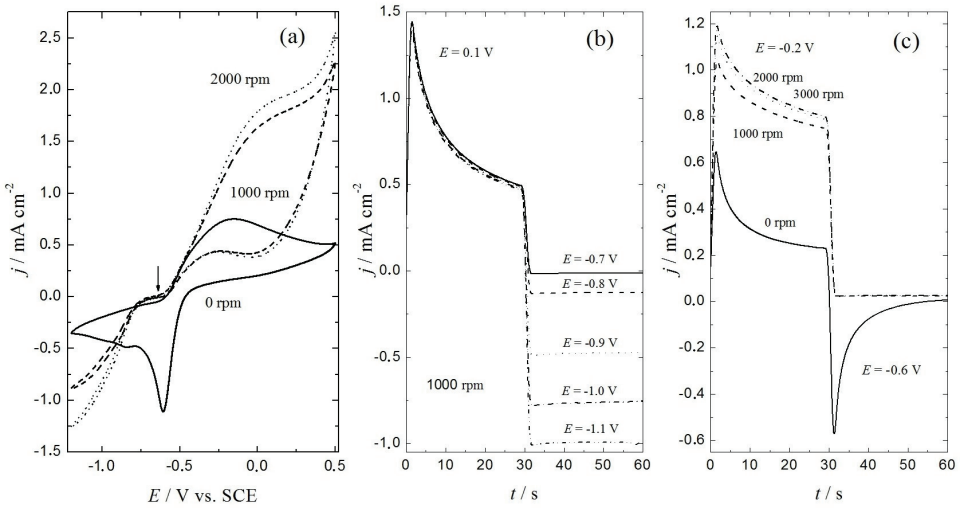

Fig. 6. a) CVs recorded at v = 100 mV s^{-1} for different rotation speeds (marked in the figure) in the solutions containing 0.01 mol dm^{-3} $CoCl_2$ + 0.2 mol dm^{-3} (en). b) Potentiostatic j *vs.* t transients recorded at different cathodic potentials (marked in the figure) and constant anodic potential E = 0.1 V at 1000 r.p.m. (c) Potentiostatic j *vs.* t transients at constant anodic and cathodic potentials (marked in the figure) recorded at different rotation speeds (marked in the figure).

Electrochemical behavior of Co^{2+} + Co^{3+} in 0.2 mol dm^{-3} ethylenediamine

The CVs recorded at a sweep rate of 100 mV s^{-1} on a stationary and rotating electrode (1000 rpm) in a solution containing 0.001 mol dm^{-3} $CoCl_2$ + 0.001 mol dm^{-3} $Co(en)_3Cl_3$ + 0.2 mol dm^{-3} (en) are shown in Fig. 7a. The potential was swept in the anodic direction from the starting potential marked with the arrow. In comparison with the results obtained in the solution containing only 0.001 mol dm^{-3} $CoCl_2$ (Fig. 5a), a small anodic peak for the 1st was detected at the stationary electrode, while for the subsequent sweeps, this peak was identical to that obtained in pure 0.001 mol dm^{-3} $CoCl_2$ solution. At the same time, the cathodic peak corresponding to the reduction of $[Co(en)_3]^{3+}$ to $[Co(en)_3]^{2+}$ was much better defined since the $[Co(en)_3]^{3+}$ complex was present in the solution at a concentration slightly higher than 0.001 mol dm^{-3} (taking into account that a certain amount of the $[Co(en)_3]^{3+}$ complex was formed by the oxidation of $[Co(en)_3]^{2+}$).

Under conditions of convective diffusion, the increase in the anodic current density without a plateau confirmed that the oxidation process was not diffusion controlled, while the shape of cathodic current density wave indicated the occurrence of two processes, the first one corresponding to reduction of $[Co(en)_3]^{3+}$ to $[Co(en)_3]^{2+}$ (potential range between –0.7 and –0.8 V) and the second one at more negative potentials, which was less pronounced, corresponded to further reduction of $[Co(en)_3]^{2+}$. The potentiostatic pulse responses presented in the inset of Fig. 7a clearly show that only a certain number of species formed during the reduction process could be oxidized during the anodic pulse (E = –0.2 V) and that the oxidation was independent of the rotation speed. The j^{-1} *vs.* $\omega^{-1/2}$ dependences presented in Fig. 7b confirmed, as in the case of 0.001 mol dm^{-3} $CoCl_2$ solution, that the reduction process was complex in the presence of Co^{2+}.

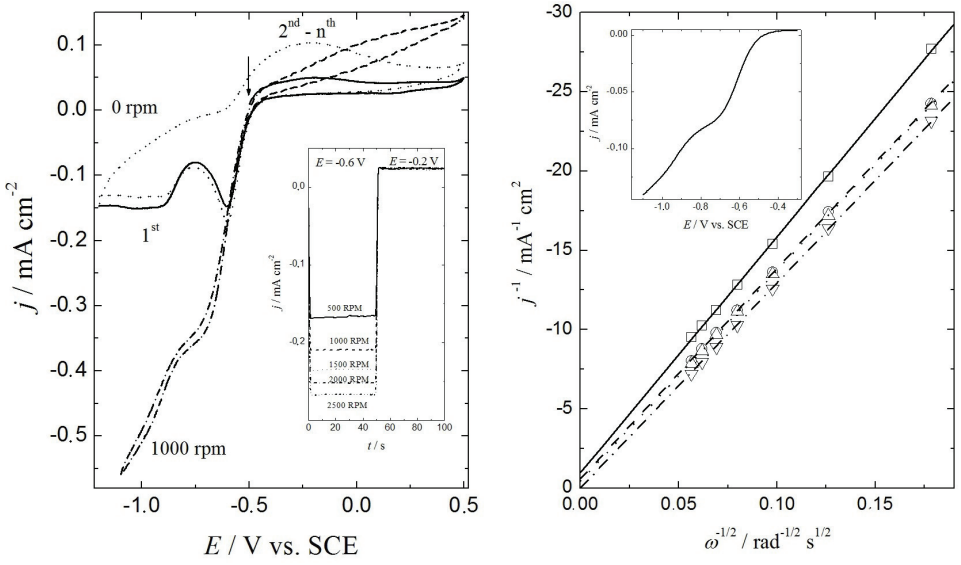

Fig. 7. a) CVs recorded with v = 100 mV s^{-1} at different rotation speeds (marked in the figure) in a solution containing 0.001 mol dm^{-3} $CoCl_2$ + 0.001 mol dm^{-3} $Co(en)_3Cl_3$ + 0.2 mol dm^{-3} (en). Inset: potentiostatic j *vs.* t transients recorded at different cathodic potentials (marked in the figure) and constant anodic potential E = -0.2 V at 1000 rpm. b) The j^{-1} *vs.* $\omega^{1/2}$ dependences obtained from the potentiostatic j *vs.* t transients. Inset: polarization curve for the reduction process recorded at a sweep rate of 1 mV s^{-1}.

CONCLUSIONS

From the results presented in this work, it could be concluded that different cobalt complexes are present in a solution containing 0.2 mol dm^{-3} ethylenediamine, with the $[Co(en)_3]^{3+}$ complex being the most stable one at all pH values. Its reduction to the $[Co(en)_3]^{2+}$ complex represents a totally irreversible,

one electron exchange reaction, while further reduction of $[Co(en)_3]^{2+}$ is a complex process leading to cobalt deposition at potentials more negative than –1.45 V. The process of $[Co(en)_3]^{2+}$ oxidation is also complex and most probably coupled with a chemical reaction.

Acknowledgement. The authors would like to thank the Ministry of Education, Science and Technological Development of the Republic of Serbia for financial support through Project No. 172045.

И З В О Д

ЕЛЕКТРОХЕМИЈА КОБАЛТ–ЕТИЛЕНДИАМИН КОМПЛЕКСА ПРИ ВИСОКИМ pH ВРЕДНОСТИМА

СНЕЖАНА М. МИУЛОВИЋ, ВЛАДИМИР М. НИКОЛИЋ, ПЕТАР З. ЛАУШЕВИЋ, ДАНКА Д. АЋИМОВИЋ, ГВОЗДЕН С. ТАСИЋ и МИЛИЦА П. МАРЧЕТА КАНИНСКИ

Институт за нуклеарне науке „Винча“, Лабораторија за физичку хемију, Универзитет у Београду, Мике Аласа 12–14, 11000 Београд

Испитивано је електрохемијско понашање кобалта у присуству етилендиамина у великом вишку при pH 12. Испитивања су извршена методама цикличне волтаметрије, потенциостатског пулса и мерењем поларизационих кривих на стационарној и ротирајућој електроди од стакластог угљеника. Показано је да се у раствору формира шеснаест различитих врста које садрже $Co(en)_3$ и да је најстабилнији $[Co(en)_3]^{3+}$ при свим pH вредностима. Показано је да је редукција $[Co(en)_3]^{3+}$ до $[Co(en)_3]^{2+}$ потпуно иреверзибилна једноелектронска реакција. Утврђено је да је даља редукција $[Co(en)_3]^{2+}$ сложен процес који води ка таложењу кобалта на потенцијалима негативнијим од –1,45 V у односу на засићену каломелову електроду. Процес оксидације $[Co(en)_3]^{2+}$ такође је комплексан и највероватније спрегнут са хемијском реакцијом.

(Примљено 27. марта, ревидирано 23. јуна, прихваћено 30. јуна 2015)

REFERENCES

1. A. Werner, *Ber. Dtsch. Chem. Ges.* **45** (1912) 121
2. D. Witiak, J. C. Clardy, D. S. Martin, *Acta Crystallogr., B* **28** (1972) 2694
3. J. Bjerrum, S. E. Rasmussen, *Acta Chem. Scand.* **6** (1952) 1265
4. H. A. Laitinen, M. W. Grieb, *J. Am. Chem. Soc.* **77** (1955) 5201
5. P. Kivalo, *J. Am. Chem. Soc.* **77** (1955) 2678
6. S. Sahami, M. J. Weaver, *J. Electroanal. Chem.* **122** (1981) 171
7. S. Sahami, M. J. Weaver, *J. Electroanal. Chem.* **122** (1981) 155
8. S. Sahami, M. J. Weaver, *J. Electroanal. Chem.* **124** (1981) 35
9. U. Mayer, A. Kotocova, V. Gutmann, W. Gerger, *J. Electroanal. Chem.* **100** (1979) 875
10. M. M. Jakšić, Č. M. Lačnjevac, *Chem. Tech.* **37** (1985) 257
11. M. M. Jakšić, *Int. J. Hydrogen Energy* **11** (1986) 519
12. M. M. Jakšić, *Mater. Chem. Phys.* **22** (1987) 1
13. M. P. Marceta Kaninski, D. Lj. Stojic, Dj. P. Saponjic, N. I. Potkonjak, S. S. Miljanic, *J. Power Sources* **157** (2006) 758
14. S. Lj. Maslovara, S. M. Miulovic, M. P. Marceta Kaninski, G. S. Tasic, V. M. Nikolic, *Appl. Catal., A* **451** (2013) 216
15. S. M. Miulovic, S. Lj. Maslovara, I. M. Perovic, V. M. Nikolic, M. P. Marceta Kaninski, *Appl. Catal., A* **451** (2013) 220

16. M. P. Marceta Kaninski, V. M. Nikolic, G. S. Tasic, Z. Lj. Rakocevic, *Int. J. Hydrogen Energ.* **34** (2009) 703
17. M. P. Marceta Kaninski, A. D. Maksic, D. Lj. Stojic, S. S. Miljanić, *J. Power Sources* **131** (2004) 107
18. P. R. Rowland, *Nature* **218** (1968) 945
19. P. R. Rowland, *J. Electroanal. Chem.* **32** (1971) 109
20. A. E. Martell, R. M. Smith, *NIST critically selected stability constants of metal complexes: version 8.0*, NIST standard reference database 46, 2004
21. A. J. Bard, L. R. Faulkner, *Electrochemical methods, fundamentals and applications*, Wiley, New York, 2001, pp. 339–343, 471–517
22. H. Gomez Meier, J. R. Vilche, A. J. Arvia, *J. Electroanal. Chem.* **138** (1982) 367.

Journal of the Serbian Chemical Society
JSCS-info@shd.org.rs • www.shd.org.rs/JSCS
J. Serb. Chem. Soc. 80 (12) 1529–1540 (2015)
JSCS–4817
UDC 546.462+661.183.8:66.091.7:
544.022:519.23:544.773.42/.43:536.5
Original scientific paper

Study of the effect of Mg(II) addition and the annealing conditions on the structure of mesoporous aluminum oxide using Plackett–Burman design

TATJANA B. NOVAKOVIĆ[1*#], LJILJANA S. ROŽIĆ[1#], SRĐAN P. PETROVIĆ[1#], ZORICA M. VUKOVIĆ[1] and MIODRAG N. MITRIĆ[2]

[1]ICTM-Department of Catalysis and Chemical Engineering, University of Belgrade, Njegoševa 12, Belgrade, Serbia and [2]Institute of Nuclear Sciences „Vinča", University of Belgrade, Mike Petrovića Alasa 12–14, Belgrade, Serbia

(Received 13 November 2014, revised 26 June, accepted 6 July 2015)

Abstract: A statistical design was used to investigate the effect of various processing conditions on the structure of sol–gel derived Mg(II) doped alumina. Six process variables were selected based on the Plackett–Burman design: concentration of magnesium nitrate, time and temperature of alcohol evaporation, temperature and time of annealing and heating rate were changed at two levels. For every set of conditions, samples with different specific surface area and degree of crystallinity were obtained. Analysis of the results showed that the annealing temperature, heating rate and concentration of magnesium nitrate were the main factors affecting the average crystallite size of the predominant alumina phase. In the case of the specific surface area, two of selected six variables had pronounced effects; however, the temperature of annealing was more effective than others. The present results showed that the proposed model that uses crystallite size as a response variable is preferable to other research.

Keywords: magnesium-doped alumina; statistical design; sol–gel.

INTRODUCTION

Mesoporous alumina is a very interesting material with broad applicability as an adsorbent, coating, porous ceramics, catalyst, and catalyst support.[1–7] Active alumina does not occur naturally and it is primarily prepared by hydrothermal or thermal transformations of aluminum hydroxides or alumogel. During annealing, organic groups are removed and the gel transforms to a more stable solid phase. This evolution involves chemical modification, crystallographic trans-

* Corresponding author. E-mail: tnovak@nanosys.ihtm.bg.ac.rs
# Serbian Chemical Society member.
doi: 10.2298/JSC141113056N

formation of the solid matter, and reorganization of the solid network and of the pore geometry.[8]

At temperatures below 1000 °C, alumina phases that are often formed are not thermodynamically stable. The temperature of the transformation of metastable phases of alumina into α-Al_2O_3, which is the only thermodynamically stable phase, is influenced by various factors, such as particle size, morphology, crystalline form and organic and inorganic additives.[9] Additives have a great influence on the kinetics of the transformation. The addition of lanthanum species greatly improves the thermal stability, which inhibits the sintering and phase transformations of alumina.[3,10,11] Magnesia, which has a high melting point above 2500 °C, also affects the surface stability of alumina even at temperatures exceeding 1000 °C[7] and produces different accelerating effect depending on the initial surface area.[12] A few studies showed that alumina undergoes phase transformation with increasing calcination temperature, and that the average pore diameter increases with a high temperature while the pore volume and surface area should decrease until the pore structure collapses.[8,13] The performance of alumina as a catalyst or catalyst support largely depends on its crystalline structure, and chemical, and textural properties.[14–16] These properties of transformed alumina, such as morphology, and structural and textural characteristic, are affected not only by the synthesis methodology but also by the subsequent calcinations conditions.[17–21]

Although a large number of parameters could be modified during the preparation of alumina, a great majority of experimental studies on the synthesis of alumina use the conventional method.[22] The conventional multifactor experimental design requires only one variable to be changed at a time to determine its effect. However, when there are many parameters, this procedure may be very long and does not allow a clear identification and influence of linked parameters. These limitations of conventional method can be eliminated by optimizing the affecting parameters collectively by statistical experimental design. The Plackett–Burman (PB) design provides an efficient way for handling a large number of variables and identifying the most important ones. Therefore, this type of design is useful in preliminary studies.[23–25] The design analyzes the input data and presents a rank ordering of the variables with magnitude of effect and designates signs to the effects to indicate whether an increase in factor value is advantageous or not.[26] However, the simultaneous effect of parameters of sol–gel synthesis and calcinations conditions on the pore structure formation of Mg(II)-doped alumina has not been investigated. There are six parameters in the sol–gel synthesis and three calcination variables and thus, a great number of experiments should be simultaneously run, and their possible interactions should be studied.

The aim of this study was to examine the influence of a large number of variables on the structural properties of Mg(II)-doped alumina and to indentify

the most significant ones. PB experimental design at two levels was used to identify the key variables. A graphical display of data, Pareto charts and main effect plots can be used to find a relationship between the input variables and the system response.

EXPERIMENTAL

Preparation of Mg(II)-doped alumina

Mg(II) doped alumina was prepared by sol–gel method using aluminum alkoxide as a precursor. To prepare boehmite sols, aluminum isopropoxide was hydrolyzed in an excess amount of water (100:1, H_2O:Al^{3+} mole ratio) at 80 °C, followed by peptization with the appropriate amount of HNO_3 (0.07:1, H^+:Al^{3+} mole ratio) to form a stable colloidal sol.[27] The sol was kept at a constant temperature for the desired time under reflux conditions, during which most of the alcohol was evaporated. The freshly prepared boehmite sol and polyethylene glycol (PEG, mol. wt. 5600 g mol^{-1}, mol. radius 2.3 nm) or a variable concentration of magnesium nitrate solution combined with PEG, were mixed together and then vigorously stirred in order to obtain a homogeneous Mg(II)-doped boehmite sol. The doped boehmite sols were then gelled at 40 °C. The gels were heated from room temperature to the final temperature, which ranged between 500 and 1100 °C. The heating rate ranged between 2 and 10 °C min^{-1}. The samples were kept at final temperatures for a fixed period, which ranged from 1 to 10 h.

Experimental design

In this study, a PB design was applied for twelve trials in order to evaluate the significance of six variables on the formation of Mg(II)-doped alumina. The independent variables screened were annealing temperature (X_1), heating rate (X_2), time of annealing (X_3), concentration of magnesium nitrate (X_5), time of the evaporation of alcohol (X_7) and temperature of the evaporation of alcohol (X_9). Each independent variable was tested at two levels, a high and a low level, which were denoted by (+1) and (–1), respectively (Table I). Dummy variables (X_4, X_6 and X_8) were employed to evaluate the standard errors of the experiment.

TABLE I. Variables and levels used in the PB experimental design matrix

Variable	Symbol	Unit	Low (–1)	High (+1)
Annealing temperature	X_1	°C	500	1100
Heating rate	X_2	°C min^{-1}	2	10
Time of annealing	X_3	h	1	10
Concentration of Mg(II)	X_5	mol Mg/mol Al_2O_3	0.03	0.06
Time of evaporation	X_7	h	60	72
Temperature of evaporation	X_9	°C	85	95

The data obtained from the PB design experiments were analyzed using Minitab 16 statistical package software trial version (Pennsylvania State University).

The main effect of each variable was calculated as the difference between the average of measurements made at the high and low levels of that factor. The PB design is based on the first order model:

$$Y = b_0 + \sum b_i X_i \quad (1)$$

where Y is the predicted response, X_i are the input variables that affect the response Y, b_0 is the intercept term and b_i are the linear terms. This model does not describe interaction among factors and it is used to screen and evaluate the important factors that influence the response.[24]

Characterization of Mg(II)-doped alumina

The phase structure of the samples after the thermal treatments was studied by the X-ray diffraction method (Philips PW 1710 powder diffractometer with CuK_α radiation (40 kV, 30 mA, λ = 0.154178 nm)) in the 2θ range from 3 to 70°. The crystallite size was determined from XRD patterns using the Scherer equation:

$$D = \frac{0.9\lambda}{\beta \cos\theta} \tag{2}$$

where D represents the crystallite size in nm, λ is the CuK_α radiation wavelength, β is the full width at half maximum in radian and θ is the Bragg angle.

Nitrogen adsorption was performed at –196 °C in the relative pressure interval between 0.05 and 0.98 using an automatic adsorption apparatus (Sorptomatic 1990 Thermo Finningen). Before each measurement, the sample was degassed at 250 °C under vacuum for a sufficient time (4 h < t < 10 h) to observe the absence of significant changes in vacuum stability. The adsorbed amount of nitrogen was measured by volume at standard temperature and pressure. The specific surface areas S_{BET} *a*nd C were calculated by the BET method[28-30] from nitrogen adsorption–desorption isotherms, using data up to p/p_0 = 0.3, and the pore size distribution was computed from the desorption branch of the isotherms.[30]

RESULTS AND DISCUSSION

The Plackett–Burman (PB) design enabled the influence of the six variables to be established with only twelve experiments. This optimized method permits an estimation of the main effects of the variables and disregards interactions between them. The twelve experiments were summarized in the matrix and are listed in Table II.

TABLE II. PB experimental design matrix with the responses specific surface area (Y_1) and crystallite size (Y_2)

Run	X_1	X_2	X_3	X_4	X_5	X_6	X_7	X_8	X_9	Y_1	Y_2
1	1	–1	1	–1	–1	–1	1	1	1	10.0	90.7
2	1	1	–1	1	–1	–1	–1	1	1	79.9	58.4
3	–1	1	1	–1	1	–1	–1	–1	1	275.6	6.4
4	1	–1	1	1	–1	1	–1	–1	–1	35.8	84.1
5	1	1	–1	1	1	–1	1	–1	–1	84.5	48.8
6	1	1	1	–1	1	1	–1	1	–1	14.5	52.3
7	–1	1	1	1	–1	1	1	–1	1	279.1	14.7
8	–1	–1	1	1	1	–1	1	1	–1	301.6	8.5
9	–1	–1	–1	1	1	1	–1	1	1	285.3	12.2
10	1	–1	–1	–1	1	1	1	–1	1	76.4	68.2
11	–1	1	–1	–1	–1	1	1	1	–1	307.2	21.3
12	–1	–1	–1	–1	–1	–1	–1	–1	–1	315.7	19.5

From the nitrogen adsorption–desorption isotherms, the specific surface area (Y_1 / m^2 g^{-1}) for all Mg(II)-doped alumina samples were calculated. The obtained results are presented in Table II and used as a dependent variable (Y_1) in the PB design. The second response in the PB design was crystallite size (Y_2 / nm), determined from the XRD patterns using Eq. (2).

The specific surface areas obtained for each combination of the variables were calculated from the nitrogen adsorption–desorption isotherms shown in Fig. 1, whereby a wide variation in the specific surface area from 316 to 10 m^2 g^{-1} was found.

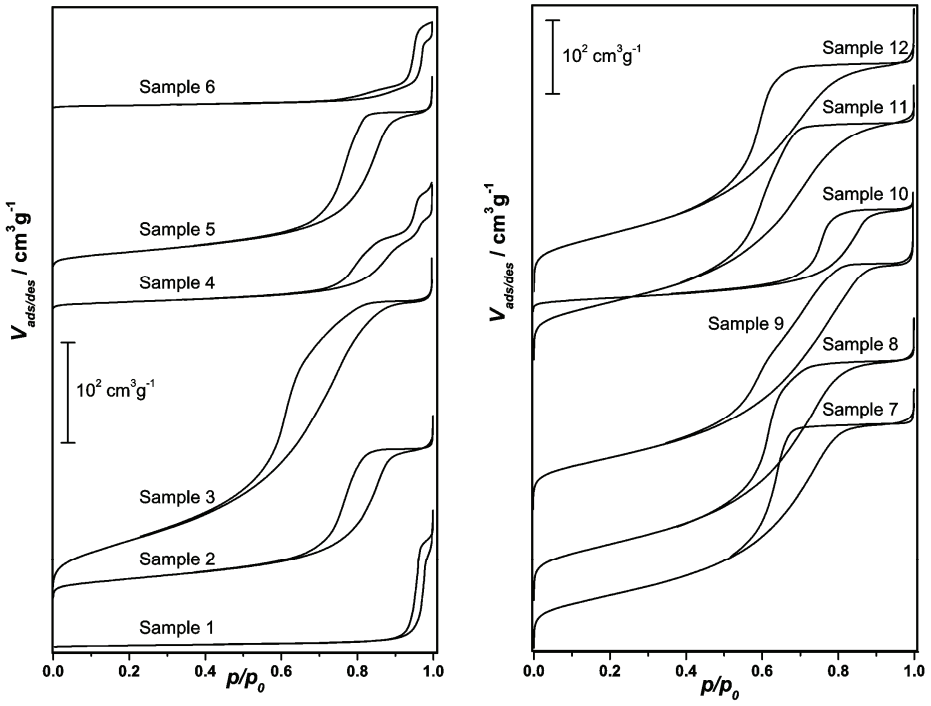

Fig. 1. Nitrogen adsorption–desorption isotherms for the Mg(II)-doped alumina samples.

The alumina samples obtained in experiment 3, 7–9, 11 and 12 annealed at 500 °C were characterized by a type IVa isotherm with a hysteresis loop of the H2 type, indicating the presence of mesopores, within a well-defined pore shape type.[28,30] The samples 1, 2, 5 and 10 annealed at 1100 °C could be described as having type IVa isotherm, the initial region of which was closely related to Type II isotherms, leveling off at high relative pressures with a characteristic saturation plateau, although this could be short and reduced to an inflexion point. A type IVa isotherm is encountered when adsorption occurs on low porosity material or on material with mostly mesoporous pore diameters. The isotherms for samples 4

and 6 were stepwise (Type VI), which are associated with layer-by-layer sorption on a highly uniform surface. The isotherms for samples 4 and 6 also showed hysteresis on the desorption isotherm curve with a smaller desorption step. Although samples 1, 2, 4–6 and 10 were all annealed at 1100 °C, sample 2, 5 and 10 aluminas show different specific surface area compared to samples 1, 4 and 6. These results highlight that the specific surface area of alumina samples depends not only on the annealing temperature, but also on the heating rate and the period in which they were kept at this temperature.

The plot of the pore size distribution (Fig. 2) shows two regions of pore size. The first one reflects a very narrow distribution of mesopores with diameters between 4.9 and 5.7 nm. The smaller average diameter and homogeneity of the mesopores were obtained in experiments 3, 7, 8, 9, 11 and 12 in comparison with the samples annealed at 1100 °C (experiment 1, 2, 4–6 and 10). With increasing annealing temperature, the maximum in pore size distribution was shifted to a larger pore diameter and the distribution became broader, as shown in Fig. 2. The samples obtained in experiments 1, 4 and 6 showed bimodal distributions, characteristics for the spinel structure of magnesium aluminates.[5] These distributions describe the charge transferring pores with radius 5 nm depending on annealing conditions and water exchange inside-delivering or communication mesopores with radius 10 nm, depending on the specific surface area of the Mg(II)-doped alumina. Thus, it could be concluded that the synthesis of bimodal porous alumina depended not only on the annealing temperature, but also on the concentration of magnesium nitrate, heating rate and period for which they were kept at this temperature.

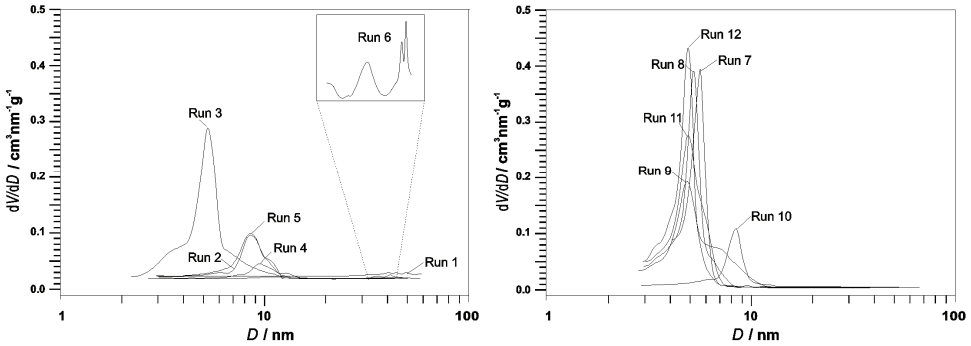

Fig. 2. Pore size distributions of Mg(II)-doped alumina samples.

The XRD patterns (Fig. 3) identified η-Al_2O_3 (PDF-2: 77-0396), γ-Al_2O_3 (PDF-2: 75-0921) and θ-alumina (PDF-2: 86-1410) as crystalline phases for the samples obtained in the experiments 3, 7–9, 11 and 12. X-Ray diffraction could not clearly distinguish between η- and γ-Al_2O_3 and thus, they will be denoted as γ-Al_2O_3. Besides θ-Al_2O_3 in the case of the samples obtained in the experiment

2, 5 and 10, δ-Al_2O_3 (PDF-2: 46-1215) was identified. Lines detected at 25.5, 34, 36.6 and 50.8° related to the presence of well crystalline α-Al_2O_3 (PDF-2: 74--1081) obtained in experiments 1, 4 and 6. In addition, the magnesium aluminate spinel phase ($Mg_{0.4}Al_{2.4}O_4$, PDF-2: 84-0378) was identified in the samples from these experiments. The X-ray diffraction pattern analysis indicated that the formation of $Mg_{0.4}Al_{2.4}O_4$ starts at a temperature of about 1100 °C. These results are in good agreement with those of Orosco *et al.*[31]. In addition, it was observed that the larger degree of crystallinity is detected in samples obtained in experiment 1, 4 and 6 compared to the other samples. The stronger diffraction peaks for these samples suggest that they underwent a higher degree of phase transformation.

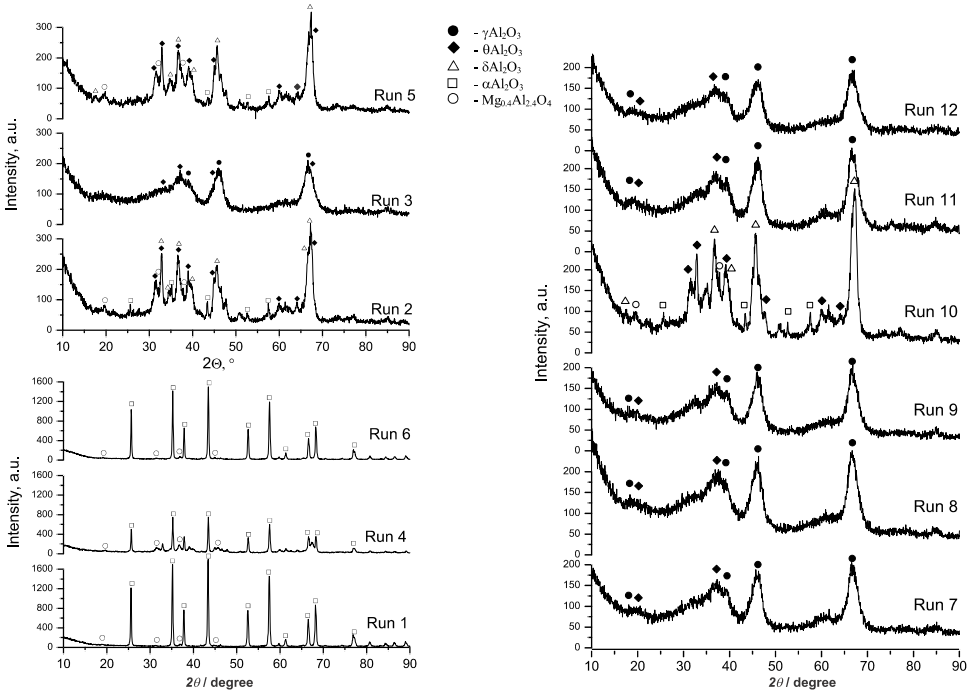

Fig. 3. XRD patterns of the Mg(II)-doped alumina samples.

The average crystallite size (Table II), which may be a good indicator of how surface area changed in Mg(II)-doped alumina under these experimental conditions, increased with increasing annealing temperature. There was a clear difference between the samples annealed at 500 °C (experiment 3, 7–9, 11 and 12) and those obtained at 1100 °C (experiment 1, 2, 4–6 and 10). However, the observed peaks for samples (experiment 3, 8 and 9) were very broad, which could be attributed to disordered arrangement of the very small crystallites making up the pores. Indeed, the calculated mean crystallite sizes according to the Scherer equation were approximately 6–12 nm. For all samples, the mean

crystallite size of the $\gamma(\eta)$-Al_2O_3 phase varied in the range 6.4–21.3 nm, while for the α-Al_2O_3 phase, it was up to 90 nm.

The phase transformations are accompanied by changes in the porous structure of Mg(II)-doped alumina. At higher temperatures (1100 °C), the formation of larger pores was notable, probably due to the collapse of the pores with shrinkage of the material structure. This also resulted in a strong increase in crystallite size and decrease in the surface area and pore volume.[8] The rapid collapse of the fine mesoporous structure started as conversion to the stable α-Al_2O_3 phase occurred at 1100 °C.

In order to determine the influence of the most important variables, a standardized Pareto chart (Fig. 4) was employed. It consists of bars with a length proportional to the absolute value of the estimated effects, divided by the standard error. The bars are displayed in order of the magnitude of the effects, with the largest effect at the top. Moreover, the chart includes a vertical line at the critical *t*-value, and the effect of its bar is smaller than the critical *t*-value is considered as not significant and not affecting the response variable.

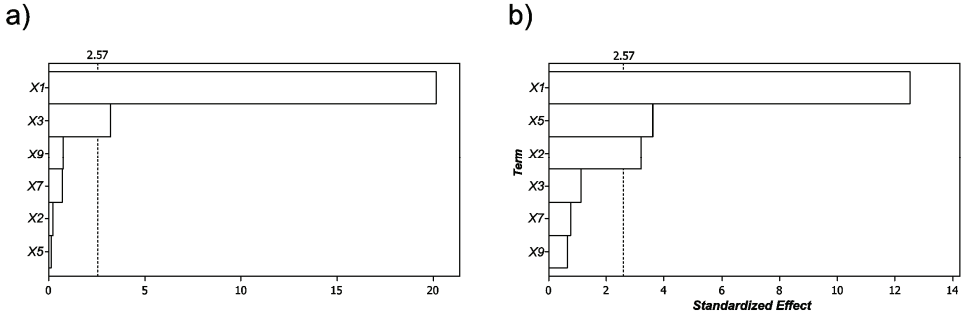

Fig. 4. Pareto chart of the estimated effects of six variables on: a) specific surface area (Y_1) and b) crystallite size (Y_2); $\alpha = 0.05$.

The Pareto chart (Fig. 4a) revealed that the annealing temperature (X_1) had the maximum standardized effect at 95 % confidence interval, while the heating rate (X_2), the concentration of magnesium nitrate (X_5), the time of alcohol evaporation (X_7) and temperature of alcohol evaporation (X_9) did not have a significant effect on the specific surface area. These findings were comparable with reports of Huang *et al.*[18] who investigated the influence of some operation parameters, *i.e.*, calcination temperature and time, and heating rate on the surface area, pore volume and pore size of alumina.

The Pareto chart for the variable Y_2 is presented in Fig. 4b, which confirmed that three variables were very significant: temperature of annealing (X_1), heating rate (X_2) and concentration of magnesium nitrate (X_5). The influences of the

other independent variables on this response were evaluated as having insignificant effects over the studied range of the variables.

In contrast to the Pareto chart, which compares absolute values of the effects, the main effect plot (Fig. 5) provides additional information on whether a change between the two variables levels decreases or increases the response.

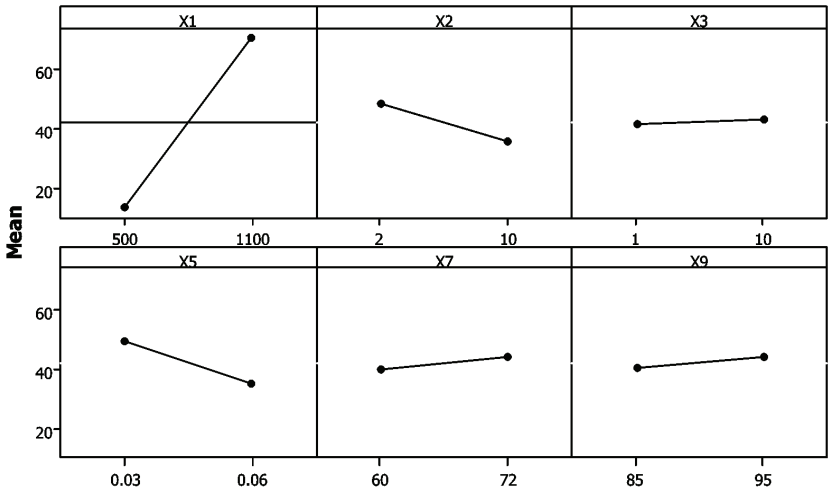

Fig. 5. Main effect plots for Y_2; data given are mean values.

The main effect plot illustrates the trends of all effects and it shows that increasing the annealing temperature leads to an increase in crystallite size, but decreases of the other variables results in the formation of small crystallites. Furthermore, the thermal shock caused by the high heating rate may accelerate the dehydration process, creating structure of magnesium aluminate spinel phase ($Mg_{0.4}Al_{2.4}O_4$) and leading toits formation.

The analysis of variance (ANOVA) was applied to test the suitability of PB design for the response Y_2 and the results are given in Table III.

TABLE III. Effects of the variables and statistical analysis of the PB design

Variable	Symbol	Effect	Coefficient	*P*-value
Annealing temperature	X_1	53.317	26.658	0.000
Heating rate	X_2	–13.550	–6.775	0.024
Time of annealing	X_3	4.717	2.358	0.318
Concentration of Mg(II)	X_5	–15.383	–7.692	0.015
Time of evaporation	X_7	3.217	1.608	0.484
Temperature of evaporation	X_9	2.683	1.342	0.556

P-values lower than 0.05 indicate that the model term is statistically significant. Analysis of the *P*-values showed that among the variables tested, the

temperature of annealing, heating rate and the concentration of magnesium nitrate had significant effects on the crystallite size. The model equation obtained from PB regression analysis for predicting the crystallite size could be written as:

$$Y_2 = -42.151 + 0.089X_1 - 1.694X_2 + 0.524X_3 - 512.778X_5 + \\ +0.268X_7 + 0.268X_9 \quad (3)$$

The model was found to fit adequately all experimental data with a coefficient of determination (R^2) of 0.9733, which indicates that 97.33 % of the variability of the response could be explained by the model. At the same time, the adjusted coefficient of determination R^2_{Adj} (0.9413) was also very high, which indicates the high significance of the model.

CONCLUSIONS

Mg(II)-doped alumina was prepared by the sol–gel method. The PB-design that was applied in this study could identify the main factors from a large number of variables in the synthesis of Mg(II)-doped alumina for the desired response variables. The results obtained from the present investigation revealed that the temperature of annealing, heating rate and concentration of magnesium nitrate were found to affect the crystallite size of the predominant phase of alumina. Among selected variables, annealing temperature was found to be the most significant parameter affecting the structural properties of alumina for both dependent variables. The fundamental information and this design were supportive for preliminary studies where the aim was to identify variables that could be fixed or modified in further investigations.

Acknowledgement. This work was supported by the Ministry of Education, Science and Technological Development of the Republic of Serbia (Project Nos. 172015 and 172001).

И З В О Д

ПРОУЧАВАЊЕ УТИЦАЈА ДОДАТКА МАГНЕЗИЈУМА И УСЛОВА ТЕРМИЧКЕ ОБРАДЕ НА СТРУКТУРНА СВОЈСТВА МЕЗОПОРОЗНОГ АЛУМИНИЈУМ-ОКСИДА ПРИМЕНОМ PLACKETT–BURMAN ДИЗАЈНА

ТАТЈАНА Б. НОВАКОВИЋ[1], ЉИЉАНА С. РОЖИЋ[1], СРЂАН П. ПЕТРОВИЋ[1], ЗОРИЦА М. ВУКОВИЋ[1] и МИОДРАГ Н. МИТРИЋ[2]

[1]*ИХТМ-Центар за катализу и хемијско инжењерство, Универзитет у Београду,Његошева 12, Београд и* [2]*Институ за нуклеарне науке "Винча", Универзитет у Београду, Мике Петровића Аласа 12–14, Београд*

Применом статистичког дизајна проучаван је утицај услова синтезе сол–гел поступком и термичке обраде на структурна својства алуминијум оксида са додатком Mg(II). На основу Plackett–Burman дизајна извршен је избор процесних параметара који показују значајан утицај на структурна својства добијених узорака. Шест процесних варијабли: концентрација магнезијум-нитрата, време и температура испаравања алкохола, температура и време термичке обраде и брзина загревања су варирани на два нивоа. Као излазни параметри посматрани су: специфична површина синтетисаних узорака и величина кристалита доминантне фазе алуминијум-оксида. Резултати су показали да темпе-

ратура и брзина термичке обраде и концентрација магнезијум-нитрата имају најзначајнији утицај на средњу величину кристалита доминантне фазе алуминијум-оксида, док на вредности специфичне површине доминантан утицај има температура термичке обраде. Свеобухватна анализа добијених резултата показала је да је предложени модел који користи величину кристалита као излазни параметар погоднија за даља истраживања.

(Примљено 13. новембра 2014, ревидирано 26. јуна, прихваћено 6. јула 2015)

REFERENCES

1. E. J. A. Pope, J. D. Mackenzie, *J. Non-Cryst. Solids* **87** (1986) 185
2. S. M. Maliyekkal, A. K. Sharma, L. Philip, *Water Res.* **40** (2006) 3497
3. T. Novakovic, N. Radic, B. Grbic, V. Dondur, M. Mitric, D. Randjelovic, D. Stoychev, P. Stefanov, *Appl. Surf. Sci*. **255** (2008) 3049
4. A. L. Ahmad, N. N. N. Mustafa, *J. Hydrogen Energ*. **32** (2007) 2010
5. H. Klym, A. Ingram, I. Hadzaman, O. Shpotyuk, *Ceram. Int.* **40** (2014) 8561
6. J. Čejka, *Appl. Catal., A* **254** (2003) 327
7. H. Arai, M. Machida, *Appl. Catal., A* **138** (1996) 161
8. A. C. Pierre, *Ceram. Int.* **23** (1996) 229
9. N. Radić, B. Grbić, Lj. Rožić, T. Novaković, S. Petrović, D. Stoychev, P. Stefanov, *J. Non-Cryst. Solids* **357** (2011) 3592
10. M. Ozawa, Y. Nishio, *J. Alloy. Compd.* **374** (2004) 397
11. Y. Wang, J. Wang, M. Shen, W. Wang, *J. Alloy. Compd*. **467** (2009) 405
12. P. Burtin, J. P. Brunelle, M. Pijolat, M. Soustelle, *Appl. Catal.* **34** (1987) 225
13. P. Exter, L. Winnubst, T. H. P. Leuwernik, A. J. Burgg, *J. Am. Ceram. Soc*. **77** (1994) 2376
14. M. Riad, *Appl. Catal., A* **327** (2007) 13
15. M. Crişan, M. Zaharescu, V. D. Kumari, M. Subrahmanyam, D. Crişan, N. Drăgan, M. Răileanu, M. Jitianu, A. Rusu, G. Sadanandam, J. K. Reddy, *Appl. Surf. Sci.* **258** (2011) 448
16. A. Khaleel, S. Al-Mansouri, *Colloids Surfaces, A* **369** (2010) 272
17. G. S. Walker, D. R. Pyke, C. R. Werrett, E. Williams, A. K. Bhattacharya, *Appl. Surf. Sci.* **147** (1999) 228
18. W. L. Huang, S. H. Cui, K. M. Liang, Z. F. Yuan, S. R. Gu, *J. Phys. Chem. Solids* **63** (2002) 645
19. S. Da Ros, E. Barbosa-Coutinho, M. Schwaab, V. Calsavara, N. R. C. Fernandes-Machad, *Mater. Charact*. **80** (2013) 50
20. B. Huang, C. H. Bartholomew, B. F. Woodfield, *Micropor. Mesopor. Mat.* **177** (2013) 37
21. S. Ghanizdeh, X. Bao, B. Vaidhyanathan, J. Binner, *Ceram. Int.* **40** (2014) 1311
22. A. S. Kaigorodov, V. R. Khrustov, V. V. Ivanov, A. I. Medvedev, A. K. Shtol'ts, *Sci. Sinter.* **37** (2005) 35
23. A. Vatanara, A. R. Najafabadi, K. Gilani, R. Asgharian, M. Darabi, M. Rafiee-Tehrani, *J. Supercrit. Fluid.* **40** (2007) 111
24. S. Menecier, J. Jarrige, J. C. Labbe, P. Lefort, *J. Eur. Ceram. Soc*. **27** (2007) 851
25. P. Wang, Z. Wang, Z. Wu, *Chem. Eng. J.* **193**–**194** (2012) 50
26. A. S. Guzun, M. Stroescu, S. I. Jinga, G. Voicu, A. M. Grumezescu, A. M. Holban, *Mat. Sci. Eng., C* **42** (2014) 280
27. B. E. Yoldas, *Am. Ceram. Soc. Bull*. **54** (1975) 289

28. F. Rouquerol, J. Rouquerol, K. S. W. Sing, P. Llewellyn, G. Maurin, *Adsorption by Powders and Porous Solids, Principles, Methodology and Applications*, Academic Press, New York, 2012
29. B. C. Lippens, B. G. Linsen, J. H. de Boer, *J. Catal*. **3** (1964) 32
30. K. Sing, D. Everet, R. Haul, L. Moscou, R. Pierotti, J. Rouquerol, T. Siemieniewska, *Pure Appl. Chem*. **57** (1985) 603
31. P. Orosco, L. Barbosa, M. C. Ruiz, *Mater. Res. Bull*. **59** (2014) 337.

Journal of the Serbian Chemical Society
JSCS-info@shd.org.rs • www.shd.org.rs/JSCS
J. Serb. Chem. Soc. 80 (12) 1541–1552 (2015)
JSCS–4818
UDC 546.73'76'77–034:66.017:577.11+
57.001.365:576+615.9:616.314
Original scientific paper

In vitro biocompatibility assessment of Co–Cr–Mo dental cast alloy

IVANA DIMIĆ[1]*#, IVANA CVIJOVIĆ-ALAGIĆ[2], NATAŠA OBRADOVIĆ[1], JELENA PETROVIĆ[3], SLAVIŠA PUTIĆ[3], MARKO RAKIN[3] and BRANKO BUGARSKI[3]

[1]*University of Belgrade, Innovation Centre of the Faculty of Technology and Metallurgy, Karnegijeva 4, 11120 Belgrade, Serbia,* [2]*University of Belgrade, Institute of Nuclear Sciences „Vinča", P. O. Box 522, 11001 Belgrade, Serbia and* [3]*University of Belgrade, Faculty of Technology and Metallurgy, Karnegijeva 4, 11120 Belgrade, Serbia*

(Received 5 May, revised 13 August, accepted 26 August 2015)

Abstract: Metallic materials, such as Co–Cr–Mo alloys, are exposed to aggressive conditions in the oral cavity that represents an ideal environment for metallic ion release and biodegradation. The metallic ions released from dental materials can cause local and/or systemic adverse effects in the human body. Therefore, dental materials are required to possess appropriate mechanical, physical, chemical and biological properties. The biocompatibility of metallic materials is very important for dental applications. Accordingly, the aim of this study was to examine metallic ion release and cytotoxicity of Co–30Cr–5Mo cast alloy as the initial phase of biocompatibility evaluation. Determination of the viability of human (MRC-5) and animal (L929) fibroblast cells were conducted using three *in vitro* test methods: the colorimetric methyl-thiazol-tetrazolium (MTT) test, the dye exclusion test (DET) and the agar diffusion test (ADT). Furthermore, the morphology and growth of the cells were analyzed using scanning electron microscopy (SEM). The obtained results indicated that Co–30Cr–5Mo alloy did not release harmful elements in concentrations high enough to have detrimental effects on human and animal fibroblasts under the given experimental conditions. Moreover, the fibroblast cells showed good adhesion on the surface of the Co–30Cr–5Mo alloy. Therefore, it could be concluded that Co–30Cr–5Mo alloy is a biocompatible material that could be safely used in dentistry.

Keywords: Co-based alloy, biomaterials, cytotoxicity, fibroblasts.

INTRODUCTION

The most extensively used metallic materials in dental practice are commercially pure titanium (CPTi), and titanium- and cobalt-based alloys, whilst

* Corresponding author. E-mail: idimic@tmf.bg.ac.rs
# Serbian Chemical Society member.
doi: 10.2298/JSC150505070M

stainless steels were abandoned primarily due to nickel-induced hypersensitivity of the organism.[1] CPTi and its alloys are mostly used as endosseous implants, while Co–Cr–Mo alloys have been widely applied as subperiosteal implants and removable partial denture frameworks due to their outstanding mechanical properties and high corrosion resistance.[2,3] In fact, Co–Cr–Mo alloys have better mechanical strength and corrosion resistance compared to stainless steel.[4] Chromium, the main alloying element in Co–Cr–Mo alloys, is added to advance the formation of a stable passive oxide layer that contributes to corrosion resistance, while molybdenum is also frequently added to increase alloy resistance to pitting and crevice corrosion. The composition of Cr and Mo in commercial alloys lies within the range of 11–25 mass % and the corrosion behaviour of Co–Cr–Mo alloys depends primarily on the Cr and Mo levels in the alloy, *i.e.*, alloys with lower amounts of Cr and Mo are found to be more susceptible to corrosion.[5] Although the metallic dental materials are considered to have excellent corrosion resistance, numerous studies showed that metallic ions could be released into the surrounding environment.[6,7] The released metallic ions from dental materials could diffuse into mucosal tissue or could be distributed throughout the human body and cause adverse biological effects, depending on the ion type and concentration.[4,8] For instance, Ichinose *et al.*[9] showed that Co–Cr–Mo alloys disintegrate easily in cells, *i.e.*, Co dissolves from the peripheral areas of the cells although Cr remains within them. The main factors affecting metallic ion release from dental materials are the quantity and quality of the saliva, plaque, pH value, temperature and presence of proteins. Additionally, the physical and chemical properties of food and liquids as well as oral health conditions have great influences on ion release.[10] Furthermore, the composition and pre-treatment of the materials are very important factors that have a significant influence on metallic ion release.[11,12] Consequently, the contact between Co–Cr–Mo alloys and human saliva leads to the release of metallic ions.[13,14] It should be emphasized that biocorrosion of Co–Cr–Mo alloys is one of the major problems during their application as dental materials.[4] Many authors reported toxic and carcinogenic effects induced when humans and animals are exposed to certain metals.[11] Thus, the requirements of dental materials are primarily non-toxicity and biocompatibility. It should be underlined that biocompatibility of metallic materials is dependent on the release of elements from the materials.[12] Therefore, the main purpose of this study was to examine metallic ion release in artificial saliva and *in vitro* cytotoxicity of Co–30Cr–5Mo alloy. The cytotoxicity of the mentioned alloy was assessed using human (MRC-5) and animal (L929) fibroblast cell lines according to ISO 10993-5 and ISO 7405 standards, respectively.[15,16] The effects of Co–30Cr–5Mo cast alloy on cell viability, morphology and spreading on the surface were also determined in this study. Determination of cells viability was conducted using three *in vitro* test methods: the colorimetric methyl-thiazol-

-tetrazolium (MTT) test, the dye exclusion test (DET) and the agar diffusion test (ADT). Although only the ADT assay has been prescribed in ISO 7405 standard,[17] the use of different test methods is highly advisable.[18] For the purpose of cells morphology and spreading analyses, scanning electron microscopy (SEM) was used. It is very important to mention that the increased worldwide interest in utilizing Co-based alloys for dental applications is related to their low cost and adequate mechanical properties,[3] and therefore Co–30Cr–5Mo alloy was chosen for examination in this study.

MATERIALS AND METHODS

Material preparation

The chemical composition of Co–30Cr–5Mo alloy (Wironit® extra-hard, Bego, Germany) used in this study was (in mass %): Co 63.0, Cr 30.0, Mo 5.0, max. 0.4 C, and trace amounts of Si and Mn. The physicochemical properties of the examined alloy were presented in a previous study.[13] The Co–30Cr–5Mo alloy in the as-cast condition was selected for consideration in this study for two reasons: 1) Co-based alloys are most often used in cast or cast and annealed metallurgic conditions[2] and 2) this type of alloy is widely used in dental practice, mostly for the manufacture of crowns, bridges and denture bases,[19] regardless of some results which indicate that harmful effects were induced by released ions and cells damage were caused by Co–Cr–Mo alloys.[1,9] The cylindrically-shaped specimens (8.0 mm in diameter and 15.8 mm in height) were cut into disc-shaped samples (8.0 mm in diameter and 4.0 mm in thickness). Subsequently, the samples were ground to 1200 grit with silicon carbide (SiC) papers and polished using diamond paste. Thereafter, the samples were cleaned in an ultrasonic bath with ethanol for 15 min followed by rinsing with distilled water for 5 min in order to eliminate surface impurities.

Microstructure characterization and hardness determination

The microstructure characterization of Co–30Cr–5Mo alloy used in this study was realized using a Carl Zeiss Opton Axioplan optical microscope (OM) and a JEOL JSM 5800 scanning electron microscope (SEM), which was operated at an accelerating voltage of 25 keV. Before the microscopic analysis, the examined material was etched using a solution containing 92mL HCl, 5mL H_2SO_4 and 3mL HNO_3. The Vickers hardness, HV, was measured on the polished mirror-like surface of the samples using a Buehler Identamet microindentation hardness tester, model 1114, under a load of 2.94 kN for 5 s.

Metallic ion release

After standard metallographic preparation of the samples and their ultrasonic cleaning, each sample was placed in a separate glass test tube with 5 mL of artificial saliva (Helvepharm AG, Switzerland) and thermostated at 37 °C. In order to designate the effect of the pH value of the artificial saliva on metallic ion release from Co–30Cr–5Mo alloy, the pH value was set to different levels (7.5, 5.5 and 4.0). The concentrations of released metallic ions were quantified after 1, 3 and 6 weeks using an Agilent ICP MS 7500ce inductively coupled plasma-mass spectrophotometer (ICP-MS).

Cell lines

The human (MRC-5) and animal (L929) fibroblast cell lines were grown attached to the surface of flasks (Costar, 25 cm^3) in Eagle's medium modified by Dulbecco (DMEM, Gibco

BRL, UK) with 4.5 g L^{-1} glucose and 10 % foetal calf serum, FCS (Sigma). The medium contained the antibiotics penicillin 100 IU mL^{-1} and streptomycin 100 μg mL^{-1}. The cell lines were maintained under standard conditions at 37 °C under 5 % CO_2 humidified environment (Heraeus). The cell lines were transplanted twice weekly, and the logarithmic phase of growth between the third and tenth transplantation was used in the assays. The cell number and percentage of viable cells were determined by the colour test rejection with 0.1 % trypan blue. The viability of cells used in the assays was over 90 %.

Cell morphology

For the purpose of the morphological characterization of MRC-5 cells on the surface of Co–30Cr–5Mo alloy, the cells were collected during the logarithmic phase of growth, trypsinized, resuspended and counted in 0.1 % trypan blue. Subsequently, the cells (1×10^5 cells mL^{-1}) were seeded directly on the material surface and cultivated at 37 °C under a 5 % CO_2 humidified environment for 48 h. After the incubation period, the MRC-5 cells were photographed with a Canon 1100D camera attached to an inverted microscope Reichert–Jung Biostar 1820 E with 20 and 40× magnification objectives. SEM analysis of MRC-5 cells was performed on the same sample using SEM MIRA3 Tescan operated at an accelerating voltage of 20 keV. Before the SEM observations, the MRC-5 cells were fixed in 2.5 % glutaraldehyde for 48 h and dehydrated using the following solutions: 3 % acetic acid, 3 % acetic acid and 25 % ethanol at a ratio 1:1, 3 % acetic acid and 50 % ethanol at a ratio 1:1, and 70 % ethanol. Subsequently, the MRC-5 cells were coated with a thin Au–Pd layer using a Baltec SCD 005 sputter coater.

In vitro *cytotoxicity tests*

The Co–30Cr–5Mo alloy cytotoxicity was measured as the percentage of cell growth inhibition using three types of *in vitro* tests: the colorimetric methyl-thiazol-tetrazolium (MTT) test, the dye exclusion test (DET) and the agar diffusion test (ADT), which are briefly described in the Supplementary material to this paper.

RESULTS AND DISCUSSION

Microstructure characterization and hardness determination

The OM and SEM micrographs of Co–30Cr–5Mo alloy in as-cast condition are shown in Fig. 1. The microstructure of examined material consisted of

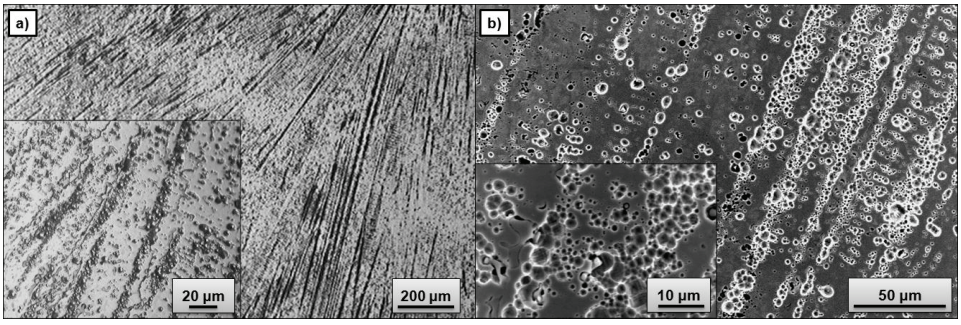

Fig. 1. a) OM and b) SEM micrographs showing the microstructure of the Co–30Cr–5Mo alloy in as-cast condition.

dendrites (dark parts in Fig. 1a; light parts in Fig. 1b) and interdendritic regions (light parts in Fig. 1a; dark parts in Fig. 1b).

Similarly, Xin *et al.*[20] showed that the microstructure of a Co–Cr–Mo alloy obtained by traditional casting has a typical dendritic microstructure. Likewise, Patel *et al.*[21] described the microstructure of a Co–Cr–Mo alloy in details; the microstructure consisted of a solid Co matrix with interdendritic phases and carbides. The carbides were a combination of carbon and either Co, Cr or Mo, and were denoted as M_nC_n where M is Co, Cr or Mo. Furthermore, XRD analysis performed by the same authors indicated that the Co–Cr–Mo alloy (ASTM F75) consisted of face-centred cubic (fcc) Co, $M_{23}C_6$ and a sigma (σ) phase. It should be mentioned that the allotropic phase transformation of pure Co from the high temperature α phase (fcc) to the low temperature ε phase (hexagonal close-packed, hcp) occurs at about 420 °C.[22,23] Alloying elements, such as Fe and Ni, can stabilize the α phase, while Cr and Mo tend to stabilize the ε phase. Furthermore, Saji and Choe[22] using EDS analysis showed that the chemical compositions of the dendrites and interdendritic regions are similar. However, the dendritic regions are slightly rich in Cr and poor in Co. The obtained hardness of the Co–30Cr–5Mo alloy investigated in this study was 287.6±36.7 HV. According to Patel *et al.*,[21] the hardness of a Co–Cr–Mo alloy is correlated with its carbide content.

Metallic ion release

The metallic ion release testing in artificial saliva was preceded in this study by an *in vitro* cytotoxicity examination. As mentioned earlier, Co–Cr–Mo alloys are usually used to fabricate dental prostheses and subperiosteal implants, which are in contact with gingiva, and therefore artificial saliva was used as the testing solution. The obtained results are shown in Fig. 2.

As can be seen from the diagrams, the concentrations of released metallic ion increased almost linearly with increasing immersion time, a conclusion that was also reached by Nejatidanesh *et al.*[24] Furthermore, the metallic ion release rate increased with decreasing pH value of the artificial saliva. The most pronounced effect of the pH value of the artificial saliva on metallic ion release could be observed in the case of Co after 6 weeks of immersion. Similarly, Denizoglu *et al.*[25] investigated ion release from a Co-based alloy (alloy composition: Co 64.0, Cr 28.65, Mo 5.0, Mn 1.0, Si 1.0, C 0.35) and showed that the pH value of the testing solution significantly affected the total and Co ion release, but not Cr ion release. The concentrations of the released Cr and Mo did not differ drastically, but the weight content of Mo in the Co–Cr–Mo alloy was much smaller than that of Cr. Therefore, it could be concluded that the concentrations of released metallic ions do not reflect their weight contents in the alloy.[13,25] Many authors examined the corrosion resistance of Co–Cr–Mo alloys

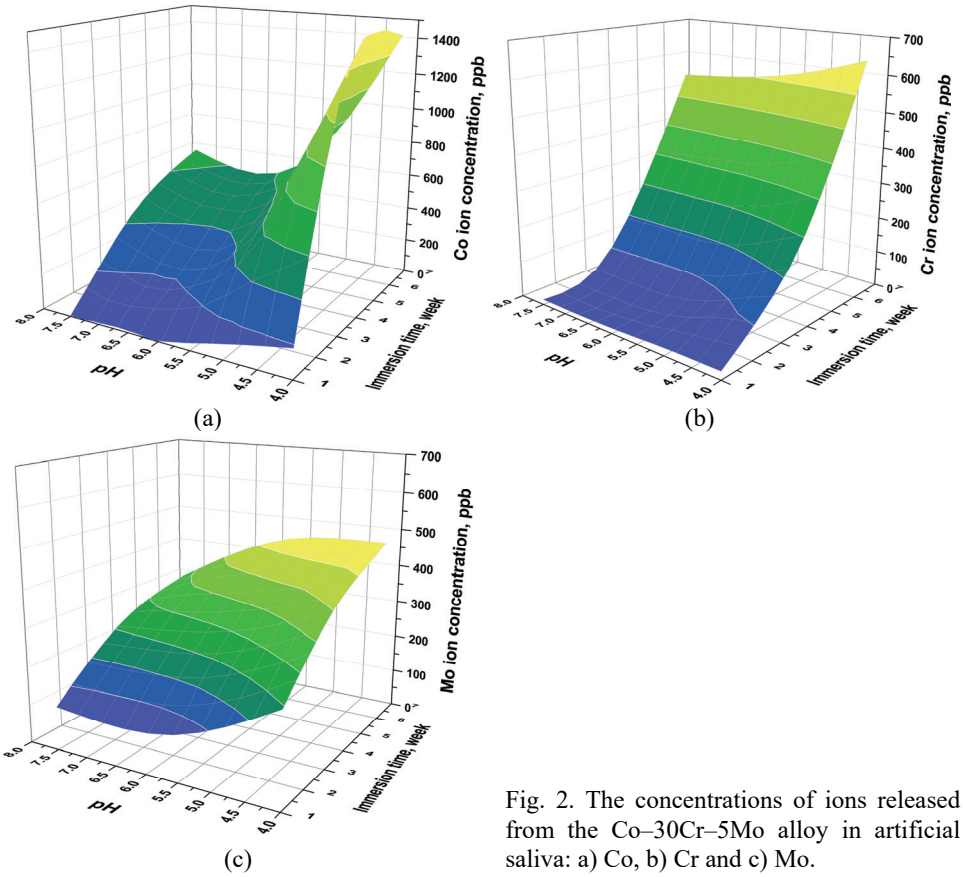

Fig. 2. The concentrations of ions released from the Co–30Cr–5Mo alloy in artificial saliva: a) Co, b) Cr and c) Mo.

and metallic ion release as a direct consequence of corrosion. For instance, Branzoi *et al.*[14] showed that the corrosion resistance of a Co–Cr–Mo alloy was higher than in the case of a Co–Cr–Ti alloy because the stability of the passive oxide film present on the Co–Cr–Mo surface was higher. Jevremović *et al.*[18] examined the release of ions from a Co-based alloy fabricated using both traditional casting and selective laser melting (SLM) techniques and concluded that the ion release rate was lower in the case of the SLM prepared alloy. Furthermore, Doni *et al.*[26] presented that a Co–Cr–Mo alloy showed a lower tendency to corrosion in a NaCl solution under sliding compared to the Ti–6Al–4V alloy. Puškar *et al.*[27] examined the behaviour of a Co–Cr–Mo alloy in artificial saliva at 37 °C for 7 days and concluded that the quantities of released Co, Cr and Mo were far below the permitted levels. According to the ISO 22674 standard, the quantity of an element released from the alloy should not exceed 200 μg cm^{-2} during 7 days.[28] In this study, Mo had the highest release rate after 7 days, but the amounts of the released ions never exceeded 2 μg cm^{-2}. Thus, the quantities

of released ions were 100-fold lower than the permitted quantities. It is important to note that Beer-Lech and Surowska[29] showed that a Co–Cr–Mo alloy had very good passivation ability. Many authors linked metallic ion release with biocompatibility of dental materials.[24,25,30] It was observed that the concentration of released ions from the examined Co-based alloy was significantly higher when compared to other Co–Cr–Mo alloys[13] and it should therefore provide more information about the cytotoxicity potential of this alloy and the possibility of using an untreated Co–Cr–Mo cast alloy for dental applications.

In vitro *cytotoxicity tests as the initial phase of biocompatibility examination*

The results of the colorimetric methyl-tiasol-tetrazolium (MTT) and dye exclusion test (DET) assays, presented in Fig. 3, showed that the Co–30Cr–5Mo alloy did not exhibit cytotoxic effect either in contact with MRC-5 or L929 fibroblast cells. In fact, the results of the MTT test (Fig. 3a) indicate a gradual increase in cell viability with increasing contact time. After 72 h, both MRC-5 and L929 cells in contact with the Co–30Cr–5Mo alloy showed almost the same viability as the cells in the control sample. After 96 h, the cell viability further increased, meaning that the Co–30Cr–5Mo alloy did not exhibit toxic effects on the cells. The diagram of the DET results (Fig. 3b) shows an enhancement in cell viability with increasing contact time. As can be seen, the Co–30Cr–5Mo alloy showed excellent cytocompatibility with MRC-5 cells after 96 h, whilst the L-929 cells in contact with Co–30Cr–5Mo alloy had slightly lower survival rates than the MRC-5 cells. These differences, caused by the cell type which was used for testing, are negligibly small. Furthermore, since the decolourization index was 0 (no decolourization detectable around or under the disc-shaped samples) and the lysis index was 0 (no cell lysis detectable), the examined material was

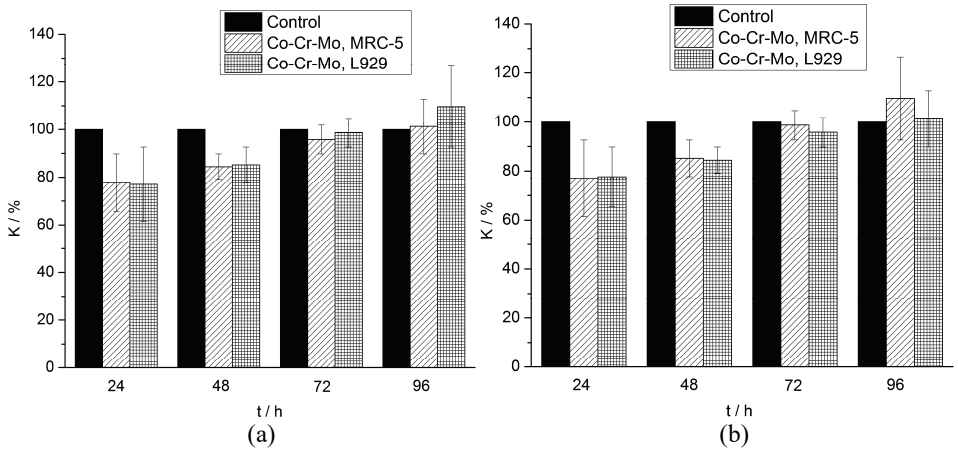

Fig. 3. Fractions of surviving fibroblast cells compared with the respective control (*K*) in: a) the MTT and b) the DET assay.

not cytotoxic according to agar diffusion test (ADT).

These results are in accordance with the observation of Jevremović *et al.*[18] who demonstrated that an ASTM F75 Co-based alloy obtained by casting and SLM did not release harmful elements that could cause acute effects against animal fibroblast cells (L929). Similarly, Xin *et al.*[20] showed good spreading of mouse fibroblasts (3T3) on the surface of a Co-based cast alloy. The advantage of present study compared to studies by Jevremović *et al.*[18] and Xin *et al.*[20] is that the cytotoxicity of the Co–30Cr–5Mo alloy was examined using both human and animal fibroblast cells, because the use of human cells provides more valid results and better insight into the behaviour of this alloy in the human body. Different and often contradictory studies regarding cytotoxicity/cytocompatibility of Co–Cr–Mo alloys can be found in the literature. On the one hand, Čairović *et al.*[31] emphasized that cells adapted to the presence of a Co-based alloy after an initial toxic effect. On the other hand, it was shown that CPTi, Ti–Al–V and Co–Cr–Mo alloys caused cell damage in direct contact with cells, while in indirect contact, only the Co–Cr–Mo alloy caused cell damage.[1] Furthermore, Fleury *et al.*[32] demonstrated that Cr^{3+} (0–150 ppm) and Co^{2+} (0–10 ppm) ions have a cytotoxic effect on oesteoblast-like cells (MG-63). Microscopic analysis demonstrated changes in the shape, size and number of cells, whereas Co^{2+} had a greater effect on these parameters than Cr^{3+}. Even if there are articles in the literature that highlighted the cytotoxicity of Cr and Co, the results in this study indicated that the Co–30Cr–5Mo alloy did not exhibit cytotoxic effects and these results are similar to some published data.[18,20,31,33]

Cells morphology and adhesion

The photograph of MRC-5 cells in culture and in contact with the Co–30Cr––5Mo alloy is shown in Fig. 4. It can be clearly seen that the cells are attached to the edge of the disc-shaped sample of the Co–30Cr–5Mo alloy and that cells are mutually connected.

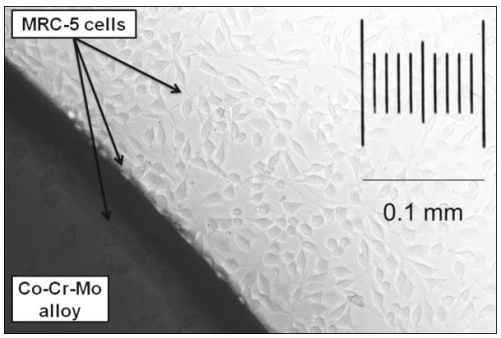

Fig. 4. MRC-5 cells in contact with Co–30Cr–5Mo alloy surface.

The SEM micrographs of MRC-5 cells on the surface of the Co–30Cr–5Mo alloy are presented in Fig. 5. MRC-5 cells can have different shapes: triangle, spindle, elongated, oval, and flat[34,35] and in this study, the cells were rounded (Fig. 5a) and spindle elongated (Fig. 5b). The rounded cells were slightly smaller than spindle elongated cells, but they are very well spread on the Co–30Cr–5Mo alloy surface. Furthermore, these micrographs revealed the voluminous nature of the cells, which indicates that the cells are metabolically active. Excellent cell spreading is shown in Fig. 5c, which demonstrates that Co–30Cr–5Mo alloy is not harmful to the appearance of MRC-5 cells. It is obvious that the MRC-5 cells show good adhesion on the Co–30Cr–5Mo alloy surface, as can be seen in Fig. 5d, and thus the biocompatibility of the alloy was demonstrated.

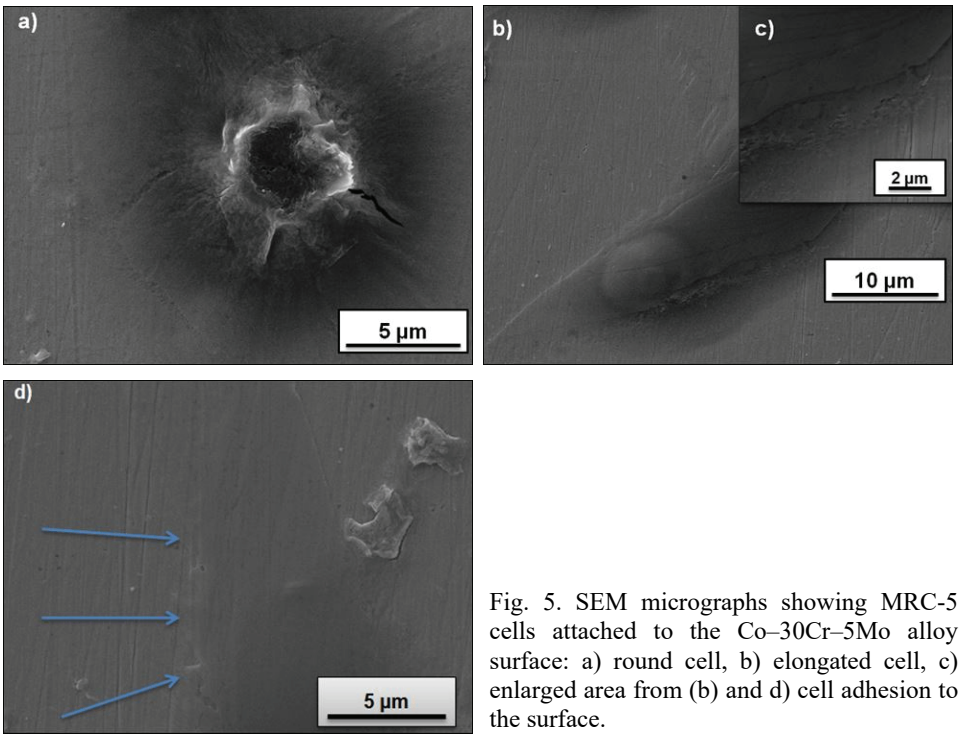

Fig. 5. SEM micrographs showing MRC-5 cells attached to the Co–30Cr–5Mo alloy surface: a) round cell, b) elongated cell, c) enlarged area from (b) and d) cell adhesion to the surface.

CONCLUSIONS

On the grounds of realized and presented research, the following conclusions were reached: 1) The ion release rate of the Co–30Cr–5Mo alloy was small enough, *i.e.*, the quantities of released ions were 100-fold lower than those permitted according to the ISO 22674 standard. 2) The metallic ion release depended on many factors, such as the pH value of artificial saliva and the immersion time. 3) The results of MTT, DET and ADT assays showed that examined

Co–30Cr–5Mo alloy did not exhibit cytotoxic effect either in contact with human (MRC-5) or animal (L929) fibroblast cells. 4) The human fibroblasts showed excellent adhesion and spreading on the surface of the Co–30Cr–5Mo alloy. Furthermore, the voluminous nature of the cells indicated that the cells were metabolically active and thus the biocompatibility of the Co–30Cr–5Mo alloy was demonstrated.

Based on this *in vitro* biocompatibility examination, it could be concluded that Co–30Cr–5Mo alloy is a biocompatible material that could safely be used in dentistry.

Acknowledgements. The authors gratefully acknowledge support from the Ministry of Education, Science and Technological Development of the Republic of Serbia through the projects III 46010 and ON 174004. The authors would like to express their gratitude to Vesna Kojić, PhD, Oncology Institute of Vojvodina, for her generous help in conducting the cytotoxicity tests and Đorđe Veljović, PhD, University of Belgrade, Faculty of Technology and Metallurgy for the SEM analysis.

ИЗВОД

IN VITRO ПРОЦЕНА БИОКОМПАТИБИЛНОСТИ Co–Cr–Mo ДЕНТАЛНЕ ЛИВЕНЕ ЛЕГУРЕ

ИВАНА ДИМИЋ[1], ИВАНА ЦВИЈОВИЋ-АЛАГИЋ[2], НАТАША ОБРАДОВИЋ[1], ЈЕЛЕНА ПЕТРОВИЋ[3], СЛАВИША ПУТИЋ[3], МАРКО РАКИН[3] и БРАНКО БУГАРСКИ[3]

[1]Универзитет у Београду, Иновациони центар Технолошко–металуршког факултета, [2]Универзитет у Београду, Институт за нуклеарне науке „Винча“ и [3]Универзитет у Београду, Технолошко–металуршки факултет

Метални материјали, као што су Co–Cr–Mo легуре, су изложени агресивним условима у усној дупљи која представља идеалну средину за отпуштање металних јона и биоразградњу. Јони отпуштени из денталних материјала могу да изазову локалне и/или системске штетне ефекте у људском организму. Због тога се захтева да дентални материјали поседују одговарајућа механичка, физичка, хемијска и биолошка својства. Биокомпатибилност металних материјала је веома битна за денталну примену. Према томе, циљ рада је био да се одреди отпуштање јона и цитотоксичност Co–30Cr–5Mo ливене легуре, као почетна фаза процене биокомпатибилности. Одређивање вијабилности људских (MRC-5) и животињских (L929) ћелија фибробласта је спроведено применом три теста: колориметријског MTT теста, теста губљења боје (DET) и агар дифузионог теста (ADT). Осим тога, морфологија и раст ћелија су анализирани коришћењем скенирајуће електронске микроскопије (SEM). Добијени резултати указују на то да Co–30Cr–5Mo легура не отпушта штетне елементе у високим концентрацијама које би могле да проузрокују штетне ефекте на људским и животињским фибробластима под датим експерименталним условима. Осим тога, ћелије фибробласта показују веома добру адхезију на површини Co–30Cr–5Mo легуре. Према томе, може се закључити да је Co–30Cr–5Mo легура биокомпатибилни материјал који се безбедно може користити у стоматологији.

(Примљено 5. маја, ревидирано 13. августа, прихваћено 26. августа 2015)

REFERENCES

1. J. B. Brunski, *An introduction to materials in medicine,* in *Biomaterials science,* B. D. Ratner, A. S. Hoffman, F. J. Schoen, J. E. Lemons, Eds., Academic Press, San Diego, CA, 1996, pp. 111–128
2. B. C. Muddugangadhar, G. S. Amarnath, S. Tripathi, S. Dikshit, M. S. Divya, *IJOICR* **2** (2011) 13
3. Y. S. Al Jabbari, *J. Adv. Prosthodont*. **6** (2014) 138
4. M. Geetha, D. Durgalakshmi, R. Asokamani, *Recent Pat. Corros. Sci.* **2** (2010) 40
5. A. Takaichi, T. Nakamoto, N. Joko, N. Nomura, Y. Tsutsumi, S. Migita, H. Doi, S. Kurosu, A. Chiba, N. Wakabayashi, Y. Igarashi, T. Hanawa, *J. Mech. Behav. Biomed.* **21** (2013) 67
6. H.-Y. Lin, J. D. Bumgardner, *J. Orthop. Res*. **22** (2004) 1231
7. S. Karimi, T. Nickchi, A. M. Alfantazi, *Appl. Surf. Sci.* **258** (2012) 6087
8. J. C. Wataha, R. G. Craig, C. T. Hanks, *J. Dent. Res.***70** (1991) 1014
9. S. Ichinose, T. Muneta, I. Sekiya, S. Itoh, H. Aoki, M. Tagami, *J. Mater. Sci. Mater. Med*. **14** (2003) 79
10. A. C. L. Faria, R. C. S. Rodriques, R. P. A. Antunes, M. G. C. de Mattos, A. L. Rosa, R. F. Ribeiro, *J. Appl. Oral Sci.* **17** (2009) 421
11. J. Stevanović, J. Stajić-Trošić, V. Ćosović, V. Panić, O. Pešić, B. Jordović, *Metall. Mater. Trans., B* **41** (2010) 80
12. G. Sjogren, G. Sletten, J. E. Dahl, *J. Prosthet. Dent.* **84** (2000) 229
13. I. Dimić, I. Cvijović-Alagić, I. Kostić, A. Perić-Grujić, M. Rakin, S. Putić, B. Bugarski, *Chem. Ind. Chem. Eng. Q.* **20** (2014) 571
14. I. V. Branzoi, M. Iordoc, M. M. Codescu, *U.P.B. Sci. Bull., B* **69** (2007) 11
15. ISO 10993-5: *Biological evaluation of medical devices - Part 5: Tests for* in vitro *cytotoxicity*, 2009
16. ISO 7405, *Dentistry – Evaluation of biocompatibility of medical devices used in dentistry*, 2008
17. ISO 7405, *Dentistry – Evaluation of biocompatibility of medical devices used in dentistry – Test methods for dental materials*, 2008
18. D. Jevremović, V. Kojić, G. Bogdanović, T. Puškar, D. Eggbeer, D. Thomas, R. Williams, *J. Serb. Chem. Soc.* **76** (2011) 43
19. K. Yoda, A. Takaichi, N. Nomura, Y. Tsutsumi, H. Doi, S. Kurosu, A. Chiba, Y. Igarashi, T. Hanawa, *Acta Biomater.* **8** (2012) 2856
20. X. Z. Xin, N. Xiang, J. Chen, B. Wei, *Mater. Lett.* **88** (2012) 101
21. B. Patel, G. Favaro, F. Inam, M. J. Reece, A. Angadji, W. Bonfield, J. Huang, M. Edirisinghe, *Mater. Sci. Eng., C* **32** (2012) 1222
22. V. S. Saji, H.-C. Choe, *Trans. Nonferrous Met. Soc. China* **19** (2009) 785
23. J. V. Giacchi, C. N. Morando, O. Fornaro, H. A. Palacio, *Mater. Charact.* **62** (2011) 53
24. F. Nejatidanesh, O. Savabi, A. Yazdanparast, *J. Dent. (Tehran)* **2** (2005) 168
25. S. Denizoglu, Z. Yesil Duymus, S. Akyalcin, *J. Int. Med. Res.* **32** (2004) 33
26. Z. Doni, A. C. Alves, F. Toptan, J. R. Gomes, M. Buciumeanu, L. Palaghian, F. S. Silva, *Mater. Design* **52** (2013) 47
27. T. Puškar, D. Jevremović, D. Eggbeer, A. Lapčević, B. Trifković, D. Vukelić, R. J. Williams, *J. Prod. Eng.* **16** (2012) 77
28. ISO 22674: *Dentistry – Metallic materials for fixed and removable restorations and appliances*, 2006
29. K. Beer-Lech, B. Surowska, *Eksploat. Niezawodn.* **17** (2015) 90

30. Y. S. Hedberg, B. Qian, S. Virtanen, I. O. Wallinder, *Dent Mater.* **30** (2014) 525
31. A. Čairović, I. Đorđević, M. Bulatović, M. Mojić, M. Momčilović, S. Stošić-Grujičić, V. Maksimović, D. Maksimović-Ivanić, S. Mijatović, D. Stamenković, *Dig. J. Nanomater. Bios.* **8** (2013) 1003
32. C. Fleury, A. Petit, F. Mwale, J. Antoniou, D. J. Zukor, M. Tabrizian, O. L. Huk, *Biomaterials* **27** (2006) 3351
33. L.-C. Rusu, C. M. Bortun, G. Tanasie, A. C. Podariu, F. Baderca, C. Solovan, L. Ardelean, *Rom. J. Morphol. Embryol*. **55** (2014) 111
34. Ž. Radovanović, Đ. Veljović, B. Jokić, S. Dimitrijević, G. Bogdanović, V. Kojić, R. Petrović, Đ. Janaćković, *J. Serb. Chem. Soc.* **77** (2012) 1787
35. Đ. Veljović, M. Čolić, V. Kojić, G. Bogdanović, Z. Kojić, A. Banjac, E. Palcevskis, R. Petrović, Đ. Janaćković, *J. Biomed. Mater. Res., A* **100** (2012) 3059.

Journal of the Serbian Chemical Society
JSCS@tmf.bg.ac.rs • www.shd.org.rs/JSCS
J. Serb. Chem. Soc. 80 (12) S389–S390 (2015) *Supplementary material*

SUPPLEMENTARY MATERIAL TO

In vitro biocompatibility assessment of Co–Cr–Mo dental cast alloy

IVANA DIMIĆ[1]*, IVANA CVIJOVIĆ-ALAGIĆ[2], NATAŠA OBRADOVIĆ[1], JELENA PETROVIĆ[3], SLAVIŠA PUTIĆ[3], MARKO RAKIN[3] and BRANKO BUGARSKI[3]

[1]University of Belgrade, Innovation Centre of the Faculty of Technology and Metallurgy, Karnegijeva 4, 11120 Belgrade, Serbia, [2]University of Belgrade, Institute of Nuclear Sciences „Vinča", P. O. Box 522, 11001 Belgrade, Serbia and [3]University of Belgrade, Faculty of Technology and Metallurgy, Karnegijeva 4, 11120 Belgrade, Serbia

J. Serb. Chem. Soc. 80 (12) (2015) 1541–1552

IN VITRO CYTOTOXICITY TESTS

Colorimetric methyl-thiazol-tetrazolium (MTT) test.

The MTT test is based on the ability of mitochondrial succinate dehydrogenase (SDH) to convert yellow 3-(4,5-dimethylthiazol-2-yl)-2,5 diphenyl tetrazolium bromide (MTT) into the insoluble, dark purple formazan product in metabolically active cells. The procedure was described in detail previously.[1,2] Briefly, viable cells (2×10^5 cells mL^{-1}) were sown in Petri dishes (50 mm, Centre well, Falcon) which contained disc-shaped Co–30Cr–5Mo alloy. Control samples did not contain the examined metallic material. The Petri dishes with sown cells were thermostated at 37 °C with 5 % CO_2 for 48 h and then the cells were resown in fresh medium. Viable cells (5×10^3 cells 100 μL^{-1}) were sown in 96-well microtiter plates and incubated at 37 °C with 5 % CO_2 for 48 h, 72 h and 96 h. MTT solution (10 μL) was added to each well of the plate and the incubation was continued for a further 3 h. Afterwards, 100 μL of 0.04 M HCl in 2-propanol was added to each well. The absorbance readings were performed immediately after incubation period using a microtiter plate reader (Multiscan, MCC/ /340) at a wavelength of 540 nm with reference to 690 nm. The wells that contained only medium and MTT solution without cells were used as blanks. The fraction of surviving cells (%*K*) was expressed as:

$$\%K = \frac{100N_s}{N_k} \quad (1)$$

where N_s is the number of surviving cells with the examined material and N_k is the number of surviving cells in the control sample.

Dye exclusion test (DET)

The Petri dishes which contained Co–30Cr–5Mo alloy with sown cells were incubated at 37 °C in 5 % CO_2 for 48 h. At the end of the incubation period, the cells were counted in the

* Corresponding author. E-mail: idimic@tmf.bg.ac.rs

counting chambers after 48 h, 72 h and 96 h using an inverted microscope Reichert–Jung, Biostar, model 1820E. After that, 100 μL of cells was taken and added to 100 μL of 0.1 % trypan blue. After intensive shaking, a few drops were placed on the counting fields of the Neubauer chamber in order to determine the number of cells. Trypan blue painted dead cells but not living ones. The fraction of surviving cells (%*K*) was obtained using Eq. (1).

Agar diffusion test (ADT)

For the purpose of the ADT testing, cells (2×10^5 cells mL^{-1}) were sown in Petri dishes and 10 mL of the suspension was incubated at 37 °C in 5 % CO_2 for 24 h. Sterile agar was heated and a nutrient medium was added. The cells were combined with the agar-nutrient mixture and allowed to solidify over 30 min. The cells were stained with a neutral red solution and kept in the dark for 15–20 min. The Co–30Cr–5Mo alloy discs were placed in Petri dishes and were incubated at 37 °C in 5 % CO_2 for 24 h. Any interaction between Co–30Cr–5Mo alloy and the cells, causing the cells death, was recorded using an inverted microscope. It is well known that living cells retain the red dye. Thus, the decolorized zones of dead cells were measured using a ruler and analyzed according to the ISO 7405 standard.[3] The results were evaluated according to decolourization index and lysis index:

$$\text{Cell response} = \text{decolourization index/lysis index} \quad (2)$$

REFERENCES

1. D. Jevremović, V. Kojić, G. Bogdanović, T. Puškar, D. Eggbeer, D. Thomas, R. Williams, *J. Serb. Chem. Soc.* **76** (2011) 43
2. Ž. Radovanović, Đ. Veljović, B. Jokić, S. Dimitrijević, G. Bogdanović, V. Kojić, R. Petrović, Đ. Janaćković, *J. Serb. Chem. Soc.* **77** (2012) 1787
3. ISO 7405, Dentistry – *Evaluation of biocompatibility of medical devices used in dentistry – Test methods for dental materials*, 2008.

Journal of the Serbian Chemical Society
JSCS-info@shd.org.rs • www.shd.org.rs/JSCS
J. Serb. Chem. Soc. 80 (12) 1553–1565 (2015)
JSCS–4819
UDC 549.676+546.62'72'46:628.345:628.336+546.28–145.15:628.3
Original scientific paper

Preparation of aluminum–ferric–magnesium polysilicate and its application on oily sludge

SI LI, SHUANG-CHUN YANG*, YI PAN and JIN-HUI ZHANG

Liaoning Shihua University, FuShun 113001, China

(Received 29 December 2014, revised 9 March, accepted 17 March 2015)

Abstract: Aluminum–ferric–magnesium polysilicate (PAFMS) was prepared by introducing aluminum, ferric and magnesium metal ions into polysilicon acid solution. In this study, PAFMS was applied in the treatment of oily wastewater from the treatment of oily sludge, and the coagulation performance was evaluated by the efficiency of the removal of turbidity and color. The structure and morphology of PAFMS were characterized by Fourier transform infrared spectroscopy (FTIR), X-ray diffraction (XRD) and scanning electronic microscopy (SEM). The results indicated that the mole ratio 6:4:15 of Al:Fe:Mg is beneficial to the formation of Al–O–Si, Fe–O–Si and Mg–Si–O. Fe played the main inhibition role among the three metals. XRD analysis showed that the addition of Al, Fe and Mg into polysilicic acid did not produce a simple mixture, but resulted in the formation of new chemical structures. The intensity of peaks was influenced by the mole ratios of metals. SEM showed that PAFMS appeared to be a spatial structure consisting of many irregular protuberant parts. The removal efficiency of turbidity and color in oily water from the treatment of oily sludge was better when the mole ratio of (Al+Fe+Mg):Si was 0.5 and if the mole ratios of Al:Fe:Mg are kept at 6:4:15. Moreover, when the dosage of PAFMS was 1.4–1.8 % and the pH value in range of 8–9, the efficiency of turbidity and color removal were up to 97.3 and 96.8 %, respectively.

Keywords: coagulation; flocculants; aluminum–ferric–magnesium polysilicate; oily sludge; magnesium; inorganic polymer.

INTRODUCTION

Coagulation is one of the important steps in the water and wastewater treatment process. Flocculants could be divided into two categories: organic and inorganic. Organic polymer flocculants, which can exert perfect flocculation effect at small dose, are expensive and toxic. However, inorganic flocculants are cheaper and wider applied. Polysilicic acid (PSi), which was synthesized in 1937, is difficult to store because of its poor stability.[1] Metals flocculants have the bad

* Corresponding author. E-mail: yangchun_bj@126.com
doi: 10.2298/JSC141229057L

effect of coagulation at low temperatures. This is because the hydrolysis reaction is difficult under low temperatures, however, the floc of metal flocculants mainly rely on the hydrolysis reaction. Furthermore, metallic residues will be present in the effluent from water treated by metals flocculants. Hence, metal polysilicate flocculants were developed to address this issue; they can unite the features of PSi and metals to exert charge neutralization, adsorption bridging and network capturing. In recent years, metal polysilicate flocculants have been the focus of research into inorganic flocculants.[2–4]

Silicic acid monomers can be isolated when strong acid is added into a Na_2SiO_4 solution and PSi formation follows in the condensation polymerization of monomeric silicic acid.[5] The mechanism is as follows:

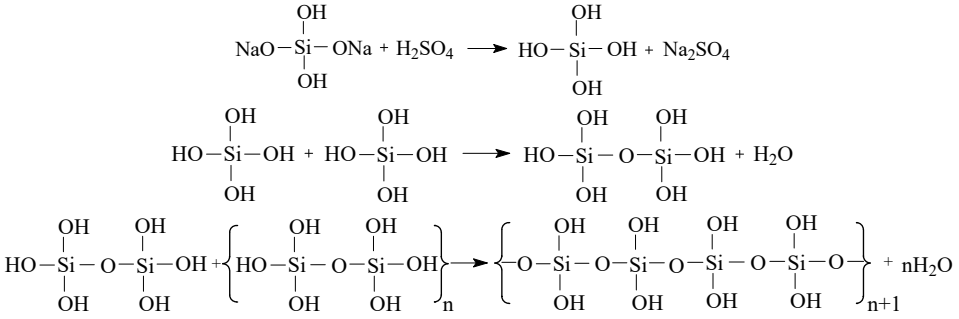

At higher degrees of polymerization, PSi gels and looses its flocculation effect. However, metals can prevent the gelation of PSi by reacting with the –OH on the PSi chain ends. In addition, metals supply positive charges to the PSi surface, which make PSi capable of "charge neutralization" and "network capturing".[6]

Flocculants with aluminum ions produce larger but looser flocs that are difficult to settle. There is also the possibility of biologically toxic residual Al in the treated water. Ferric ions can make the flocs more compact and easy to settle, but the color of the effluent is pronounced.[7] However, magnesium ions can play a decolorizing role because they can create insoluble complexes (for example, $MgHN_3PO_4{\cdot}6H_2O$).[8] Magnesium can reduce the Al^{3+} and Fe^{3+} residuals.[9] Al polysilicate and Fe polysilicate were investigated in many studies,[10–13] but there are only a few studies about magnesium-containing flocculants. Yanjie[14] prepared ferric–magnesium polysilicate (PSIFM) by copolymerization, and its removal for COD (chemical oxygen demand) and SS (suspended substances) was found to be up to 80 and 90 %, respectively. Polysilic aluminum–magnesium sulfate was prepared and applied in the treatment of oily wastewater by Tianbin *et al.*,[15]and its maximum turbidity removal can reach 97.6 %.

Oily sludge is one of the main pollutants in the petrochemical industry. It is a key factor constraining the improvement of the environmental quality in oil-

fields.[16] It has a complex composition and is difficult to treat. The hot washing method was a widely used method for oily sludge treatment. The reagents used in the hot washing method included surfactants, sodas and flocculants. Flocculants play the role of turbidity removal and dewatering. The development of flocculants has a very important significance for the hot washing method of oily sludge treatment. Oily sludge can be separated into three phases, oil, sludge and water, because of de-emulsification by the addition of a hot soda or surfactant solution. However, the aqueous phase still has a high turbidity.[17] Thus, in this paper, the aqueous phase from oily sludge treatment with Tween 80 was used as the object to be treated.

The subject of this study was to prepare aluminum–ferric–magnesium polysilicate (PAFMS), a new type of polysilicate coagulant, by introducing aluminum, ferric and magnesium ions into polysilicic acid. The preparation and application conditions were optimized in terms of the removal of turbidity and color from oily wastewater obtained by phase separation of oily sludge. Finally, the PAFMS powders were characterized by FTIR spectroscopy, XRD analysis and SEM.

EXPERIMENTAL

Wastewater samples

The oily sludge used in these experiments was tank sludge obtained from the Liaohe Oilfield of CNPC, China. Its water content was 33.9 %, the oil content was 11.4 % and the sand content was 54.7 %. It was treated by the hot washing method using Tween 80 under the following conditions: temperature, 60 °C and a solid–liquid ratio of 1:6. The oily wastewater, the water phase obtained from oily sludge treatment, was the subject of further experiments.

Preparation of flocculants

PAFMS was prepared by co-polymerization (hydroxylation of a mixture of Al^{3+}, Fe^{3+} and Mg^{2+} and fresh polysilicic acid (PSi)). The following solutions were prepared: 0.5 mol L^{-1} Na_2SiO_4, 0.233 mo L^{-1} H_2SO_4, 0.5 mol L^{-1} $AlCl_3$, 0.5 mol L^{-1} $Fe_2(SO_4)_3$ and 0.5mol L^{-1} $MgCl_2$. The pH of 10 mL Na_2SiO_4 solution was adjusted to 5.5 with dilute sulfuric acid.[18] The mixture of Na_2SiO_4 solution and dilute sulfuric acid was stirred until a pale blue appeared color. The "pale blue" implied the beginning of polymerization of the silicic acid monomers. The pale blue solution was fresh PSi. Three metal salts solution of different volumes were mixed to form mixed metal solution at different metal mole ratios. Finally, fresh PSi was poured into mixed metal solution. Then mixed solution was stirred constantly and then aged.

Batch coagulation–flocculation test

The pH of wastewater was adjusted to 9 by adding NaOH. The wastewater with appropriate amount of PAFMS was stirred rapidly at 180 rpm for 2 min, and then slowly at 60 rpm for 10 min. Wastewater after treatment was left to precipitate for 30 min.

According to GB13200-91 (Chinese National Standard),[19] the turbidity was measured at a wavelength of 680 nm. The turbidity removal efficiency (*RE*) was calculated as follows:

$$TRE = 100\frac{T_0 - T_i}{T_0} \quad (1)$$

where T_0 is the turbidity of the wastewater and T_i is the turbidity of the wastewater after treatment.

The absorption peaks of wastewater were determined for the analysis of wastewater color by scanning the wavelengths from 280 to 500 nm. The highest absorption peak appeared at 482 nm. The color removal efficiency (*CRE*) was calculated using the absorbance at 482 nm by applying Eq. (2):

$$CRE = 100\frac{A_0 - A_i}{A_0} \quad (2)$$

where A_0 is the absorbance of the wastewater and A_i is the absorbance of the wastewater after treatment.

Characterization

The liquid samples of PAFMS were dried at 50 °C for 10 h and then placed in a desiccator to cool to room temperature. The solid PAFMS was ground for the further characterization studies. The chemical bonds in PAFMS were analyzed by Fourier transform infrared spectroscopy using the KBr pellet method. The spectra were recorded in the range 400–4000 cm^{-1} at a scan resolution of 2 cm^{-1}. X-Ray diffraction analysis was applied for the determination of crystalline phases in the solid PAFMS using a D/MAX-RB X-ray diffractometer with CuK_α radiation in the 2θ range 10–70° at a scan rate of 8° min^{-1}. The morphology was determined by scanning electron microscopy (SEM) at an acceleration voltage of 30 kV and a magnification of 1000×.

RESULTS AND DISCUSSION

The optimization of metal ratio

The optimal mole ratios of Al:Fe:Mg and (Al+Fe+Mg):Si were determined and the results are shown in Figs. 1–3.

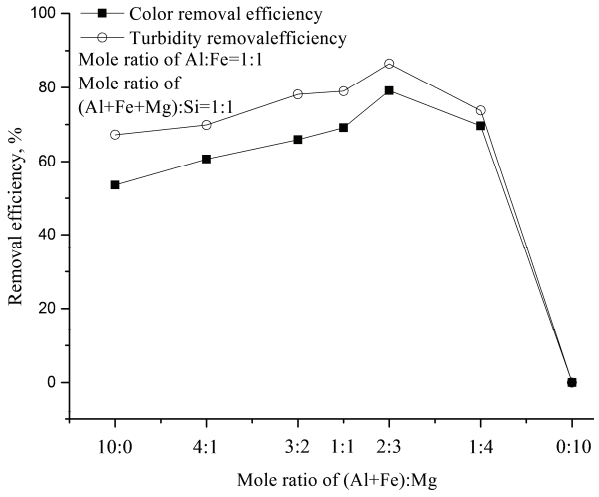

Fig. 1. Effect of the volume of $MgCl_2$ solution (V_{MgCl_2}) on the coagulation performance.

The changes in the removal efficiency when the mole ratios of (Al+Fe): Mg were 10:0, 4:1, 3:2, 1:1, 2:3, 1:4 and 0:10 are indicated in Fig 1. Before the

maximum removal efficiencies of turbidity and color were achieved, the, removal efficiencies increased with increasing mole ratio of Mg. This illustrates that Mg^{2+} improves the coagulation performance and the decolorizing function of PAFMS. The optimum mole ratio of (Al+Fe):Mg was 2:3. After this maximum, further increases in the amount of Mg^{2+} would result in decreased removal efficiencies of turbidity and color. There are two reasons for this decrease in removal efficiency First Mg^{2+} has less positive charges than Al^{3+} and Fe^{3+}. Once the mole ratio of (Al+Fe):Mg exceeds 2:3, the overall charges on the PAFMS would decrease resulting in a weak charge neutralization function of PAFMS. The second reason is Mg^{2+} has smaller molecular mass than Al^{3+} and Fe^{3+}. When mole ratios of (Al+Fe):Mg exceeded 2:3, the settlement velocity would become slow leading to a decrease in the removal efficiency. From Fig. 1, it can be seen that when only Mg^{2+} was added into PSi ((Al+Fe):Mg mole ratio is 0:10), the removal efficiency was 0. This is because PAFMS gelled rapidly to lose the flocculant function in coagulation process, which implies Mg cannot effectively inhibit the gelation of PSi.

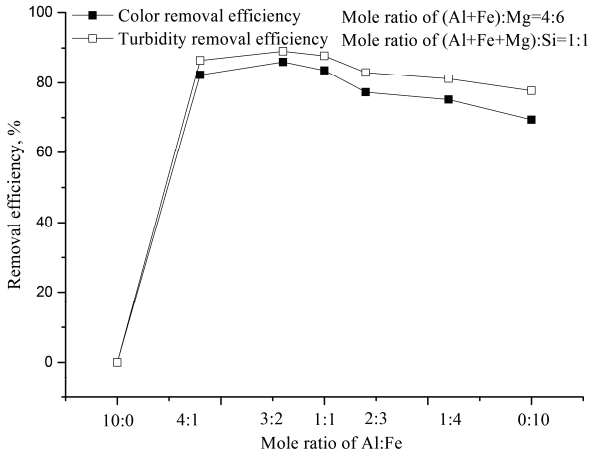

Fig. 2. Effect of volume of $Fe_2(SO_4)_3$ solution ($V_{Fe_2(SO_4)_3}$) on the coagulation performance.

The removal efficiencies of turbidity and color when the mole ratios of Al:Fe were 10:0, 4:1, 3:2, 1:1, 2:3, 1:4 and 0:10 are shown in Fig. 2. The removal efficiency was zero when no Fe^{3+} (Al:Fe mole ratio 10:0) was added to the PSi, which illustrates Fe plays the main inhibition role among the three kinds of metals (Fe, Al and Mg). With the increasing amount of Fe^{3+}, the removal efficiency gradually achieved its maximum value, and then started to decrease. The maximum removal efficiency appeared when mole ratio of Al:Fe was 3:2. The reason of decreasing removal efficiency of turbidity is that the settlement velocity of PAFMS could be accelerated with the increasing amount of Fe, which has a larger molecular weight than Al.[20] On the other hand, Fe^{3+} has color and its

floc is smaller than that of Al^{3+}, and a mole ratio of Al: Fe exceeding 2:3 lead to decreasing color removal efficiency. According to the results shown in Figs. 1 and 2, the favorable mole ratio of Al:Fe:Mg is 6:4:15.

The changes in removal efficiencies when the mole ratios of (Al+Fe+Mg):Si were 0.25:1, 0.5:1, 0.75:1, 1:1, 1.25:1, 1.5:1 and 2:1 are displayed in Fig. 3. The optimum value of the mole ratio of (Al+Fe+Mg):Si was 0.5. Before the removal efficiency achieved the maximum, the removal efficiency increased with the increasing of content of (Al+Fe+Mg). After this maximum, with continuing increases in the amount of metals, the removal efficiencies decreased. Before the optimal mole ratio, the charge of PAFMS increased because of the increasing mole ratio of (Al+Fe+Mg):Si, which led to a better charge neutralization function. After the optimal mole ratio, the adsorption bridging function of PAFMS was weakened by the decreasing amount of Si.

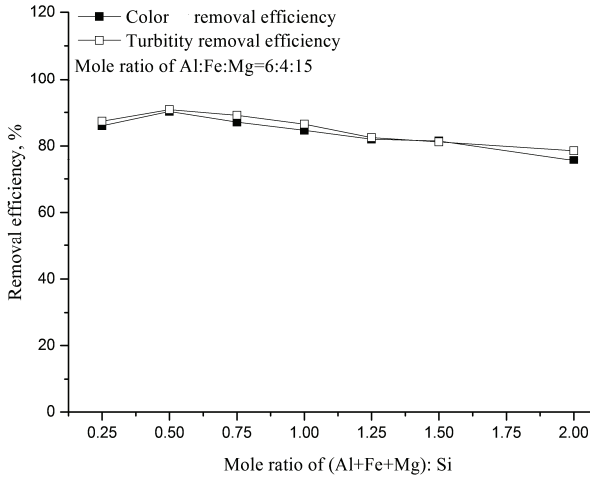

Fig. 3. Effect of mole ratio of (Al+Fe+Mg):Si on the coagulation performance.

Effect of PAFMS dosage on coagulation performance

The changes in the removal efficiencies when the PAFMS dosages were 0.5, 1.0, 1.4, 1.6, 1.8, 2.0 and 3.0 % are shown in Fig. 4. The optimum value for the PAFMS dosage was 1.6 %, however, the removal efficiency was always more than 85.0 % when the PAFMS dosage was within the range 1.4–1.8 %. Before the removal efficiency achieved its maximum value, the removal efficiency increased with increasing PAFMS dosage. After this maximum, a continuing increase in the PAFMS dosage resulted in decreased removal efficiency. When the dosage of PAFMS exceeded 2.0 %, because the positive charges from PAFMS adhered around the suspended matter in the wastewater and the native charges on suspended matters became positive. This made the suspension of the matter in

the wastewater stable. For this reason, the removal efficiency decreased. Thus, the dosage of PAFMS should lie in the range 1.4 %–1.8 % to avoid higher costs.

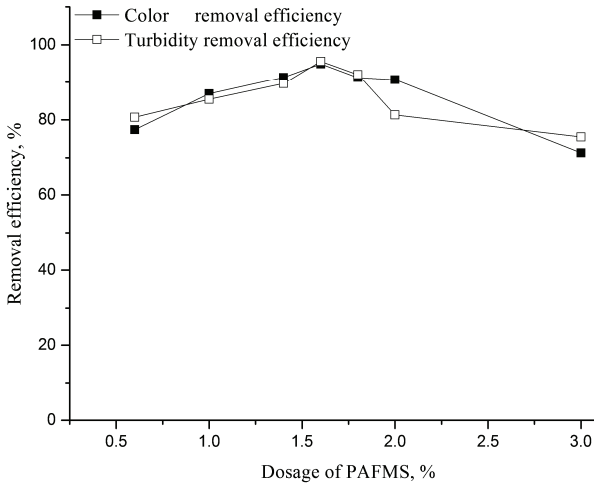

Fig. 4. Effect of PAFMS dosage on the coagulation performance.

Effect of pH of oily wastewater on coagulation performance

The changes in the removal efficiencies when the pH values of the wastewater were set at 7, 8, 9, 10 and 11 are shown in Fig. 5. With increasing pH value, the removal efficiency gradually achieved its maximum value, and then started to decrease. When the pH value was in the range 8–9, the maximum efficiency of turbidity removal and color removal were 97.3 % and 96.8 %, respectively. In this pH range, Al^{3+}, $Fe^{3+}$and Mg^{2+} have rich variety of hydrolysates

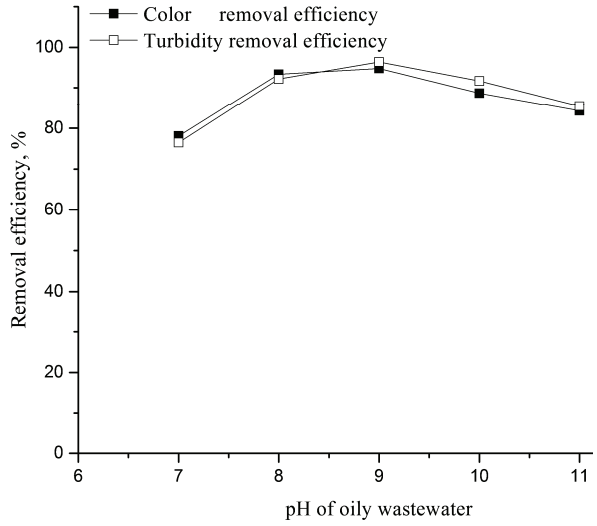

Fig. 5. Effect of the pH of the oily wastewater on coagulation performance.

and hence a large amount of polynuclear complexes and hydroxy complex ions[21] are generated, leading to improved adsorption bridging and network capturing functions by PAFMS. Furthermore, PAFMS exhibited a positive potential, but the suspended matters has a negative potential. This illustrates that a pH value in the range 8–9 is the best range for charge neutralization. However, when the pH value exceeded 9, the degree of dissociation of PSi was too large[22] for PSI exhibit an adsorption bridging function.

Characterization of the PAFMS

FTIR analysis. The FTIR spectrum of PSI is shown in Fig. 6a, while the FTIR spectra of PAFMS with different mole ratios of the metals are presented in Fig. 6b–d. In Fig. 6b, the mole ratio of Al:Fe:Mg was 6:4:15, and (Al+Fe+Mg):Si ratio was 0.5:1, *i.e.*, it shows the spectrum of the PAFMS with the optimal metal ratios. In Fig. 6c, the mole ratio of (Al+Fe):Mg was 4:1, and (Al+Fe+Mg):Si was 1:1, *i.e.*, it shows the spectrum of the PAFMS with a lower amount of Mg^{2+}. In Fig. 6d, the mole ratio of Al:Fe:Mg was 6:4:15, and (Al+Fe+Mg):Si was 1.5:1, *i.e.*, it shows the spectrum of the PAFMS with an excessive amount of (Al+Fe+Mg).

In Fig. 6b–d, characteristics peaks at 3700–3900 cm^{-1} could be attributed to the symmetric and antisymmetric stretching of M–OH (Al–OH, Fe–OH and Mg–OH).[23] This peak does not appear in Fig. 6a, which indicated that the metals had reacted with the –OH on the PSi chain ends. Intensity of peaks in Fig. 6b and d are stronger than those in Fig. 6c. This illustrates that Mg^{2+} is better for the formation of M–OH bonds.

The peaks at 3500–3300 cm^{-1} were assigned to the stretching vibration of –OH.[24] In Fig. 6b and d, there are shoulder peaks around 3500–3300 cm^{-1} and peak area is larger than in Fig. 6a. This implies that the amount of –OH increased. This phenomenon could be attributed to an increase in absorbed water and –OH linked with Al^{3+}, Fe^{3+} and Mg^{2+}.

The peaks at 1660–1640 cm^{-1} corresponded to bending vibrations of H–O–H, which implies all four samples were hydroxyl polymers[25]. There is a strong absorption peak at 1099.9 cm^{-1} in the spectrum presented in Fig. 6a, which could be attributed to the stretching vibration of Si–O–Si groups, which arose because of the condensation polymerization of silicic acid monomers. However, all Si–O–Si peaks shown in Fig. 6b–d are weaker than in Fig. 6a, and blue-shifted to 1150.5, 1105.5 and 1139.2 cm^{-1}, respectively. Peaks at 1150.5, 1105.5 and 1139.2 cm^{-1} are assigned to the characteristics peaks of Al–OH–Al, Fe–OH–Fe and Mg–OH–Fe, respectively. This proves that metals can prevent the gelation of PSi. This corresponds to the research results of Yuemei.[26] There is another possibility, the peaks around 1100 cm^{-1} could also be attributed to the characteristics peaks of SO_4^{2-}. From Fig.6a–d, it could be seen that the peaks around 1100 cm^{-1} of Fig. 6a are stronger than those of Figs. 6b–d (at 1150.5,

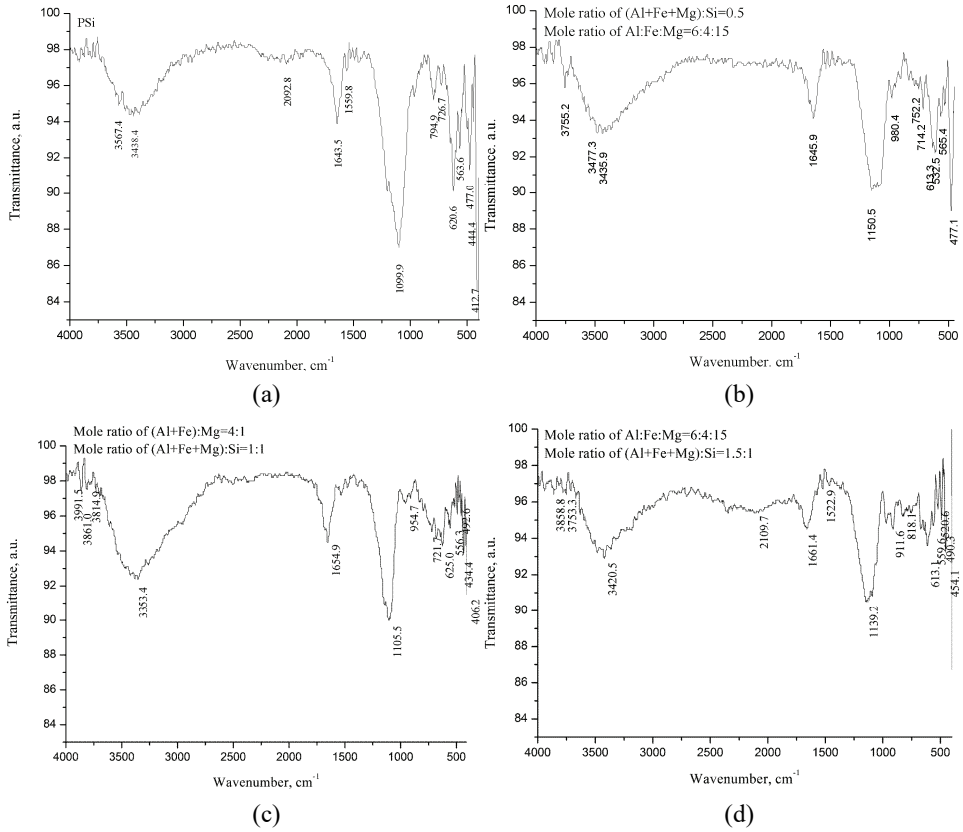

Fig. 6. FTIR spectra of PSi and PAFMS with different mole ratios of metals: a – PSi; b – PAFMS prepared under mole ratio of (Al+Fe+Mg):Si = 0.5, mole ratio of Al:Fe:Mg = 6:4:15; c – PAFMS prepared under mole ratio of (Al+Fe+Mg):Si = 0.5, mole ratio of (Al+Fe):Mg = 4:1; d – PAFMS prepared under mole ratio of (Al+Fe+Mg):Si = 1.5, mole ratio of Al:Fe:Mg = 6:4:15.

1105.5 and 1139.2 cm^{-1}, respectively). This indicates SO_4^{2-} would coordinate with metal ions and participate in the polymerization when metal salts were added into PSi.[27]

Characteristic peaks at 910–960 cm^{-1} in Figs. 6b–d could be attributed to the stretching vibration of Al–O–Si and Fe–O–Si.[14] The intensity of this peak is closely related to the coagulation performance. The peak intensity at 960.4 cm^{-1} in Fig. 6b is the strongest. The peak at 532.5 cm^{-1} in Fig. 6b and the peak at 520.6 cm^{-1} in Fig. 6d were assigned to the stretching vibration of Si–O–Mg,[25] but they did not appear in Fig. 6c. This implies that greater amount of Mg would form more Si–O–Mg groups. In a word, the generation of Al–O–Si, Fe–O–Si and Mg–O–Si indicate the metals had polymerized with PSi. The peak at 794.0 cm^{-1}

in Fig. 6a, assigned to the connection of tetrahedron of Si–O–Si,[25]did not appear in Figs. 6b–d. This indicates PAFMS has a reticular formation.

In conclusion, FTIR analysis supports the formation of new chemical species of PAFMS consisting of aluminum, iron, magnesium and silica.

XRD analysis

Figure 7 illustrates The XRD patterns of PSi and PAFMS with different mole ratios of metals are illustrated in Fig. 7.

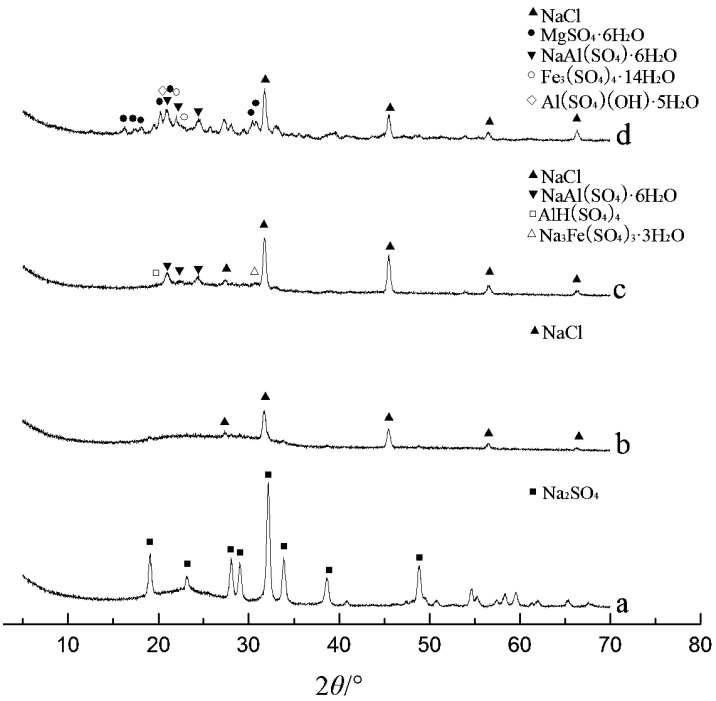

Fig. 7. XRD spectra of PSi and PAFMS with different mole ratios of metals: a – PSi; b – PAFMS prepared under mole ratio of (Al+Fe+Mg):Si = 0.5, mole ratio of Al:Fe:Mg = 6:4:15; c – PAFMS prepared under mole ratio of (Al+Fe+Mg):Si = 0.5, mole ratio of (Al+Fe):Mg = 4:1; d – PAFMS prepared under mole ratio of (Al+Fe+Mg):Si=1.5, mole ratio of Al:Fe:Mg= 6:4:15.

The XRD spectrum of PSi has clear diffraction peaks, but the spectra of PAFMS have no diffraction peaks. With the introduction of metal ions, the intensity of peaks was weakened and the width of peaks was broadened. There is a diffuse peak group, which indicates PAFMS is a new type of multipolymer without fixed regular structures; it is a kind of macromolecule with long-range disorderly structures. Diffraction crystal peaks of Na_2SO_4 (at 2θ 19.035, 23.153, 28.027, 28.990, 32.123, 33.826, 38.615 and 49.443°) were only found in the spectrum of

PSi, which implies the introduction of metals impelled SO_4^{2-} to participate in the copolymerization. This corresponds to the results of the FTIR analysis.

Crystal peaks NaCl (at 2θ 27.334, 31.692, 45.449, 56.477 and 66.227°) appeared in the patterns of the PAFMS samples (Fig. 7, b–d), which illustrates Cl^- did not fully participate in the polymerization reaction. The intensity of NaCl crystal peaks in Fig. 7, c, were stronger than in Fig. 7, b and d, which implies that the increasing amount of Mg^{2+} could promote Cl^- to polymerize with PSi.

Polymerization between metals and PSi could produce an amorphous substance and hence, the more complete is the polymerization reaction, the smoother is the amorphous peak groups at 2θ 18–30°. Obviously, the peak shape in Fig. 7, b, is more regular, and the amorphous peak groups at 2θ 18–30° is smoother. This indicates the PAFMS had a better coagulation performance with more amorphous substance.

Crystal peaks of metal ions were observed in Fig. 7, d, *i.e.*, $MgSO_4 \cdot 6H_2O$ (at 2θ 16.250, 17.688, 18.164, 20.211, 21.983, 24.640, 30.084 and 30.367°), $NaAl(SO_4)_2 \cdot 6H_2O$ (at 2θ 21.034, 24.366 and 30.818°) and $Fe_3(SO_4)_4 \cdot 14H_2O$ (at 2θ 21.950 and 22.336°), which indicates that excessive metals do not participate in the polymerization reaction.

Diffraction patterns of crystals, such as $AlCl_3$, $Fe_2(SO_4)_3$, $MgCl_2$, Al_2O_3, Fe_2O_3, Fe_3O_4, MgO, $Al(OH)_3$, $Fe(OH)_3$, $Mg(OH)_3$ and SiO_2 were not observed in Fig. 7, b, which confirms that the metal ions had polymerized with PSi. Amorphous or new compounds were formed in PAFMS. The XRD analysis shows that the addition of Al^{3+}, Fe^{3+} and Mg^{2+} did not produce a simple mixture in PSi, but resulted in the formation of new chemical structures. The intensity of the peaks was influenced by the mole ratios of the metals.

SEM micrography

The surface morphology of PAFMS powder with optimal metal ratios, which is a reticular formation consisting of many irregular and non-direction protuberant parts, is presented in Fig. 8. This corresponds to the results of FTIR analysis. A series of holes of different width and depth are distributed, which indicates PAFMS presents a large surface area. The reasons for the formation of this structure is that metal ions adsorbed or polymerized with the –OH at the of the chain ends of PSi.

CONCLUSIONS

A new inorganic coagulant PAFMS was prepared in this study, the mole ratios of metals and application conditions were optimized. The structure and surface characteristics of PAFMS were analyzed by FTIR, XRD and SEM.

As the experiment results showed, the characteristics of PAFMS were largely affected by the mole ratios of metals. Removal efficiency was maximal when the

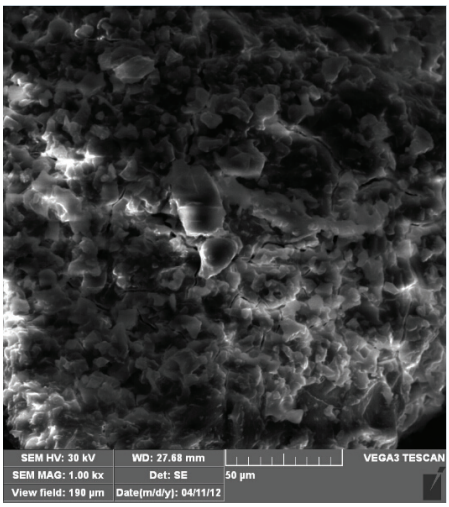

Fig. 8. SEM image of PAFMS.

mole ratio of (Al+Fe+Mg):Si was 0.5 and the mole ratio of Al:Fe:Mg was 6:4:15. Moreover, when the dosage of PAFMS was 1.6 % and wastewater pH value in range of 8–9, the removal efficiency of turbidity and color were up to 97.3 % and 96.8 %, respectively. The results of the FTIR analysis indicated that there were bonds formed by polymerization between metals and PSi in PAFMS, such as Al–OH, Fe–OH, Mg–OH, Al–OH–Al, Fe–OH–Fe, Mg–OH–Mg, Al–O–Si, Fe–O–Si and Mg–Si–O. Moreover, the intensities of the FTIR peaks were influenced by the mole ratios of the metals. In XRD patterns of PAFMS, there was an amorphous group of peaks at 2θ 18–30°. This implies PAFMS is a kind of amorphous multipolymer with no regular structure. The peak shape in XRD spectra of PAFMS under optimal conditions was more regular. Meanwhile, in SEM microphotograph, PAFMS showed a reticular formation consisting of many irregular protuberant parts. In conclusion, as a new type inorganic flocculant, PAFMS has further research value.

Acknowledgements. This work was supported by the Project of Liaoning Provincial Industrial Magnesium Resources Protection Office (The synthesis and application of magnesium-based polymeric flocculants) and Training Programs of Innovation and Entrepreneurship for Undergraduates of Liaoning Provincial (Research and development of composite flocculant special for acrylic fiber wastewater).

ИЗВОД

СПРАВЉАЊЕ АЛУМИНИЈУМ–ФЕРИ–МАГНЕЗИЈУМ–ПОЛИСИЛИКАТА И ЊЕГОВА ПРИМЕНА НА НАФТНОМ МУЉУ

SI LI, SHUANG-CHUN YANG, YI PAN и JIN-HUI ZHANG

Liaoning Shihua University, FuShun 113001, China

Поли-алуминијум–фери–магнезијум-силикат (PAMFC) је справљен уношењем јона метала алуминијума, гвожђа и магнезијума у кисели раствор. Учинак коагулације је

оцењиван уклањањем мутноће и обојења отпадне воде од третмана нафтног муља. Структура и морфологија PAMFC су карактерисане инфрацрвеном спектроскопијом са Фуријe трансформацијом (FTIR), рентгенском дифракцијом (XRD) и сканирајућом електронском микроскопијом (SEM). Резултати су указали да је однос 6:4:15 метала Al:Fe:Mg погодан за формирање Al–O–Si, Fe–O–Si и Mg–Si–O. Од ова три метала, гвожђе је највише играло улогу инхибитора. XRD анализа је показала да додатак Al, Fe и Mg у полимерну силицијумову киселину доводи до формирања нове хемијске врсте, а не обичне смеше. Интензитет пикова је зависио од молских фракција метала. Према SEM, PAMFC се показао као просторна структура која се састоји од много неправилних истурених делова. Када је молски однос (Al+Fe+Mg):Si био 0,5, а Al:Fe:Mg на 6:4:15, ефекат уклањања је био бољи. Штавише, када је дозирање PAMFC било 1,4–1,8 % или 8–9 %, тада је уклањање мутноће и обојења било 97,31, односно 96,76 %.

(Примљено 29. децембра 2014, ревидирано 9. марта, прихваћено 17. марта 2015)

REFERENCES

1. S. L. Yu, L Liu, X. Y. Liu, *J. Harbin. Univ. Civil Eng. Arch.* **30** (1997) 62 (in Chinese)
2. Z. L. Yang, B. Liu, B. Y. Gao, *Sep. Purif. Technol.* **111** (2013) 119
3. Z. M. Qiu, W. T. Jiang, Z. J. He, *J. Hazard. Mater.* **166** (2009) 740
4. G. C. Zhu, H. L. Zheng, W. Y. Chen, W. Fan, P. Zhang, T. Tshukudu, *Desalination* **285** (2012) 315
5. S. L. Yu, X. Y. Liu, L. Liu, *J. Harbin. Univ. Civ. Eng. Arch.* **29** (1996) 111 (in Chinese)
6. X. Xu, S. L. Yu, W. X. Shi, *Sep. Purif. Technol.* **66** (2009) 486
7. C. J. Wang, N. Y. Gao, S. J. Zhao. *Sichuan Environ.* **28** (2009) 119 (in Chinese)
8. J. X. Zhang, J. R. Lu, B. T. Shan, *Ind. Water Treat.* **8** (2009) 56 (in Chinese)
9. L. Chen, L. Sha, Z. H. Zhang, *Tech. Water Treat.* **37** (2011) 42 (in Chinese)
10. B. Y. Gao, Q. Y. Yue, Y. H. Song. *Environ. Chem.* **2** (1998) 170 (in Chinese)
11. H. Y. Yang, F. Y. Cui, Q. L. Zhao, *J. Zhejiang. Univ.: Sci.* **5 (**2004) 721
12. Z. M. Lu, C. S. Wu, Y. J. Diao. *Guangzhou Chem.* **35** (2010) 28 (in Chinese)
13. W. B. Lv, X. L. Zhu, J. G. Li, *Pap. Sci. Technol.* **30** (2011) 86 (in Chinese)
14. Y. J. Wen, C. Y. Han, L. D. Zhang, *J. Beijing Univ. Chem. Technol. (Nat. Sci.)* **39** (2012) 90 (in Chinese)
15. T. B. Li, W. Chen, Y. B. Wan, *J. Yangtze Univ. (Nat. Sci. Ed.)* **8** (2011) 18 (in Chinese)
16. X. B. Li, J. T. Liu, Y. Q. Xiao, *J. Cent. South Univ. Technol.* **18** (2011) 367
17. B. C. A. Pinheiro, J. N. F. Holandan. *Ceram. Int.* **39** (2013) 57
18. Y. B. Duan, S. Z. Yi. *Environ. Prot. Chem. Ind.* **25** (2005) 239 (in Chinese)
19. GB13200-91, Water quality-Determination of turbidity (in Chinese)
20. Y. Fu, S. L. Yu, Y. Z. Yu, *J. Environ. Sci.* **19** (2007) 678
21. Y. Z. Li. *Shandong Chem. Ind.* **41** (2013) 51 (in Chinese)
22. G. Z. Zhu. *Pes. Ind.* **22** (2009) 28 (in Chinese)
23. H. Liu, Y. M. Fang, J. Shao, J. Liang. *Chem. Eng.* **127** (2006) 55 (in Chinese)
24. T. Song, C. H. Sun, G. L. Zhu, *Desalination* **268** (2011) 270
25. R. Li, C. He, Y. L. He, *Desalination* **319** (2013) 85
26. Y. M. Fang. *Ind. Safety Env. Prot.* **10** (2007) 22 (in Chinese)
27. K. Müller, G. Lefèvre, *Langmuir* **27** (2011) 6830.

Journal of the Serbian Chemical Society
JSCS-info@shd.org.rs • www.shd.org.rs/JSCS
J. Serb. Chem. Soc. 80 (12) 1567–1580 (2015)
JSCS–4820
UDC 504.75+504.06:377+378.4
Original Scientific paper

"It happened, what's the problem?" and "A guide through the problem" – A model for consideration of ecological issues in chemistry education

JASMINKA N. KOROLIJA[1#], SNEŽANA RAJIĆ[2], MILENA TOŠIĆ[1#] and LJUBA M. MANDIĆ[1*#]

[1]*Faculty of Chemistry, University of Belgrade, Belgrade, Serbia and* [2]*Secondary School St. Sava, Belgrade, Serbia*

(Received 22 May, revised 11 August, accepted 9 September 2015)

Abstract: In order to improve the ability to apply knowledge of chemistry (acquired in the existing educational system) in real life, the model for consideration of ecological issues was developed and applied in high school. The model consists of a continuous text "It Happened, What's the Problem?" and a test with non-continuous text "A Guide Through the Problem", which were prepared for consideration of the problem of eutrophication. All results obtained (average achievement of 70.9±14.3 %) showed that the application of the model enabled: understanding of an ecological problem based on scientific representations of the term eutrophication given in the continuous text, realization that pollution of the environment may be directly related to modern life, application of acquired knowledge of chemistry to observe and understand the cause and effect of eutrophication in the environment, to draw a scientific conclusion, and understanding the importance of science and technology discoveries for solving ecological problems. In addition, the model contributed to the development of student's environmental literacy (ecological knowledge and cognitive skills), ability to think critically, and provided possibilities for classroom knowledge to become applicable in real life.

Keywords: environmental education; ecological problem-eutrophication; environmental literacy; application of chemistry knowledge.

INTRODUCTION

The results of the PISA (Program for International Student Assessment) and TIMSS (Trends in International Mathematics and Science Study) international evaluation of educational achievements are good indicators of the effectiveness of the educational system in a country. In Serbia, in these studies, the overall

* Corresponding author. E-mail: ljmandic@chem.bg.ac.rs
# Serbian Chemical Society member.
doi: 10.2298/JSC150522072K

achievement of Serbian eighth grade students in natural sciences was statistically significantly lower than that of the international average.[1–6]

TIMSS 2007 in Serbia indicated that the achievement of the students in "factual knowledge" of chemistry was good (26–93.6 %). In the domain of "conceptual knowledge", achievements were in the range from 5.1 to 89.7 %, whilst in the domain of "reasoning and analysis", the results were lower (6.7–73.2 %). The results achieved per level of scientific literacy in PISA 2012 demonstrated that 35 % of pupils possessed "limited scientific knowledge applicable only in a small number of well-known situations" (level 1).[7] "Adequate scientific knowledge necessary for providing explanations and deduction in simple explorations of well-known contexts" (level 2) was possessed by a slightly lower number of students (32.4 %). Level 3 that implies "limited associating, interpreting and use of scientific concepts from different disciplines" was achieved by only 22.8 % the students. For levels 4 and 5, which involve developed abilities for giving not only explanations based on "critical analysis" but also possessing "scientific knowledge of many complex life situations", the results were low (8.1 and 1.6 %). Only 0.1 % of the students encompassed in PISA 2012 testing achieved level 6, where "progressive scientific opinions" and willingness to make "suggestions and decisions" are expected in complex personal, socio-economic and global life situations.[7]

Causes for low students' achievements can be seen in the rather extensive curricula, and in the fact that "Practical knowledge in action" (recognizing questions as scientific, identifying relevant evidence, critically evaluating conclusions, and communicating scientific ideas) is rare with students.[4,8–10] In regular school classes, insufficient attention was directed to the teaching of concepts through their practical application in real life. Therefore, students find classes frustrating because the material is difficult, boring, and irrelevant for their lives. Overall, students in Serbia have fairly good scientific knowledge of single facts ("factual knowledge"),[5] but difficulties emerge in identifying and applying acquired knowledge in diverse life situations, perception of problem situations from the aspect of scientific concepts from different disciplines and scientific knowledge and solving tasks that demand analysis and deduction based on pieces of information presented in the form of continuous and non-continuous texts.

The above-mentioned difficulties have lead to the following question: What can be done in the existing state-of-the-art? The existing problems could be overcome by applying the experience attained by TIMSS and PISA testing in preparing models appropriate to make the knowledge of science, especially chemistry, applicable in real life.[11,12] Taking into account that student's awareness of the connections between chemistry and real-life issues[13] could be raised by learning chemistry in the context[14] of a specific environmental problem,[15] a model based on consideration of ecological problems was designed in this study. The

main goal of environmental education is to contribute to the development of environmental literacy (ecological knowledge, cognitive skills and affective attitudes towards the environment)[16–19] and responsible citizen, so that they could have a proper relationship with the environment in which they live.[20–22] In Serbia, as well as in many European countries, environmental issues are encompassed of several teaching subjects.[23] Pupils who received environmental education only during regular class hours were successful in components of environmental knowledge (factual knowledge and conceptual understanding), but did not perform as well in reasoning and analysis.[5] In addition, awareness and environmentally responsible behavior are difficult to be achieved,[24,25] even in eco-school pupils'.[16] Therefore, the goal of environmental education to increase environmental literacy was also included in the Model design. Students' environmental literacy is evaluated based on their ability in using and dealing with information on an ecological issue and using chemical knowledge and skills to understand information about an everyday problem. The "problem-based approach" was chosen because of the achievements and possibilities this teaching method provides.[26–28]

Thus, the model was designed to let students read about a real ecological problem, apply scientific principles to find out its causes and effects and offer problem solutions. Such an approach translates everyday situations into chemical problems and leads to an increase in the student's awareness of the connections between chemistry and real life-issues, as well as in their interest in science. Ultimately, the model should provide an efficiency check in acquiring, understanding and applying knowledge, while, simultaneously, serving as a guide for problem solving.

EXPERIMENTAL

Design of the model

A model that provided steps (the partial goals are presented in Fig. 1) necessary for achieving knowledge applicable in everyday life was developed and used. The basis for the model was demands for evaluation of the students' scientific literacy, which are stated by the Program for International Student Assessment (PISA). As mentioned above, PISA tends to focus on "practical knowledge in action", namely recognizing questions as scientific, identifying relevant evidence, critically evaluating conclusions, and communicating scientific ideas.[4,8-10] Another emphasis in PISA is the extent to which the education systems in the participating countries prepare students to become life-long learners able to play constructive roles as citizens in society. In addition, the model is in accordance with general aims that are defined by socio-scientific issues (SSI) and Chemistry in Context projects,[13,14] because all the approaches emphasize the preparation of students for life and citizenship, complex reasoning and reflective practices, and robust understandings of the nature of science, particularly as it is practiced in society.[29]

For the realization of this model, it was necessary to:

– Select a problem from a real life context, which will interest students, and whose understanding requires the application of science knowledge (chemistry knowledge).

Design of the texts related to the problem:

– a continuous text with information related to the problem („It Happened, What's the Problem?");

– a test with a non-continuous text ("A Guide Through the Problem");

– apply the Model in the classroom;

– analyze the obtained results.

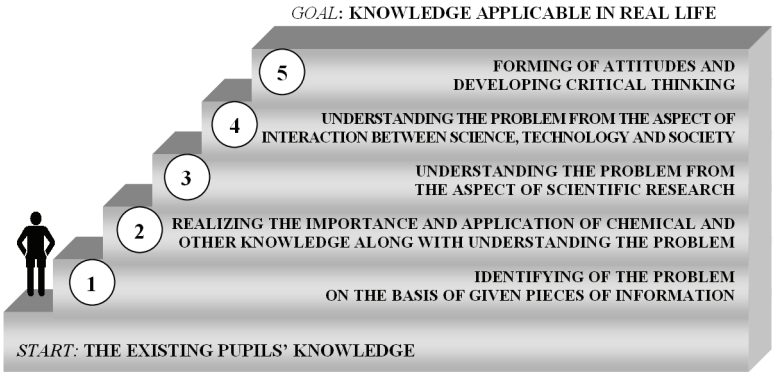

Fig. 1. Steps in the model for achieving the goal – make the existing knowledge applicable in real life.

Preparation of texts concerning the ecological problem

Continuous text about the ecological problem: "It Happened, What's the Problem?" Students are informed about ecological problems everyday through the media. An understanding of these problems requires application of knowledge of natural sciences. To accomplish the set-up steps in the model (Fig. 1), pieces of information about the ecological problem (without many scientific facts and explanations) are given in the form of a continuous text "It Happened, What's the Problem?" Keyword, ecological problem and real life event (Fig. 2, I–III) were selected before preparation of the text.

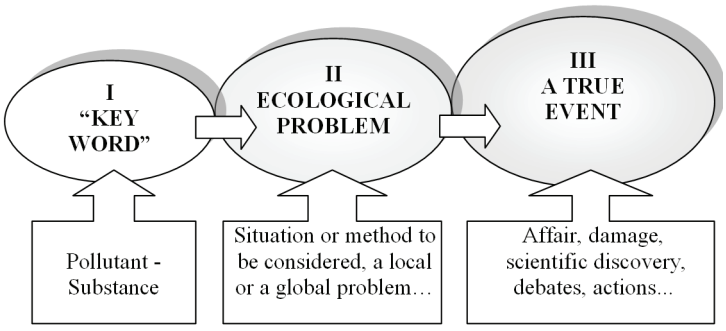

Fig. 2. Selection of content determinants in the preparation of the continuous text "It Happened, What's the Problem?"

Keyword (a substance that is covered in regular chemistry classes) may be a direct or indirect cause for the emergence of an ecological problem. Ecological problem may be chosen to illustrate the influence of humans (society) on the ecosystem from two aspects: "humans as a cause of the problem" and "humans (science) who solve the problem" (Fig. 3).

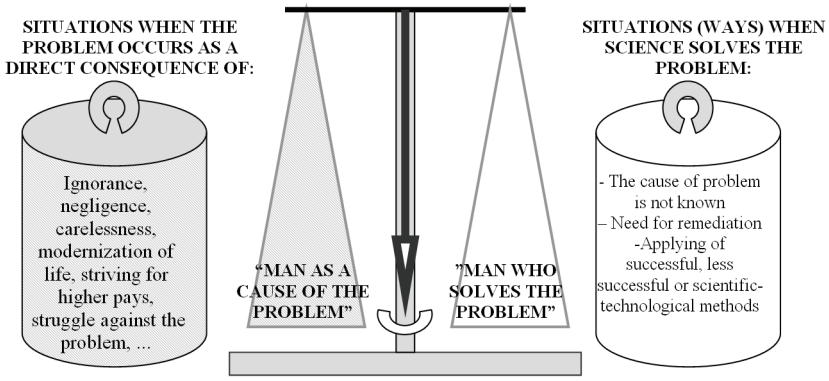

Fig. 3. Situation "Man as a cause of the problem" and "Man who solves the problem".

A true event may be chosen such as a historical event, *i.e*. a case that happened long ago but its consequences are still present in an ecosystem and lessons people have learned from it, and a contemporary event – a case of short- and long-term consequences at local and global level. It could be described from two points of view: the consequences that people noticed, and "What does science say?" (scientific explanation of changes/consequences in the environment). If the cause of the problem was unknown, there follows the description of scientific–technological method applied to find the real cause (pollutant substance) without too many scientific facts. The content of the continuous text provides key information that, in combination with existing knowledge of chemistry (and other science subjects), enables conclusions about the cause of the ecological problems and making suggestions for solutions and future accident prevention. Structural elements of the continuous text and those (IV–VII) that may be advanced in composing the text based on set goals (steps in Fig. 1) are presented in Fig. 4.

Such way of writing the text enabled the anticipation and understanding of the problem from the aspect of interactions in science–technology–society (STS):

a) both benefits and harms that scientific–technological development brings about,
b) differences between scientific proofs and personal opinion/attitude,
c) importance and role of science and technology,
d) limits and relationships between science and technology and
e) alternative solutions.

In addition, such written text encourages the formation of opinions and the development of critical thinking in students (step 5 in the presented model, Fig. 1).

The interrelation of partial goals in the model (steps 1–5, Fig. 1) with structural elements of the continuous text (I–VII, Figs. 2 and 4), with interactions that should be perceived and understood is shown in Fig. 5 (a.–e.). Such a presentation enabled anticipation of how by a stepwise approach through the text the goal could be accomplished: application of existing knowledge of science in real life.

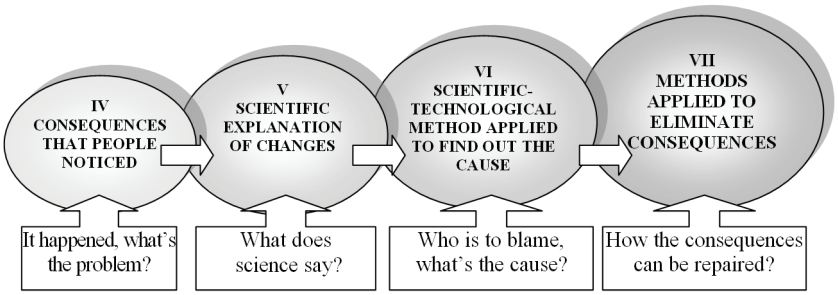

Fig. 4. Structural elements and theses of the continuous text "It Happened, What's the Problem?"

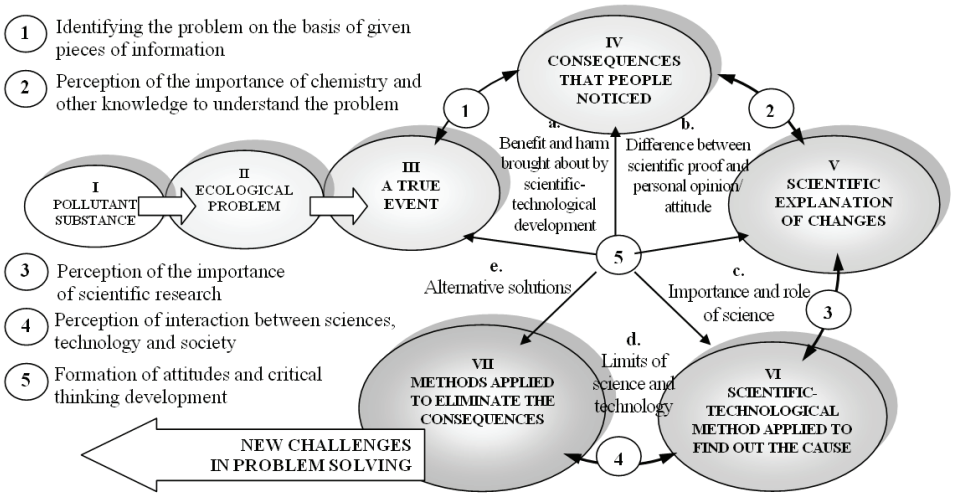

Fig. 5. Relationship between set-up steps 1–5 in the model, structural elements of the continuous text (I–VII), and interactions to be perceived through the text (a.–e.).

"It Happened, What's the Problem?" – Eutrophication as an example

"Detergent" (keyword), "eutrophication" (ecological problem) and "algal blooming" (true event – blooming of the sea on the Adriatic coast of Montenegro) were chosen before the preparation of two continuous texts (documents 1 and 2).

First, students were presented with the ecological problem and the real life event through document 1, which begins with the headline from a newspaper "SWIMMERS STOP! – BLOOMING OF THE ADRIATIC SEA IS IN PROGRESS". The following text describes the outcome and changes that occurred in the sea from the viewpoint of tourists and swimmers, and then the eutrophication from the viewpoint of science (increase in biomass concentration, development of anaerobic conditions, and degradation of biomaterial down to methane, hydrogen sulfide and ammonia).[30-32] The cause of eutrophication was not disclosed in document 1, rather it was called "a nutrient". As guidance for the evaluation of the nutrient, Radfield's discovery was presented that organic mechanisms (biota) control the movement of nitrogen and phosphorous in the ocean according to a constant atomic stoichiometry of

106C:16N:1P.[33] The "Experienced formula" of algae ($C_{106}H_{263}O_{110}N_{16}P$) based on their chemical components was offered as a scientific discovery to solve the cause of eutrophication.[34]

Document 2 entitled "WITH WHAT DO WE FEED THE SEA?" deals with the history of detergent and softener use. In the conclusion of the text, it was stated that softeners are polyphosphates. This text does not indicate the importance of Redfield's discovery for determining the cause of eutrophication, but it was left to the students to use pieces of information they had read to discover the relationship between eutrophication, "experienced formula" of algae (document 1) and polyphosphate softeners (document 2). A schematic presentation of the text for considering eutrophication according to the given model is shown in Fig. 6.

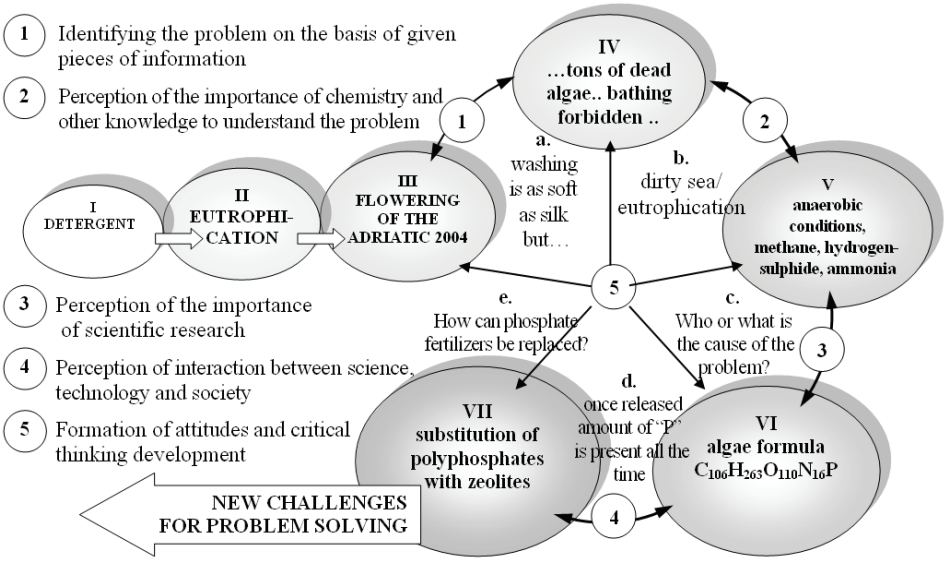

Fig. 6. Structural elements of the continuous text about eutrophication.

The test with a non-continuous text "A Guide through the Problem"

The questions in the test "A Guide through the Problem" contain extracts either from the continuous text or from new pieces of information (given in the form of non-continuous text – graphs, pictures, schemes, tables, *etc*.) about pollutant substances and changes in the ecosystem. They help perceive the problem from the viewpoint of scientific knowledge, whereby all capacities are directed to essentially scientific perception of the problem. The form and sequence of questions are arranged to follow the story of the continuous text and make students pass through the set-up steps presented in Fig. 1. Questions are classified into six groups and interrelated with the steps (partial goals) in the model as follows.

First group: Existing student's knowledge about pollutant substance (start). Questions refer to general, special and single items of knowledge about the substance, which is a direct or indirect cause of the occurrence of the ecological problem ("keyword"). Questions help to connect the chemical structure of a pollutant substance with outcomes that may be caused in an ecosystem by the substance.

Second group: Identifying the problem based on pieces of information in the continuous text "It Happened, What's the Problem?" (step 1, Fig. 1). This group of questions examines the ability to understand that which has been read, and of collecting, using and interpreting information items given in the text.

Third group: Application of chemistry and other knowledge to the understanding of the outcomes and changes in the environment (step 2, Fig. 1). Questions should encourage identifying and applying those teaching contents of chemistry and/or other scientific disciplines that are crucial to understand the essence of the described problem, as well as to interpret scientific arguments and results of scientific and/or technological measurements that explain causes and consequences of ecological problems.

Fourth group: Understanding steps in scientific research methodology (step 3, Fig. 1). These questions require assuming a researcher's role, which involves hypothesis proposal, suggesting and testing of the method for solving the assumption and drawing a conclusion.

Fifth group: Understanding interactions between science, technology and society in solving ecological problems (step 4, Fig. 1). The responses provide the possibility to estimate the extent to which the problem is perceived over political, economic and ethical aspects of solving, whether limits of science and technology as well as likely risks are perceived.

Sixth group: Questions where statements of student opinions towards ecological problems, deduction and generalizations are expected (step 5, Fig. 1). The responses should contain an opinion on given or some other situations, on the (un)acceptability of some methods, and the suggestions of alternative solutions.

Application of the model in the classroom

The Model was used in the upper secondary school "St. Sava School", Belgrade, Serbia. The total number of students was 60 (34 boys and 26 girls) from the senior chemistry class (ages 18–19). Before the application of the model, the students were not familiar with the term eutrophication. Two steps were involved in the application of the model in the classroom. First, the students read the continuous test and solved the test with the non-continuous text within 90 min. Subsequently, the obtained results of the test were analyzed and discussed. The students were divided in groups with the task to discuss the questions and decide on the correct answers within their group. After the representatives of each group presented their results and a general discussion within the whole class was organized and coordinated by the teacher.

The students' progress was evaluated by analysis of individual results and combined results of all (60) students. The success analysis realized for each of (six) question groups gave a progress report on the level of the students' chemical/environmental literacy.

RESULTS AND DISCUSSION

Assessment of the model applicability

In the first part of the test, an examination was performed on the chemistry knowledge of soaps, detergents and softeners (their chemical composition and action) acquired in regular classes. The achieved results (77.3–92.4 %) showed that the student had satisfactory knowledge that could help them in the search for an answer to the question: What substances could be a cause of the occurrence of eutrophication and why?

The next group of questions in the test was related to information items given in the continuous text about eutrophication. A multiple-choice task was used to check how much of this phenomenon was understood from the information read in the text. The achieved result (81.8 % of correct answers) showed a high understanding of the read text.

The term "nutrients", mentioned several times in the continuous text, masks polyphosphate softeners, the real cause of eutrophication. 74.2 % of students chose polyphosphate softener as nutrients. Incorrect responses (22.7 %) indicated that a certain number of students did not have a clear understanding of the difference between changes and outcomes of the described phenomenon (algae and bacteria, 7.6 and 10.6 %, respectively), potential cause (detergents, 4.5 %) and real cause (polyphosphate softeners).

One question, with seven statements (given in the form of alternative choice) required interpretation of scientific facts based on reaction equation, which describes the generation of algae bioplasm ($C_{106}H_{263}O_{110}N_{16}P$) through photosynthesis:[34]

$$106CO_2 + 16HNO_3 + H_3PO_4 + 122H_2O \xrightarrow{\text{Energy and microelements}} \rightarrow C_{106}H_{263}O_{110}N_{16}P + 138O_2$$

The percentage of correct responses was in the 63.6–84.8 % range. The cause (small concentration of phosphate, 1 mol H_3PO_4) which leads to abrupt development of algae (biomass increase), *i.e.*, that P is main limiting factor in control of algal growth in water, was perceived by 84.8 % of the pupils. The lowest result (63.6 %) was achieved for the question referring to the action of oxygen on algae decomposition.

Understanding of how science comes to discoveries was tested by four questions. Responses involved hypothesis formulation, proposal and testing the Method for solving the assumption and deduction. For the question "What makes Redfield's discovery of the algae formula critically important for finding out the real cause of eutrophication?" a high percentage (81.8 %) of the students deduced correctly how important the discovery of the elements C, H, N, O and P, necessary for algae formation was for the identification of a substance causing eutrophication. After the algae formula had been discovered, scientists perceived the problem and asked the question, "Why don't algae reproduce in unpolluted waters?" This question required the analysis of the offered assumptions and 87.9 % of the students chose the correct hypothesis. To the question, "After the proposed assumption, what would you do to find out the real cause of eutrophication?" 70.0 % of the students gave a correct proposal for the choice of method to be used for hypothesis testing. This figure should be supplemented by 6.1 % of the students who expanded the correct response by their proposals, such as "test the role of surplus of those elements in the laboratory, not in clean waters at all",

"decrease and increase the phosphorus concentration", "perform laboratory experiment with algae in the water with and without softeners". The task: "The results of an analysis of polluted and unpolluted waters indicated that eutrophication does not occur in unpolluted waters because…" had good responses (68.8 %).

Final testing of the understanding and application of the concept of eutrophication was realized through two tasks. Solving the the first question involved the listing of other sources of pollution (substances) which may lead to eutrophication, apart from detergents (Fig. 7). 51.5 % of students correctly listed substances that may be potential sources of phosphates (fertilizers and pesticides applied in agriculture, salts from factories wastewaters). Solving the second question depended equally on knowledge of chemistry and geography, and demanded relating them to pieces of information from the text; the solving success was slightly lower (45.0 %) in comparison to the first question.

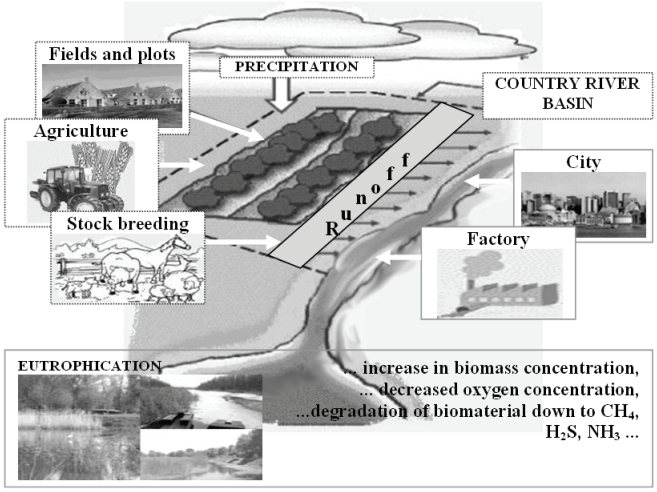

Fig. 7. Text of the Task 12: There are estimates that rivers annually bring to North Adriatic about 28,000 tons of phosphorus in phosphate form and a large part (about 90%) is anthropogenic (man is the cause). Look at Figure above and deduce what *substances* can be a potential source of phosphorus in waters?

The final question of the test required actual deduction of why danger of eutrophication was not entirely eliminated but only alleviated by replacing phosphates in washing powders with zeolites or polycarboxylates. That considerable amounts of phosphates run off with rain from the soil, where phosphate fertilizers were applied was confirmed by 83.3% of students. A slightly higher percentage (89.4 %) of students was familiar with the problem of non-filtering or insufficient filtering of large amounts of municipal wastewaters containing phosphates. A certain percentage (65.2 %) thought that the amount of phosphates once released

was permanently present in water due to the indestructibility of phosphates and the existence of their cycle in nature.

All the obtained results (Fig. 8, average achievement of 70.9±14.3 %) showed that the application of the model enabled:

– Understanding of an ecological problem, based on the scientific definition of the term eutrophication given in the continuous text (biological indicators of eutrophication, elements inducing or limiting eutrophication, their origin in water, other factors influencing eutrophication).

– Realization that the pollution of our environment may be directly related to modern life.

– Application of acquired knowledge of chemistry, to observe and understand the cause and effect of eutrophication in our environment and to draw a scientific conclusion (from a hypothesis to a conclusion).

– Understanding the importance of science and technology discoveries for solving ecological problems.

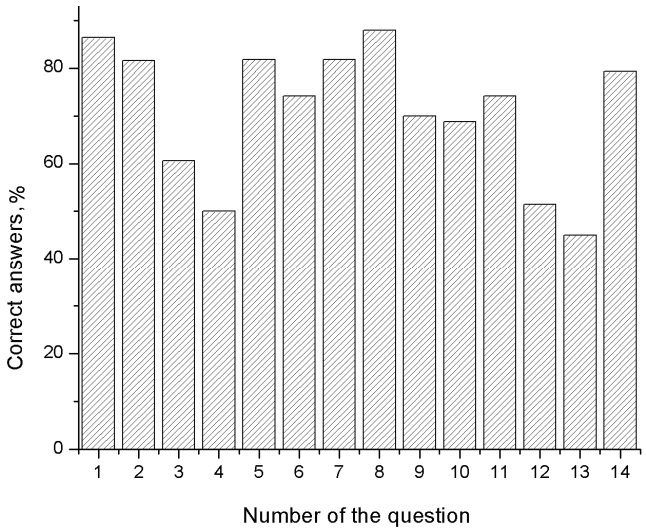

Fig. 8. Percent of correct answers obtained on the test with the non-continuous text.

Misconceptions that students had (*e.g.*, about the role of some elements in the eutrophication process) were corrected by the analysis of results obtained on the test, as was described in the section Application of the Model in the classroom. Such an approach resulted in an even better success rate of students and in their self-realization of the results achieved.

All the results indicated that the Model studied fulfilled its goal, that it inspired students to think about the ecological problem described and enabled them to use and apply their scientific knowledge during the recognition and discussion

of the problems from real life. It should be noted also that the model contributed to the rise of student's environmental literacy (ecological knowledge – knowledge and understanding of important concepts in ecology, principles of how the system works and its interaction with the environment of social systems; cognitive skills: the ability to analyze, synthesize and evaluate information on environmental issues).

Questionnaire

In addition, the importance of the quality of applied model was confirmed by a questionnaire. Some of the questions (Q) and answers (A) ae selected here.

Q: Was the continuous text on eutrophication interesting for you?

A: Very much (61 %), a lot (30 %), a little (8 %), no answer (1 %)

Q: Which characteristics of the text were the most important?

A: Story about real event; chemical explanation on the use of softeners and the history of washing machines; There is not much chemistry; it is obvious that science is not perfect; citations.

Q: How much did the questions in the test help you to understand the essence of the concept of eutrophication?

A: Very much (15 %), a lot (65 %), a little (5 %), not at all (2 %), no answers (12 %).

CONCLUSIONS

The general goals of environmental education are to deepen knowledge about environmental problems, to develop cognitive skills for research and to develop awareness and attitudes towards the environment (*i.e.*, environmental literacy). These goals are difficult to achieve only during regular class hours of several teaching subjects. In eco-schools, in which the program was adopted, the full achievement of the general objectives of environmental education also failed. These objectives could be attained by way of realistic, active class work oriented towards problem solving. Therefore, in this paper, a Model suitable for providing students with tools to identify ecological issues, to use existing knowledge of natural sciences in the consideration of an ecological problem and to explain phenomena scientifically was developed and applied. The didactic material "It Happened, What's the Problem?" made possible new knowledge of science to add to that existing. The test with non-continuous text "A Guide through the Problem" and the following discussion enabled the exercise of applying knowledge of chemistry, giving scientific explanations, generalizations, whereby understanding of the essence of the studied problem was realized. All the achieved results, over 70 % of correct responses, indicated that such a method of work had been accepted. With such an approach, environmental education has a chance to encourage action competence in pupils, which is the basis for the development different behaviors and attitudes.

Environmental education in practice is completely in the hands of individual teachers, its realization depends on how prepared they are to adopt their subjects to environmental education. The examined model could help the teachers in the preparation and realization of their classes. Considerations of the ecology contents provide great possibilities for classroom knowledge to become applicable in real life.

Acknowledgements. This paper was supported by the Ministry of Education, Science and Technological Development of the Republic of Serbia (Project No. 179048).

ИЗВОД

„ДЕСИЛО СЕ, У ЧЕМУ ЈЕ ПРОБЛЕМ?“ И „ВОДИЧ КРОЗ ПРОБЛЕМ“ – МОДЕЛ ЗА РАЗМАТРАЊЕ ЕКОЛОШКИХ ПРОБЛЕМА У НАСТАВИ ХЕМИЈЕ

ЈАСМИНКА Н. КОРОЛИЈА[1], СНЕЖАНА РАЈИЋ[2], МИЛЕНА ТОШИЋ[1] и ЉУБА М. МАНДИЋ[1]

[1]Хемијски факултет, Универзитет у Београду, Београд и [2]Гимназија Сш. Сава, Београд

У циљу побољшања способности примене знања из хемије (стечених у постојећем систему образовања) у реалном животу, развијен је модел који омогућава разматрање еколошких проблема. Састоји се од континуалног текста „Десило се, у чему је проблем?“ и теста са неконтинуалним текстом „Водич кроз проблем“, у којима је разматрана еутрофикација. Модел је примењен на часовима хемије у гимназији. Добијени резултати (средња вредност 70,9±14,3 %) показали су да је примена приказаног модела омогућила: разумевање еколошког проблема еутрофикације на основу научних одредница појма датих у континуираном тексту, сагледавање како загађење животне средине може бити директно последица модернизације свакодневног живота, примену стечених хемијских знања за сагледавање и разумевање узрока и последица еутрофикације у животној средини, и за долажење до закључка путевима како то ради наука, као и сагледавање значаја научно–технолошких открића за решавање еколошких проблема. Осим тога, примена модела доприноси развоју ученичке писмености о животној средини (еколошко знање и когнитивне способности), способности критичког мишљења, и обезбеђује да знање стечено у учионици буде применљиво у реалном животу.

(Примљено 22. маја, ревидирано 11. августа, прихваћено 9. септембра 2015)

REFERENCES

1. M. O. Martin, I. V. S. Mullis, E. J. Gonzales, S. J. Chrostowski, in *TIMSS 2003, International science report: Findings from IEA's Trends in International Mathematics and Science Study in the fourth and eighth grades*, Boston College, Chestnut Hill, MA, 2004
2. M. O. Martin, I. V. S. Mullis, P. Foy, in *TIMSS 2007 International science report: Findings from IEA's Trends in International Mathematics and Science Study in the fourth and eighth grades*, TIMSS & PIRLS International Study Center, Boston College, Chestnut Hill, MA, 2008
3. Organization for Economic Co-operation and Development (OECD-PISA), *Executive Summary PISA 2006: Science Competencies for Tomorrow's World / Pisa project*, http://www.pisa.oecd.org/ (last revised 2007)
4. Organization for Economic Co-operation and Development (OECD-PISA), *Assessment of scientific literacy in the OECD/Pisa project*, http://www.pisa.oecd.org/ (last revised 2005)

5. D. Šišović, in *TIMSS 2003 in Serbia*, R. Antonijevic, D. Janjetovic, Eds., Institute for pedagogical investigations, Belgrade, 2005, p. 215 (in Serbian)
6. D. Trivić, E. Lazarević, M. Bogdanović, in TIMSS 2007 in Serbia, S. Gasic-Pavisic, D. Stankovic, Eds., Institute for pedagogical investigations, Belgrade, 2011, p. 97 (in Serbian)
7. D. Pavlović-Babić, A. Baucal, *Support me, inspires me, PISA 2012 in Serbia: the first results*, Institute for psychology, Belgrade, 2013, p. 69
8. Y. Shwartz, R. Ben-Zvi, A. Hofstein, *Chem. Educ. Res. Pract.* **7** (2006) 203
9. W. Harlen, *Studies Sci. Educ.* **36** (2001) 79
10. P. J. Fensham, W. Harlen, *Int. J. Sci. Educ*. **21** (1999) 755
11. J. Holbrook, *Chem. Educ. Int.* **6** (2005) 1
12. J. Reguli, *Chem. Listy* **98**(4) (2004) 201
13. D. L. Zeadler, T. D. Sadler, M. L. Simmons, E. V. Howes, *Sci. Educ.* **89** (2005) 357
14. D. King, S. M. Ritchie, *Learning Science through Real-World Contexts*, in *Second International Handbook of Science Education,* B. J. Fraser, K. Tobin, C. J. McRobbie, Eds., Springer, New York, 2012, p. 69
15. S. Kegley, A. M. Stacy, M. K. Carroll, *Chem. Educ.* **1** (1996) 1
16. D. Krnel, S. Naglič, *Sci. Educ. Int.* **20** (2009) 5
17. T. Meagher, *Electron. J. Sci. Educ.* **13** (2009) 1
18. K. Kostova, E. Vladimirova, *Chemistry* **19** (2010) 50
19. M. Littledyke, *Environ. Educ. Res.* **14** (2008) 1
20. M. Erdogan, Z. Kostova, T. Marcinkowski, *Eurasia J. Math. Sci. Technol. Educ*. **5** (2009) 15
21. H. E. Chu, E. A. Lee, H. R. Ko, D. H. Shin, M. N. Lee, B. M. Min, K. H. Kang, *Int. J. Sci. Educ.* **29** (2007) 731
22. H. R. Hungerford, T. L. Volk, *J. Environ. Educ*. **21** (1990) 8
23. S. Stanisic, S. Maksic, *J. Environ. Educ.* **45** (2014) 118
24. F. Maulidya, A. Mudzakir, Y. Sanjaya, *Int. J. Sci. Res*. **3** (2014) 193
25. D. Chapman, K. Sharma, *Environmentalist* **21** (2001) 265
26. C. Wood, *Chem. Educ. Res. Pract.* **7** (2006) 96
27. G. M. Bodner, J. D. Herron, in *Chemical Education: Towards Research-Based Practice*, J. K. Gilbert, O. De Jong, R. Justi, D. F. Treagust, J. H. Van Driel, Eds., Kluwer Academic Publishers, Dordrecht, 2002, p. 235
28. A. H. Johnstone, *University Chem. Educ.* **5** (2001) 69
29. T. D. Sadler, D. L. Zeidler, *J. Res. Sci. Teaching* **46** (2009) 909
30. E. M. F. Ribeiro, J. de Oliveira, E. J. Wartha, *Quimica Nova Escola* **32** (2010) 169
31. L. B. Cahoon, J. R. Kucklick, R. H. Kiefer, J. D. Willey, *J. Elisha Mitchell Sci. Soc.* **109** (1993) 123
32. H. Simola, *Hydrobiologia* **106** (1983) 43
33. A. C. Redfield, B. H. Ketchum, F. A. Richards, in *The Sea*, Vol. 2., M. N. Hill, Ed., Wiley–Interscience, New York, 1963, p. 26
34. X. Yang, X. Wu, H. Hao, Z. He, *J. Zhejiang Univ. Sci., B* **9** (2008) 197.

Journal of the Serbian Chemical Society
JSCS@tmf.bg.ac.rs • www.shd.org.rs/JSCS
J. Serb. Chem. Soc. 80 (12) 1581–1591 (2015)

Contents of Volume 80

NUMBER 1

Biochemistry and Biotechnology

H. D. Yan, *H. C. Liu* and *Z. Wang*: Optimization of the fermentation conditions and substrate specifity of mycelium-bound ester hydrolases of *Aspergillus oryzae* Cs007 1

J. Wang, *W. Wu*, *X. Wang*, *M. Wang* and *F. Wu*: An effective GC method for the determination of the fatty acid composition in silkworm pupae oil using a two-step methylation process 9

M. Dodevska, *S. Šobajić* and *B. Djordjević*: Fibre and polyphenols of selected fruits, nuts and green leafy vegetables used in Serbian diet..... 21

Inorganic Chemistry

S. Saha, *D. Brahman* and *B. Sinha*: Cu(II) complexes of an ionic liquid-based Schiff base [1-{2-((2-hydroxybenzylidene)amino)ethyl}-3-methylimidazolium]PF_6: Synthesis, characterization and biological activities 35

A. Tavman and *C. Sayil*: Synthesis, crystal structure and properties of $[Co(L)_2](ClO_4)_2$ (L = 1,3-bis(1*H*-benzimidazol-2-yl)-2-oxapropane)..... 45

Theoretical Chemistry

Y. Jing and *X. Tan*: A theoretical study on the mechanism of the reaction between azacyclopropenylidene and oxirane 53

Physical Chemistry

Z. M. Marković, *J. R. Prekodravac*, *D. D. Tošić*, *I. D. Holclajtner-Antunović*, *M. S. Milosavljević*, *M. D. Dramićanin* and *B. M. Todorović-Marković*: Facile synthesis of water-soluble curcumin nanocrystals..... 63

Electrochemistry

M. V. Tomić, *M. M. Petrović*, *S. Stanković*, *S. I. Stevanović* and *J. B. Bajat*: Ternary Zn–Ni–Co alloy: anomalous codeposition and corrosion stability..... 73

Analytical Chemistry

N. Hui, *A. Liang*, *C. Xue* and *W. Sun*: Polarographic determination of DNA based on its interaction with the phenanthroline–zinc(II) complex 87

Polymers

B. Zeytuncu, *M. H. Morcali*, *S. Akman* and *O. Yucel*: Influence of the amount of poly-(vinyl alcohol) on the *in situ* production of photo-crosslinked thioamide functionalized nanofiber membranes 97

Materials

E. R. Ivanović, *N. D. Nikolić* and *V. R. Radmilović*: Randomly oriented twin domains in electrodeposited silver dendrites..... 107

Environmental

Y. S. Perng and *M. H. Bui*: The feasibility of *Cassia fistula* gum with polyaluminum chloride for the decolorization of reactive dyeing wastewater 115

NUMBER 2

Organic Chemistry

H.-T. Zhao, *S.-M. Zhong*, *J.-K. Qin* and *H. Tang*: Novel hybrids of oxoisoaporphine––tryptamine as inhibitors of acetylcholinesterase-induced β-amyloid aggregation with improved antioxidant properties 127

L. Maamria, *H. Haba*, *C. Lavaud*, *D. Harakat* and *M. Benkhaled*: An isoflavane and saponins from *Astragalus depressus* L. (Short communication) 137

Biochemistry and Biotechnology

S. Pantović, *D. Božović*, *G. Nikolić*, *M. Martinović*, *P. Mitrović*, *L. Radulović*, *A. Isaković* and *I. Marković*: Markers of inflammation and antioxidant enzyme activities in restenosis following percutaneous coronary intervention 143

D. Ćujić, *Ž. Bojić-Trbojević*, *N. Kolundžić*, *T. Kadoya* and *Lj. Vićovac*: Molecular forms of galectin-1 from human placenta and trophoblast cells 159

Y. Wang, *C. X. You*, *K. Yang*, *R. Chen*, *W. J. Zhang*, *Y. Wu*, *Z. L. Liu*, *S. S. Du* and *Z. W. Deng*: Chemical constituents and insecticidal activities of the essential oil from *Alpinia blepharocalyx* rhizomes against *Lasioderma serricorne* 171

Inorganic Chemistry

V. V. Divarova, *K. T. Stojnova*, *P. V. Racheva*, *V. D. Lekova* and *A. N. Dimitrov*: Liquid––liquid extraction of ion-association complexes of cobalt(II)–4-(2-pyridylazo)resorcinol with ditetrazolium salts 179

Theoretical Chemistry

Z. Mohajeri Avval, *E. Pourbasheer*, *M. R. Ganjali* and *P. Norouzi*: Application of genetic algorithm – multiple linear regressions to predict the activity of RSK inhibitors 187

Electrochemistry

V. M. Maksimović, *N. D. Nikolić*, *V. B. Kusigerski* and *J. L. Blanuša*: Ternary Zn–Ni–Co alloy: anomalous codeposition and corrosion stability 197

Analytical Chemistry

M. Krstić, *S. Ražić*, *D. Vasiljević*, *Đ. Spasojević* and *S. Ibrić*: Application of experimental design in the examination of the dissolution rate of carbamazepine from formulations. Characterization of the optimal formulation by DSC, TGA, FT-IR and PXRD analysis 209

Polymers

A. Janevski and *G. Bogoeva-Gaceva*: The influence of glass fibers on the morphology of β-nucleated isotactic polypropylene evaluated by differential scanning calorimetry 223

Materials

M. S. Djošić, *M. Mitrić* and *V. B. Mišković-Stanković*: The porosity and roughness of electrodeposited calcium phosphate coatings in simulated body fluid 237

Chemical Engineering

N. Anu, *S. Rangabhashiyam*, *A. Rahul* and *N. Selvaraju*: Evaluation of optimization methods for solving the receptor model for chemical mass balance 253

Environmental

N. Yang and *R. Wang*: Molecular sieve-supported ionic liquids as efficient adsorbents for CO_2 capture 265

Erratum 277

NUMBER 3

M. G. Rikalović, *M. M. Vrvić* and *I. M. Karadžić*: Rhamnolipid biosurfactant from *Pseudomonas aeruginosa* – from discovery to application in contemporary technology (Review) 279

Organic Chemistry

D. Ashok, *B. V. Lakshmi*, *S. Ravi* and *A. Ganesh*: Microwave-assisted synthesis of some new coumarin–pyrazoline hybrids and their antimicrobial activity 305

Biochemistry and Biotechnology

N. S. Radulović, *Z. Stojanović-Radić*, *P. Stojanović*, *N. Stojanović*, *V. Dekić* and *B. Dekić*: A small library of 4-(alkylamino)-3-nitrocoumarin derivatives with potent antimicrobial activity against gastrointestinal pathogens 315

Inorganic Chemistry

I. Djordjević, *S. Grubišić*, *M. Milčić* and *S. Niketić*: Derivation of a new set of force field parameters for ammine complexes of chromium(III) containing halogenido ligands: modeling of the *trans*-influence of halogenido ligands 329

Theoretical Chemistry

J.-B. Tong, *J. Chang*, *S.-L. Liu* and *M. Bai*: A quantitative structure–activity relationship (QSAR) study of peptide drugs based on a new descriptor of amino acids 343

Physical Chemistry

Y. Zaynali and *S. M. Alavi*: Higher propene yield by tailoring operating conditions of propane oxidative dehydrogenation over $V_2O_5/\gamma\text{-}Al_2O_3$ 355

Materials

L. Almásy, *D. Creanga*, *C. Nadejde*, *L. Rosta*, *E. Pomjakushina* and *M. Ursache-Oprisan*: Wet milling *versus* co-precipitation in magnetite ferrofluid preparation 367

Chemical Engineering

S. Nemoda, *M. Mladenović*, *M. Paprika*, *D. Dakić*, *A. Erić* and *M. Komatina*: Euler–Euler granular flow model of the combustion of liquid fuels in a fluidized reactor 377

Metallurgy

S. Stanković, *I. Morić*, *A. Pavić*, *S. Vojnović*, *B. Vasiljević* and *V. Cvetković*: Bioleaching of copper from samples of old flotation tailings (Copper Mine Bor, Serbia) 391

Environmental

A. Kőnig-Péter, *F. Kilár*, *A. Felinger* and *T. Pernyeszi*: Biosorption characteristics of *Spirulina* and *Chlorella* cells for the accumulation of heavy metals 407

L. J. Stamenković, *D. Z. Antanasijević*, *M. Đ. Ristić*, *A. A. Perić-Grujić* and *V. V. Pocajt*: Modeling of methane emissions using the artificial neural network approach 421

History of and Education in Chemistry

B. Tomašević and *D. Trivić*: Chemistry curricular knowledge of secondary school teachers 435

NUMBER 4

Organic Chemistry

H. Beyzaei, *R. Aryan* and *H. Moghadas*: Novel one-pot process for the synthesis of ethyl 2-imino-4-methyl-2,3-dihydrothiazole-5-carboxylates (Short communication) 453

H. Djahaniani, *L. Aghadadashi-Abhari* and B. M*ohtat*: *N*-Methylimidazole-mediated synthesis of aryl alkyl ethers under microwave irradiation and solvent free conditions (Short communication)..... 459

Biochemistry and Biotechnology

K. Sahayaraj, *P. Kombiah*, *A. K. Dikshit* and *J. M. Rathi*: Chemical constituents of the essential oils of *Tephrosia purpurea* and *Ipomoea carnea* and their repellent activity against *Odoiporus longicollis*..... 465

J. Šućur, *A. Popović*, *M. Petrović*, *G. Anačkov*, *V. Bursić*, *B. Kiprovski* and *D. Prvulović*: Allelopathic effects and insecticidal activity of aqueous extracts of *Satureja montana* L. 475

Inorganic Chemistry

L. Udrescu, *L. Sbârcea*, *A. Fuliaş*, *I. Ledeţi*, *T. Vlase*, *P. Barvinschi* and *L. Kurunczi*: Physicochemical characterization of zofenopril inclusion complex with 2-hydroxypropyl-β-cyclodextrin 485

Theoretical Chemistry

L. Jiao, *X. Wang*, *S. Bing*, *Z. Xue* and *H. Li*: QSPR study of supercooled liquid vapour pressures of polybrominated diphenyl ethers using the molecular distance–edge vector index..... 499

Physical Chemistry

S. Soltanpour and *Z. Bastami*: Thermodynamic solubility of piroxicam in propylene glycol + water mixtures at 298.2–323.2 K – data report and modeling 509

Analytical Chemistry

M. Voicescu and *S. Ionescu*: 3-Hydroxyflavone–bovine serum albumin interaction in dextran medium 517

Polymers

M. S. Nikolić, *N. Đorđević*, *J. Rogan* and *J. Đonlagić*: Influence of clay organic modifier on the morphology and performance of poly(ε-caprolactone)/clay nanocomposites .. 529

Environmental

I. Tomanović, *S. Belošević*, *A. Milićević* and *D. Tucaković*: Modeling of the reactions of a calcium-based sorbent with sulfur dioxide..... 549

S.-F. Li, *S.-C. Yang*, *S.-L. Zhao*, *P. Li* and *J.-H. Zhang*: Microwave and acid-modified talc for the adsorption of Methylene Blue in aqueous solution..... 563

Geochemistry

N. Đoković, *D. Mitrović*, *D. Životić*, *D. Španić*, *T. Troskot-Čorbić*, *O. Cvetković* and *K. Stojanović*: Preliminary organic geochemical study of lignite from the Smederevsko Pomoravlje field (Kostolac Basin, Serbia) – Reconstruction of geological evolution and potential for rational utilization..... 575

EuCheMS News

I. Leito, *W. Buchberger* and *P. Worsfold*: European Analytical Column No. 43 589

NUMBER 5

Organic Chemistry

N. Janković, *Z. Bugarčić* and *S. Marković*: Double catalytic effect of $(PhNH_3)_2CuCl_4$ in a novel, highly efficient synthesis of 2-oxo- and thioxo-1,2,3,4-tetrahydropyrimidines ... 595

O. Farsa, *Š. Sedláková*, *J. Podlipná* and *J. Maxa*: Aminopeptidase N inhibition could be involved in the anti-angiogenic effect of dobesilates ... 605

Biochemistry and Biotechnology

B. Rašković, *N. Babić*, *J. Korać* and *N. Polović*: Evidence of *β*-sheet structure induced kinetic stability of papain upon thermal and sodium dodecyl sulfate denaturation ... 613

N. Hacihasanoglu Cakmak and *R. Yanardag*: Edaravone, a free radical scavenger, protects liver against valproic acid induced toxicity ... 627

Inorganic Chemistry

R. Mehrotra, *S. N. Shukla* and *P. Gaur*: A study on tailor made ruthenium sulphoxide complexes: Synthesis, characterization and application ... 639

Theoretical Chemistry

B. G. Oliveira: Solvent effect on ternary complexes formed by oxirane and hydrofluoric acid ... 651

Physical Chemistry

T. Olariu, *V. Vlaia*, *C. Ciubotariu*, *D. Dragoş*, *D. Ciubotariu* and *M. Mracec*: Quantitative relationships for the prediction of the vapor pressure of some hydrocarbons from the van der Waals molecular surface ... 659

A. Simion, *C.-C. Huzum*, *I. Carlescu*, *G. Lisa*, *M. Balan* and *D. Scutaru*: Unsymmetrical banana-shaped liquid crystalline compounds derived from 2,7-dihydroxynaphthalene ... 673

Electrochemistry

S. Milošević, *I. Stojković*, *M. Mitrić* and *N. Cvjetićanin*: High performance of solvothermally prepared VO_2(B) as an anode for aqueous rechargeable lithium batteries ... 685

Thermodynamics

S. Hamidi and *A. Jouyban*: Solubility of atenolol in ethanol + water mixtures at various temperatures ... 695

Materials

M. Milošević, *A. Krkobabić*, *M. Radoičić*, *Z. Šaponjić*, *V. Lazić*, *M. Stoiljković* and *M. Radetić*: Antibacterial and UV protective properties of polyamide fabric impregnated with TiO_2/Ag nanoparticles ... 705

Environmental

J. A. Milovanović, *R. E. Stensrød*, *E. M. Myhrvold*, *R. Tschentscher*, *M. Stöcker, S. S. Lazarević* and *N. Z. Rajić*: Modification of natural clinoptilolite and ZSM-5 with different oxides and a study of the obtained products in lignin pyrolysis ... 717

NUMBER 6

Organic Chemistry

C. Ibis, *A. H. Shntaif*, *H. Bahar* and *S. S. Ayla*: An investigation of nucleophilic substitution reactions of 2,3-dichloro-1,4-naphthoquinone with various nucleophilic reagents ... 731

H. B. Lad, *R. R. Giri*, *Y. L. Chovatiya* and *D. I. Brahmbhatt*: Synthesis of modified pyridine and bipyridine substituted coumarins as potent antimicrobial agents s..... 739

Biochemistry and Biotechnology

K. Pavlović, *Lj. Grbović*, *B. Vasiljević*, *A. Župunski*, *M. Putnik-Delić*, *I. Maksimović* and *S. Kevrešan*: The influence of naphthenic acids and their fractions on cell membrane permeability (Short communication)..... 749

Inorganic Chemistry

B. Parveen, *I. H. Bukhari*, *S. Shahzadi*, *S. Ali*, *S. Hussain*, *K. Ghulam Ali* and *M. Shahid*: Synthesis and spectroscopic characterization of mononuclear/binuclear organotin(IV) complexes with 1*H*-1,2,4-triazole-3-thiol: Comparative studies of their antibacterial/antifungal potencies..... 755

Theoretical Chemistry

L. H. Mendoza-Huizar: Analysis of the chemical reactivity of aminocyclopyrachlor herbicide through the Fukui function..... 767

Physical Chemistry

A. Khorshidi, *B. Heidari* and *H. Inanlu*: Anisotropic silver nanoparticles deposited on zeolite A for selective Hg^{2+} colorimetric sensing and antibacterial studies..... 779

Electrochemistry

N. Keshtkar, *M. A. Taher* and *H. Beitollahi*: Voltammetric determination of carbidopa and folic acid using a modified carbon nanotubes paste electrode..... 789

M. Vujković: Comparison of lithium and sodium intercalation materials (Extended abstract)..... 801

Analytical Chemistry

Lj. Damjanović, *O. Marjanović*, *M. Marić Stojanović*, *V. Andrić* and *U. B. Mioč*: Spectroscopic investigation of two Serbian icons painted on canvas..... 805

Polymers

J. K. Milenković, *J. J. Hrenović*, *I. S. Goić-Barišić*, *M. D. Tomić* and *N. Z. Rajić*: Antibacterial activity of copper-containing clinoptilolite/PVC composites toward clinical isolate of *Acinetobacter baumannii*..... 819

Environmental

N. Grba, *F. Neubauer*, *A. Šajnović*, *K. Stojanović* and *B. Jovančićević*: Heavy metals in Neogene sedimentary rocks as a potential geogenic hazard for sediment, soil, and surface and groundwater contamination (eastern Posavina and the Lopare Basin, Bosnia and Herzegovina)..... 827

NUMBER 7

Organic Chemistry

N. Božinović, *I. Novaković*, *S. Kostić Rajačić*, *I. M. Opsenica* and *B. A. Šolaja*: Synthesis and antimicrobial activity of azepine and thiepine derivatives..... 839

Biochemistry and Biotechnology

J. Wang, *A. Gong*, *S. Gu*, *H. Cui* and *X. Wu*: Ultrafast synthesis of isoquercitrin by enzymatic hydrolysis of rutin in a continuous-flow microreactor..... 853

Inorganic Chemistry

Ž. K. Jaćimović, *M. Kosović*, *S. B. Novaković*, *G. Giester* and *A. Radović*: Synthesis and crystal structure of Cu(II) and Co(II) complexes with the 1,3-dimethylpyrazole-5--carboxylic acid ligand 867

Theoretical Chemistry

Lj. Andjelković, *M. Perić*, *M. Zlatar* and *M. Gruden-Pavlović*: Nucleus-independent chemical shift profiles along the intrinsic distortion path for Jahn–Teller active molecules. Study on the cyclopentadienyl radical and cobaltocene 877

Physical Chemistry

Z. Hou, *W. Zhu*, *H. Song*, *P. Chen* and *S. Yao*: The adsorption behavior and mechanistic investigation of Cr(VI) ions removal by poly(2-(dimethylamino)ethyl methacrylate)/poly(ethyleneimine) gels 889

Electrochemistry

D. Ž. Mijin, *V. D. Tomić* and *B. N. Grgur*: Electrochemical decolorization of the Reactive Orange 16 dye using a dimensionally stable Ti/PtO*x* anode 903

Polymers

H. Zeghioud, *S. Lamouri*, *Z. Safidine* and *M. Belbachir*: Chemical synthesis and characterization of highly soluble conducting polyaniline in mixtures of common solvents 917

Thermodynamics

J. M. Vuksanović, *I. R. Radović*, *S. P. Šerbanović* and *M. Lj. Kijevčanin*: Experimental study of the thermodynamic and transport properties of binary mixtures of poly(ethylene glycol) diacrylate and alcohols at different temperatures 933

Environmental

B. Majkić-Dursun, *A. Petković* and *M. Dimkić*: The effect of iron oxidation in the groundwater of the alluvial aquifer of the Velika Morava River, Serbia, on the clogging of water supply wells 947

Letters to the Editor

O. Nedić and *A. Dekanski*: A survey on publishing policies of the Journal of the Serbian Chemical Society – On the occasion of the 80th volume 959

NUMBER 8

Organic Chemistry

S. Z. Hejazi, *A. F. Shojaei*, *K. Tabatabaeian* and *F. Shirini*: Preparation and characterization of ZrO_2-supported Fe_3O_4-MNPs as an effective and reusable superparamagnetic catalyst for the Friedländer synthesis of quinoline derivatives 971

Biochemistry and Biotechnology

D. S. Milojković, *D. H. Anđelković*, *G. M. Kocić* and *T. D. Anđelković*: Evaluation of a method for phthalate extraction from milk related to the milk dilution ratio 983

Inorganic Chemistry

M. Dehestani and *L. Zeidabadinejad*: QTAIM investigation of a dipyrazol-1-ylmethane derivative and its Zn(II) complexes ($ZnLX_2$, X = Cl, Br or I) 997

Theoretical Chemistry

I. Gutman, *B. Furtula* and *X. Li*: Multicenter Wiener indices and their applications 1009

Physical Chemistry

P. Subramaniam and *N. Thamil Selvi*: Dynamics of cetyltrimethylammonium bromide-mediated reaction of phenylsulfinylacetic acid with Cr(VI): Treatment of pseudo-phase models 1019

Electrochemistry

K. Nikolić, *M. M. Aleksić*, *V. Kapetanović* and *D. Agbaba*: Voltammetric and theoretical studies of the electrochemical behavior of cephalosporins at a mercury electrode 1035

Analytical Chemistry

L. Liu, *M. Chen* and *X. Chen*: Analysis of alcohol dehydrogenase inhibitors from *Desmodium styracifolium* using centrifugal ultrafiltration coupled with HPLC–MS 1051

Polymers

C. Kizilkaya, *M. Bicen*, *S. Karatas* and *A. Gungor*: Structural effects of the monomer type on the properties of copolyimides and copolyimide–silica hybrid materials..... 1061

Thermodynamics

G. R. Ivaniš, *A. Ž. Tasić*, *I. R. Radović*, *B. D. Djordjević*, *S. P. Šerbanović* and *M. Lj. Kijevčanin*: An apparatus proposed for density measurements in compressed liquid regions at pressures of 0.1–60 MPa and temperatures of 288.15–413.15 K 1073

Environmental

T. Perunović, *K. Stojanović*, *M. Kašanin-Grubin*, *A. Šajnović*, *V. Simić*, *B. Jovančićević* and *I. Brčeski*: Geochemical investigation as a tool in the determination of the potential hazard for soil contamination (Kremna Basin, Serbia) 1087

NUMBER 9

Organic Chemistry

K. Gokula Krishnan, *R. Sivakumar* and *V. Thanikachalam*: Synthesis, structural characterization and antimicrobial evaluation of some novel piperidin-4-one oxime esters . 1101

Biochemistry and Biotechnology

L. T. Izrael Živković, *Lj. S. Živković*, *B. M. Jokić*, *A. B. Savić* and *I. M. Karadžić*: Adsorption of *Candida rugosa* lipase onto alumina: effect of surface charge 1113

M. N. Filimon, *S. O. Voia*, *D. L. Vladoiu*, *A. Isvoran* and *V. Ostafe*: Temperature dependent effect of difenoconazole on enzymatic activity from soil 1127

Theoretical Chemistry

M. Haghdadi, *H. Amani* and *N. Nab*: Theoretical study on the Diels–Alder reaction of bromo-substituted 2*H*-pyran-2-ones and some substituent vinyls..... 1139

Physical Chemistry

O. N. Kononova, *N. S. Karplyakova* and *E. V. Duba*: Sorption recovery of platinum(II,IV) in presence of copper(II) and zinc(II) from chloride solutions 1149

Analytical Chemistry

B. N. Olana, *S. A. Kitte* and *T. R. Soreta*: Electrochemical determination of ascorbic acid at *p*-phenylenediamine film–holes modified glassy carbon electrodes 1161

Polymers

P. Spasojević, *V. Panić*, *S. Šešlija*, *V. Nikolić*, *I. G. Popović* and *S. Veličković*: Poly(methyl methacrylate) denture base materials modified with ditetrahydrofurfuryl itaconate: Significant applicative properties 1177

Materials

S. S. Lazarević, *I. M. Janković-Častvan*, *B. M. Jokić*, *Dj. T. Janaćković* and *R. D. Petrović*: Sepiolite functionalized with *N*-[3-(trimethoxysilyl)propyl]ethylenediamine triacetic acid trisodium salt. Part I: Preparation and characterization 1193

Environmental

J. Milovanović, *S. Eich-Greatorex*, *T. Krogstad*, *V. Rakić* and *N. Rajić*: The use in grass production of clinoptilolite as an ammonia adsorbent and a nitrogen carrier..... 1203

Errata 1215

NUMBER 10

K. Đ. Popović and *J. D. Lović*: Formic acid oxidation at platinum–bismuth catalysts (Review)..... 1217

Organic Chemistry

S. M. Gomha, *I. M. Abbas*, *M. A. A. Elneairy*, *M. M. Elaasser* and *B. K. A. Mabrouk*: Antimicrobial and anticancer evaluation of a novel synthetic tetracyclic system obtained by Dimroth rearrangement 1251

G. M. Ziarani, *M. Rahimifard*, *F. Nouri* and *A. Badiei*: Green one-pot, four-component synthesis of spiro[indoline-3,4′-pyrano[2,3-*c*]pyrazole] derivatives using amino-functionalized nanoporous silica SBA-15 under solvent-free conditions..... 1265

P. A. Hadžić, *M. M. Popsavin* and *S. Z. Borozan*: Alkylating ability of carbohydrate oxetanes: Practical synthesis of bolaform skeleton derivatives..... 1273

Biochemistry and Biotechnology

B. Dojnov, *M. Grujić*, *B. Perčević* and *Z. Vujčić*: Enhancement of amylase production by *Aspergillus* sp. using carbohydrates mixtures from triticale 1279

Inorganic Chemistry

X.-Y. Wang, *Z.-Y. Zhao*, *Q. Han*, *M. Yu* and *D.-Y. Kong*: A new zinc(II) supramolecular square: synthesis, crystal structure, thermal behavior and luminescence..... 1289

Physical Chemistry

R. Hercigonja, *V. Rac*, *V. Rakić* and *A. Auroux*: Effect of transition metal cations on the commensurate freezing of *n*-hexane confined in micropores of ZSM-5 1297

Analytical Chemistry

R. Rezaee, *M. Qomi* and *F. Piroozi*: Hollow-fiber micro-extraction combined with HPLC for the determination of sitagliptin in urine samples..... 1311

Education in and Hystory of Chemistry

V. D. Milanovic, *D. D. Trivic* and *B. I. Tomasevic*: Secondary-school chemistry textbooks in the 19th century 1321

NUMBER 11

Organic Chemistry

D. M. Opsenica, *J. Radivojević*, *I. Z. Matić*, *T. Štajner*, *S. Knežević-Ušaj*, *O. Djurković-Djaković* and *B. A. Šolaja*: Tetraoxanes as inhibitors of apicomplexan parasites *Plasmodium falciparum* and *Toxoplasma gondii* growth and anti-cancer molecules.. 1339

D. Ashok, *S. Ravi*, *B. V. Lakshmi* and *A. Ganesh*: One-pot synthesis of carbazole based 3-hydroxy-4*H*-chromen-4-ones by a modified Algar–Flynn–Oyamada reaction and their antimicrobial activity 1361

Y.-W. Li and *S.-T. Li*: Facile synthesis and antifungal activity of dithiocarbamate derivatives bearing an amide moiety 1367

Biochemistry and Biotechnology

B. Dojnov, *M. Grujić* and *Z. Vujčić*: Highly efficient production of *Aspergillus niger* amylase cocktail by solid-state fermentation using triticale grains as a well-balanced substrate 1375

Inorganic Chemistry

D. Li, *G.-Q. Zhong* and *Z.-X. Wu*: Solid–solid synthesis, characterization and thermal decomposition of a homodinuclear cobalt(II) complex 1391

Theoretical Chemistry

M. Gruden, *S. Stepanović* and *M. Swart*: Spin state relaxation of iron complexes: The case for OPBE and S12g 1399

Physical Chemistry

C. Karunakaran, *S. Karuthapandian* and *P. Vinayagamoorthy*: Light-induced oxidative transformation of diphenylamine on ZrO_2. Synergism by ZnO and ZnS 1411

Thermodynamics

G. R. Ivaniš, *A. Ž. Tasić*, *I. R. Radović*, *B. D. Djordjević*, *S. P. Šerbanović* and *M. Lj. Kijevčanin*: Modeling of density and calculations of derived volumetric properties for *n*-hexane, toluene and dichloromethane at pressures 0.1–60 MPa and temperatures 288.15–413.15 K 1423

Polymers

H. Zeghioud, *S. Lamouri*, *Y. Mahmoud* and *T. Hadj-Ali*: Preparation and characterization of a new polyaniline salt with good conductivity and great solubility in dimethyl sulphoxide 1435

Materials

M. Jabbarzadeh and *A. R. Golkarian*: The influence of interlayer interactions on the mechanical properties of polymeric nanocomposites 1449

NUMBER 12

Organic Chemistry

L. I. Socea, *G. Saramet*, *C. Draghici*, *B. Socea*, *V. D. Constantin* and *M. A. Radu-Popescu*: Synthesis of new derivatives of hydrazinecarbothioamides and 1,2,4-triazoles, and an evaluation of their antimicrobial activities 1461

V. Alagarsamy, *V. Raja Solomon*, *G. Krishnamoorthy*, *M. T. Sulthana* and *B. Narendar*: Syntheses and antimicrobial activities of 1-(3-benzyl-4-oxo-3,4-dihydroquinazolin-2-yl)-4-(substituted) thiosemicarbazide derivatives 1471

V. Dobričić, *B. M. Francuski*, *V. Jaćević*, *M. V. Rodić*, *S. Vladimirov*, *O. Čudina* and *Dj. Francuski*: Synthesis, crystal structure and local anti-inflammatory activity of the L-phenylalanine methyl ester derivative of dexamethasone-derived cortienic acid (Short communication) 1481

Inorganic Chemistry

W. Śmiszek-Lindert, *A. Michta*, *A. Tyl*, *G. Małecki*, *E. Chełmecka* and *S. Maślanka*: X-Ray, Hirshfeld surface analysis, spectroscopic and DFT studies of polycyclic aromatic hydrocarbons: fluoranthene and acenaphthene..... 1489

Physical Chemistry

M. Momčilović, *J. Ciganović*, *D. Ranković*, *U. Jovanović*, *M. Stoiljković*, *J. Savović* and *M. Trtica*: Analytical capability of the plasma induced by IR TEA CO_2 laser pulses on copper-based alloys..... 1505

Electrochemistry

S. M. Miulović, *V. M. Nikolić*, *P. Z. Laušević*, *D. D. Aćimović*, *G. S. Tasić* and *M. P. Marčeta Kaninski*: Electrochemistry of cobalt ethylenediamine complexes at high pH.... 1515

Materials

T. B. Novaković, *Lj. S. Rožić*, *S. P. Petrović*, *Z. M. Vuković* and *M. N. Mitrić*: Study of the effect of Mg(II) addition and the annealing conditions on the structure of mesoporous aluminum oxide using Plackett–Burman design 1529

I. Dimić, *I. Cvijović-Alagić*, *N. Obradović*, *J. Petrović*, *S. Putić*, *M. Rakin* and *B. Bugarski*: *In vitro* biocompatibility assessment of Co–Cr–Mo dental cast alloy 1541

Environmental

S. Li, *S.-C. Yang*, *Y. Pan* and *J.-H. Zhang*: Preparation of aluminum–ferric–magnesium polysilicate and its application on oily sludge..... 1553

History of and Education in Chemistry

J. N. Korolija, *S. Rajić*, *M. Tošić* and *Lj. M. Mandić*: "It happened, what's the problem?" and "A guide through the problem" – A model for consideration of ecological issues in chemistry education..... 1567

Contents of Volume 80 1581

Author index 1593

Journal of the Serbian Chemical Society
JSCS-info@shd.org.rs • www.shd.org.rs/JSCS
J. Serb. Chem. Soc. 80 (12) 1593–1596 (2015)

Author Index

Abbas, M. I., 1251
Aćimović, D. D., 1515
Agbaba, D., 1035
Aghadadashi-Abhari, L., 459
Akman, S., 97
Alagarsamy, V., 1471
Alavi, M. S., 355
Aleksić, M. M., 1035
Ali, S., 755
Almásy, L., 367
Amani, H., 1139
Anačkov, G., 475
Anđelković, D. T., 983
Anđelković, H. D., 983
Andjelković, Lj., 877
Andrić, V., 805
Antanasijević, Z. D., 421
Anu, N., 253
Aryan, R., 453
Ashok, D., 305, 1361
Auroux, A., 1297
Ayla, S. S., 731

Babić, N., 613
Badiei, A., 1265
Bahar, H., 731
Bai, M., 343
Bajat, B. J., 73
Balan, M., 673
Barvinschi, P., 485
Bastami, Z., 509
Beitollahi, H., 789
Belbachir, M., 917
Belošević, S., 549
Benkhaled, M., 137
Beyzaei, H., 453
Bicen, M., 1061
Bing, S., 499
Blanuša, L. J., 197
Bogoeva-Gaceva, G., 223
Bojić-Trbojević, Ž., 159
Borozan, Z. S., 1273
Božinović, N., 839
Božović, D., 143
Brahman, D., 35
Brahmbhatt, I. D., 739
Brčeski, I., 1087
Buchberger, W., 589
Bugarčić, Z., 595
Bugarski, B., 1541
Bui, H. M., 115
Bukhari, H. I., 755
Bursić, V., 475

Carlescu, I., 673
Chang, J., 343
Chen, M., 1051
Chen, P., 889
Chen, R., 171
Chen, X., 1051
Chovatiya, L. Y., 739
Ciganović, J., 1505
Ciubotariu, C., 659
Ciubotariu, D., 659
Constantin, D. V., 1461
Creanga, D., 367
Cui, H., 853
Cvetković, O., 575
Cvetković, V., 391
Cvijović-Alagić, I., 1541
Cvjetićanin, N., 685
Čudina, O., 1481
Ćujić, D., 159

Dakić, D., 377
Damjanović, Lj., 805
Dehestani, M., 997
Dekanski, A., 959
Dekić, B., 315
Dekić, V., 315
Deng, W. Z., 171
Dikshit, K. A., 465
Dimić, I., 1541
Dimitrov, N. A., 179
Dimkić, M., 947
Divarova, V. V., 179
Djahaniani, H., 459
Djordjević, B., 21
Djordjević, D. B., 1073, 1423
Djordjević, I., 329
Djošić, S. M., 237
Djurković-Djaković, O., 1339
Dobričić, V., 1481
Dodevska, M., 21
Dojnov, B., 1279, 1375
Draghici, C., 1461
Dragoş, D., 659
Dramićanin, D. M., 63
Du, S. S., 171
Duba, V. E., 1149
Đoković, N., 575
Đonlagić, J., 529
Đorđević, N., 529

Eich-Greatorex, S., 1203
Elaasser, M. M., 1251
Elneairy, A. A. M., 1251
Erić, A., 377

Farsa, O., 605
Felinger, A., 407
Filimon, N. M., 1127
Francuski, Dj., 1481
Francuski, M. B., 1481
Fuliaş, A., 485
Furtula, B., 1009

Ganesh, A., 305, 1361
Ganjali, R. M., 187
Gaur, P., 639
Ghulam, Ali K., 755
Giester, G., 867
Giri, R. R., 739
Goić-Barišić, S. I., 819
Gokula Krishnan, K., 1101
Golkarian, A. R., 1449
Gomha, M. S., 1251
Gong, A., 853
Grba, N., 827
Grbović, Lj., 749
Grgur, N. B., 903
Grubišić, S., 329
Gruden, M., 1399
Gruden-Pavlović, M., 877
Grujić, M., 1279, 1375
Gu, S., 853
Gungor, A., 1061
Gutman, I., 1009

Haba, H., 137
Hacihasanoglu Cakmak, N., 627
Hadj-Ali, T., 1435
Hadžić, A. P., 1273
Haghdadi, M., 1139
Hamidi, S., 695
Han, Q., 1289
Harakat, D., 137
Heidari, B., 779
Hejazi, Z. S., 971
Hercigonja, R., 1297
Holclajtner-Antunović, D. I., 63
Hou, Z., 889
Hrenović, J. J., 819
Hui, N., 87
Hussain, S., 755
Huzum, C.-C., 673

Ibis, C., 731
Ibrić, S., 209
Inanlu, H., 779
Ionescu, S., 517
Isaković, A., 143
Isvoran, A., 1127
Ivaniš, R. G., 1073, 1423
Ivanović, R. E., 107
Izrael Živković, T. L., 1113

Jabbarzadeh, M., 1449
Jaćević, V., 1481
Jaćimović, K. Ž., 867

Janaćković, T. Dj., 1193
Janevski, A., 223
Janković, N., 595
Janković-Častvan, M. I., 1193
Jiao, L., 499
Jing, Y., 53
Jokić, M. B., 1113, 1193
Jouyban, A., 695
Jovančićević, B., 1087, 827
Jovanović, U., 1505

Kadoya, T., 159
Kapetanović, V., 1035
Karadžić, M. I., 1113, 279
Karatas, S., 1061
Karplyakova, S. N., 1149
Karunakaran, C., 1411
Karuthapandian, S., 1411
Kašanin-Grubin, M., 1087
Keshtkar, N., 789
Kevrešan, S., 749
Khorshidi, A., 779
Kijevčanin, Lj. M., 933, 1073, 1423
Kilár, F., 407
Kiprovski, B., 475
Kitte, A. S., 1061
Kizilkaya, C., 1061
Knežević-Ušaj, S., 1339
Kocić, M.G., 983
Kolundžić, N., 159
Komatina, M., 377
Kombiah, P., 465
Kong, D.-Y., 1289
Kőnig-Péter, A., 407
Kononova, N. O., 1149
Korać, J., 613
Korolija, N. J., 1567
Kosović, M., 867
Kostić Rajačić, S., 839
Krishnamoorthy, G., 1471
Krkobabić, A., 705
Krogstad, T., 1203
Krstić, M., 209
Kurunczi, L., 485
Kusigerski, B. V., 197

Lad, H. B., 739
Lakshmi, V. B., 305
Lamouri, S., 917, 1435
Laušević, Z. P., 1515
Lavaud, C., 137
Lazarević, S. S., 1193, 717
Lazić, V., 705
Ledeţi, I., 485
Leito, I., 589
Lekova, D. V., 179
Li, D., 1391
Li, H., 499
Li, P., 563
Li, S., 1553
Li, S.-F., 563
Li, S.-T., 1367
Li, X., 1009
Li, Y.-W., 1367
Liang, A., 87
Lisa, G., 673
Liu, H. C., 1
Liu, L. Z., 171
Liu, L., 1051
Liu, S.-L., 343
Lović, D. J., 1217

Maamria, L., 137
Mabrouk, A. K. B., 1251
Mahmoud, Y., 1435
Majkić-Dursun, B., 947
Maksimović, I., 749
Maksimović, V. M., 197
Mandić, M. Lj., 1567
Marčeta Kaninski, P. M., 1515
Marić Stojanović, M., 805
Marjanović, O., 805
Marković, I., 143
Marković, M. Z., 63
Marković, S., 595
Martinović, M., 143
Matić, Z. I., 1339
Maxa, J., 605
Mehrotra, R., 639
Mendoza-Huizar, H. L., 767
Mijin, Ž. D., 903
Milanovic, D. V., 1321
Milčić, M., 329
Milenković, K. J., 819
Milićević, A., 549
Milojković, S. D., 983

Milosavljević, S. M., 63
Milošević, M., 705
Milošević, S., 685
Milovanović, A. J., 717
Milovanović, J., 1203
Mioč, B. U., 805
Mišković-Stanković, B. V., 237
Mitrić, N. M., 237, 685, 1529
Mitrović, D., 575
Mitrović, P., 143
Miulović, M. S., 1515
Mladenović, M., 377
Moghadas, H., 453
Mohajeri Avval, Z., 187
Mohtat, B., 459
Momčilović, M., 1505
Morcali, H. M., 97
Morić, I., 391
Mracec, M., 659
Myhrvold, M. E., 717

Nab, N., 1139
Nadejde, C., 367
Narendar, B., 1471
Nedić, O., 959
Nemoda, S., 377
Neubauer, F., 827
Niketić, S., 329
Nikolić, D. N., 107, 197
Nikolić, G., 143
Nikolić, K., 1035
Nikolić, M. V., 1515
Nikolić, S. M., 529
Nikolić, V., 1177
Norouzi, P., 187
Nouri, F., 1265
Novaković, B. S., 867
Novaković, B. T., 1529
Novaković, I., 839

Obradović, N., 1541
Olana, N. B., 1061
Olariu, T., 659
Oliveira, G. B., 651
Opsenica, M. D, 1339
Opsenica, M. I., 839
Ostafe, V., 1127

Pan, Y., 1553
Panić, V., 1177
Pantović, S., 143
Paprika, M., 377
Parveen, B., 755
Pavić, A., 391
Pavlović, K., 749
Perčević, B., 1279
Perić, M., 877
Perić-Grujić, A. A., 421
Perng, S. Y., 115
Pernyeszi, T., 407
Perunović, T., 1087
Petković, A., 947
Petrović, D. R., 1193
Petrović, J., 1541
Petrović, M. M., 73
Petrović, M., 475
Petrović, P. S., 1529
Piroozi, F., 1311
Pocajt, V. V., 421
Podlipná, J., 605
Polović, N., 613
Pomjakushina, E., 367
Popović, Đ. K., 1217
Popović, A., 475
Popović, G. I., 1177
Popsavin, M. M., 1273
Pourbasheer, E., 187
Prekodravac, R. J., 63
Prvulović, D., 475
Putić, S., 1541
Putnik-Delić, M., 749

Qin, J.-K., 127
Qomi, M., 1311

Rac, V., 1297
Racheva, V. P., 179
Radetić, M., 705
Radivojević, J., 1339
Radmilović, R. V., 107
Radoičić, M., 705
Radović, A., 867
Radović, R. I., 933, 1073, 1423
Radulović, L., 143
Radulović, S. N., 315
Radu-Popescu, A. M., 1461

Rahimifard, M., 1265
Rahul, A., 253
Rajić, N., 1203
Rajić, S., 1567
Rajić, Z. N., 717, 819
Rakić, V., 1203, 1297
Rakin, M., 1541
Rangabhashiyam, S., 253
Ranković, D., 1505
Rašković, B., 613
Rathi, M. J., 465
Ravi, S., 305, 1361
Ražić, S., 209
Rezaee, R., 1311
Rikalović, G. M., 279
Ristić, Đ. M., 421
Rodić, V. M., 1481
Rogan, J., 529
Rosta, L., 367
Rožić, S. Lj., 1529

Safidine, Z., 917
Saha, S., 35
Sahayaraj, K., 465
Saramet, G., 1461
Savić, B. A., 1113
Savović, J., 1505
Sayil, C., 45
Sbârcea, L., 485
Scutaru, D., 673
Sedláková, Š., 605
Selvaraju, N., 253
Shahid, M., 755
Shahzadi, S., 755
Shirini, F., 971
Shntaif, H. A., 731
Shojaei, F. A., 971
Shukla, N. S., 639
Simić, V., 1087
Simion, A., 673
Sinha, B., 35
Sivakumar, R., 1101
Socea, B., 1461
Socea, I. L., 1461
Solomon, V.R., 1339
Soltanpour, S., 509
Song, H., 889
Soreta, R. T., 1061
Spasojević, Đ., 209
Spasojević, P., 1177
Stamenković, J. L., 421
Stanković, S., 391, 73
Stensrød, E. R., 717
Stepanović, S., 1399
Stevanović, I. S., 73
Stöcker, M., 717
Stoiljković, M., 705, 1505
Stojanović, K., 1087, 575, 827
Stojanović, N., 315
Stojanović, P., 315
Stojanović-Radić, Z., 315
Stojković, I., 685
Stojnova, T. K., 179
Subramaniam, P., 1019
Sulthana, M. T., 1471
Sun, W., 87
Swart, M., 1399
Šajnović, A., 1087, 827
Šaponjić, Z., 705
Šerbanović, P. S., 933, 1073, 1423
Šešlija, S., 1177
Šobajić, S., 21
Šolaja, A. B., 839, 1339
Španić, D., 575
Štajner, T., 1339
Šućur, J., 475

Tabatabaeian, K., 971
Taher, A. M., 789
Tan, X., 53
Tang, H., 127
Tasić, S. G., 1515
Tasić, Ž. A., 1073, 1423
Tavman, A., 45
Thamil Selvi, N., 1019
Thanikachalam, V., 1101
Todorović-Marković, M. B., 63
Tomanović, I., 549
Tomašević, B., 435, 1321
Tomić, D. M., 819
Tomić, D. V., 903
Tomić, V. M., 73
Tong, J.-B., 343
Tošić, D. D., 63
Tošić, M., 1567
Trivić, D., 435, 1321

Troskot-Čorbić, T., 575
Trtica, M., 1505
Tschentscher, R., 717
Tucaković, D., 549

Udrescu, L., 485
Ursache-Oprisan, M., 367

Vasiljević, B., 391, 749
Vasiljević, D., 209
Veličković, S., 1177
Vićovac, Lj., 159
Vijaya Lakshmi, B., 1361
Vinayagamoorthy, P., 1411
Vladimirov, S., 1481
Vladoiu, L. D, 1127
Vlaia, V., 659
Vlase, T., 485
Voia, O. S., 1127
Voicescu, M., 517
Vojnović, S., 391
Vrvić, M. M., 279
Vujčić, Z., 1279, 140
Vujković, M., 801
Vuković, M. Z., 1529
Vuksanović, M. J., 933

Wang, J., 9, 853
Wang, M., 9
Wang, R., 265
Wang, X., 499
Wang, X., 9
Wang, X.-Y., 1289
Wang, Y., 171
Wang, Z., 1
Worsfold, P., 589
Wu, F., 9
Wu, W., 9
Wu, X., 853
Wu, Y., 171
Wu, Z.-X., 1391

Xue, C., 87
Xue, Z., 499

Yan, H. D., 1
Yanardag, R., 627
Yang, S.-C., 1553
Yang, K., 171
Yang, N., 265
Yang, S.-C., 563
Yao, S., 889
You, X. Z., 171
Yu, M., 1289
Yucel, O., 97

Zaynali, Y., 355
Zeghioud, H., 917, 1435
Zeidabadinejad, L., 997
Zeytuncu, B., 97
Zhang, J. W., 171
Zhang, J.-H., 563, 1553
Zhao, H.-T., 127
Zhao, S.-L., 563
Zhao, Z.-Y., 1289
Zhong, G.-Q., 1391
Zhong, S.-M., 127
Zhu, W., 889
Ziarani, M. G., 1265
Zlatar, M., 877
Živković, S. Lj., 1113
Životić, D., 575
Župunski, A., 749

Subject Index of Vol. **80** and List of Referees in 2015 are given in the electronic form at the Internet address of the Journal of the Serbian Chemical Society: http://www.shd.org.rs/JSCS/Vol80/No12.html

End of Volume 80.

Journal of the Serbian Chemical Society
JSCS-info@shd.org.rs • www.shd.org.rs/JSCS
Volume *80* (2015)

Subject index

1-(2-aminoethyl)-3-methylimidazolium hexafluorophosphate, 35
1,2,4-triazol-3-thiole, 1461
1,4-naphthoquinone, 731
17β-carboxamide steroids, 1481
1*H*-1,2,4-triazole-3-thiol, 755
2-(9-ethyl-9*H*-carbazol-3-yl)-3-hydroxy--4*H*-chromen-4-ones, 1361
2-(dimethylamino)ethyl methacrylate, 889
2,5-dihydroxybenzenesulfonic acid salt, 605
2,7-dihydroxynaphthalene, 673
2,7-naphthalenediol, 673
2-aminopyridine, 639
2-hydroxynicotinate, 1289
3-hydroxyflavone–bovine serum albumin, 517
4-(alkylamino)coumarins, 315
absorption, 1177
acenaphthene, spectroscopic studies of, 1489
acetylcholinesterase inhibitor, 127
acetylcholinesterase, 127
acidification, 563
Acinetobacter baumannii, 819
activated carbon, 407
acylhydrazinecarbothioamide, 1461
AdSDPV, 1035
adsorbent, 1203
adsorption capacity, 265
adsorption, 563, 899, 1113, 1297
AFM, 73
AGOA, 651
alcohol dehydrogenase, 1051
alcohols, 933
aldehydes, 595
algae, 407
aliphatic polyester, 529
alkylation, 1273
allelochemicals, 475
alloy, 1217
Alpinia blepharocalyx, 171
alumina, 1113
aluminum-ferric-magnesium polysilicate, 1553
Alzheimer's disease, 127
amide moiety, 1367
amine, 731
amino acids, 343, 819
aminocyclopyrachlor, 767
amino-functionalized silica, 1265
aminopeptidase N, 605
ammonia, 1203
annual work plan, 435
anode materials, 685
anode, 903
anti-angiogenic effect, 605
antibacterial activity, 705, 819, 839, 1471
antibacterial potency, 755
antibacterial studies, 779
antibacterial, 639
anticancer, 1251
antidiabetic drug, 1311
antifungal activity, 839, 1367
antifungal agents, 1367
antifungal potency, 755

antiinflammatory activity, 1481
antimalarials, 1339
antimicrobial activity, 305, 315, 739, 1361, 1461
antimicrobial study, 755
antimicrobial, 1101, 1251
antioxidant activity, 21, 143
antioxidant, 127, 475
antiparasitic, 1339
antitubercular activity, 1471
application, 279
aqueous extracts, 475
aqueous rechargeable lithium batteries, 685
aromadendrin, 1051
aromatic acid, 1101
aromaticity, 877
artificial neural network, 499
ascorbic acid, 1161
ASOG–VISCO parameters, 933
Aspergillus niger, 1375
Aspergillus oryzae, 1
Aspergillus sp., 1279
Astragalus depressus, 137
asymmetric bent-core, 673
atenolol, 695
atomic force microscopy, 63
ATR-FTIR, 485
azacyclopropenylidene, 53
azepines, 839
azo dye, 903
Aβ anti-aggregating activity, 127
backpropagation neural network, 421
binary mixtures, 933
biocatalysis, 853
biocompatibility, 1541
biodegradable, 529
bioleaching, 391
biological activity, 35, 1481
biological sample, 1311
biomarkers, 575
biomaterials, 1541
bio-oil, 717
biopesticides, 475
biosorption, 407
biosurfactant, 279
bipyridines, 739
bis-benzimidazole, 45
bismuth, 1217
bolaform skeleton, 1273
bond critical point, 997
Bor, 391
bromo-2*H*-pyran-2-ones, 1139
broth dilution method, 739
brushite, 237
calcium phosphate, 237
camphor, 171
cancer, 1339
Candida albicans, 315
Candida rugose, 1113
canvas, 805
carbazole, 1361
carbidopa, 789
carbon dioxide, 265
carbon nanotubes, 789
carboxylesterase, 1
carcinogenesis, 605
carrier, 1203
Cassia fistula, 115
catalase, 143
catalysts, 717
cations, 1297
CD13 activity, 605
cell membranes permeability, 749
centrifugal ultrafiltration, 1051
cephalosporins, 1035
cetyltrimethylammonium bromide, 1019
chalcones, 305
charge transfer, 997
chelates, 179
chemical mass balance, 253
chemical shift, 877
chemistry knowledge, 1567
chemistry teaching, 435, 1321
chemistry textbook, 1321
chloride solutions, 1149
chromatography, 1311
chromium(VI), 899, 1019
chromium(III) complexes, 329
cigarette beetle, 171
clay, 529
clinical isolate, 819
clinoptilolite, 717, 819, 1203
coagulation, 115, 1553
coatings, 237
cobalt complex, 1515

cobalt(II) complex, 179, 1391
cobalt(II) perchlorate, 45
cobalt, 197
cobalth-based alloy, 1541
colorimetric sensing, 779
combustion, 377
composites, 223
compressed liquid, 1073
computational electrochemistry, 1035
computational fluid dynamics model, 377
conducting polymer, 917, 1435
confinement media, 1297
conformation, 1101
consistent force field, 329
contact toxicity, 171
contamination, 827
continuous flow, 853
copolyamic acid, 1061
copper(II) complexes, 35
copper, 391, 819, 1149
copper-based alloys, 1505
co-precipitation, 367
coronary restenosis, 143
corrosion, 73
cortienic acid, 1481
coumarin, 305, 739
crystal structure, 867, 1289, 1391
crystallization, 223
CTAB micellar effect, 1019
curcumin nanocrystals, 63
curricular components, 435
curricular knowledge, 435
CV, 1035
cyclocondensation, 453
cytotoxicity, 1541**,** 1339
decolorization, 903
decomposition, 1391
dehydrogenase, 1127
denaturation, 613
dendrite, 107
density functional theory calculations, 595, 877, 1035, 1139, 1399, 1489
density, 933, 1073
dental cast alloy, 1541
dental, 1177
denture, 1177
Desmodium styracifolium, 1051
desulfurization, 549
dextran 70, 517
dialkyl acetylenedicarboxylate, 459
diatomite, 209
diazonium, 1161
dibenzo[*a*,*d*][7]annulene, 1461
dichloromethane, 1073
dichloromethane, 1423
Diels–Alder reaction, 1139
diet, 21
difenoconazole, 1127
dilution, 983
dimethyl sulfoxide, 1435
Dimroth rearrangement. 1251
dinuclear, 639
diphenylamine, 1411
dipyrazol-1-ylmethane, 997
discharge capacity, 685
ditetrazolium salts, 179
dithiocarbamate derivatives, 1367
dithiocarboxylate, 755
DNA, 87
dobesilates, 605
drug analysis, 1311
DSC, 209, 223
Dubinin–Radushkevich, 407
dye removal, 115
ear edema, 1481
eastern Posavina, 827
EC-SOD, 143
edaravone, 627
education, 1567
EDXRF, 805
EIS, 73
elastic modules, 1449
electric conductivity, 685
electrochemical impedance spectroscopy, 685
electrochemistry, 903, 1161, 1515
electrodeposition, 73, 107, 197, 237
electrolysis, 903
electrospinning, 97
elevated temperature, 1073
entropy, 1297
environmental education, 1567
environmental literacy, 1567
enzymatic activity, 1127
enzymatic hydrolysis, 853
enzyme production, 1279, 1375

enzyme, 143
ESI, 137
ESIPT, 517
essential oil, 171, 465
ester hydrolase, 1
ethanol, 695
ethylenediamine, 1515
eucalyptol, 171
Euchems news, 589
eutrophication, 1567
evaluation, 959
extraction efficiency, 983
extraction equilibria, 179
Fabaceae, 137
fatty acid methyl ester, 9
fatty acid, 9
feed composition, 355
fermentation, 1
ferrofluid, 367
fibroblasts, 1541
flavones, 517
flocculants, 1553
flotation tailings, 391
flue gas, 549
fluidized bed, 377
fluoranthene, spectroscopic studies of, 1489
fluorescence spectroscopy, 517
folic acid, 789
formic acid, 1217
formononetin, 1051
four components, 1265
fractions of fibre, 21
free radicals, 627
freezing, 1297
Freundlich isotherm, 1203
Friedländer reaction, 971
fruits, 21
FT-IR spectroscopy, 613, 805
FT-IR, 209
fuel cell anode catalysts, 1217
fuel cell, 1217
Fukui, 767
fumigant toxicity, 171
functionalization, 1193
functionalization, 1449
fungi, 1279, 1375
fungicide, 1127
galectin-1, 159
gas chromatography, 9
gas chromatography-mass spectrometry, 983
gauche interaction, 1101
gels, 889
general regression neural network, 421
genetic algorithms, 187, 253
geo-accumulation index, 827
geochemical study, 575
geochemistry, 1087
geogenic hazard, 827
glass fibers, 223
glassy carbon electrode, 1161
glucoamylase, 1279, 1375
gold nanoparticles, 1161
graphene sheet, 1449
green leafy vegetables, 21
green procedure, 971
green synthesis, 1265
groundwater over-exploitations, 947
groundwater, 827
Hammett correlation, 1019
heavy metals, 407, 827, 1087
hepatic enzymes, 727
hepatotoxicity, 627
herbicide, 767
hesperidinase, 853
heterocycles, 595, 839
heterogeneous catalyst, 971
hexadecanoic acid, 465
high angle annular dark field microscopy, 107
high pressure, 1073, 1423
Hirshfeld surface analysis, 1489
hollow-fiber micro-extraction, 1311
homobimetallic complex, 755
homodinuclear, 1391
homogeneous catalysis, 595
HPLC, 1311
HPLC–MS, 1051
hs-CRP, 143
hybrid materials, 1061
hydrazides, 453
hydrazines, 453
hydrazones, 1251
hydrocarbons, 659
hydrofluoric acid, 651

hydrogen bonds, 651
hydrophobic nature, 1061
hydroxyapatite, 237
hypochlorite, 903
hypochlorous acid, 903
icons, 805
illumination, 1411
imidization, 1061
immobilization, 1113
in vitro, 1541
inclusion complex,485
indolylquinones, 731
inflammation, 143
inhibition, 605
inorganic compound, 1061
inorganic polymer, 1553
insecticidal activity, 171, 475
interaction, 87
intercalation, 801
interlayer interactions, 1449
ion exchange, 1149
ion-association complexes, 179
ionic liquid, 35, 265
Ipomoea carnea, 465
IR spectra, 367
IR, 755
iron encrustations, 947
iron(II) complex, 1399
iron(III) complex, 1399
iron, 947
isobaric thermal expansivity, 1423
isoflavane, 137
isoquercitrin, 853
isotherm, 407
isothermal compressibility, 1423
itaconic acid, 917, 1435
itaconic, 1177
Italian ryegrass, 1203
Jahn–Teller, 877
Job's plot, 485
Jouyban–Acree model, 695
kerosene suspensions, 367
kinetic stability, 613
kinetics, 407
Kostolac Basin, 575
Kremna Basin, 1087
Krohnke reaction, 739
Lake Robule, 391
Langmuir, 407
Lasioderma serricorne, 171
layered silicate, 529
lesson plan, 435
LIBS, 1505
light-induced, 1411
lignin, 717
lignites, 575
lime, 549
linear sweep voltammetry, 87
lipase, 1, 1113
liquid crystals, 673
lithium, 801
Lopare Basin, 827
Lp(a), 143
luminescence, 1289
magnesium, 1553
magnesium-doped alumina, 1515
magnetic properties, 197
magnetite nanoparticles, 367
magnetometry, 367
maltose, 1279
manure, 1203
mass spectra, 755
MD – molecular descriptor, 659
mechanistic investigation, 899
mercury electrode, 1035
mercury, 779
mesoporous, 1515
metal clusters, 1217
metal-ion aqueous batteries, 801
metallocene, 877
methane emission, 421
methods, 279
methyl methacrylate, 1177
methylation, 9
Methylene Blue, 563
Michael addition, 305
microcalorimetry, 1297
micropores, 1297
micro-Raman spectroscopy, 805
microreactor, 853
microwave irradiation, 305
microwave, 563
microwave-assisted reaction, 459
milk, 983
mixed anhydride, 1101
mixed solvent, 695

model, 549
modeling, 509
modification, 717
modified Algar–Flynn–Oyamada reaction, 1361
modified electrodes, 789
molecular distance–edge vector index, 499
molecular form, 159
molecular graph, 1009
molecular sieve, 265
monomer, 1061
Monte Carlo method, 659
monthly work plan, 435
morphology, 197, 223, 529
MP2 method, 53
MP2, 767
multicenter Wiener index, 1009
multicomponent reactions, 595
multidrug resistance, 819
multiple linear regression, 187, 421
multivariate statistical analysis, 315
N-[3-(trimethoxysilyl)propyl]ethylene-diamine triacetic acid, 1193
nanocomposites, 1449
nanofiber membrane, 97
nanofiber, 97
nanoparticles, 705, 779
nanoporous silica, 1265
nanostructures, 237
naphthenic acid fractions, 749
naphthenic acids, 749
national emission, 421
natural coagulant, 115
natural zeolite, 717, 819
neovascularization, 605
neusilin, 209
n-hexane, 1073, 1297, 1423
N-methylimidazole, 459
NMR, 137, 755
non-conventional fuel, 377
nucleophilic substitution, 731
nuts, 21
O-alkylation, 459
Odoiporus longicollis, 465
oily sludge, 1553
olive oil, 1
one-pot, 1361
one-pot reaction, 453
one-pot synthesis, 1265
OPBE, 1399
organic matter, 5757
organic modifier, 529
organotin chloride, 755
organotin(IV) complexes, 755
orientation imaging microscopy, 107
oxapropane, 45
oxetane ring, 1273
oxidation, 947, 1217
oxidative cyclizations, 1251
oxidative transformation, 1411
oxides, 717
oxirane, 53, 651
oxLDL, 143
oxoisoaporphine–tryptamine, 127
palaeo-reconstruction, 575
palladium, 839
PANI, 917, 1435
papain, 613
partial atomic charges, 329
partial least square, 343
particle, 549
PBDEs, 499
PCM, 651, 767
peer review, 959
pendulone, 137
peptide drugs, 343
peptide, 343
permeation, 1061
peroxides, 1339
pH, 1515
phenanthroline, 87
phenol, 717
phenylsulfinylacetic acid, 1019
phosphatase, 1127
photocatalysis, 1411
photo-curable, 97
photoluminescence spectroscopy, 63
photooxidation, 1411
photoreduction, 705
phthalate esters, 983
physicochemical characterization, 485
physiological activity, 749
pigments, 805
piperidin-4-one oxime, 1101
piroxicam, 509

Piszkiewicz cooperative model, 1019
placenta, 159
Plackett-Burman design, 1529
plasma, 1505
Plasmodium falciparum, 1339
platinum, 1149, 1217
p-nitrophenyl esters,
polarography, 87
pollution, 827, 1087
poloxamer, 209
poly(ethylene glycol) diacrylate, 933
poly(vinyl alcohol), 97
poly(vinyl chloride), 819
polyaluminum chloride, 115
polyamide, 705
polyaniline, 917
polybrominated diphenyl ethers, 499
polyethyleneimine, 899
polymer, 819, 1553
polymerization, 899, 917
polymorphous transition, 209
polypropylene, 223
porosity, 237
powder, 197
p-phenyldiamine, 1161
pre-concentration, 1311
production, 279
propane to oxygen ratio, 355
propane oxidative dehydrogenation, 355
propylene glycol, 509
protease, 1127
proteins, 517
Pseudomonas aeruginosa, 279
pseudo-phase models, 1019
publishing, 959
pulses, 1505
PXRD, 209, 485
pyranopyrazole, 1265
pyrazole-based ligand, 867
pyrazolines, 305
pyridine-2,6-dicarboxylic acid, 1391
pyrolysis, 717
QSAR, 187, 343, 499, 659, 1035
QTAIM, 997
questionnaire, 959
quinazolinone, 1471
quinoline derivatives, 971
radical, 877
Raman spectroscopy, 63
rat, 627
raw starch, 1375
reaction mechanism, 53, 1139, 1251
reactive black 5, 115
reactive blue 19, 115
reactive dye, 903
Reactive Orange 16, 903
reactivity indices, 1139
reactivity, 767
receptor model, 253
redox front formation, 947
refractive index, 933
regioselectivity, 1139
repellent activity, 465
reusable catalyst, 971
rhamnolipids, 279
rhodamine B, 779
ring opening, 1273
river sediments, 827
room temperature, 1391
roughness, 237
RSK inhibitors, 187
ruthenium sulphoxide complexes, 639
ruthenium, 639
rutin, 853
S12g, 1399
salicylaldehyde, 35
Salmonella enterica, 315
saponins, 137
SAPT, 997
Satureja montana L., 475
SBA-15, 1265
scanning electron microscopy, 107, 197
scavenger, 627
Schiff base, 35
SDS resistance, 613
secondary school, 1321
secondary structure, 613
sedimentary rocks, 827
sediments, 1087
SELDI-TOF MS, 159
semi-coordination, 45
sensor, 779
sepiolite, 1193
silkworm pupae oil, 9
silver, 107, 705, 779
simulated body fluid, 237

simulation, 695
single crystal XRD, 1101
sitagliptin, 1311
skeletal vibrations, 329
sodium, 801
soil, 827,1087, 1127, 1203
sol–gel, 1061, 1515
solid surfactant drug delivery systems, 209
solid–solid reaction, 1391
solid-state fermentation, 1375
solubility properties, 917
solubility, 485, 509, 695, 1435
solution casting, 529
solvent effect, 651
solvent extraction, 179
solvent-free, 1265
solvothermal, 685
sorbent, 549
source contribution, 253
source profiles, 253
spacer, 639
spectrophotometry, 179
spectroscopy, 45
spin state relaxation, 1399
spin states, 1399
spiro indole, 1265
starch, 1279
statistical design, 1515
Steiner distance, 1009
Steiner–Wiener index, 1009
stereoselectivity, 1139
steroids, 1481
storage capacity, 801
structural mechanics, 1449
sub-band gap illumination, 1411
sulfur dioxide, 549
sulphonation, 1435
sulphoxide, 639
supercooled liquid, 499
superparamagnetic catalyst, 971
supramolecular square, 1289
surface charge, 1113
SVWGM, 343
synergism, 1411
synthesis, 1367
talcum powder, 563
TEA CO_2 laser, 1505
TEM, 367
tensile, 1177
Tephrosia purpurea, 465
ternary alloy coatings, 73
ternary complexes, 651
tetrahydropyrimidines, 595
tetraoxanes, 1339
textbook quality, 1321
textbooks, 1321
TGA, 209
theoretical study, 53, 1035
thermal analysis, 485, 1391
thermal inactivation, 613
thermodynamic, 509, 933
thiazole derivatives, 453
thienopyridines, 1251
thiepines, 839
thioamide, 97
thiocyanation, 453
thioethers, 731
thiosemicarbazide, 1471
three-component reaction, 453, 459
titanium dioxide, 705
titanium, 237
toluene, 1073, 1423
total enrichment factor, 827
total fibre, 21
total phenols, 21
toxicity, 627
Toxoplasma gondii, 1339
trans-influence, 329
transition metal complex, 867
transition metal, 1297
transmission electron microscopy, 63
trisodium salt, 1193
triticale, 1279, 1375
Trnovče, 947
trophoblast cells, 159
twinning, 107
two-fluid model, 377
UNIFAC–VISCO parameters, 933
urease, 1127
urine, 1311
utilization, 575
UV protection, 705
vacancy defect, 1449
validation study, 1399
valproic acid, 627

van der Waals molecular surface, 659
vanadia loading, 355
vapour pressure, 499, 659
vasculopathies, 605
vibronic coupling, 877
viscosity, 933
voltammetry, 789, 1035
wastewater, 115
water supply, 947
water, 695
weathering, 827, 1087
wells, 947
wet milling, 367
wide band gap, 1411
Wiener index, 1009
X-ray diffraction, 45, 197, 367, 1481
zeolite A, 779
zeolite, 1203
zinc(II) complex, 87, 997
zinc(II), 1289
zinc, 87, 997, 1149
zofenopril, 485
ZSM-5, 717, 1297
α-amylase, 1279, 1375
β-nucleated, 223

Journal of the Serbian Chemical Society
JSCS-info@shd.org.rs • www.shd.org.rs/JSCS
Volume *80* (2015)

2015 List of Referees

Editorial Board of the Journal is grateful to the following referees for reviewing the manuscripts during 2015:

Shawkat A. Abdelmohsen, *Department of Chemistry, Faculty of Science, Assiut University, Assiut, Egypt*
Hatem A. Abdel-Aziz, *Department of Applied Organic Chemistry, National Research Center, Dokki, Cairo, Egypt*
Snezana Agatonovic-Kustrin, *LaTrobe University, School of Pharmacy, Bendigo, Victoria, Australia*
Mohamed Jawed Ahsan, *Maharishi Arvind College of Pharmacy Jaipur, Rajasthan, India*
Senem Akkoç, *Erciyes University, Faculty of Science, Department of Chemistry, Kayseri, Turkey*
Mariya al-Rashida, *Department of Chemistry, Forman Christian College, Chartered University, Lahore, Pakistan*
Joan Albert, *Departament de Química Inorganica, Facultat de Química, Universitat de Barcelona, Spain*
Andrea Aliboni, *Ente Per Le Nuove Tecnologie, l'Energia e l'Ambiente, Energy and Sustainable Economic Development, Rome, Italy*
Mara Aleksić, *Faculty of Pharmacy, University of Belgrade, Serbia*
Omar M. Aly, *Medicinal Chemistry Department, Faculty of Pharmacy, Minia University, Egypt*
Jelena Arsenijević, *Faculty of Pharmacy, Department of Pharmacognosy University of Belgrade, Serbia*
Athar Ata, *Department of Chemistry, The University of Winnipeg; Winnipeg, MB, Canada*
Tarek Aysha, *Institute of Organic Chemistry and Technology, Faculty of Chemical Technology, University of Pardubice, Czech Republic*
Najmedin Azizi, *Chemistry & Chemical Engineering Research Center of Iran, Tehran, Iran*
Darko Babić, *Institut Ruđer Bosković, Zagreb*
Milica Balaban, *Faculty of Science, University of Banja Luka, Bosnia and Herzegovina*
Igor Balać, *Faculty of Mechanical Engineering, University of Belgrade, Serbia*
Taibi Ben Hadda, *Laboratoire Chimie Matériaux, Faculté Sciences, Université Med Premier, Oujda, Morocco*
Vladimir Beškoski, *Faculty of Chemistry, University of Belgrade, Serbia*
P. J. Bindu, *Department of Studies and Research in Chemistry, Kuvempu University, Shankaraghatt, India*
Irani Biswas, *University of Burdwan, Department of Botany, Bardhaman, India*
Jelena Bobić, *Institute for Multidisciplinary Research, University of Belgrade, Serbia*
Gordana Bogoeva-Gaceva, *Ss. Cyril and Methodius University, Faculty of Technology and Metallurgy, Skopje, FYR Macedonia*

Dragana Đorđević, , *Institute of Chemistry, Technology and Metallurgy, University of Belgrade, Serbia*
Milos I. Đuran, *Department of Chemistry, Faculty of Science, University of Kragujevac, Serbia*
Enis Džunuzović, *Faculty of Technology and Metallurgy, University of Belgrade, Serbia*
Michail N. Elinson, *N. D. Zelinsky Institute of Organic Chemistry, Moscow, Russia*
Oleg Farat, *Department of Chemistry, M.V. Lomonosov Moscow State University, Russian Federation*
Daniela Farinelli, *Dipartimento di Scienze Agrarie, Alimentari e Ambientali, Perugia, Italy*
M. H. Fatemi, *Mazandaran University of Babolsar, Iran*
Abel Gomes Martins Ferreira, *Departamento de Engenharia Química, Faculdade de Ciências e Tecnologia, Universidade de Coimbra, Portugal*
Sacramento Ferrer, *Departament de Química Inorgànica, Universitat de València, Burjassot, Valencia, Spain*
Boris Furtula, *Department of Chemistry, Faculty of Science, University of Kragujevac, Serbia*
Slobodan Gadžurić, *Faculty of Sciences, Dep. Of Chemistry, University of Novi Sad*
Dejan Gođevac, *Institute of Chemistry, Technology and Metallurgy, University of Belgrade, Serbia*
Gordana Gojgić-Cvijović, *Institute of Chemistry, Technology and Metallurgy, University of Belgrade, Serbia*
Snežana Gojković, *Faculty of Technology and Metallurgy, University of Belgrade, Serbia*
Encarna Gomez Plaza, *University of Murcia, Faculty of Veterinary, Spain*
Juozas Vidas Grazulevicius, *Department of Organic Technology, Kaunas University of Technology, Lithuania*
Ludwig Gruber, *Fraunhofer IVV, Freising, Germany*
Sonja Grubišić, *Faculty of Chemistry, University of Belgrade. Serbia*
Maja Gruden, *Faculty of Chemistry, University of Belgrade. Serbia*
Mikhail Goubko, *Russian Academy of Sciences, Moscow, Russia*
Ivan Gutman, *Department of Chemistry, Faculty of Science, University of Kragujevac, Serbia*
Valéria Guzsvány, *Faculty of Sciences, Department of Chemistry, Biochemistry and Environmental Protection, University of Novi Sad,*
Milica Gvozdenovic, *Faculty of Technology and Metallurgy, University of Belgrade, Serbia*
Ladislav Habala, *Faculty of Pharmacy, Comenius University Bratislava, Slovakia*
Sotiris K. Hadjikakou, *Department of Chemistry, University of Ioannina, Greece*
Linda Hall, *Faculty of Agricultural, Life & Environmental Sciences, University of Alberta, Edmonton, AB Canada*
Richard Haynes, *Centre for Infection, Division of Cellular and Molecular Medicine, St George's, University of London, UK*
Hooshang Hamidian, *Department of Chemistry, Payame Noor University (PNU), Tehran, Iran*
Berta Barta Holló, *Department of Chemistry, Biochemistry and Environmental Protection Faculty of Sciences, University of Novi Sad, Serbia*
Tingjun Hou, *Institute of Functional Nano & Soft Materials; Soochow University, China*
Nenad Ignjatović, *Institute of Technical Sciences of the Serbian Academy of Sciences and Arts, Belgrade, Serbia*
Mirela Iličić, Mirela Iličić, *University of Novi Sad, Serbia*
Moustafa Issa , *Faculty of Science, Cairo University, Giza, Egypt*
Ivana Ivančev-Tumbas, *University of Novi Sad, Serbia*
Radmila Jančić Heinemann, *Faculty of Technology and Metallurgy, University of Belgrade, Serbia*

Ingrid Milošev, *Jozef Stefan Institute, Ljubljana, Slovenia*
Ahmed Mkadmh, *Chemsitry Department, Faculty of Science, Al Aqsa University Gaza Palestine*
Keith Murray, *School of Chemistry, Monash University, VIC, Autralia*
Shanmugam Muthusubramanian, *Department of Organic Chemistry, School of Chemistry, Madurai Kamaraj University, India*
Muhammad Naseer, *Department of Chemistry, Quaid-i-Azam University, Islamabad, Pakistan*
Bojana Nedić Vasiljević, *Faculty of Physical Chemistry, University of Belgrade, Serbia*
Olgica Nedić, *Institute for the Application of Nuclear Energy, University of Belgrade, Serbia*
Aleksandra Nešić, *Faculty of Technology and Metallurgy, University of Belgrade, Serbia*
Biljana Nigovic, *Department of Pharmaceutical, Analysis, Faculty of Pharmacy and Biochemistry, University of Zagreb, Croatia*
Katarina Nikolić, *Faculty of Chemistry, University of Belgrade, Serbia*
Milan Nikolić, *Faculty of Chemistry, University of Belgrade, Serbia*
Paolino Ninfali, *Universita degli Studi di Urbino, Dipartimento di Scienze Biomolecolari, Urbino, Italy*
Emiliya V. Nosova, *Chemical Technology Institute, Urals Federal University, Ekaterinburg, Russia*
Miroslav Novaković, *Institute of Chemistry, Tehnology and Metallurgy, University of Belgrade, Serbia*
Tatjana Novaković, *Institute of Chemistry, Tehnology and Metallurgy, University of Belgrade, Serbia*
Jean Ondo, *Aix-Marseille Université, CNRS, LCE, Marseille, France*
Dejan Opsenica, *Faculty of Chemistry, University of Belgrade, Serbia*
Igor Opsenica, *Faculty of Chemistry, University of Belgrade, Serbia*
Adil A. Othman, *Faculty of Sciences, University of Sciences and Technology of Oran-Mohamed Boudiaf-USTO-MB, Oran, Algeria*
Magdalena Owczarek, *Faculty of Chemistry, University of Wroclaw, Poland*
Sibel A. Ozkan, *Faculty of Pharmacy, Ankara University, Turkey*
Jose Palacios, *The University of New Mexico, Albuquerque, USA*
Vladimir Panić, *Institute of Chemistry, Tehnology and Metallurgy, University of Belgrade, Serbia*
Andrea Penoni, *Dipartimento di Scienza e Alta Tecnologia Università degli Studi dell'Insubria, Como, Italy*
Marija Pergal, *Institute of Chemistry, Technology and Metallurgy, University of Belgrade, Serbia*
Miljenko Perić, *Faculty of Physical Chemistry, University of Belgrade, Serbia*
Milena Petković, *Faculty of Physical Chemistry University of Belgrade, Serbia*
Menka Petkovska, *Faculty of Technology and Metallurgy, University of Belgrade, Serbia*
Srđan Petrović, *Institute of Chemistry, Technology and Metallurgy, University of Belgrade, Serbia*
Rada Petrović, *Faculty of Technology and Metallurgy, University of Belgrade, Serbia*
José Luis Pérez Pavón, *Facultad de Química, Salamanca, Spain*
Andrej Perdih, *National Institute of Chemistry, Ljubljana, Slovenia*
Slobodan D. Petrović, *Faculty of Technology and Metallurgy, University of Belgrade, Serbia*
Velimir Popsavin, *Faculty of Science, University of Novi Sad, Serbia*
Radivoje Prodanović, *Department of Biochemistry, Faculty of Chemistry, University of Belgrade, Serbia*

Vladimir Šukalović, *Institute of Chemistry, Technology and Metallurgy - Department of Chemistry, University of Belgrade, Serbia*
Aziz Tekin, *Ankara University, Turkey*
Vele Tešević, *Faculty of Chemistry, University of Belgrade, Serbia*
Shiliang Tian, *University of Illinois at Urbana-Champaign, Urbana, IL, USA*
Manisha Tiwari, *Dr. B.R. Ambedkar Centre for Biomedical Research, University of Delhi, India*
Theivasanthi Thirugnanasambandan, *International Research Centre, Kalasalingam University, Tamil Nadu, India*
Tamara Todorović, *Faculty of Chemistry, University of Belgrade, Serbia*
Simonida Tomić, *Faculty of Technology and Metallurgy, University of Belgrade, Serbia*
Dragica Trivić, *Faculty of Chemistry, University of Belgrade, Serbia*
Hakki Türker Akcay, *Recep Tayyip Erdoan University, Rize, Turkey*
Vlatka Vajs, *Institute of Chemistry, Technology and Metallurgy - Department of Chemistry, University of Belgrade, Serbia*
S. Venkata Mohan, *Bioengineering and Environmental Sciences (BEES), CSIR-Indian Institute of Chemical Technology (CSIR-IICT), Hyderabad, India*
Vesna Vasić, *Vinča Institute of Nuclear Sciences, Belgrade, Serbia*
Cristina Vázquez, *Universidad de Buenos Aires, Facultad de Ingeniería, Buenos Aires, Argentina*
H. Venkatachalam, *Department of Chemistry, Kasturba Medical College International Center, Manipal University, India*
Zhivko Velkov, *South-West University ''Neofit Rilski'', Bulgaria*
Tatjana Ž. Verbić, *Faculty of Chemistry, University of Belgrade, Serbia*
Miguel Vilas Vilas-Boas, *Escola Superior Agraria Braganca, Braganca, Portugal*
Zoran Višak, *Centro de Química Estrutural, Instituto Superior Tecnico, Universidade de Lisboa, Portugal*
Vesna Vitnik, *Department of Chemistry, Institute of Chemistry, Technology and Metallurgy, University of Belgrade, Serbia*
Željko Vitnik, *Department of Chemistry, Institute of Chemistry, Technology and Metallurgy, University of Belgrade, Serbia*
Maja Vukašinović-Sekulić, *Faculty of Technology and Metallurgy, University of Belgrade, Serbia*
Tatjana Vulić, *Faculty of Technology, University of Novi Sad, Serbia*
Agnieszka Ewa Wiącek, *Department of Interfacial Phenomena, Faculty of Chemistry, UMCS Lublin, Poland*
Cheli Wang, *Changzhou University, School of Petrochemical Engineering, Changzhou, PR China*
Limin Wang, *Key Laboratory of Advanced Materials and Institute of Fine Chemicals, East China University of Science and Technology, Shanghai, PR China*
Julian Weghuber, *University of Applied Sciences Upper Austria, School of Engineering and Environmental Sciences, Steyr, Austria*
Hong Wei Xi, *Technological University, Singapore*
Yumei Xiao, *Department of Applied Chemistry, China Agricultural University, Beijing, P. R. China*
Takehiko Yamato, *Department of Applied Chemistry, Faculty of Science and Engineering, Saga University, Japan*
Okan Zafer Yeşilel, *Eskisehir Osmangazi Univ., Eskisehir, Turkey*
George A. Zachariadis, *Aristotle University of Thessaloniki, Greece*